Towards a methanol economy: Zeolite catalyzed production of synthetic fuels

Mentzel, Uffe Vie

Publication date:
2010

Towards a methanol economy:
Zeolite catalyzed production of synthetic fuels

Methanol ⟶ Fuels and chemicals

Uffe Vie Mentzel

PhD Thesis
Technical University of Denmark
Department of Chemistry
November 2010

Centre for Catalysis and Sustainable Chemistry

DTU

Towards a methanol economy:

Zeolite catalyzed production of synthetic fuels

Uffe Vie Mentzel

PhD Thesis
Technical University of Denmark
Department of Chemistry
November 2010

Danish National Research Foundation´s
Center for Sustainable and Green Chemistry

Preface

This thesis is submitted in candidacy of the PhD degree from the Technical University of Denmark (DTU). The work was initiated at the Center for Sustainable and Green Chemistry under the supervision of Professor Claus Hviid Christensen. When Claus sought new carrier opportunities in the summer of 2008, the supervision was taken over by Professor Rasmus Fehrmann and the work was continued and finalized in the Centre for Catalysis and Sustainable Chemistry. The work has been co-sponsored by Haldor Topsøe A/S, the Danish National Research Foundation, and the Technical University of Denmark.

The objective of the project has been to develop new chemical processes with relevance to the concept of "the methanol economy", which is a possible future scenario where methanol acts as the main energy carrier and building block in the chemical industry. The main focal point of the experimental work performed during the PhD project is zeolite catalyzed production of hydrocarbon fuels.

Most of the work presented in this thesis has been done in close collaboration with other PhD students. The experiments concerning co-conversion of ethane and methanol to higher hydrocarbons (Chapter 3) were done in collaboration with Anne Krogh Rovik, while the experiments on conversion of C_1-C_4 alcohols (Chapter 4) and other oxygenates (Chapter 5) to hydrocarbons were done in collaboration with Martin Spangsberg Holm. I think we have had an excellent cooperation, and it has been a pleasure to benefit from Martin's drive and broad knowledge on zeolite synthesis, characterization, and properties. Karen Thrane Leth has synthesized some of the zeolites used in the work, for which I am grateful.

Alongside the work on zeolite catalyzed production of hydrocarbons, I have worked on a side project concerning gold catalyzed aerobic oxidation of amines and alcohols to imines, oximes, amides, and esters. This has been done in collaboration with several students, especially post. doc. Søren Kegnæs who has been the main facilitator for the project. The results from these experiments are not part of this thesis, and the publications are not included in the appendix.

Furthermore, I would like to thank former PhD students Asbjørn Klerke and Jeppe Rass-Hansen for assistance and advice concerning practical and technical issues in connection with the construction of experimental setups.

_____

Uffe Vie Mentzel

Kgs. Lyngby, November 2010

Abstract

The main focus of this thesis is zeolite catalyzed conversion of oxygenates to hydrocarbon fuels and chemicals. Furthermore, conversion of ethane to higher hydrocarbons has also been studied.

After a brief introduction to the concept of "the methanol economy" in the first chapter, the second chapter is a literature study of Mobil's "methanol-to-hydrocarbons" (MTH) process, giving an overview of the history of the process, the nature of the employed catalysts, and the reaction mechanism.

In the third chapter, a series of experiments concerning co-conversion of ethane and methanol over a commercial H-ZSM-5 zeolite impregnated with gallium and/or molybdenum is described. The object was to investigate if the presence of methanol in the feed could enhance the conversion of ethane, but in all cases the opposite is observed; the presence of methanol actually suppresses the conversion of ethane. This suppression of ethane conversion is most likely due to simple composition for the active sites. Isotopic labeling studies performed with ^{13}C labeled methanol and unlabeled ethane showed that in the very first minutes of the reaction, large amounts of carbon atoms from ethane are incorporated into the products. This observation is attributed to a stoichiometric reaction between ethane and the metal oxide species in the catalyst, leading to the oxidation of ethane to ethene, which is readily converted and incorporated into the products.

Conversion of methanol, ethanol, 2-propanol, and 1-butanol to hydrocarbons over various zeolite catalysts is studied in Chapter 4. When 2-propanol or 1-butanol is converted over H-ZSM-5, the total conversion capacities of the catalyst are more than 25 times higher than for conversion of methanol and ethanol. Furthermore, for conversion of C_{3+} alcohols, the selectivity shifts during the experiment, and after around one third of the total run-time, the product mixture consists almost exclusively of alkenes, which is in stark contrast to conversion of methanol and ethanol where the catalyst produces large amounts of aromatics until full deactivation. When zeolite H-Beta is employed, the conversion capacities for all four alcohols are markedly lower than for H-ZSM-5, and H-Beta has higher conversion capacity for methanol than the other alcohols. Furthermore, conventional and mesoporous H-Ga-MFI was employed in the conversion of methanol and 2-propanol. These catalysts showed a lower selectivity towards aromatics than H-ZSM-5 and the mesoporous H-Ga-MFI deactivated extremely slowly during the conversion of 2-propanol and only very small amounts of coke were deposited on the gallium based zeolites compared to H-ZSM-5.

In the fifth chapter the direct zeolite catalyzed production of hydrocarbons from other oxygenates such as glycerol, methyl lactate, and acetic acid is studied. In general, very fast deactivation due to coke deposition is observed, but dilution of the reactants in methanol has a distinct positive effect on this, and reasonable conversion capacities are achieved in this way. The incorporation of the carbon atoms from the oxygenates into the hydrocarbon products was confirmed by isotopic labeling experiments. More than 25 different oxygenates are converted over H-ZSM-5 as 10 % solutions in methanol, and the effect of the H/C atomic ratio of the dehydrated reaction mixture and the specific functional groups in the reactant on the catalyst lifetime, product selectivity, and formation of coke is addressed.

Dansk resumé

Hovedemnet for denne afhandling er zeolit-katalyseret konversion af oxygenater til kulbrintebaseret brændstof og kemikalier, og konversion af ethan til højere kulbrinter er også blevet undersøgt.

Det første kapitel er en kort introduktion til konceptet "the methanol economy", som er et fremtidsscenarie, hvor methanol fungerer som energibærer og byggesten i den kemiske industri. Det andet kapitel er et litteraturstudium af Mobils "methanol-to-hydrocarbons" proces. Her gives et overblik over processens historie, de anvendte katalysatorers egenskaber og reaktionsmekanismen.

I det tredje kapitel beskrives en række forsøg omhandlende co-konversion af ethan og methanol over en kommerciel H-ZSM-5 zeolite imprægneret med gallium og/eller molybdæn. Formålet var at undersøge, om tilstedeværelsen af methanol i fødestrømmen kunne forøge konversionen af ethan, men i alle tilfælde blev det modsatte observeret, idet tilstedeværelsen af methanol undertrykker konversionen af ethan. Dette skyldes højst sandsynligt simpel konkurrence om de aktive sites. Isotopmærkningsstudier udført med ^{13}C-mærket methanol og umærket ethan viste, at i de første minutter af reaktionen, bliver der inkorporeret store mængder carbon fra ethan i produkterne. Dette tilskrives en støkiometrisk reaktion mellem ethan og metaloxider på katalysatoren, hvorved ethan oxideres til ethen, som uden videre bliver konverteret og inkorporeret i produkterne.

Fjerde kapitel omhandler konversion af methanol, ethanol, 2-propanol og 1-butanol til carbonhydrider over forskellige zeolit-katalysatorer. Når 2-propanol eller 1-butanol bliver konverteret over H-ZSM-5 er katalysatoren i stand til at konvertere mere end 25 gange så meget reaktant før deaktivering i forhold til konversion af methanol eller ethanol. Ydermere ændrer selektiviteten sig under forsøget, når C_{3+} alkoholer konverteres over H-ZSM-5, og efter omkring en tredjedel af den totale reaktionstid består produktblandingen næsten udelukkende af alkener, hvilket er i skarp kontrast til konversion af methanol og ethanol, hvor katalysatoren producerer store mængder aromater, indtil den er helt deaktiveret. Når H-Beta anvendes som katalysator, sker deaktiveringen langt hurtigere end for H-ZSM-5, og H-Beta har længere levetid for konversion af methanol end de andre alkoholer. Herudover er konventionel og mesoporøs H-Ga-MFI blevet anvendt til konversion af methanol og 2-propanol. Disse katalysatorer udviser lavere selektivitet til aromater end H-ZSM-5, og mesoporøs H-Ga-MFI deaktiverer ekstremt langsomt under konversion af 2-propanol. Der aflejres kun ganske små mængder coke på de galliumbaserede zeolitter sammenlignet med H-ZSM-5.

I det femte kapitel studeres den direkte zeolitkatalyserede produktion af carbonhydrider fra andre oxygenater som glycerol, methyllactat og eddikesyre. Generelt observeres meget hurtig deaktivering pga. dannelse af coke, men fortynding af reaktanterne i methanol har en markant positiv effekt på dette, og fornuftige levetider opnås på denne måde. Inkorporering af carbonatomer fra de forskellige oxygenater i de producerede carbonhydrider blev bekræftet vha. isotopmærkningsforsøg. Mere end 25 forskellige oxygenater blev konverteret over H-ZSM-5 som 10 % opløsninger i methanol, og effekten af det atomare H/C-forhold i den dehydrerede reaktionsblanding og de specifikke funktionelle grupper i reaktanten på katalysatorens levetid, produktselektivitet og dannelse af coke på katalysatoren behandles.

List of publications and conference contributions during the PhD project

Scientific publications in international peer-reviewed journals

Mentzel, U. V., Holm, M. S., "Utilization of biomass: Conversion of model compounds to hydrocarbons over H-ZSM-5", submitted, **2010**

Kegnæs, S., Mielby, J., Mentzel, U. V., Christensen, C.H., Riisager, A., "Formation of imines by selective gold-catalysed aerobic oxidative coupling of alcohols and amines under ambient conditions", *Green Chem.* **2010,** *12,* 1437

Mentzel, U. V., Saravanamurugan, S., Hruby, S. L., Christensen, C. H., Holm, M. S., "High Yield of Liquid Range Olefins Obtained by Converting *i*-Propanol over Zeolite H-ZSM-5", *J. Am. Chem. Soc.* **2009**, *131*, 17009

Mentzel, U. V., Rovik A. K., Christensen C. H., "Co-Conversion of Ethane and Methanol into Higher Hydrocarbons over Ga/H-ZSM-5, Mo/H-ZSM-5 and Ga-Mo/H-ZSM-5", *Catal. Lett*. **2008**, *127*, 44

Klitgaard, S. K., Egeblad, K., Mentzel, U. V., Popov A. G., Jensen, T., Taarning, E., Nielsen, I. S., Christensen, C. H., "Oxidations of amines with molecular oxygen using bifunctional gold-titania catalysts", *Green Chem.* **2008**, *10*, 419

Oral presentations at international conferences

Mentzel, U. V., Shunmugavel, S., Christensen, C. H., Holm, M. S., "Advances in methanol-to-hydrocarbons (MTH) chemistry: High yield of liquid range olefins obtained by converting higher alcohols over zeolite H-ZSM-5", *ACS National Meeting*, San Francisco, March 21st -25th, **2010**

Mentzel, U. V., Klitgaard, S. K., Christensen, C. H., "Green Oxidations: Synthesis of Amides, Oximes and Imines by Gold Catalyzed Oxidation of Amines and Alcohols", *2nd EuCheMS Chemistry Congress*, Turin, Italy, September 16th -20th, **2008**

Mentzel, U. V., Rovik, A. K., Christensen, C. H., "Co-Conversion of Ethane and Methanol over Ga/H-ZSM-5", *Tenth International Symposium on Heterogeneous Catalysis*, Varna, Bulgaria, August 23rd – 27th, **2008**

Mentzel, U. V., Klitgaard, S. K., Christensen, C. H., "Gold Catalyzed Aerobic Oxidation of Alcohols and Amines in the Synthesis of Amides, Oximes and Imines", *Tenth International Symposium on Heterogeneous Catalysis*, Varna, Bulgaria, August 23rd – 27th, **2008**

Poster presentations at international conferences

Mentzel, U. V., Holm, M. S., "Conversion of oxygenates over zeolite H-ZSM-5: Towards direct production of hydrocarbon fuels from biomass", *14th Nordic Symposium on Catalysis*, Helsingør, Denmark, August 29th – 31st, **2010**

Mentzel, U. V., Shunmugavel, S., Hruby, S. L., Holm, M. S., "Conversion of C_1-C_4 Alcohols over H-ZSM-5 Zeolite: Increase in Conversion Capacity and Decrease in the Production of Aromatics", *16th International Zeolite Conference, 7th International Mesostructured Materials Symposium*, Sorrento, Italy, July 4th – 7th, **2010**

Mentzel, U. V., Holm, M. S., Shunmugavel, S., Hruby, S. L., Christensen, C. H., "Conversion of Methanol and Higher Alcohols over H-ZSM-5", *EuropaCat IX: Catalysis for a Sustainable World*, Salamanca, Spain, August 30th – September 4th, **2009**

Mentzel, U. V., Popov, A. G., Egeblad, K., Taarning, E., Christensen, C. H., "Catalytic Oxidations of Amines with Molecular Oxygen Facilitated by TiO_2", *Europacat VIII*, Turku, Finland, August 26th – 31st, **2007**

Mentzel, U.V., Popov, A.G., Egeblad, K., Taarning, E., Christensen, C.H., "Green Oxidations of Amines With Air Using a TiO2 Catalyst: A New Route to Cyclohexanone Oxime", *3rd International Conference on Green and Sustainable Chemistry*, Delft, The Netherlands, July 1st – 5th, **2007**

Book chapter

Mentzel, U. V., Egeblad, K., Christensen, C. H., "Bioraffinaderiet - Nanokatalysatorer i aktion", *Nanoteknologiske Horisonter*, DTU**, 2008**

Table of Contents

1 The methanol economy

Due to environmental concerns and diminishing oil reserves a new structure of the energy sector will be needed in the not so distant future. Since the discovery and implementation of crude oil in the 19th century it has served as the main energy source and energy carrier of the world. Due to the increasing energy demand of mankind, it is not plausible to replace the energy supply from oil with another single technology, all relevant energy sources and processes must play a role, including solar, wind, hydro, wave, geo/hydrothermal, biomass, etc. Despite environmental concerns, nuclear power and coal will most likely also contribute significantly to the total worldwide energy supply.

Hydrogen has been acknowledged as the energy carrier of the future, leading to the terms "hydrogen economy" or "hydrogen society", which refers to a possible future society where hydrogen acts as the main energy carrier [1, 2]. This scenario is very attractive due to the possibility of the energy and transport sectors being completely independent of carbon based technologies. Hydrogen is currently produced from fossil sources (mainly natural gas) through gasification or steam reforming, but it can also be produced from various alternative power sources via electrochemical splitting of water to its elements [3].

The proposed use of hydrogen is not straightforward; there are technical barriers to overcome. For instance, storage and release of hydrogen is of major importance, and a sufficiently simple and efficient method has not been discovered yet, though efforts have been made in the fields of metal hydrides [4, 5] and indirect storage of hydrogen in ammonia containing salts [6, 7]. The use of hydrogen as a transportation fuel requires development and implementation of sufficiently effective and cheap fuel cells. Furthermore, simple handling of hydrogen is not unproblematic, since it is very explosive and any leaks could be disastrous. Hydrogen will not become the energy carrier of the world before the mentioned issues are solved.

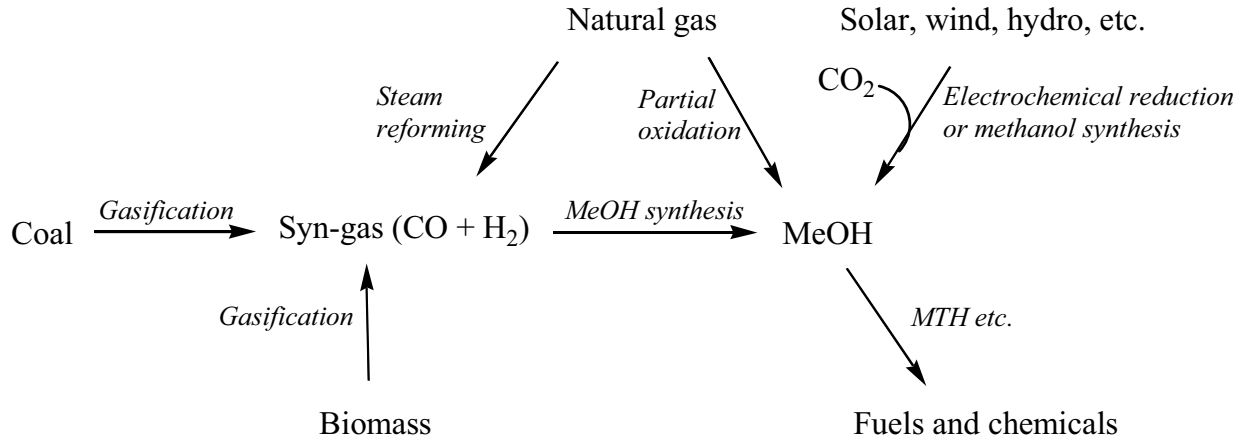

Figure 1: Main routes for production of methanol

An alternative to the hydrogen based economy is "the methanol economy" [3, 8], where methanol acts as the main energy carrier and building block in the chemical industry. Methanol is currently produced from fossil-based syn-gas (mainly based on natural gas) [3], but as illustrated in Figure 1, it can also be produced from various other sources.

The partial oxidation of methane to methanol has been a desired goal for researchers for many years, but no process has yet been developed with the necessary selectivity, yield and catalyst stability [3]. The main problem of the reaction is that the oxidation products (methanol, formaldehyde, and formic acid) are more reactive in the oxidation than methane itself, leading to the formation of CO_2 and water.

Methanol can also be produced from alternative power sources such as wind or solar power, either electrochemically from CO_2 [9] or via formation of hydrogen from electrolysis of water followed methanol synthesis by hydrogenation of CO_2 [10]. In this way the chemical energy of hydrogen can be stored indirectly as methanol, which is much more convenient for storage and transport than hydrogen [3].

Methanol can be used as a fuel directly, either in a combustion engine or by employing a “direct methanol fuel cell” (DMFC) [11], but it can also be converted to fuel grade hydrocarbons through Mobil’s methanol-to-hydrocarbons (MTH) process, which is described in detail in Chapter 2. In this way it is possible to produce gasoline which is virtually identical to normal petrochemical gasoline and the implementation of new types of vehicles and infrastructure is not necessary. Besides the use as an energy carrier, methanol is also a carrier of carbon and can thus serve as the main building block in the synthesis of solvents, materials etc. In this context, the MTH reaction is very important, since hydrocarbon bulk chemicals (e.g. toluene, xylenes, and small olefins) are available through this process.

2 The methanol-to-hydrocarbons (MTH) reaction

In the methanol-to-hydrocarbons (MTH) reaction, methanol is converted in a one-step process to a mixture of different hydrocarbons over a solid acid catalyst (typically a zeolite or zeotype). A simplified reaction pathway is shown in Figure 2. Initially methanol is partly dehydrated to an equilibrium mixture of methanol, dimethylether (DME), and water. Methanol and DME are then completely dehydrated and catalytically converted to olefins under the formation of carbon-carbon bonds. The formed olefins react further to form paraffins and aromatics. The overall product composition can be expressed as $(CH_2)_n$ corresponding to complete dehydration of methanol.

$$2\ CH_3OH \rightleftharpoons CH_3OCH_3 + H_2O$$

$$\begin{matrix} CH_3OH \\ CH_3OCH_3 \end{matrix} \xrightarrow{-H_2O} \text{Olefins} \longrightarrow \begin{matrix} \text{Paraffins} \\ \text{Aromatics} \end{matrix}$$

Figure 2: Simplified MTH reaction pathway

Depending on the catalyst, reactor design, and reaction conditions, the selectivity of the MTH reaction can be shifted towards gasoline production (the methanol-to-gasoline (MTG) reaction) or towards production of olefins (the methanol-to-olefins (MTO) reaction).

The MTH reaction was discovered in the early 1970s by two groups of researchers at Mobil Oil. One group was attempting to convert methanol to other oxygenates, such as ethylene oxide over zeolite H-ZSM-5 but they only observed hydrocarbons as products. Later, another group attempted to methylate isobutane with methanol over H-ZSM-5, leading to an unexpected production of aromatic compounds and paraffins all coming from methanol [12]. Mobil published their results on methanol conversion in the open literature in 1976 and 1977 [13, 14]. Due to the oil crisis in the 1970s, great effort was put into developing this reaction, since it offers an alternative to the ordinary petrochemically derived gasoline. The MTG reaction was acknowledged as the first new route to synfuels in 50 years since the discovery of the Fischer Tropsch process, i.e. conversion of synthesis gas to diesel fuel [15].

In 1979 the government of New Zealand chose Mobil's new MTG technology over the well known Fischer Tropsch technology to convert their large reserves of natural gas to gasoline [16]. By 1986 a full scale plant including production of synthesis gas from methane, methanol synthesis, and the MTG reaction employing Mobil's zeolite H-ZSM-5 catalyst was producing 600,000 ton gasoline pr. year, corresponding to a third of the nations demand. In the following years the price of crude oil dropped, leading to a shut-down of the gasoline synthesis, but the methanol synthesis was left online [16]. During the last decade the price of crude oil has again been on the rise, which has sparked new interest in the MTG process, and today ExxonMobil are offering licenses for the process and several have already been sold [17].

UOP/Hydro has developed an MTO process employing SAPO-34 as the catalyst. The process has successfully been scaled up to 275 tons pr. year in a demonstration plant in Norway proving the ability

to produce ethylene and propylene in high selectivity while the catalyst is regenerated continuously. The technology is licensed and available for purchase [18].

The methanol-to-propylene (MTP) process, a variation of the MTO process, has been developed by Lurgi. In this ZSM-5 based process, propylene selectivity is increased to above 70% by optimizing the catalyst and process conditions. The process is also available for purchase, and the construction of a plant with a capacity of 100,000 ton pr. year in the Middle East has been announced [19].

Haldor Topsøe A/S has also developed an MTG process known as the TIGAS (Topsøe Integrated GAsoline Synthesis) process. In the TIGAS process, the methanol synthesis and the MTG process are integrated into a single synthesis loop, thus eliminating methanol as an isolated intermediate [20]. A demonstration plant in Houston was operated successfully for 10,000 h, but the experimental program was terminated in 1987 [21].

2.1 MTH catalysts

Before Mobil's discovery of the zeolite catalyzed MTH reaction, several other catalysts have been employed in the conversion of methanol to hydrocarbons, including $ZrCl_2$ [19], $ZnCl_2$ [22] and Al_2O_3 [23, 24], but the real breakthrough came with Mobil's discoveries within solid Brønsted acidic zeolite catalysis in the 1970s. A short introduction to zeolites, their structure and properties is given in the following.

Zeolites are crystalline inorganic materials composed of silicon atoms, bridged through oxygen atoms to form an ordered structure containing micropores of molecular sizes throughout the entire crystal, leading to a massive internal surface area. Today 179 different framework structures have been reported [25] and more are discovered regularly. In general, zeolites contain silicon, oxygen and aluminum, but it is possible to synthesize materials of the same structure as zeolites, but with different elements such as phosphorous or germanium or others. These materials are known as zeotypes [26].

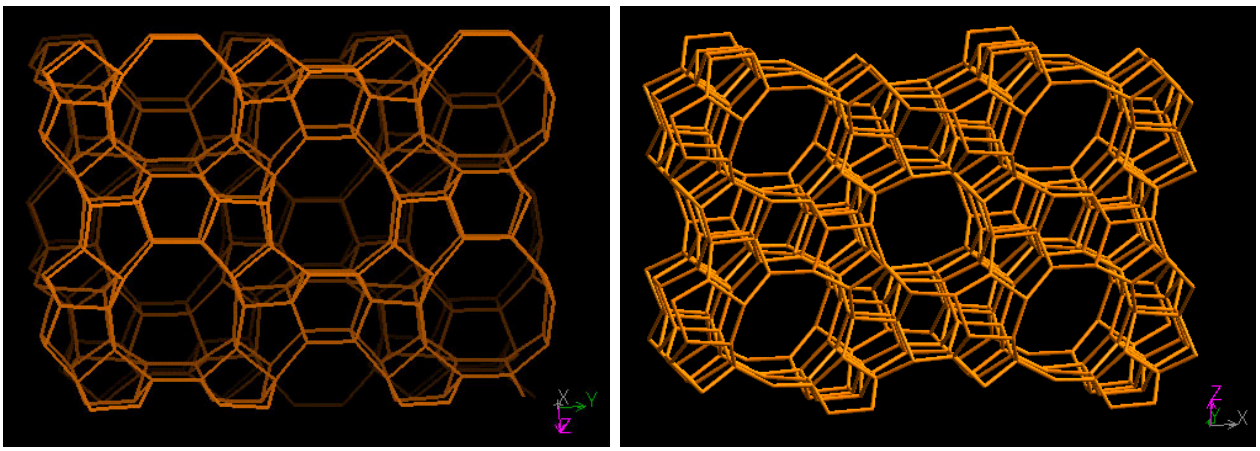

Figure 3: Illustration of the pores in the MFI (ZSM-5) structure. Left: Sinusoidal pores, right: Straight pores [25]

All zeolitic structures are assigned a 3 letter code. In Figure 3 an illustration of the MFI structure, the structure of Mobil's ZSM-5 zeolite is shown. The material has a three dimensional pore system. Importantly, these pores are of molecular size, meaning that reactants are able to enter the crystal to

find the catalytically active sites and be converted to products, which are allowed to leave through the pores. This gives rise to one of the unique features of zeolite catalysts, namely the size selectivity. Reactants must be small enough to enter the pores and products must be able to diffuse out after they are formed. This implies that the size of the pores in a specific zeolite structure is very important when it comes to product (and reactant) selectivity.

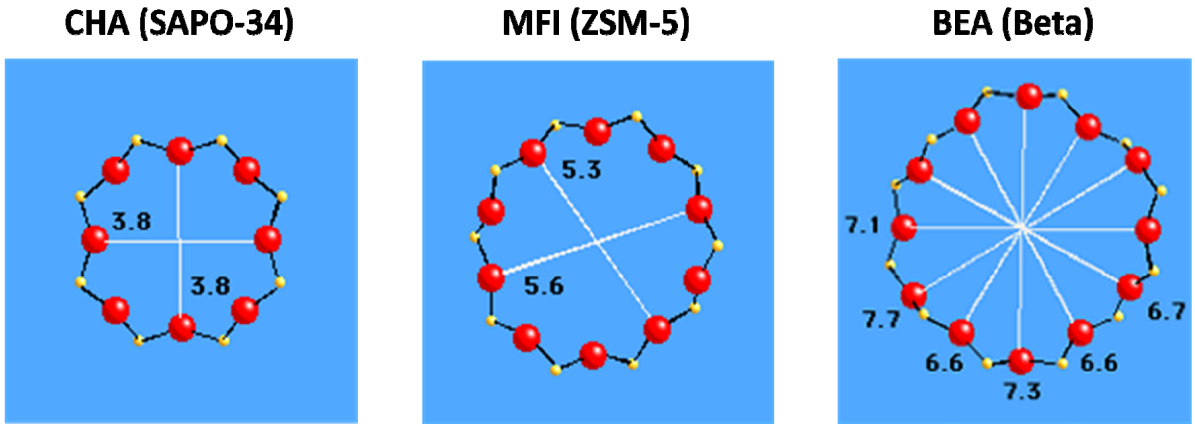

Figure 4: Illustration of the pore sizes in the CHA (SAPO-34), BEA (Beta) and MFI (ZSM-5) structures [25]

The pore sizes of two other zeolite structures relevant to the MTH reaction, CHA and BEA (the structures of SAPO-34 and zeolite Beta) are shown in Figure 4 alongside MFI. The pores of the three structures contain 8, 10 or 12 tetrahedrally coordinated atoms (known as T-atoms) between the bridging oxygen atoms and they are defined as small (CHA), medium (MFI), and large pores (BEA), respectively. It should be noted that SAPO-34 is not a zeolite, but a zeotype aluminumphospate consisting of tetrahedrally coordinated aluminum and phosphorous atoms bridged by oxygen atoms.

The consequences on a molecular level of the different pore dimensions of the three materials are illustrated schematically in Figure 5. At the intersections of the pores, SAPO-34 has large cavities of a size around 10 Å which are able to house larger compounds, but due to the narrow pores, only small compounds are able to leave the cages, which is why this catalyst is employed in the MTO reaction. In contrast to SAPO-34, the medium size pores of ZSM-5 allows aromatic compounds to leave the catalyst interior opening a broader window for product selectivity. The largest compound able to leave the catalyst pores is durene (1,2,4,5-tetramethylbenzene) [15], but at the pore intersections larger compounds such as pentamethylbenzene (pentaMB) and hexamethylbenzene (hexaMB) can be formed, but they are not able to diffuse through the pore system [27, 28]. Due to the large pores of zeolite Beta, the product selectivity is shifted even further towards larger products and even hexaMB and naphthalene are able to diffuse through the pore system to leave the catalyst.

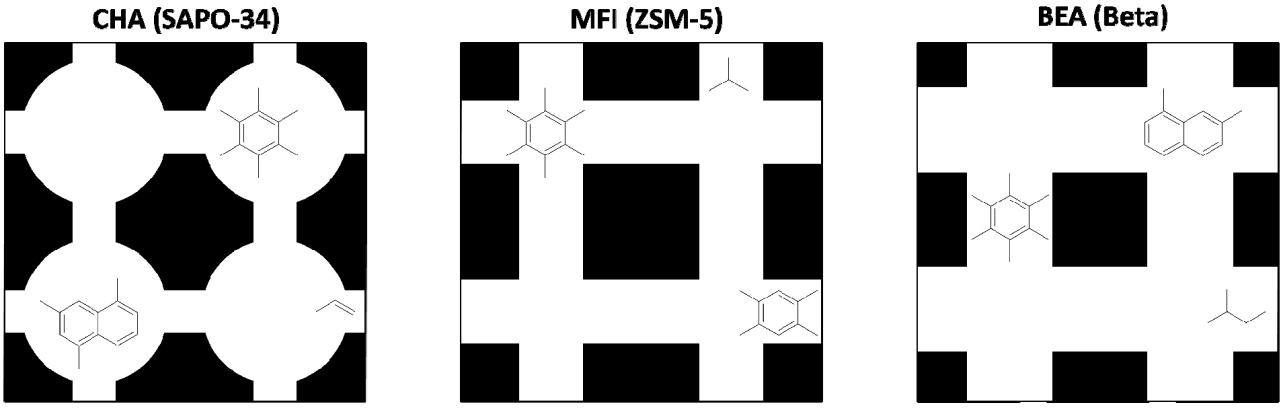

Figure 5: Illustration of the pore and cage sizes of CHA, MFI and BEA

In the MTH reaction, the zeolite owes its catalytic activity to the presence of Brønsted acidic sites situated inside the zeolitic pores (and on the surface). The origin of the catalytic site in ZSM-5 is replacement of a silicon atom in the zeolite framework by an aluminum atom leading to a charge deficiency, which must be offset by a cation. If this cation is a proton, an acidic site has been created. In SAPO-34 an acidic site is created in a similar manner by the replacement of a phosphorous atom by silicon atom.

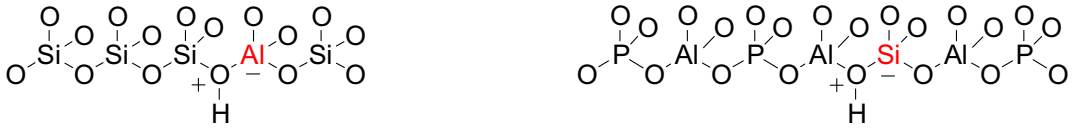

Figure 6: Structure of a single acidic site in H-ZSM-5 (left) and H-SAPO-34 (right)

The acid density of a zeolite catalyst is dictated by how many silicon atoms have been replaced with aluminum, and it is denoted as the ratio between silicon and aluminum (Si/Al) in the structure, i.e. a low value of Si/Al corresponds to high acid density. The strength of the acid site is dictated by the local molecular environment and is therefore dependent on the structure of the zeolite.

2.2 MTH catalysis

The mechanism behind the MTH reaction is highly complex and has been debated in literature since the discovery of the reaction. Numerous reviews have been published within the area [16, 19, 21, 29, 30, 31, 32, 33].

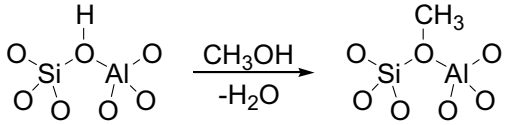

Figure 7: Binding of methanol to an acidic site in a zeolite

The initial step in the MTH reaction is binding of methanol to the zeolite catalyst as shown in Figure 7 creating a surface methoxy group [16]. This initial reaction step does not give any indication on how further bond formation between the C_1 species occurs, and this has been the main focus of the suggested mechanisms for zeolite catalyzed methanol conversion, thus more than 20 different mechanisms on formation of the initial C-C bond have been presented [16]. In lack of solid evidence, the

early mechanisms are mostly based on speculations and chemical intuition. Figure 8 summarizes some of the early suggested mechanisms. All of these mechanisms describe the formation of a chemical bond between two carbon atoms from methanol, to form ethene, which is able to react further to produce the final products. In Mobil's original paper [13] a mechanism involving carbene formation from methanol, followed by coupling with another methanol molecule is suggested, see Figure 8 (A).

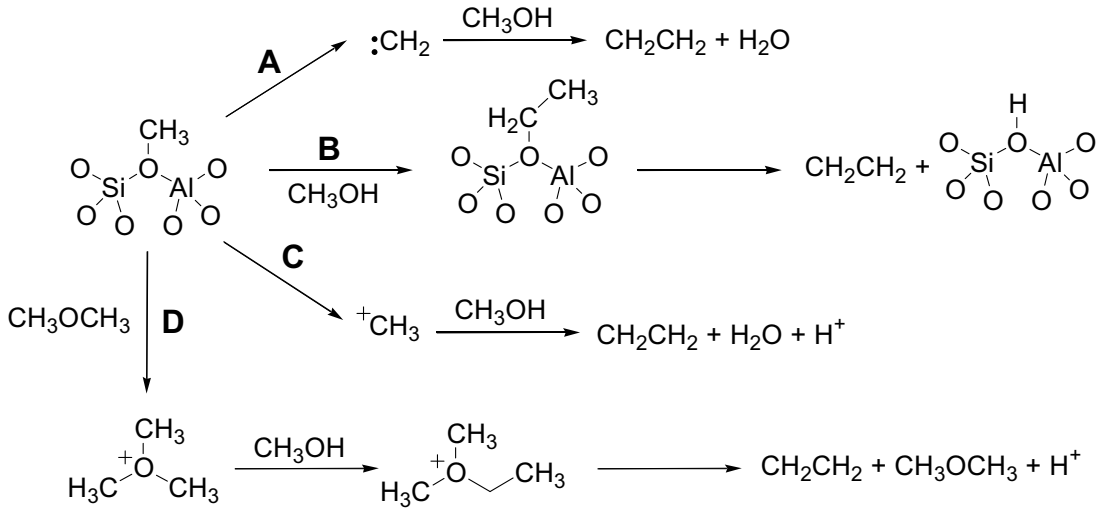

Figure 8: Several of the early suggested mechanisms to account for the formation of carbon-carbon bonds between C_1 species from methanol; the carbene mechanism (A) [13], the rake mechanism (B) [34] (alkoxy chain growth), carbocationic mechanism (C) [35] and the oxonium ylide mechanism (D) [36, 37, 38]

Figure 8 also shows other suggested mechanistic pathways including alkoxy chain growth (B), the formation of carbocations (C) and oxonium ylides (D). Radicals have also been proposed as reaction intermediates [39] (not shown in Figure 8). All of these mechanistic proposals go via high energy intermediates and lack solid evidence.

In 1993 Dahl and Kolboe suggested the indirect "hydrocarbon pool mechanism", illustrated in Figure 9 [40, 41]. In this mechanism methanol does not pass over high energy barriers to be activated, it is simply added to hydrocarbon species inside the zeolite, which in turn split off hydrocarbon products. Produced alkenes are able to be reinserted into the hydrocarbon pool, while alkanes and aromatics are end products. The concept of the hydrocarbon pool mechanism has gained general acceptance amongst researchers within the field [15, 16, 30], but the mechanistic details are far from fully understood, and the nature of the active hydrocarbon pool is discussed intensively.

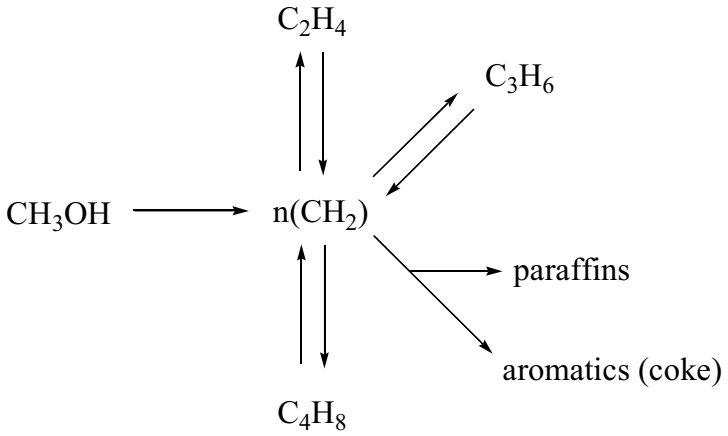

Figure 9: The hydrocarbon pool mechanism [40, 41]

The basic concept of methanol being converted via reaction with other hydrocarbon species in the zeolite pores was not new, but Dahl and Kolboe formulated a more general mechanism. As early as 1982 Langner observed that addition of small amounts of co-reactant, e. g. cyclohexanol resulted in an increased initial reactivity of methanol over H-ZSM-5 [42]. He proposed the mechanism shown in abbreviated form in Figure 10, where C_1 species from methanol (or DME) are continuously added to cyclohexene resulting in a polymethylated compound which in turn splits off olefins.

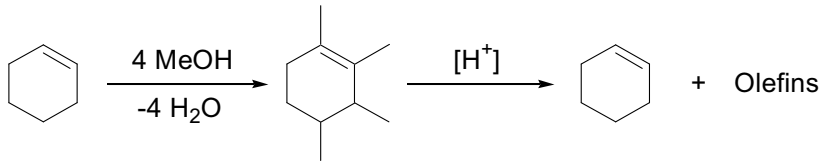

Figure 10: Early mechanism for the co-reaction of cyclohexanol and methanol proposed by Langner in 1982 [42]

A key experimental technique in the clarification of mechanistic details in the MTH reaction has been conversion of isotopically labeled methanol typically with a co-reactant. This allows for tracing the origin of the different products by analyzing their isotopic distribution. Thus, in 1982 Dessau and La Pierre observed that co-conversion of ^{13}C labeled methanol with different olefins resulted in a product mixture containing isotopically scrambled products [43]. To explain these observations, the authors proposed a mechanism based on olefin methylation and cracking reactions, see Figure 11. Based on experiments with different contact times, Desssau later concluded that ethylene is only formed from cracking at long contact times, indicated by the dotted line in Figure 11 [44].

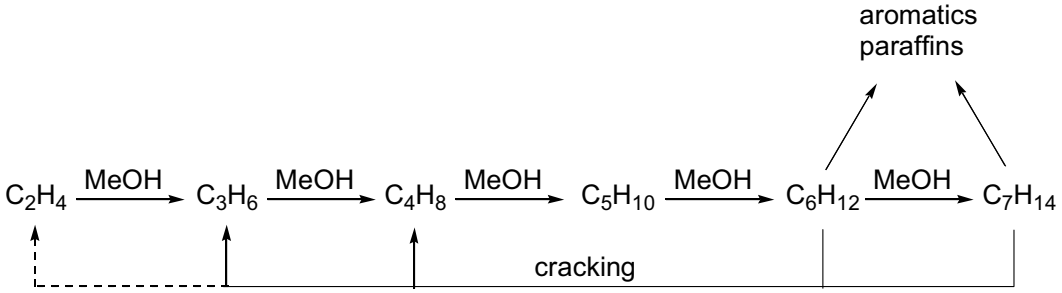

Figure 11: Dessau's olefin methylation and cracking mechanism, proposed in 1982 [43] and refined in 1986 [44]

Around 20 years after Dessau's discoveries, Svelle *et al.* studied the H-ZSM-5 catalyzed co-conversion of ^{13}C labeled methanol and ethene, propene and butene at low contact times [45, 46]. These experiments showed that the methylation reaction is first order in the olefin and zero order in methanol, and that the methylation rate increased in the order: Ethene < propene < butene. Another important finding was that the presence of methanol suppresses the interconversion reactions of alkenes (oligomerization, isomerization, cracking). These observations indicate, that when methanol is present in the catalyst bed, most of the active sites bind a methanol molecule (as a surface methoxy) giving rise to the zero order kinetics in methanol and the suppression of alkene interconversion (no free sites are available to perform the reaction). At low methanol concentrations methanol starts to play a role in the kinetics of methylation, and alkene interconversions starts to take place [46]. This reflects that the occupancy of the active sites by methanol is lower.

Mole *et al.* [47] also used isotopic labeling in an attempt to elucidate mechanistic information on the conversion of methanol over H-ZSM-5. The authors co-fed ^{13}C labeled methanol and unlabeled methylbenzenes, and a mixture of isotopes was observed in ethene formed in the reaction. They also observed dealkylation of ethylbenzene and *n*-propylbenzene. These observations led them to propose the mechanism shown in Figure 12 in abbreviated form [30].

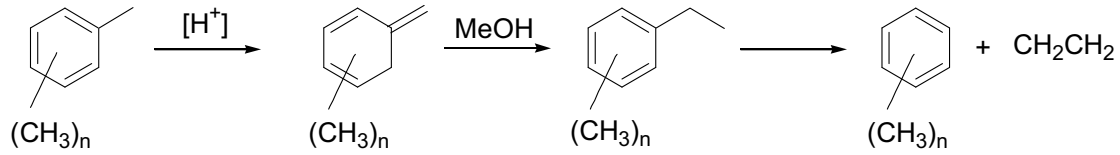

Figure 12: Mole's mechanism for methanol conversion via *exo*-methylene-cyclohexadiene [30, 41]

In the line of Mole's early experiments, Mikkelsen *et al.* observed isotopic scrambling in the olefinic products when co-converting ^{13}C methanol and toluene over H-ZSM-5, H-mordenite and H-beta [48]. Based on their results, the authors conclude that a hydrocarbon pool type mechanism is responsible for the production of ethene and propene, and that the catalytically active hydrocarbon complex inside the zeolite pores is most likely an arene or a compound easily derived from an arene. This is the case for all three zeolites studied. It is also evident from the results that propene is formed from the hydrocarbon pool since the produced propene has the same isotopic composition as ethene indicating that propene is produced directly from the hydrocarbon pool and not from subsequent methylation of ethene [48]. If the ratio between methanol and toluene in the feed is raised, the selectivity towards propene increases indicating that higher substituted arenes has a higher tendency towards producing propene.

The exocyclic methylation mechanism, also known as the side chain alkylation mechanism, is shown in Figure 13 [29, 30, 49]. It is essentially a refinement of Mole's original mechanism. In this mechanism hexamethylbenzene (hexaMB) is methylated to the heptamethylbenzenium ion (heptaMB$^+$), which is deprotonated to 1,2,3,3,4,5-hexamethyl-6-methylene-1,4-cyclohexadiene (HMMC). This is followed by exocyclic methylation by one or two methanol derived C_1 entities and ethene or propene are split off as products. Through a series of methyl shifts and deprotonation hexaMB is reformed and the catalytic cycle is complete. The formation of heptaMB$^+$ from hexaMB in zeolite beta was confirmed through NMR spectroscopy by Song *et al.* in 2002 [50] and in 2003 Bjørgen *et al.* used IR spectroscopy to show that

hexaMB is protonated in the zeolite when fed directly to a beta zeolite [51]. Shortly after, the formation of HMMC in the pores of zeolite beta from co-conversion of benzene and methanol was shown through ex-situ NMR [52]. The reactivity of polymethylbenzenium ions was confirmed through gas phase ionization and fragmentation by Svelle *et al.* in 2006. Indeed, small olefins are among the fragmentation products confirming that polymethylbenzenes play a role in olefin formation [53].

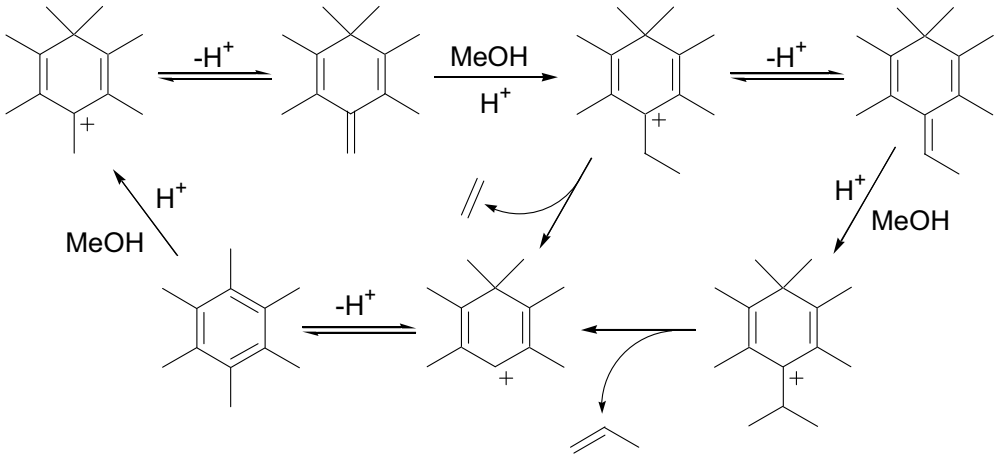

Figure 13: Formation of ethene and propene via the exo-cyclic methylation mechanism

An alternative mechanism dealing with the formation of olefins from methanol via polymethylbenzens known as “the paring mechanism” is shown in Figure 14. The mechanism was originally suggested by Sullivan *et al.* to explain the formation of *i*-butane (via *i*-butene) and other paraffins in the hydrocracking of hexaMB over silica/alumina supported nickel particles [54]. The mechanism was later adapted to the MTH reaction [29, 49]. As illustrated in Figure 14, the paring reaction predominantly leads to the formation of propene and *i*-butene [49].

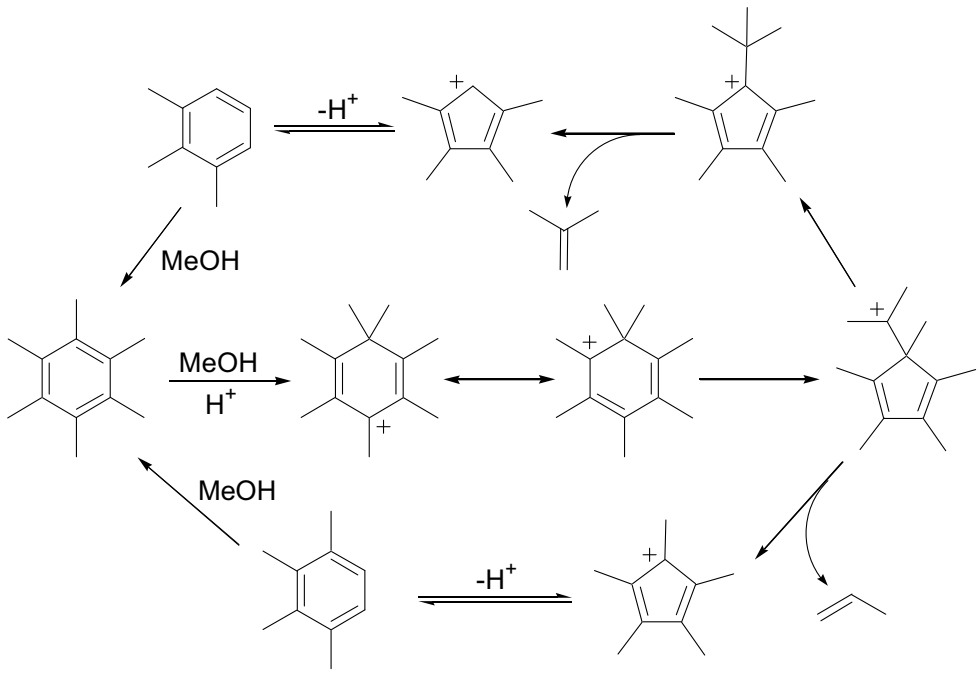

Figure 14: Formation of propene and *i*-butene via the paring reaction

The central mechanistic feature of the paring reaction is the ring contraction, which is responsible for the formation of an isopropyl substituted intermediate. This intermediate is able to split off propene or undergo methyl shift and split off *i*-butene. The exocyclic methylation mechanism and the paring reaction are generally accepted as possible pathways for methanol conversion via hydrocarbon pool species in the zeolite pores.

In 2002 Sassi *et al.* performed a very thorough study of the reaction of polymethylbenzenes over a series of beta zeolites with different acid densities (Si/Al = 37.5, 75, and 150, respectively) at 450 °C with and without ^{13}C labeled methanol present [55]. If the paring reaction is active, ^{13}C atoms from methanol would over time be inserted into the aromatic ring, while the exocyclic mechanism only can account for labeling in the methyl positions. Based on the isotopic distributions of the aromatic products Sassi *et al.* conclude that the main pathway for olefin formation is the exocyclic mechanism, while the paring reaction might play a minor role. The authors note that for the zeolite catalyst with highest acid density (Si/Al = 37.5) some ^{13}C incorporation to the aromatic ring is observed indicating that the paring mechanism is active. Nevertheless this observation could also arise from formation of aromatics from ^{13}C labeled alkenes produced from the hydrocarbon pool.

In a similar series of experiments Bjørgen *et al.* co-converted benzene and ^{13}C labeled methanol over high acid density beta zeolite (Si/Al = 12) at 210-330 °C. In these experiments incorporation of ^{13}C to the aromatic ring carbons was pronounced and increasing with temperature. Observation of ^{12}C carbon atoms originating from benzene in propene and *i*-butane (formed via *i*-butene) confirmed the validity of the paring mechanism. The results obtained by Bjørgen *et al.* confirm the observation by Sassi *et al.*, that the activity of the paring reaction seems to be more pronounced at higher acid densities. Bjørgen's experiments are performed at much lower temperature than Sassi's, which might also play a role in this context.

In general, mechanistic studies performed on the MTH reaction show similar trends when different zeolite catalysts are employed. The beta zeolite has been a popular choice for mechanistic investigations, due to its large pores allowing the direct reaction of proposed reaction intermediates such as hexaMB. Even though the same types of mechanisms are active in the different zeolites, the exact nature of the active hydrocarbon pool species differs.

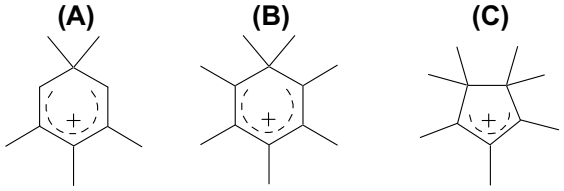

Figure 15: Carbenium ions observed by employing NMR spectroscopy to spent zeolite catalysts. A was observed in H-ZSM-5 [56], B in H-Beta [57] and C in H-SAPO-34 [58]

Through NMR spectroscopy Haw's research group has identified different carbenium ions in different zeolite catalysts [56, 57, 58]. The carbenium ion (B) in Figure 15 observed in H-beta is in good correspondence with the exocyclic methylation and paring mechanisms shown above. For H-ZSM-5 the ion (A) is observed and in H-SAPO-34 (C) is observed. These intermediates (A and C) are most likely part

of the same types of mechanisms as (B), but due to pore structure and dimensions of the different zeolite structures the specific structure of the active hydrocarbon pool differs. It should be noted that structure (C) is derived from acetone conversion over SAPO-34 [58].

As mentioned above hexaMB has been verified as a key intermediate in methanol conversion over H-Beta. In 2001 Arstad and Kolboe [59] performed isotopic labeling experiments where they built up a hydrocarbon pool by reacting unlabelled methanol over SAPO-34. After switching to ^{13}C labeled methanol and feeding this for a short time, the reaction was stopped and the spent zeolite was dissolved in hydrofluoric acid to analyze the hydrocarbon species inside the zeolite pores. Incorporation of ^{13}C in the methylbenzenes retained in the zeolite was observed and importantly the degree of ^{13}C incorporation is highest for the more substituted compounds, i.e. all the methylbenzenes seem to be participating in the reaction, but as for H-Beta hexaMB has the highest activity for methanol conversion over H-SAPO-34.

In a similar series of experiments with switching between unlabeled and ^{13}C labeled methanol, Bjørgen *et al.* investigated the mechanism behind conversion of methanol over H-ZSM-5 [27, 28]. A very low degree of ^{13}C incorporation in hexaMB and pentaMB is observed, while tetraMB's and especially triMB's contain a large number of labeled carbon atoms. This implies that in contrast to H-SAPO and H-Beta, the less substituted aromatics seem more important as active hydrocarbon pool species for H-ZSM-5. Apart from being inactive in the methanol conversion, flushing experiments show that pentaMB and hexaMB are immobilized inside the zeolite pores. They are not able to diffuse out of the zeolite structure, and they are not able to split off small olefins to escape as smaller molecules, i.e. they act as internal coke blocking the pores inside the zeolite.

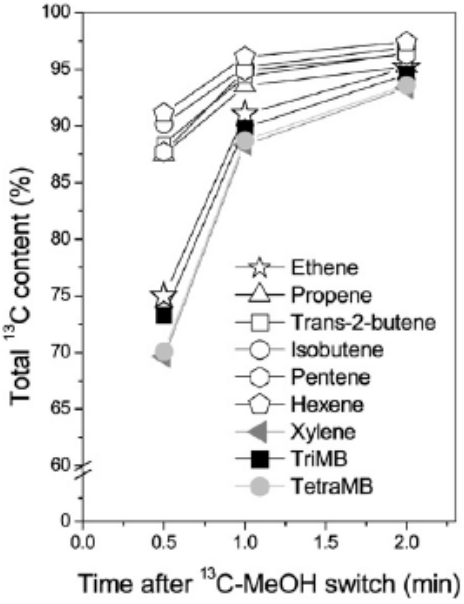

Figure 16: ^{13}C contents of alkenes and aromatics in the effluent after switch to ^{13}C labeled methanol [28]

Another important mechanistic feature unraveled by these isotopic labeling experiments is that ethene contains much less ^{13}C after the switch from ^{12}C methanol to ^{13}C methanol than the larger alkenes; see Figure 16 [28]. This implies that ethene is produced from a different reaction mechanism than the larger

alkenes. The degree of ^{13}C labeling of ethene groups with the aromatic compounds in the effluent, indicating that the formation of ethene is coupled to the formation of aromatics. The authors suggest that the reactions proceeding in a working catalyst can be summarized into the "dual cycle mechanism" shown in Figure 17. In this mechanism methanol is converted to hydrocarbons through two catalytic cycles. Cycle I is methylation of aromatics and subsequent release of ethene, while cycle II is repeated methylation of C_{3+} alkenes followed by isomerization and cracking reactions. The alkenes produced in cycle II are able to undergo cyclization and hydrogen transfer reactions to produce alkanes and aromatics, which participate in cycle I. The mechanism is essentially an elegant combination of Dessau's methylation/cracking mechanism, and the paring/exocyclic methylation mechanisms catalyzed by methylbenzenes. Even though methanol is shown as the reactant in Figure 17, DME is also participating significantly in the reaction; in fact kinetic studies have shown that DME is 2.5 times more active for propene methylation than methanol [60].

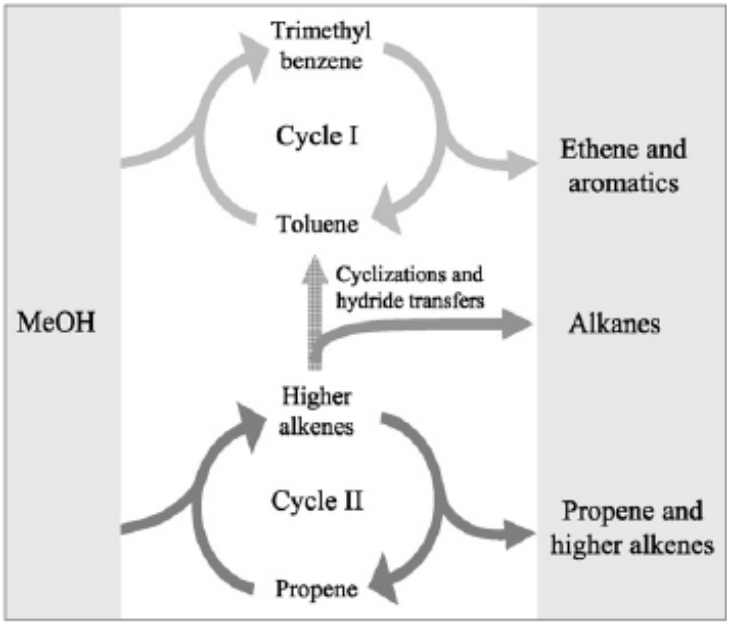

Figure 17: The "dual cycle mechanism" suggested by Bjørgen *et al.* [28]

An important point discussed by the authors [28] regarding this mechanism is whether the two cycles are able to run independently. Cycle I is dependent on a continuous feed of aromatics from cycle II, but in principle cycle II could be able to run alone, but in the case of H-ZSM-5, there is a continuous production of aromatics, which will allow cycle I to run. If cycle II could run alone, it would be possible to obtain a product mixture consisting solely of alkenes.

PolyMB's in the zeolite pores are able to split of C_2-C_4 alkenes according to the reaction mechanisms for the paring and the exocyclic methylation reactions shown above. As mentioned, it has been shown that hexaMB and pentaMB are inactive for methanol conversion over H-ZSM-5, but tetraMB is active and one could imagine that it is possible to split off larger fragments than ethene from this compound. This issue was recently addressed by Bjørgen *et al.* [61]. In a co-conversion experiment of p-xylene and ^{13}C methanol performed with a high feed rate to suppress cycle II, ethene and propene were detected in almost equal amounts with only traces of the higher alkenes. This implies that not only ethene, but also

propene is produced from cycle I, which the authors also mention in the original presentation of the dual cycle mechanism [28]. In a recent publication by McCann *et al.* [62] a complete catalytic cycle for the formation of *i*-butene from methanol via methylbenzenes in H-ZSM-5 is presented. The mechanism goes via the paring reaction, and is based on ^{13}C methanol and p-xylene co-conversion, NMR spectroscopy, and DFT calculations. These results indicate that cycle I, besides ethene, is also able to produce propene and C_4 alkenes (or at least *i*-butene). Nevertheless, cycle I is the only source of ethene, due the very low reactivity of ethene towards methylation and very low formation rate from cracking of higher alkenes, it does not participate significantly in cycle II.

Despite the general acceptance of the hydrocarbon pool mechanism, the mechanism behind the formation of the very first chemical bond between two C_1 fragments has not been unraveled. In 2002 Song *et al.* [63] addressed this issue. They performed methanol conversion over H-ZSM-5 and H-SAPO-34 catalysts with reagents, catalyst, carrier gas, and setup purified to an extreme level to marginalize traces of hydrocarbons present before reaction. Thus, they studied the conversion of fractionally distilled methanol containing only 11 ppm total organic impurities, and observed that the initial yield of hydrocarbons was substantially lower when this high purity methanol was converted compared to a standard methanol reagent containing 36 ppm of ethanol. This led the authors to conclude that even trace impurities are enough to establish a hydrocarbon pool and that direct coupling of C_1 species from methanol does not exist, or if it exists it is eclipsed by even trace impurities in the reactant, catalyst, or carrier gas. The failure of direct coupling of C_1 species from methanol was later supported by DFT calculations [64] and experimentally by lack of H/D exchange from zeolite bound methoxy groups [65]. Even though the direct coupling of C_1 species seems unlikely, it has never been ruled out definitively, but as stated by Dessau in 1986 [44], the origin of the initial C-C bond formation is irrelevant to the overall mechanism of the conversion of methanol.

2.3 The nature of the MTH reaction: Conversion, selectivity and deactivation

As outlined above, the mechanism behind MTH reaction is quite complex and a whole range of different chemical reactions takes place in the catalyst bed during the conversion of methanol. An illustration of a working catalyst bed after some time on stream in a plug flow reactor is shown in Figure 18. The bed can be divided into four zones; dehydration, deactivated catalyst (inactive), methanol/DME conversion, and secondary reactions (alkene oligomerization, alkylation, cracking, cyclization, hydrogen transfer, isomerization).

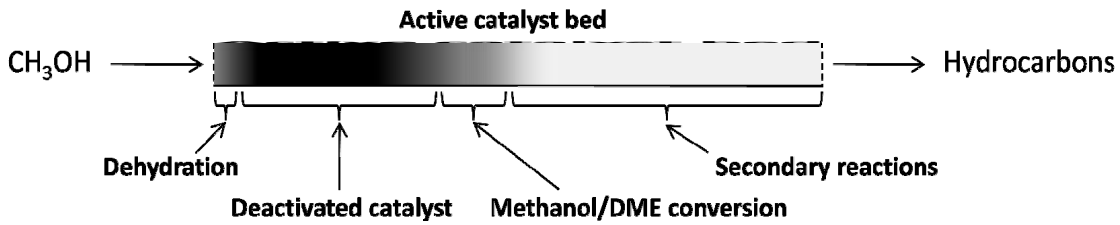

Figure 18: Illustration of a working MTH catalyst bed

The black/dark part of the catalyst bed in Figure 18 has been subjected to coking and is inactive, while the lighter parts of the bed are still active. In the dehydration zone at the very front of the bed only

minor coke deposition has taken place as methanol/DME conversion to hydrocarbons is not active at this point.

An illustration of the catalyst bed at different stages of methanol conversion is given in Figure 19. When the first methanol molecules reach the catalyst bed, there is no hydrocarbon pool in the catalyst, and the conversion to hydrocarbons is in principle zero in this induction period. After a short while active hydrocarbon pool species are formed in the zeolite (illustrated as triMB and tetraMB in Figure 19), and the hydrocarbon pool grows during the initiation period until full methanol conversion is achieved. In practice it is necessary to actively look for this induction period to actually observe it. For instance, Song *et al.* injected as little as 12.5 µl of methanol to a catalyst bed containing 300 mg H-ZSM-5 to observe the induction/initiation period [63].

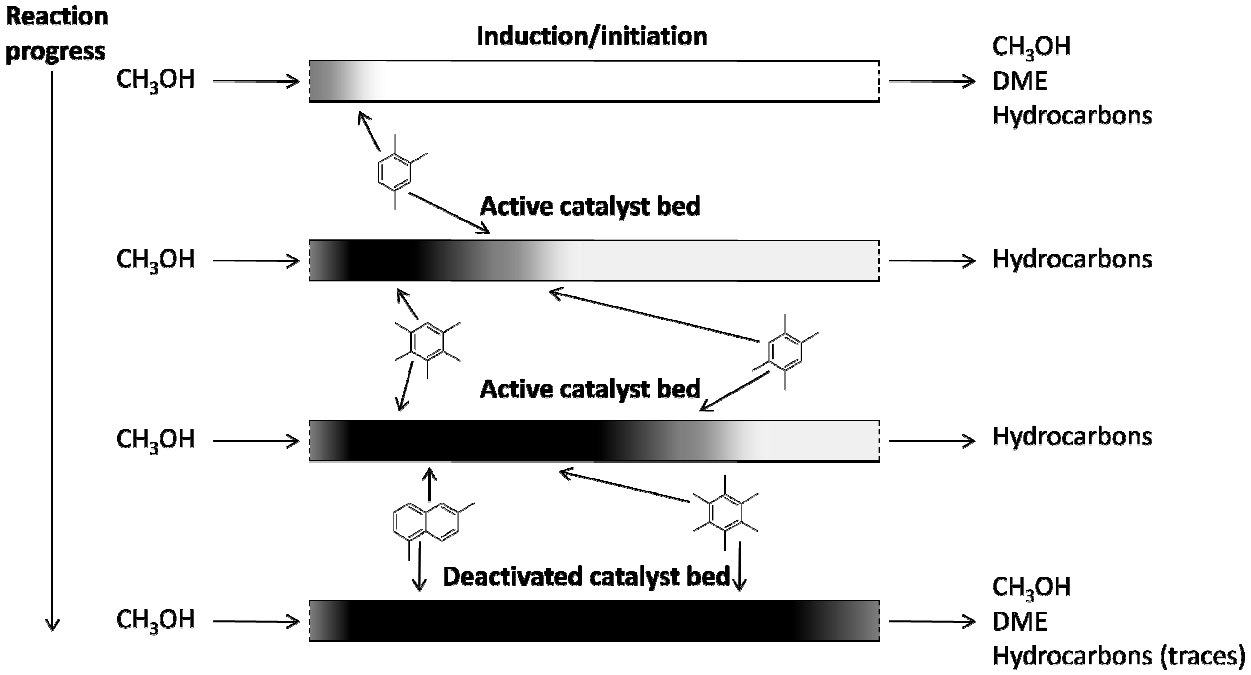

Figure 19: Illustration of the catalyst bed at different stages of the MTH reaction

As soon as an active hydrocarbon pool has been built in the zeolite pores, deactivation by deposition of coke starts to occur. When H-ZSM-5 is employed, the catalytically active species such as triMB and tetraMB might be methylated to the inactive pentaMB and hexaMB leading to formation of coke inside the zeolite pores. In H-ZSM-5 hexaMB can be formed in the channel intersections and is not able to diffuse out. Another possibility is the formation of coke on the external surface of the zeolite crystal by methylation/alkylation of aromatic compounds which are allowed to grow and block the entrance to the interior of the zeolite. In the case of conversion of methanol over H-ZSM-5 formation of coke externally on the zeolite crystals is the main path of deactivation [28]. When a part of the catalyst bed is deactivated, methanol and DME will progress further into the catalyst bed, where new hydrocarbon pool species are continuously formed. In this way, a band of active catalyst moves downstream leaving deactivated catalyst behind. This behavior was described by Haw *et al.* [66] as the “cigar burn” model, the burning tobacco being the active catalyst and the ash being the deactivated catalyst.

The product distribution from methanol conversion is plotted as a function of space time in Figure 20 [67]. When the feed rate is low (high space time), only a small fraction of the catalyst bed is necessary for dehydration and methanol conversion meaning that secondary reactions are able to convert the primary products to paraffins and aromatics over the rest of the catalyst bed. When the feed rate is increased (lower space time) the amount of catalyst for secondary reactions is smaller, leading to higher yields of olefins. At even higher feed rates the catalyst is not able to achieve full methanol conversion or even reach equilibrium between methanol and DME.

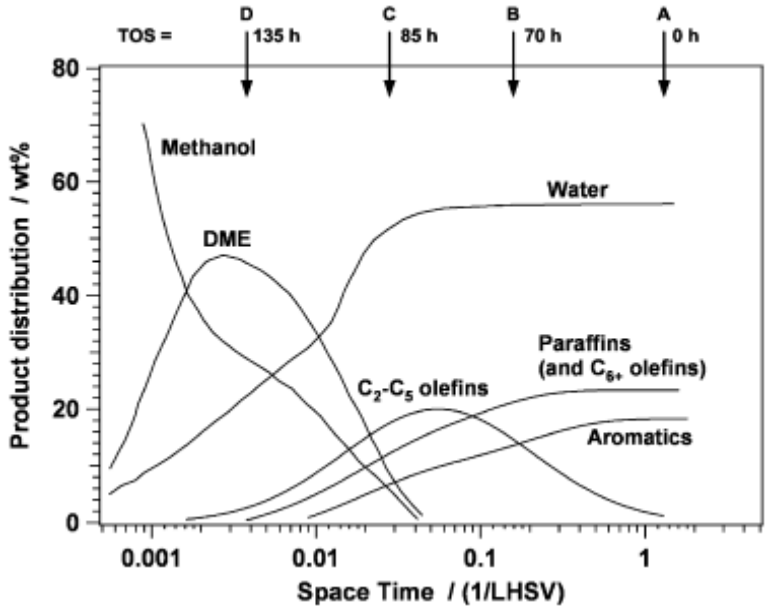

Figure 20: Product distribution as a function of space time [67]. The letters (A, B, C and D) in the top of the figure corresponds to different times on stream in Figure 21

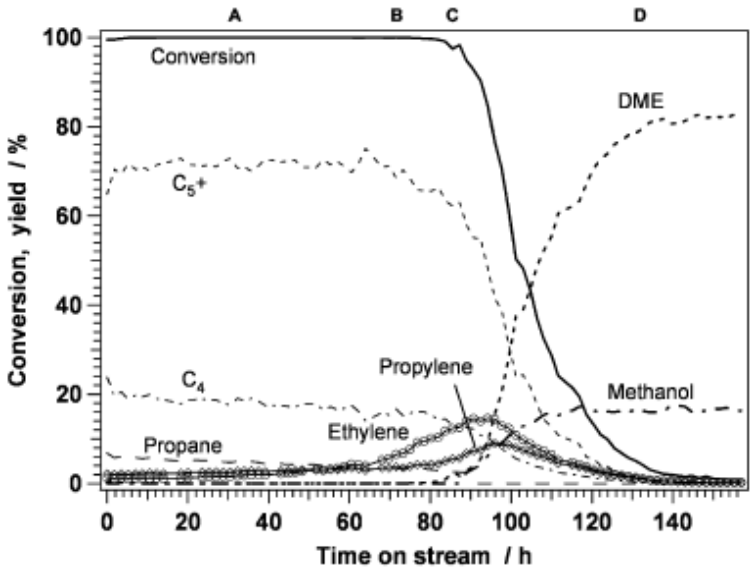

Figure 21: Methanol conversion and product yields as a function of time on stream (H-ZSM-5, 350 °C, 15 bar, WHSV= 2.8) [67]

The deactivation in the MTH reaction can be regarded as loss of active catalyst over time [67]. This implies that as the catalyst deactivates, the effective space time decreases, leading to a change in product selectivity over time. This is illustrated in Figure 21 [67], where the methanol/DME conversion and product yields are plotted against time on stream. The letters (A, B, C, and D) at different reaction times in Figure 21 corresponds to different space times in Figure 20 (A, B, C, and D). Thus the observed higher selectivity towards ethene and propene when the catalyst is close to complete deactivation (around 90 h on stream in Figure 21) is a consequence of higher effective space velocity due to loss of active catalyst.

Besides space velocity of the reactant, the performance of the MTH reaction is highly influenced by reaction conditions such as temperature and pressure. The dependence on temperature at low space velocity and pressure is illustrated in Figure 22 [13, 15]. At low temperatures the conversion of methanol/DME is incomplete, but when the temperature is raised to around 370 °C full conversion to hydrocarbons (mainly paraffins and aromatics) is achieved. A further increase in temperature leads to an increase in the activity for cracking reactions, which consume the C_{5+} aliphatics to produce small olefins and paraffins. It should be noted, that the shown case is for very low LHSV (0.6-0.7 h^{-1}) leading to a large extend of secondary reactions converting all the initially produced olefins to paraffins and aromatics (MTG mode). At higher space velocity, the yield of olefins would be much higher around 370 °C.

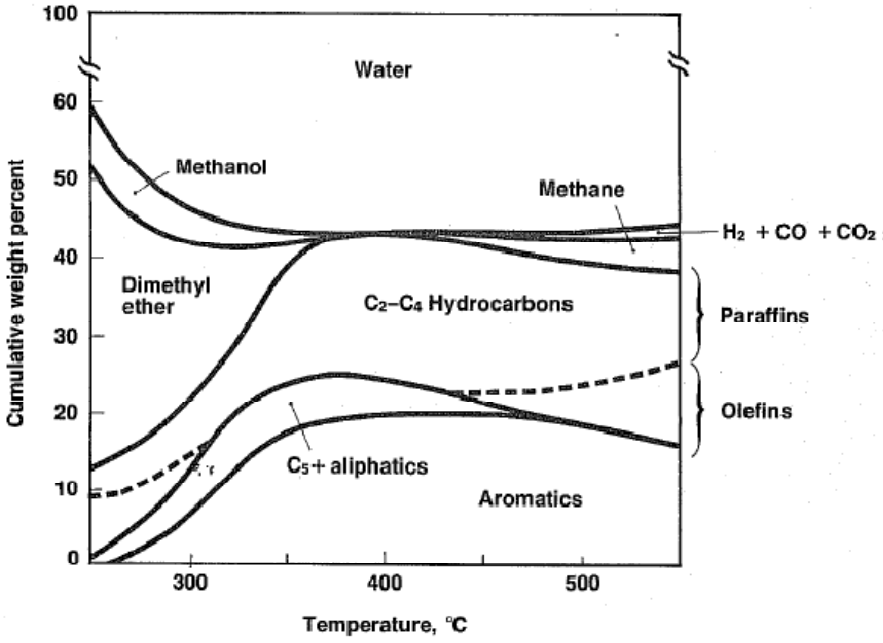

Figure 22: The influence of temperature on methanol conversion and product distribution in the reaction of methanol over H-ZSM-5 (P = 0.1 bar, LHSV = 0.6-0.7 h^{-1}) [13, 15]

The product distribution for methanol conversion over H-ZSM-5 as a function of residence time at different methanol pressures is shown in Figure 23 [15, 68]. At elevated pressure secondary reactions become more dominating which is apparent from the higher yields of paraffins and aromatics. Interaction between individual olefin molecules during the formation of aromatics and paraffins becomes much more likely at higher pressures. The co-existence of methanol/DME and aromatics is highlighted on the graphs. This is important because it opens the door for methylation of aromatics to

produce undesired polyMB which will end up in the product mixture. A methyl group on the aromatic ring is activating for further methylation so the tendency is towards total methylation, but for ZSM-5, the largest polyMB able to leave the pores is durene [15].

The MTH reaction is highly exothermic, and the removal of heat is a major challenge when designing large scale processes, so the reaction is often performed in fluid bed reactors, which makes the heat removal much more convenient. Mobil's MTG reaction was, nevertheless performed in a series of fixed bed reactors (a dehydration reactor followed by an MTG reactor) [69]. In laboratory scale the reaction is usually performed in a fixed bed reactor due to the small scale of the reactor making fluid bed systems unattractive.

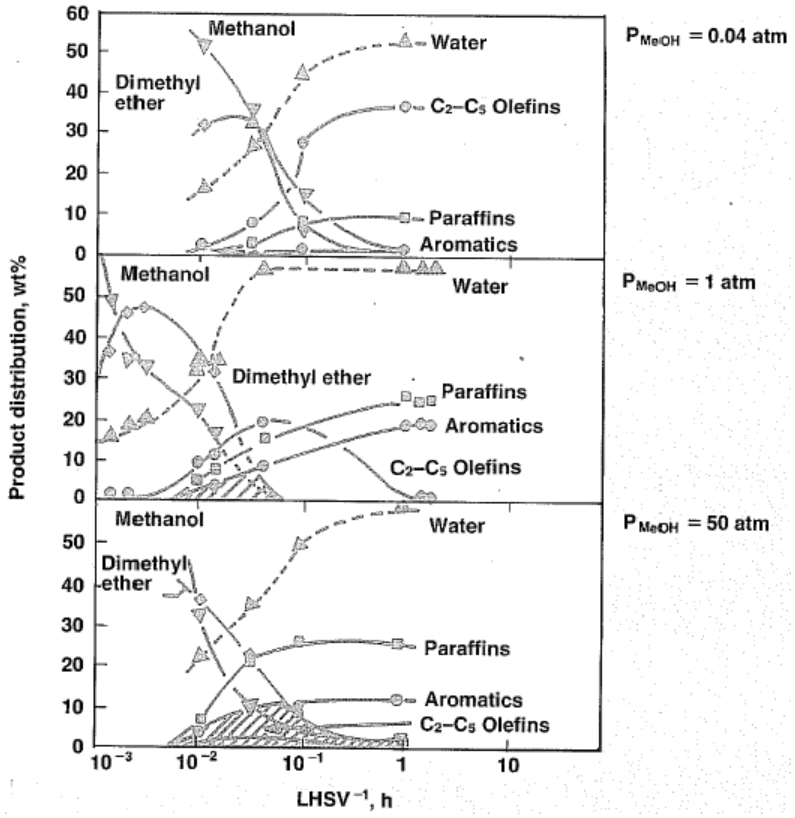

Figure 23: Product distribution as a function of residence time for conversion of methanol over H-ZSM-5 at different pressures (T = 370 °C) [15, 68]

An essential aspect in MTH catalysis is catalyst deactivation. For industrial processes frequent catalyst regeneration by burning the deposited coke with diluted oxygen is necessary, and it is one of the most desired goals within MTH research to enhance the lifetime of the catalyst between regenerations. Besides coke formation, the catalyst can also suffer from irreversible deactivation through the loss of active sites by dealumination induced by steaming of the zeolite. This typically occurs at elevated temperatures and in the presence of water. Naturally, during methanol conversion the concentration of water in the reactor is quite high, i.e. high temperatures must be avoided to suppress steaming of the catalyst [69]. When the catalyst is regenerated by coke burning, the temperature is naturally raised, which might also result in steaming if a combination of too high temperature and water presence occurs.

An important goal pursued by many research groups is to suppress the formation of aromatics and shift the selectivity towards alkenes [32, 70]. In general, zeolites with high selectivity towards alkenes typically suffer from much faster deactivation than ZSM-5, i.e. it is a major challenge to discover a catalyst/process which combines high olefin selectivity and acceptable catalyst lifetime between regenerations.

3 Co-conversion of ethane and methanol

This chapter addresses a series of experiments performed on co-conversion of ethane and methanol over gallium and molybdenum containing H-ZSM-5. The purpose of the experiments is to determine whether the presence of methanol in the reactant stream is able to enhance the conversion of ethane.

3.1 Introduction

The direct non-oxidative conversion of small alkanes such as methane [71], ethane [72, 73, 74, 75] and propane [76, 77] to aromatics and alkenes over metal containing acidic zeolites has been well investigated. Typically high temperatures are required to obtain reasonable conversions, especially the conversion of methane is extremely endothermic, and temperatures above 700 °C are necessary [78, 79]. To avoid these quite harsh conditions, methane can be activated by the presence of a co-reactant in the feed. A wide range of co-reactants have been studied in literature and the most extensively studied is ethene [80, 81, 82], but also propene and butene [83], light gasoline [84] and C_2-C_5 alkanes [85, 86] have been employed in the reaction. In these co-feeding studies, the typical reaction temperature for methane conversion is as low as 500 °C, and the catalyst is a zeolite (e.g. ZSM-5 or ZSM-11) containing a metal such as Zn, W, Ga, Mo, In, or Ag. The metal is introduced to the zeolite either by incorporation as a T-atom in the framework of the zeolite, or as metal oxide nanoparticles obtained by impregnation of the zeolite with aqueous solution of metal ions followed by calcination, or by ion exchange, replacing a proton in the active site of the zeolite with a metal ion.

In 2005 Choudhary *et al.* reported that it is possible to activate methane at low temperature by performing simultaneous conversion of methane and methanol over H-ZSM-5 containing various metals (Ga, Mo, Zn, and In) present in the zeolite as particles of metal oxide (or carbide) [87]. The authors report equimolar conversions of methane and methanol at temperatures as low as 500 °C with a molar methane/methanol ratio of 14 in the feed (at full methanol conversion). Without methanol present, methane did not convert at all under these conditions. Our research group has worked within the area of ethane dehydrogenation to ethene and aromatics over transition metal containing zeolites [88, 89]. Therefore, the work of Choudhary *et al.* prompted us to investigate if ethane could also be activated by the presence of methanol [87].

The basic concept of converting lower alkanes and methanol simultaneously is not new. The “coupled methanol hydrocarbon cracking” (CMHC) process has been developed in an attempt to ease the requirements for heat removal/supply by creating a thermoneutral process by combining exothermic methanol conversion with endothermal alkane dehydrogenation [90]. The hydrocarbon feed in this process is typically lower alkanes (C_3-C_4) [91, 92, 93, 94] but larger compounds such as decane has also been used [90]. In the case of ethane, the enthalpy of reaction for dehydrogenation to ethene and hydrogen is 136.5 kJ/mol, while the conversion of methanol to aromatics and paraffins releases -1670 kJ/kg [13] corresponding to -53.5 kJ/mol on the basis of methanol. This means that besides the possible activation of ethane due to the presence of methanol, it might also be possible to obtain a thermoneutral process, which makes reactor design much simpler.

3.2 Experimental

The performed experiments were inspired by the experiments performed on co-conversion of methane and methanol by Choudhary *et al.* [87] in terms of employed catalysts, reaction temperatures, ratio between reactants, and space velocity.

3.2.1 Catalyst preparation

The employed zeolite (H-ZSM-5, Si/Al = 15) was obtained from Zeolyst (CBV3024E) as the ammonia form. The NH_4-ZSM-5 was calcined at 550 °C to obtain the acidic form, which was impregnated with an aqueous solution of $Ga(NO_3)_3 \cdot xH_2O$, $(NH_4)_6Mo_7O_{24}$ or both, dried overnight at 110 °C and calcined at 550 °C for 4h. The catalyst powder was pressed to pellets, crushed, and sieved to obtain a particle size of 180-355 µm. Three catalysts were prepared with theoretical metal contents of 3 wt% Ga, 3 wt% Mo, and 2 wt% Ga + 2 wt% Mo, respectively (denoted Ga/H-ZSM-5, Mo/H-ZSM-5, and Ga-Mo/H-ZSM-5).

3.2.2 Catalytic tests

500 mg of catalyst was charged to a fixed bed plug flow quartz reactor with an inner diameter of 3.7 mm. The Ga/H-ZSM-5 catalyst was pretreated for 2 h at 550 °C in a flow of helium, while the molybdenum containing catalysts (Mo/H-ZSM-5 and Ga-Mo/H-ZSM-5) were pretreated at the same conditions in a flow of H_2/CH_4 (6 % H_2) to obtain the catalytically active molybdenum carbide [87]. After the pretreatment, the temperature was lowered to the reaction temperature (350 - 550 °C) in a flow of helium. The flow of ethane was 9.8 mL/min and a uniform stream of methanol (WHSV = 0.16 h^{-1}, corresponding to an ethane/methanol molar feed ratio of ~10) was created by passing a flow of helium (9.2 mL/min) through a methanol containing bubble flask at rt. followed by another flask kept at 16.0 °C. The product stream was analyzed by an online GC (HP6890A) equipped with a TCD and an FID connected in series. The conversion of ethane was calculated from the TCD signal by employing Ar as an internal standard (introduced to the product stream after the reactor), while the product composition was determined by the FID signal. Full methanol conversion was observed in all experiments. When ^{13}C methanol was used, product samples were withdrawn with a gas syringe (1 mL) and subsequently analyzed in a GC-MS (Agilent 5975 MSD/6850 GC) to identify the isotopic distributions of the products.

3.2.3 Dissolution of spent zeolites

After the catalytic tests, the spent catalysts were dissolved in hydrofluoric acid by a method introduced by Guisnet *et al.* [95] to analyze the deposited species in the zeolite. 100 mg spent catalyst was placed in a screw-cap teflon vial. 2 mL aqueous HF (20 %) was added and the zeolite was left to dissolve for 30 min. The liberated compounds were extracted by addition of 1 mL CH_2Cl_2 and the obtained organic solution was analyzed by GC-MS (Agilent 5975 MSD/6850 GC).

3.3 Catalyst characterization

The elemental compositions of the catalysts were obtained through dissolution by HF followed by ICP-OES (Inductively Coupled Plasma Optical Emission Spectroscopy) analyses performed in the analysis laboratory at Haldor Topsøe A/S. The results are shown in Table 1. When preparing Ga/H-ZSM-5 and Mo/H-ZSM-5, it was attempted to obtain a catalyst with a metal loading of 3 wt%. According to the results from ICP-OES, this has not been achieved in the case of Ga/H-ZSM-5. Also in Ga-Mo/H-ZSM-5, which was intended to contain 2 wt% of the respective metals, the gallium loading is lower than

expected. Naturally, there could be several reasons for this discrepancy, but possibly something unexpected has occurred in the impregnation process. The gallium compound used for the impregnation, $Ga(NO_3)_3 \cdot xH_2O$, contains an unknown amount of water, and it was used without any attempt of drying or determining the amount of water. Even though a fresh bottle was used to prepare the catalysts, the $Ga(NO_3)_3 \cdot xH_2O$ might contain significant amounts of water, which could explain the low amount of gallium observed in the catalysts by ICP-OES. For molybdenum the measured values correspond nicely to the expected.

	Ga (wt%)	Mo (wt%)	Al (wt%)	Si (wt%)	Si/Al
H-ZSM-5	-	-	2.37	36.7	14.9
Ga/H-ZSM-5	1.79	-	2.34	34.1	14.0
Mo/H-ZSM-5	-	3.18	2.34	33.3	13.7
Ga-Mo/H-ZSM-5	1.27	2.17	2.31	33.5	13.9

Table 1: Elemental composition of the different catalysts obtained from ICP-OES analysis. The analyses were performed in the analysis laboratory at Haldor Topsøe A/S

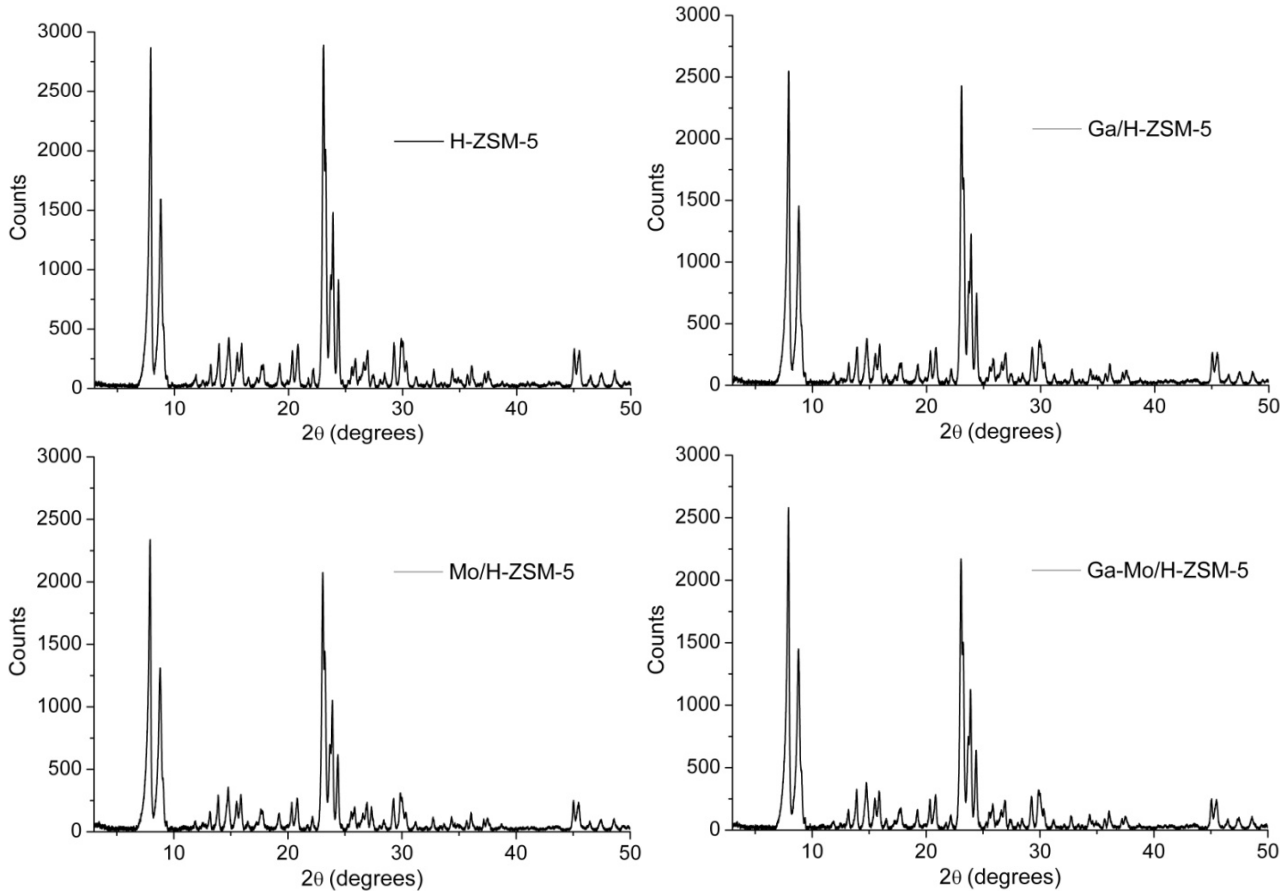

Figure 24: XRD diffractograms of H-ZSM-5, Ga/H-ZSM-5, Mo/H-ZSM-5, and Ga-Mo/H-ZSM-5 (recorded on a Huber G670 Guinier)

From the XRD diffractograms displayed in Figure 24, it is evident that the zeolite structure is not affected by the presence of gallium or molybdenum; in all cases the diffractogram is almost identical to the pure zeolite. Furthermore, no indication of the formation of a metaloxide phase is visible, which is probably due to the low metal loading.

Table 2 shows the surface areas and micropore volumes of the different catalysts. The impregnation of the zeolite causes the surface area and micropore volume to decrease slightly, but it does not appear detrimental to the accessibility to the interior of the zeolite.

	BET surface area (m^2/g)	Micropore volume (cm^3/g)
H-ZSM-5	381	0.115
Ga/H-ZSM-5	348	0.107
Mo/H-ZSM-5	350	0.101
Ga-Mo/H-ZSM-5	342	0.102

Table 2: BET surface areas and micropore volumes of the employed catalysts obtained from physisorption of nitrogen performed on a Micromeritics ASAP 2020

Temperature programmed desorption (TPD) of ammonia for the various catalyst is shown in Figure 25. The high temperature peak (around 350 °C) is the peak of interest since it arises from the strong Brønsted acidic sites in the zeolite [96]. The presence of metal oxides in the zeolite has a clear suppressing effect on this peak, indicating that the metal species are somehow interacting with the acidic site.

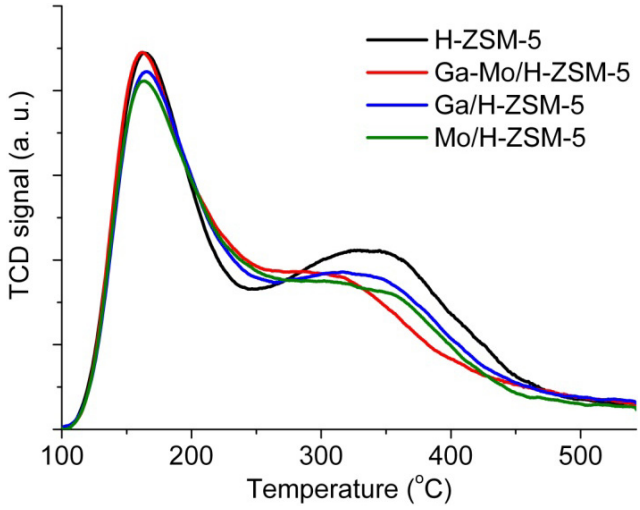

Figure 25: Temperature programmed desorption (TPD) of ammonia for H-ZSM-5, Ga-Mo/H-ZSM-5, Ga/H-ZSM-5, and Mo/H-ZSM-5 (Recorded on a Micromeritics Autochem 2920, heating ramp: 15 °C/min)

3.4 Results and discussion

The conversion of ethane with and without methanol present in the feed for the three different catalysts at 500 °C is shown in Figure 26. The WHSV of ethane is the same in all experiments, meaning that when methanol is present as a co-reactant, the catalyst is subjected to a larger amount of carbon. When methanol is not present in the feed, helium is led to the reactor along with ethane to achieve similar residence time in the different experiments. The Ga/H-ZSM-5 shows an ethane conversion around 4 %, when ethane is reacted alone, but when methanol is present in the reactant stream, the conversion drops to around 2 %. The same tendency is observed for the two other catalysts, especially for Mo/H-ZSM-5 the conversion of ethane is much lower when methanol is present, i.e. the presence of

methanol seems to suppress the conversion of ethane significantly. When ethane is reacted over H-ZSM-5 without extra framework metal sites (results not shown), no ethane conversion is observed.

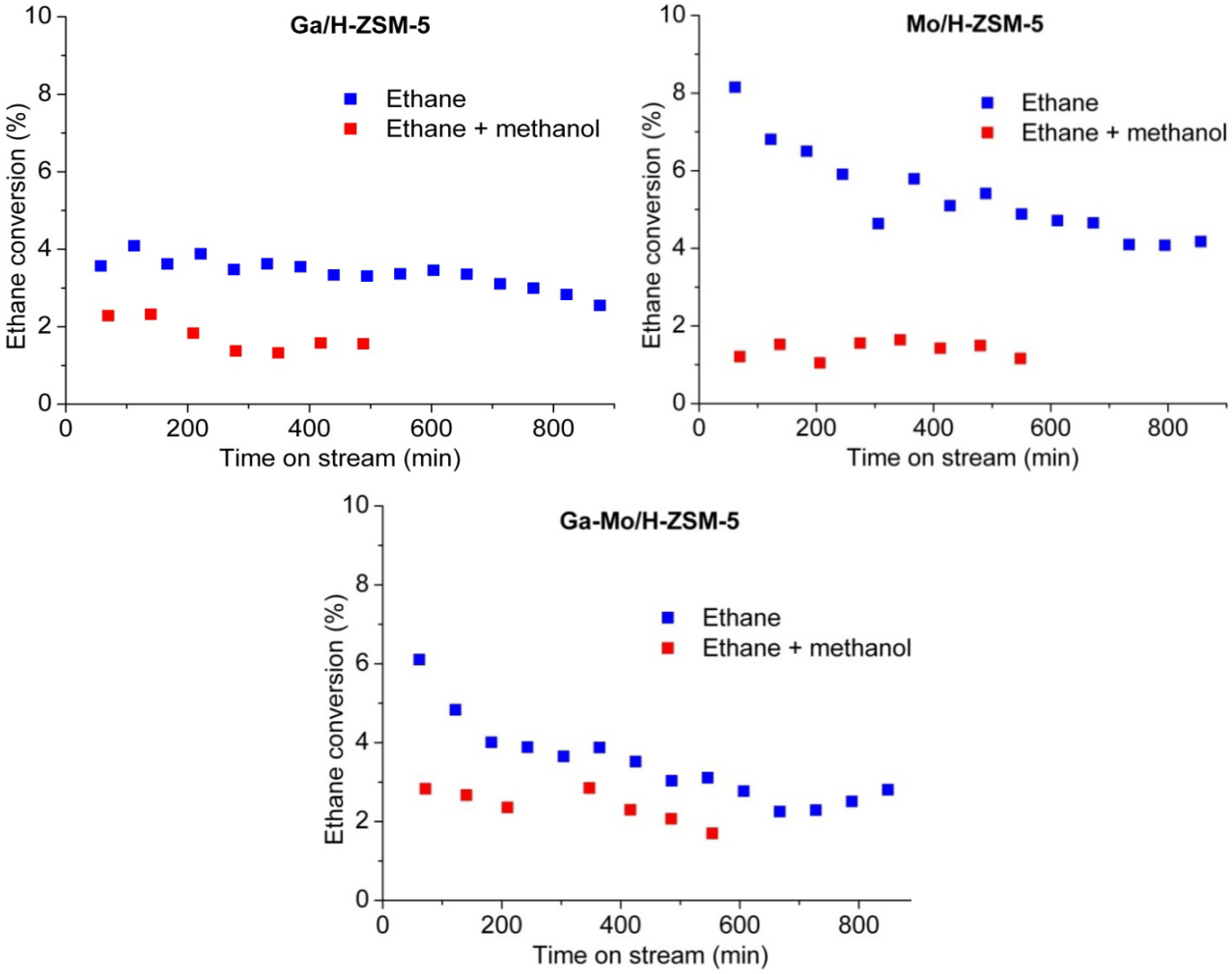

Figure 26: Conversion of ethane with and without methanol as co-reactant over Ga/H-ZSM-5, Mo/H-ZSM-5, and Ga-Mo/H-ZSM-5 at 500 °C

The product selectivities for conversion of ethane and methanol, separately and simultaneously over Ga/H-ZSM-5 at 500 °C are shown in Figure 27. The selectivities are quite constant with time on stream, so the shown selectivities after 200 min. on stream are taken as representative for the entire experiment. Compared to normal MTH conditions this reaction is performed at very high temperature and low space velocity, leading to a large extend of secondary reactions, pushing the selectivity towards small gasses and aromatics, which are the main products observed. Propane and propene are the largest aliphatic compounds observed in significant amount, the larger aliphatics are simply cracked or oligomerized/cyclizied due to the high reaction temperature, although traces of C_4 compounds were observed. It should also be noted that when methanol is converted alone a small amount of ethane is produced (~2 % selectivity), but due to the very low feed rate of methanol, this contribution to the total amount of ethane in the outlet is not nearly enough to account for the suppressed ethane conversion in the presence of methanol.

When converted alone, ethane shows a high selectivity towards ethene, while the presence of methanol markedly suppresses the ethene selectivity. Also when methanol is present in the feed, large amounts of methane are produced, which is probably produced directly from methanol circumventing the hydrocarbon pool. Within the group of aromatics, there is a clear tendency that the presence of methanol opens the route for methylation reactions leading to higher selectivities towards larger aromatics. The selectivities for Mo/H-ZSM-5 and Ga-Mo/H-ZSM-5 are very similar and are not shown here.

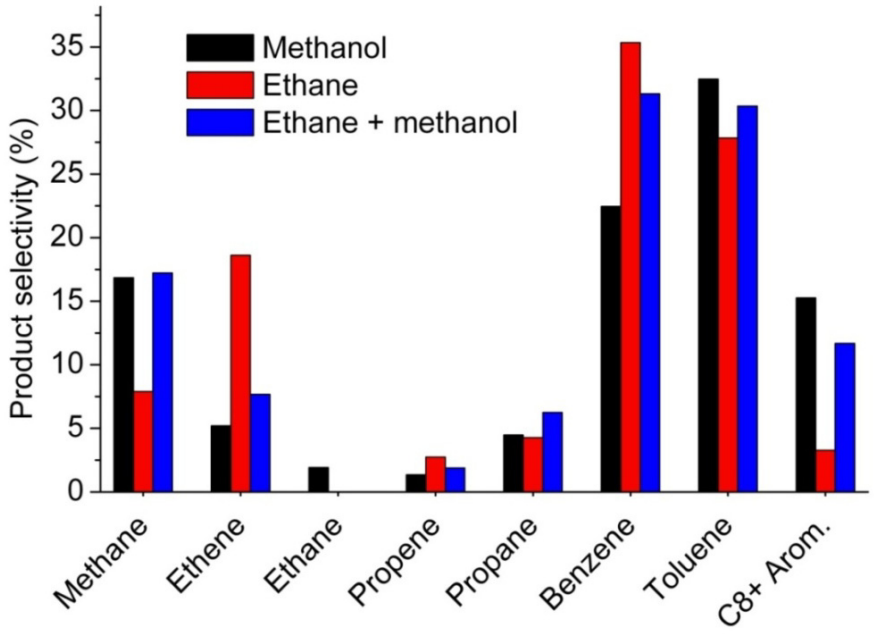

Figure 27: Product selectivities from conversion of methanol and ethane either separately or simultaneously over Ga/H-ZSM-5 after approx. 200 min on stream at 500 °C

As mentioned, the space velocity of methanol is very low in these experiments. When considering the "cigar burn" model illustrated in Figure 19, page 22, the low space velocity and high temperature means that the zone of active catalyst for methanol conversion moving down the bed is very small, while ethane is present throughout the entire catalyst bed. This is supported by the pictures of the spent catalyst beds from ethane conversion and co-conversion of ethane and methanol shown in Figure 28. When methanol is present as a reactant, the very first part of the catalyst bed is completely black due to formation of coke, illustrating that methanol is only converted at the very top of the catalyst bed. In the rest of the bed, ethane is present along with products formed from methanol (small olefins, paraffins, and aromatics). Seen from this perspective, if the presence of methanol should activate ethane, the activation should arise from the hydrocarbon species formed from methanol and not methanol itself, since it is converted almost immediately under the employed conditions.

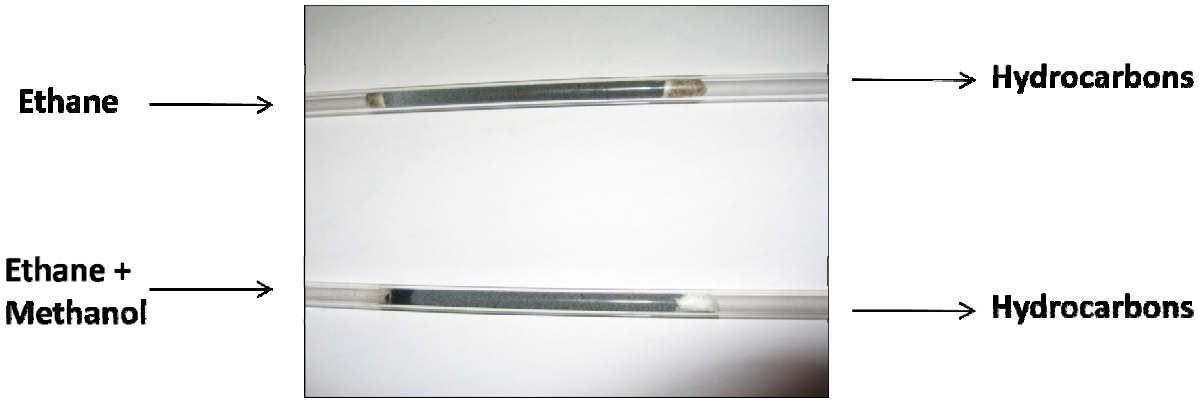

Figure 28: Pictures of catalyst beds from conversion of ethane and co-conversion of ethane and methanol over Ga/H-ZSM-5 at 500 °C after approx. 20 h on stream

Ethane needs a metal site to be converted and the hydrocarbons formed from methanol will also bind to these sites meaning that simple competition for the active sites might be the explanation for the suppressed ethane conversion. To confirm this, it would have been interesting to compare the formation of hydrogen to the conversion of ethane with and without methanol present. One could imagine, that dehydrogenation of hydrocarbons formed from methanol would contribute significantly to the production of hydrogen, confirming that competition for the active sites is taking place. Unfortunately, the TCD is not sufficiently sensitive towards hydrogen to supply such information. Dehydrogenation of alkanes formed from the reaction would lead to alkenes which will form aromatics and alkanes. These alkanes could be dehydrogenated again, resulting in very high selectivity towards aromatics (as observed).

From the product selectivities, it is possible to calculate the summarized atomic ratio between hydrogen and carbon in the hydrocarbon products (H/C). The results of such calculations are shown in Table 3. If no dehydrogenation takes place in a methanol conversion experiment, the value of H/C in the products is exactly 2, corresponding to the overall product composition $(CH_2)_n$. When methanol and ethane are converted simultaneously over a dehydrogenating catalyst, ethane is dehydrogenated to ethene, which also has an H/C ratio of 2, and if we imagine that no further dehydrogenation takes place, the value of the overall H/C ratio would still be 2. But as seen from Table 3, when Ga/H-ZSM-5 is employed as the catalyst the H/C ratio is well below 2 indicating that dehydrogenation of alkanes produced in the reaction is indeed taking place, leaving the hydrocarbon product mixture poor in hydrogen. This confirms that competition for the active sites takes place, since ethane is not the only molecule being dehydrogenated.

Reactant	Catalyst	Temp.	Calculated H/C
Methanol	Ga/H-ZSM-5	500 °C	1,61
Ethane	Ga/H-ZSM-5	500 °C	1,50
Ethane + methanol	Ga/H-ZSM-5	500 °C	1,61
Methanol (Ref.)	H-ZSM-5	500 °C	1,96

Table 3: Calculated atomic ratios of hydrogen and carbon (H/C) in the hydrocarbon product mixture from conversion of different reactants over Ga/H-ZSM-5 at 500 °C. The reference experiment (performed without dehydrogenating sites present in the catalyst) is the result of conversion of methanol over H-ZSM-5 at 500 °C

A calculation was also done on a reference experiment were the employed catalyst does not contain dehydrogenating sites. This gives an H/C ratio very close to 2 (1.96), confirming that the calculation of the H/C ratio is sufficiently precise.

Besides the competition for active sites, one could also speculate that the suppression of ethane conversion is due to methanol-induced deactivation of the catalyst, but since the initial ethane conversion is lower when methanol is present, this does not seem to be a plausible explanation. Also the coked zone shown in Figure 28 is too small to significantly affect the conversion.

In order to gain a more detailed insight into the reaction pathway, co-conversion of ethane and ^{13}C labeled methanol was performed. This allows tracing if the carbon atoms in the products are derived from ethane or methanol. Product samples were withdrawn with a gas syringe and injected to a GC-MS to obtain the isotopic distribution of the various products. In general only the aromatic products were detectable, the GC-MS was not able to separate the small gasses sufficiently for reliable results to be obtained.

From the obtained mass spectra, the distribution of molecules containing different numbers of incorporated ^{13}C atoms in a specific product specie can be calculated by using reference spectra obtained from conversion of unlabeled and ^{13}C labeled methanol, respectively. Naturally occurring ^{13}C in ethane (ca. 1 %) and ^{12}C in ^{13}C methanol (ca. 1 %) are part of the references, meaning that when the ^{13}C percent is calculated, it is in principle not the ^{13}C percent, but the percent of atoms originating from ^{13}C labeled methanol.

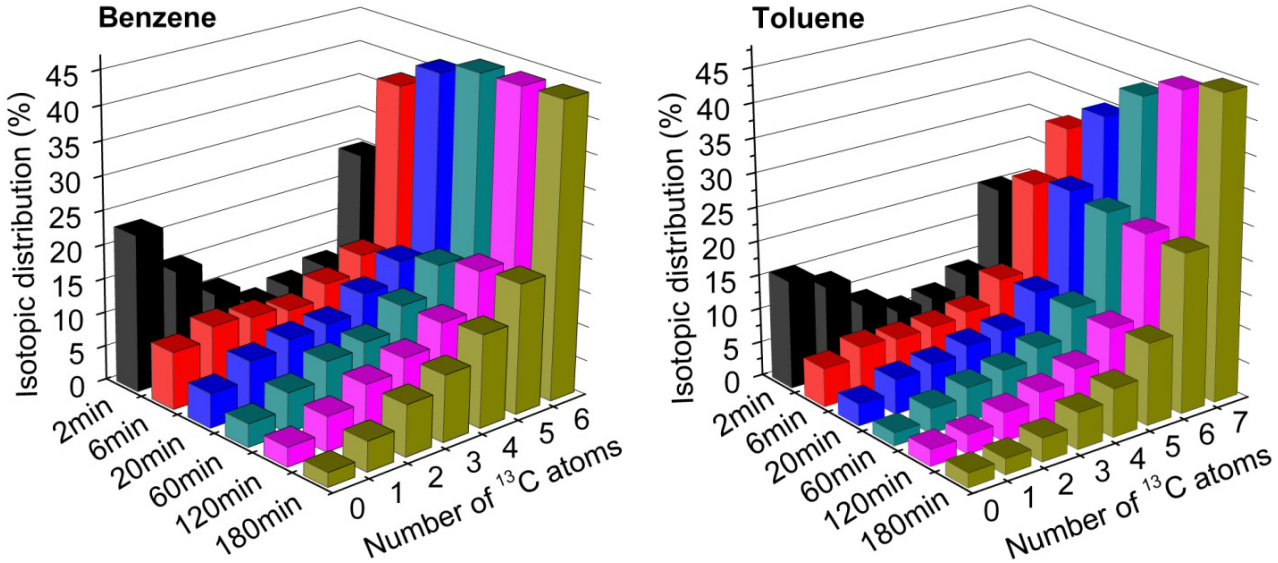

Figure 29: The distribution of the number of ^{13}C atoms in benzene (left) and toluene (right) after different reaction times in a co-conversion experiment of ethane and ^{13}C methanol over Ga/H-ZSM-5 at 500 °C

In a co-conversion experiment with ethane and ^{13}C methanol over Ga/H-ZSM-5 at 500 °C samples for GC-MS analyses were withdrawn at different reactions times. The calculated isotopic distributions for benzene and toluene are shown as a function of time on stream in Figure 29. In the first minutes of the reaction a high incorporation of ^{12}C originating from ethane is observed in both benzene and toluene.

The high ^{12}C content in the products rapidly levels off, and a more gradually declining isotopic distribution is observed after 20 min. on stream. The fact that compounds consisting of only ^{13}C and only ^{12}C are significantly overrepresented in the very beginning indicates that ethane and methanol are converted through different mechanisms or at different places in the catalyst bed in this initial period.

The fact that significant amounts of benzene contains exactly one ^{12}C atom originating from ethane, illustrates the complexity of the reaction and the large extend of secondary reactions. To form benzene with only one ^{12}C atom, a series of different reactions must take place.

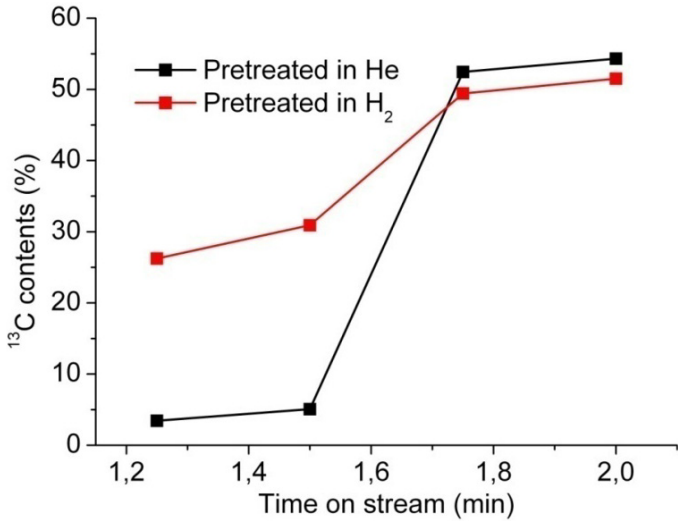

Figure 30: Initial ^{13}C contents in benzene formed from co-conversion of ethane and ^{13}C methanol over Ga/H-ZSM-5 at 500 °C. Prior to the reaction, the catalyst has been pretreated in helium or H_2 at 550 °C for 2 h.

There could be several reasons for the overrepresentation of ^{12}C in the initial period. One could imagine that methanol is not fully converted in this induction period, which would lead to lower ^{13}C content in the products, but methanol or DME was never observed in the products stream. Another explanation could be that the conversion of ethane is simply higher in the very first minutes. We propose that ethane reacts stoichiometrically with the Ga_2O_3 particles in the zeolite resulting in a reduction of Ga_2O_3 and an oxidative dehydrogenation of ethane to ethene, which is able to react further. To confirm this hypothesis, an experiment where the catalyst was reduced in a flow of H_2 prior to the reaction was performed, and indeed a difference was observed in the ^{13}C contents of benzene formed in the very beginning of the reaction, as seen in Figure 30. This tendency is observed for all aromatic products in the outlet. It should be mentioned that the volume of the reactor, tubing etc. introduces a time lack of around 1.2 minutes from the experiment is started until the product mixture reaches the septum, where the samples for GCMS are withdrawn. This means that the first data point on Figure 30 corresponds to the very first products formed in the reaction (after a few seconds). The difference in ^{13}C content of benzene is only observed in the first 30 seconds, approximately. The other aromatic compounds show the same tendency, concerning lower initial incorporation of ^{12}C after pretreatment of the catalyst in hydrogen.

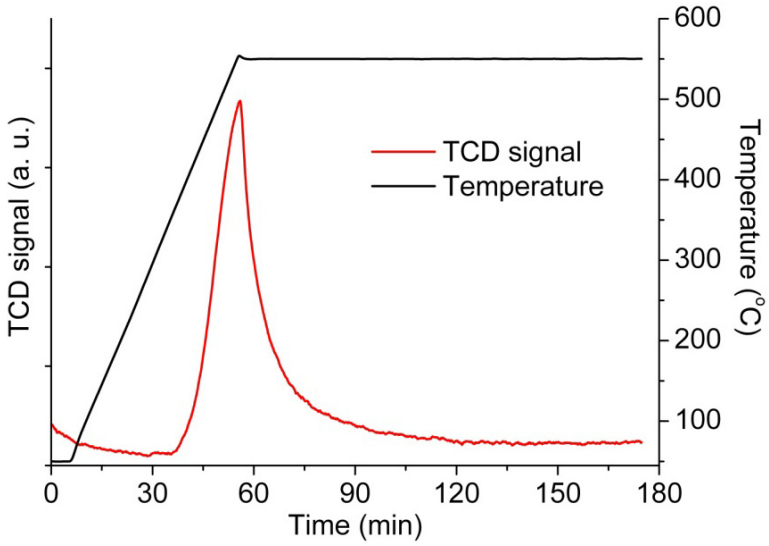

Figure 31: Temperature programmed reduction (TPR) of Ga/H-ZSM-5 in a flow of H_2. The TPR is performed at the same conditions as the catalyst pretreatment in H_2 (Figure 30)

To verify that Ga_2O_3 is actually reduced during the catalyst pretreatment in H_2, a temperature programmed reduction (TPR) was performed at the same conditions as in the catalyst pretreatment, see Figure 31. H_2 has a lower thermal conductivity than helium leading to a positive peak in the TCD signal when H_2 is consumed in the reduction. This TPR measurement only gives a qualitative indication that Ga_2O_3 is reduced during the pretreatment; we do not know which gallium species are actually formed in the zeolite during the reduction. Another important point is that it is not which gallium species are formed in the proposed stoichiometric reaction between ethane and Ga_2O_3, but the difference in ^{13}C contents for reduced and non-reduced catalyst (Figure 30) indicates that the oxidation state of gallium in the zeolite has a strong influence on the extend of the initial reaction between ethane and gallium species in the zeolite, supporting the proposed stoichiometric oxidative dehydrogenation of ethane.

A rough calculation shows that the molar amount of gallium on the employed catalyst corresponds to the amount of ethane led to the reactor during approximately 20 seconds. Even though enrichment of ^{12}C from ethane is observed in the products for several minutes of reaction time, this is definitely in a reasonable order of magnitude, because there is not full conversion of ethane. It is not at all certain that ethane and gallium oxide species react exactly in a one-to-one molar ratio, but as mentioned we do not know which gallium species are formed in the reaction. A one-to-one molar reaction between gallium oxide and ethane would lead to the formation of gallium in an oxidation state of 1.

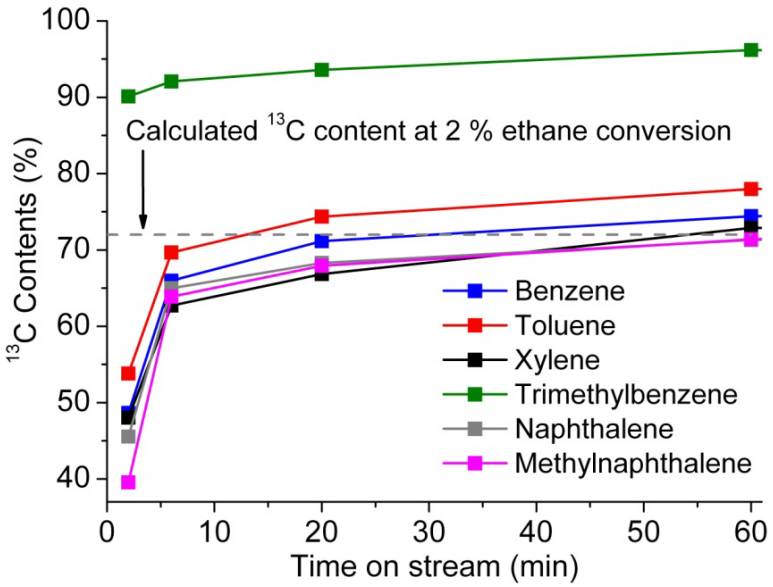

Figure 32: ^{13}C contents of different aromatic compounds in the effluent from a co-conversion experiment of ethane and ^{13}C methanol over Ga/H-ZSM-5 at 500 °C as a function of time on stream

The total ^{13}C contents of the different aromatic products formed from the co-conversion experiment of ethane and ^{13}C methanol over Ga/H-ZSM-5 at 500 °C is shown in Figure 32. The conversion of ethane in the experiment is around 2 % (see Figure 26), and from this value the expected ^{13}C contents in the products has been calculated to ~72 %, which is in very good correspondence with the isotopic data as illustrated by the dashed horizontal line in Figure 32. An initial overrepresentation of ^{12}C followed by stabilization around the calculated value is observed in all aromatic compounds in the effluent, except triMB which contains much more ^{13}C. This observation can be rationalized if we consider that methanol is most likely completely converted in the top of the reactor, while ethane is converted throughout the entire catalyst bed, as discussed above. It is hard to imagine that the lower aromatics (toluene, xylene) can be methylated to form triMB without methanol or DME present. This implies that triMB is predominantly formed in the top of the reactor where methanol is converted, and in this part of the catalyst bed, the products must be much more heavily labeled with ^{13}C, due to the high (full) conversion of methanol and low conversion of ethane. Some of the triMB formed in the top of the bed will probably decompose to small olefins and lower aromatics in the lower part of the bed, but no new triMB is formed and therefore the high level of ^{13}C incorporation is retained. TriMB might also be formed by cracking/isomerization of larger aromatic compounds (e.g. ethylbenzenes) or by transalkylation between for instance to xylene molecules which would lead to enrichment of ^{12}C in triMB, but these reactions seem to be minor (if occurring at all).

Also tetraMB (durene) is observed as a product, and it seems to contain even more ^{13}C than triMB, but the concentration is very low, and it has not been possible to quantify the ^{13}C content with sufficient accuracy. It should be mentioned that the ^{13}C contents in the individual products is completely stable from 60 min. until the end of the experiment (420 min).

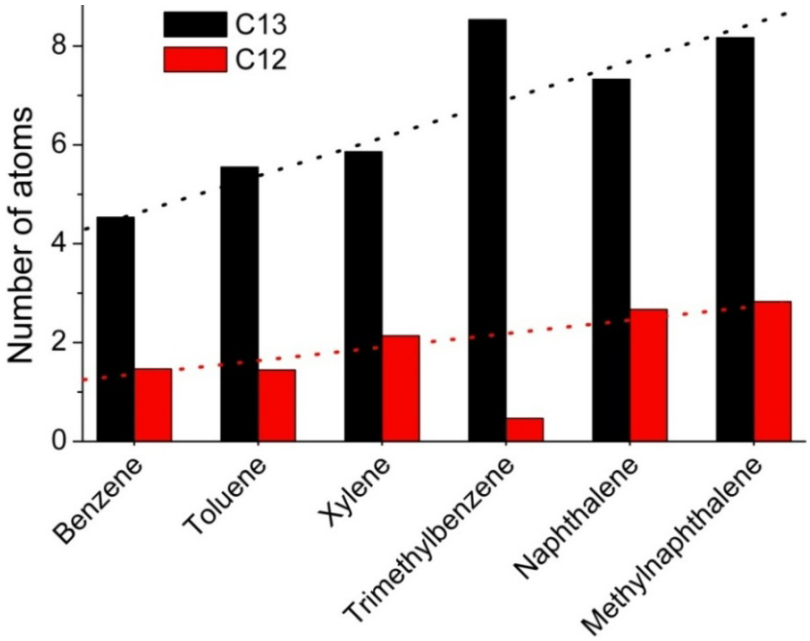

Figure 33: Average number of ^{13}C and ^{12}C atoms present in different aromatic products after 120 min. on stream in a co-conversion experiment of ethane and ^{13}C methanol over Ga/H-ZSM-5. The dotted lines represent the expected values calculated from the conversion of ethane (2 %)

Figure 33 shows the average number of ^{13}C and ^{12}C atoms in the aromatic products after 120 min. on stream. This means that the initial period with increased ^{12}C incorporation is over and steady state is attained. As discussed above triMB shows very little ^{12}C incorporation, while all the other products are quite close to the expected values. If we compare benzene and toluene, the data shows that toluene, quite precisely, contains one more ^{13}C atom than benzene. This could be interpreted as toluene being formed from methylation of benzene with ^{13}C methanol, but since methanol is only present in the very top of the reactor, this is not a plausible explanation. Another explanation could be that some of the toluene is formed from decomposition of triMB to toluene and ethene, which would lead to increased ^{13}C content in toluene. Also, the fact that xylene does not show the same overrepresentation in ^{13}C content as toluene, supports this argument, since triMB is not able to decompose to form xylene and thereby enrich the ^{13}C content in the compound.

Another reaction that might take place in the catalyst bed is transalkylation between different methylated aromatic compounds. For instance, reaction between triMB and toluene might lead to the formation of two xylene molecules. If this reaction was taking place at a significant rate, the very low ^{12}C incorporation in triMB would not be observed to the same degree. If triMB is involved in transalkylation reactions it is only to a minor extent, since the isotopic data suggests that triMB is allowed to pass through the catalyst bed without equilibration of the isotopic composition. Formation of triMB via transalkylation (for instance from two xylene molecules) is also ruled out, since this reaction would lead to a massive enrichment of the amount of ^{12}C in triMB, which is not observed.

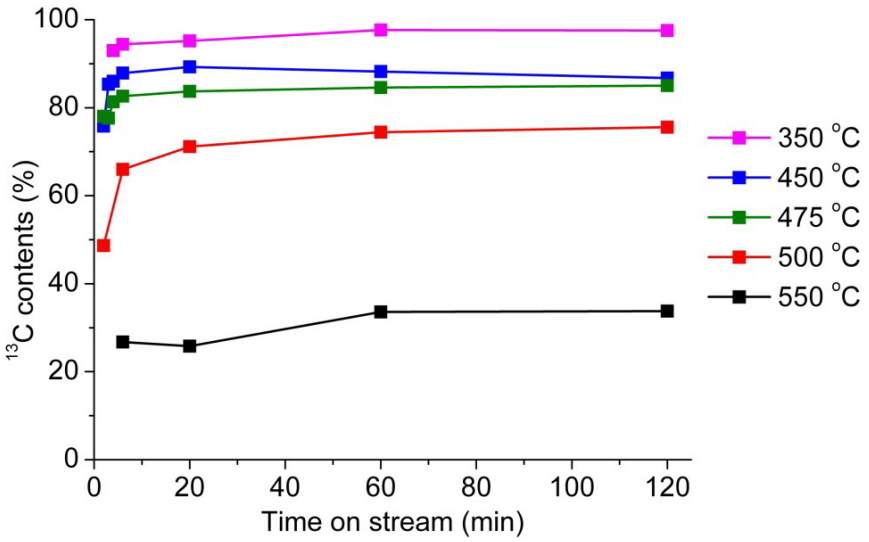

Figure 34: ^{13}C contents in benzene produced from co-conversion of ethane and ^{13}C methanol at different reaction temperatures as a function of time on stream

Co-conversion of ethane and methanol has been performed at a range of different temperatures. In general high temperatures are required for conversion of ethane (as mentioned in the introduction), but if activation of ethane could take place at lower temperature it would be very interesting. Figure 34 shows the ^{13}C contents in benzene produced from co-conversion of ^{13}C methanol and ethane over Ga/H-ZSM-5 as a function of time on stream at different reaction temperatures. In all cases full conversion of methanol is achieved, so lower ^{13}C contents in benzene reflects higher conversion of ethane. The tendency of high initial incorporation of ^{12}C is observed at all temperatures except 550 °C, but this is most likely due to lack of data for the first few minutes. At low temperatures, the conversion of ethane is very small, for instance at 350 °C the ^{13}C percentage after 60 min. on stream (98%) corresponds to an ethane conversion of only 0.1% (at full conversion of methanol). Conversions of this magnitude are not measurable in the experimental setup using the TCD detector. The ^{13}C incorporation after 60 min. at 450 and 475 °C (89 and 85 %) corresponds to ethane conversions of 0.6 and 0.9%, respectively, which is also too low to quantify with sufficient accuracy using the TCD detector. Thus, the isotopic data show that a reaction temperature of at least 500 °C is necessary to obtain reasonable conversions under the reaction conditions employed in this work.

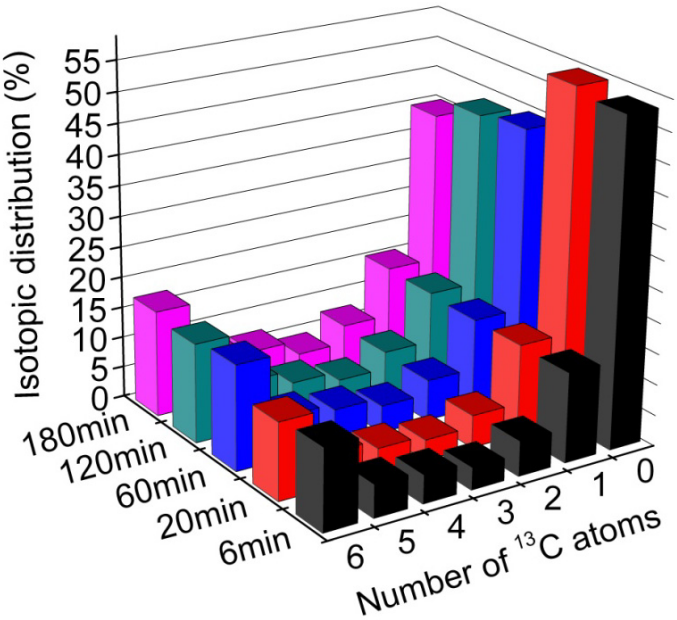

Figure 35: The distribution of the number of ^{13}C atoms in benzene after different reaction times in a co-conversion experiment of ethane and ^{13}C methanol over Ga/H-ZSM-5 performed at 550 °C

The isotopic distribution for benzene produced from co-conversion of ethane and ^{13}C methanol over Ga/H-ZSM-5 at 550 °C is shown in Figure 35. At this temperature, the incorporation of ^{12}C is much higher than at 500 °C as shown in Figure 34, and interestingly, there is a clear tendency that benzene molecules containing solely ^{13}C or ^{12}C atoms are overrepresentated, not only in the initial period, but throughout the entire catalytic experiment. This confirms the discussed hypothesis, that methanol and ethane are converted at different places in the catalyst bed, i.e. methanol is converted in the top of the bed while ethane is converted throughout the entire bed. This tendency in isotopic distribution is observed for all aromatic compounds in the product mixture.

After the catalytic tests, the spent zeolite catalysts were dissolved in aqueous hydrofluoric acid to liberate the organic compounds trapped in the zeolite pores. The acidic solution was extracted with CH_2Cl_2 followed by GC-MS analysis of the organic phase. Through this procedure, mass spectra are obtained for the species trapped inside the zeolite and the calculated ^{13}C percentages are shown in Figure 36. Generally there is slightly higher ^{12}C incorporation in the retained species than in the species in the effluent (see Figure 32), but the same tendency is observed regarding high ^{13}C contents in triMB and it is even higher in tetraMB and pentaMB indicating that these species are predominantly formed from methanol (in the top of the reactor). The naphthalenes contain slightly more ^{12}C than the simple aromatic compounds, indicating that they to some extend preferably are formed from species derived from ethane.

The fact that relatively small molecules such as benzene, toluene, and xylene are trapped in the pores of the zeolite is noteworthy, since they should be able to leave the zeolite pores with ease. An explanation could be that the pores are blocked by larger species leaving the smaller molecules trapped.

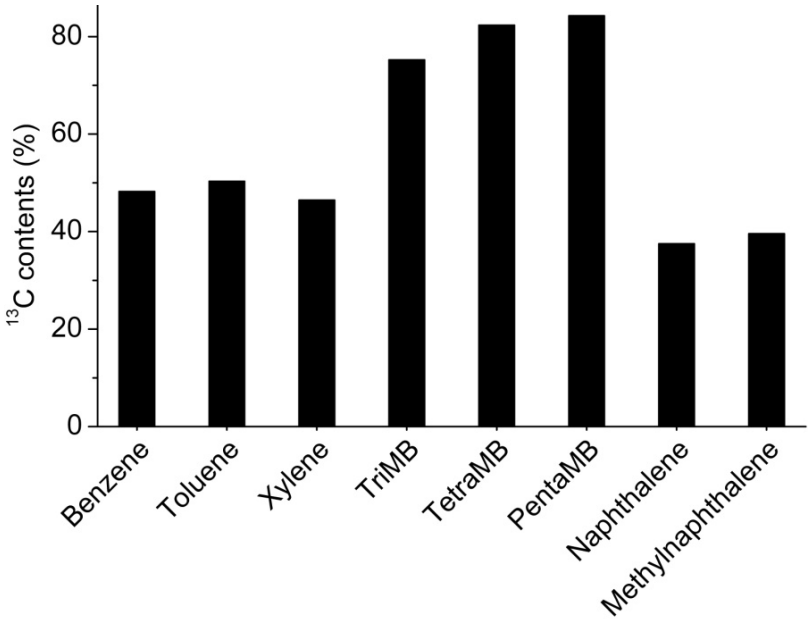

Figure 36: ^{13}C contents in carbonaceous species retained in the zeolite after co-conversion of ethane and ^{13}C methanol over Ga/H-ZSM-5 at 500 °C after 2h on stream

3.5 Conclusions

The conversion of ethane is not enhanced by the presence of methanol in the reactant stream. On the contrary, in our experiments the conversion of ethane is around twice as high without methanol present under the same reaction conditions. These results are in stark contrast to the observed activation of methane reported by Choudhary *et al.* [87] in a similar series of experiments employing methane and methanol as reactants.

Isotopic labeling studies performed with unlabeled ethane and ^{13}C labeled methanol show that carbon atoms from methanol and ethane are mixed in the products. During the first few minutes of the reaction there is a distinct overrepresentation of ^{12}C atoms originating from ethane in the products. We propose that this observation is due to a stoichiometric reaction between ethane and the metal oxide species in the zeolite. This theory is confirmed by a clear reduction in initial ^{12}C incorporation when the catalyst was pretreated in H_2 (instead of helium) in order to reduce the metal oxide species prior to the reaction.

Products containing solely ^{12}C and solely ^{13}C atoms are observed in relatively high concentrations, especially at high temperature (550 °C). This indicates that ethane and methanol are converted at different places in the catalyst bed. This can be explained by the fact that methanol is much more reactive than ethane and is converted in the very top of the catalyst bed, while ethane is converted throughout the entire bed.

Since methanol is not present in the lower part of the bed, it is naturally not able to influence the ethane conversion, but hydrocarbon species formed from methanol are present throughout the entire bed. These species could in principle act as co-catalysts to activate ethane, but as mentioned it does not seem to be the case since a negative effect is observed on the ethane conversion due to the presence of methanol in the feed. We propose that the most obvious reason for this negative effect is simple

composition for the active sites, since hydrocarbons formed from methanol will bind to the active metal sites, blocking the access for ethane.

As mentioned, our results show that the presence of methanol has a negative effect on the conversion of ethane, while Choudhary *et al.* [87] reported that methanol has a positive effect for conversion of methane. At first glance these observations seem contradictory, but if we consider dehydrogenation of methane, the direct product of this reaction is a CH_2 unit which is not able to exist on its own. Therefore, the reactivity of methane is increased if a co-reactant is able to take part in the reaction by reacting with the CH_2 unit to form a stable compound. In the case of ethane, the direct dehydrogenation product is ethene which is able to leave the active site without the need of a co-reactant. This said, a co-reactant could still have a positive effect on the conversion of ethane, but our experiments show that methanol is probably not the right choice.

4 Conversion of methanol and higher alcohols to hydrocarbons

This chapter concerns experiments performed on conversion of methanol, ethanol, 2-propanol, and 1-butanol to hydrocarbons over different zeolite catalysts. Aspects such as catalyst lifetime, coke formation, and product selectivity are discussed.

4.1 Introduction

As discussed in Chapter 2, the conversion of methanol to hydrocarbons is a well known and established reaction, but other alcohols are not nearly as well investigated in the reaction, although already in Mobil's original paper on MTG [13] a whole range of different reactants besides methanol were tested, including ethanol and higher alcohols, esters, acids, and oxy-compounds. All of these reactants were reported to produce hydrocarbons in the reaction, but methanol was the natural reactant of choice because it is produced in huge scale world-wide and is available from abundant sources such as natural gas and coal [3].

The search for alternatives to the fossil sources has sparked interest in the conversion of (bio)ethanol to hydrocarbons in a process similar to MTH and a reasonable amount of work has been done on the so-called "ethanol-to-gasoline" (ETG) process [97, 98]. In 1979, Derouane *et al.* compared methanol and ethanol as reactants over H-ZSM-5 and observed very similar product distributions [99]. This was confirmed in a recent study from our research group, where the differences in the hydrocarbon pool species retained in the zeolite is also discussed [100]. Not surprisingly, it is shown that for ethanol, ethylbenzenes are present in the zeolite pores after the reaction instead of methylbenzenes as in the case of methanol.

Besides direct dehydration to the corresponding alkenes, only scarce reports on zeolite-catalyzed conversion of higher alcohols (C_{3+}) to hydrocarbons exist in literature. As mentioned above, propanol and butanol were among the reactants originally tested by Mobil. Recently, Gayubo *et al.* also screened a large variety of different reactants, including propanol and butanol, under MTH conditions, concluding that similar product mixtures were obtained from the different alcohols [101]. Mixtures of isotopically labeled methanol and unlabeled propanol were converted over zeolite H-ZSM-5 by Tau *et al*. to uncover mechanistic details of the MTH reaction [102, 103].

Tabak *et al.* studied the conversion of propene and butene to larger hydrocarbons over H-ZSM-5 [104]. The small alkenes oligomerize to larger compounds, and by variation of the temperature and pressure it is possible to affect the reactivity of oligomerization versus cracking and thereby control the molecular weight of the products.

Recently, the conversion of C_1-C_4 alcohols over H-ZSM-5 was performed in a batch reactor by Gujar *et al*. [105]. The authors conclude that the higher alcohols produce a larger amount of liquid hydrocarbons than methanol when allowed to react for a fixed time.

Although several research groups have studied the conversion of higher alcohols over H-ZSM-5, none of the studies address the dependence of the catalyst lifetime and deactivation on the alcohol feed.

4.2 Conversion of methanol, ethanol and 2-propanol over H-ZSM-5

4.2.1 Experimental

In all experiments in this section the employed catalyst was zeolite ZSM-5 (Si/Al = 40) obtained from Zeolyst International in its ammonia form. Prior to use, the zeolite was calcined at 550 °C for 4 h to obtain the acidic form.

4.2.1.1 Non-pressurized experiments

The catalytic reactions were performed in a fixed bed reactor charged with 300 mg catalyst, which was pretreated in helium at the reaction temperature for 30 min. prior to the reaction. The reactant liquid was pumped with an HPLC pump and evaporated before reaching the reactor. The reaction temperature was 400 °C (measured inside the reactor, just below the catalyst bed). Helium was used as a carrier gas, with a flow of 20 mL/min, and the products from the reaction were analyzed by an on-line GC (HP 6890) equipped with an FID.

4.2.1.2 Pressurized experiments

The reactant liquid was pumped directly to the reactor, where it was evaporated above the catalyst bed. The reaction temperature was typically 400 °C (measured in the oven, just outside the catalyst bed) and the pressure was 5 - 20 bar. Helium was used as a carrier gas with a flow of 20 mL/min.

The pressure was induced by a back-pressure valve situated between the reactor and the online GC. Liquid products were condensed directly after the reactor, while the system was still pressurized and the product mixture was continuously led through the condenser, meaning that a mixture of carrier gas (helium) and gaseous products left the condenser to be depressurized to 1 bar and analyzed by the online GC. Naturally, depending on the vapor pressure of the individual compounds, some of the larger products will to some extent leave the condenser with the off-gas. The condensed liquid products were withdrawn periodically for offline GC or GC-MS analysis.

This experimental system means that the results from the online GC will only show gaseous products and traces of larger compounds which escape the condenser, making it almost impossible to obtain a reliable product distribution and close the mass balance. In order to circumvent this issue, the focus was placed upon the production of liquid product which was tapped in portions from the condenser during the experiment and analyzed off-line by GC or GC-MS.

4.2.1.3 Temperature programmed oxidation (TPO)

The TPO analyses were typically performed with 100 mg of spent catalyst, which was heated in a flow of 5 % O_2 in helium (20 mL/min) with a heating ramp of 2.75 °C/min to an oven temperature of 700 °C. The final temperature was maintained for 2 h to ensure complete combustion of the carbonaceous species. The concentrations of CO and CO_2 in the outlet were monitored continuously by a BINOS detector.

4.2.2 Results and discussion

The first part of the results presented here concerns the conversion of methanol, ethanol and 2-propanol over H-ZSM-5 performed at 1 bar. It should be mentioned, that when the conversions are calculated, the direct dehydration products (DME, ethene, diethylether, propene, and dipropylether,

respectively) are considered reactants. These dehydration products are still produced over a completely deactivated catalyst.

4.2.2.1 Conversion of methanol over H-ZSM-5

Figure 37 shows the methanol conversion and the formation of aromatics and aliphatics vs. time on stream. The catalyst displays full methanol conversion until around 40 h on stream, when the conversion suddenly drops and the catalyst is completely deactivated shortly thereafter. This behavior is completely normal for methanol conversion and is in good correspondence with the "cigar-burn" model described earlier (see page 22). The initial selectivity towards aromatics is around 20 % and declines slightly with time on stream allowing the selectivity towards aliphatics to rise above 80 % just before full deactivation. This behavior is due to loss of active catalyst to perform the secondary reactions such as hydrogen transfer and cyclization to convert alkenes to aromatics and alkanes. When the catalyst is deactivated an equilibrium mixture of methanol and DME is observed.

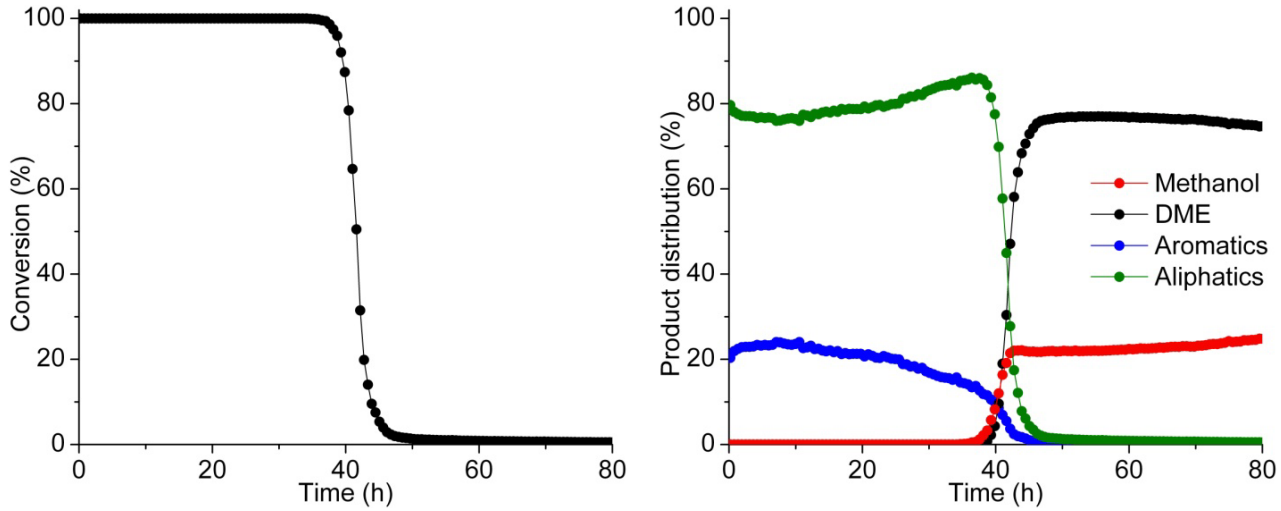

Figure 37: Conversion vs. time on stream for the reaction of methanol over H-ZSM-5 (left) and the concentrations of aromatics, aliphatics, methanol, and DME in the product stream vs. time on stream (right) (T = 400 °C, P = 1 bar, WHSV = 8.4 h^{-1})

More detailed product distributions divided into aliphatics (left) and aromatics (right) are given in Figure 38. In general a high selectivity towards C_4 and C_{5+} aliphatics is observed, but also propene and ethene are produced in significant amounts. It is also evident that especially propene, but also ethene and C_{5+} aliphatics become more dominating with time on stream, again demonstrating that the extend of secondary reactions consuming these compounds is lower as the catalyst becomes partly deactivated. The increase in selectivity towards alkenes with time on stream is accompanied by a decrease in alkane selectivity. The C_4 selectivity is rather constant throughout the entire experiment, but changes are observed within the different C_4 compounds, as alkanes become less and less dominating. The selectivity within the group of C_4 compounds will be addressed more thoroughly later.

Methane is formed throughout the entire experiment, and the selectivity is increasing with time on stream. When methane is formed it is an end product; it is not converted in the secondary reactions, so the increase in methane selectivity is not due to a decrease in the amount of secondary reactions as for the alkenes. Since methane is also formed over the completely deactivated catalyst, its formation must

be independent of the presence of a working hydrocarbon pool; it is most likely formed directly from methanol, but a detailed mechanism for its formation is not known.

Ethane is also formed throughout the entire experiment, but in very low amounts (< 0.2 %) and declining with time on stream. In order for ethane to be formed, ethene has to participate in a hydrogen transfer reaction, which is not favored under the conditions employed in this experiment.

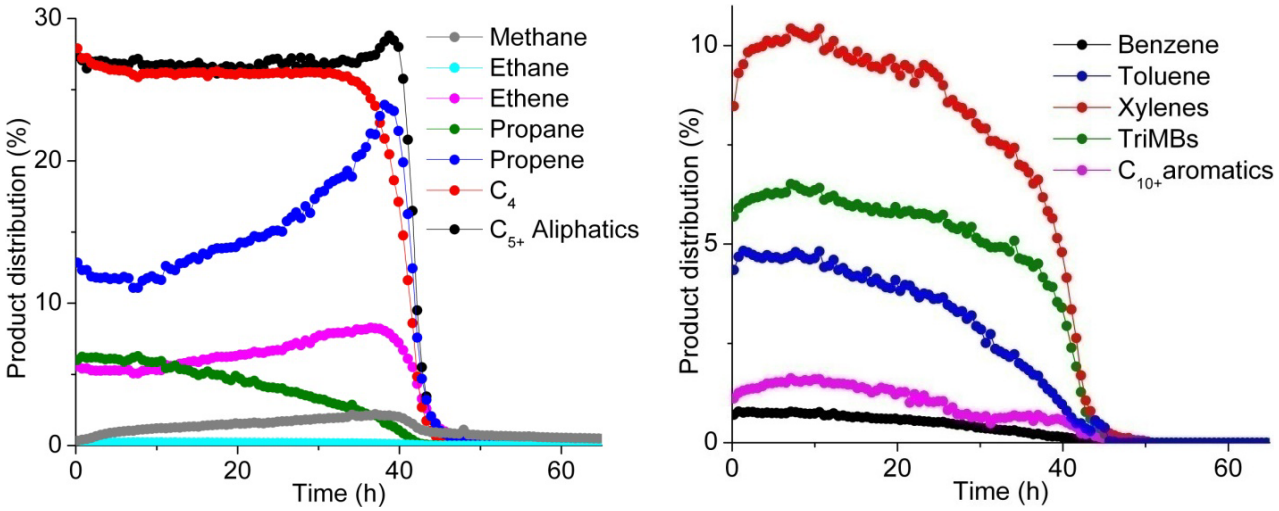

Figure 38: Detailed composition of the aliphatic (left) and aromatic (right) products for methanol conversion over H-ZSM-5 (T = 400 °C, P = 1 bar, WHSV = 8.4 h^{-1})

Among the aromatic products, xylenes are the most abundant, while trimethylbenzenes (TriMBs) and toluene are also produced in significant amounts. Larger aromatics (mainly durene, but also traces of naphthalenes) and benzene are only produced in small amounts. For all aromatic products, the selectivity declines with time on stream.

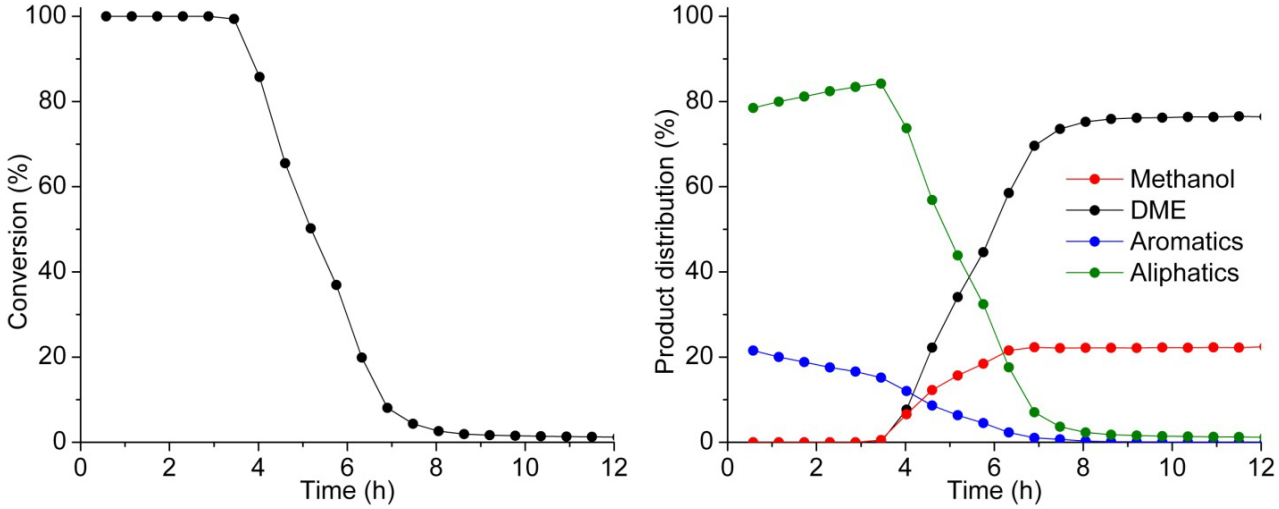

Figure 39: Conversion vs. time on stream for the reaction of methanol at high WHSV over H-ZSM-5 (left) and the concentrations of aromatics, aliphatics, methanol, and DME in the product stream vs. time on stream (right) (T = 400 °C, P = 1 bar, WHSV = 25.2 h^{-1})

A methanol conversion experiment with three times higher WHSV was performed. Conversion data and formation of aliphatics and aromatics vs. time on stream is shown in Figure 39. The most pronounced difference compared to the experiment with lower WHSV is the much shorter catalyst lifetime; the conversion starts declining already after 4 h on stream.

Interestingly, the catalyst is still able to produce around 20 % aromatics initially, even though it is much more stressed and one would expect that less catalyst is available for secondary reactions. But if we consider catalyst deactivation as loss of active catalyst, the effective space velocity increases as the catalyst deactivates. If we consider Figure 37, the selectivity towards aromatics (and the extend of secondary reactions) is quite stable for around 25 h (corresponding to around two third of the catalyst lifetime), before the effective space velocity becomes too high for catalysts to perform the same extend of secondary reactions, and the selectivity towards aromatics starts to decline. At this point the effective space velocity is comparable to the initial space velocity in the experiment with 25.2 h^{-1}, and the fact that significant amounts of aromatics are produced is therefore not surprising.

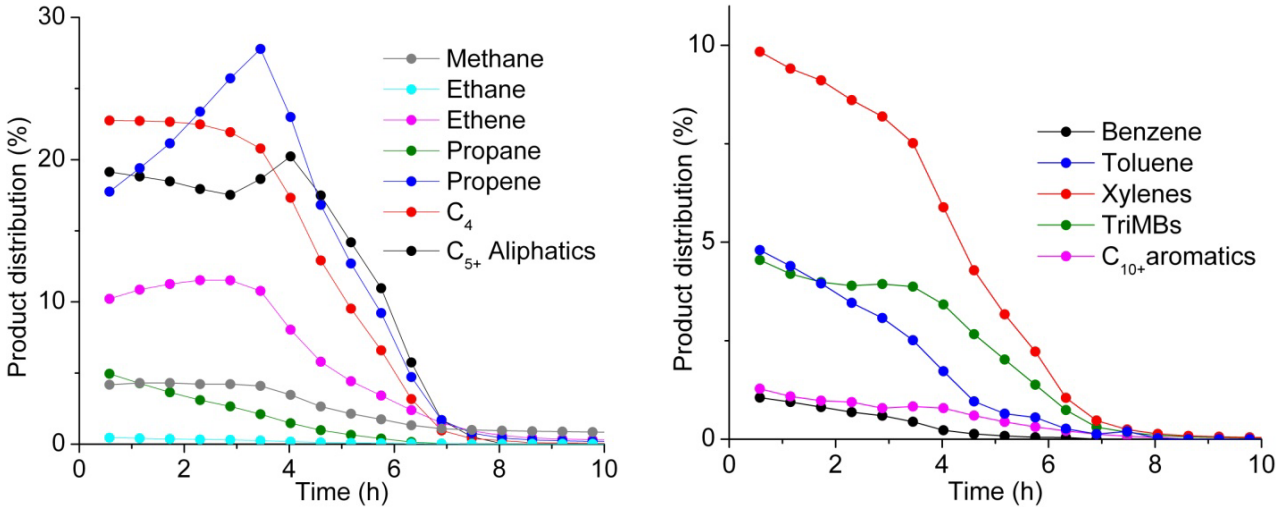

Figure 40: Detailed composition of the aliphatic (left) and aromatic (right) products for methanol conversion over H-ZSM-5 (T = 400 °C, P = 1 bar, WHSV = 25.2 h^{-1})

At high WHSV the selectivity towards small compounds such as ethene and propene is higher, and especially the propene selectivity increases from the beginning of the run due to diminishing amount of catalyst for secondary reaction. Also relatively large amounts of methane are produced. As mentioned, the mechanism behind the formation of methane is not known, but it might be connected to the formation of coke on the catalyst somehow. For the aromatics, the selectivities are very similar to the experiment at low WHSV, the main difference being that they all decline rapidly with time on stream.

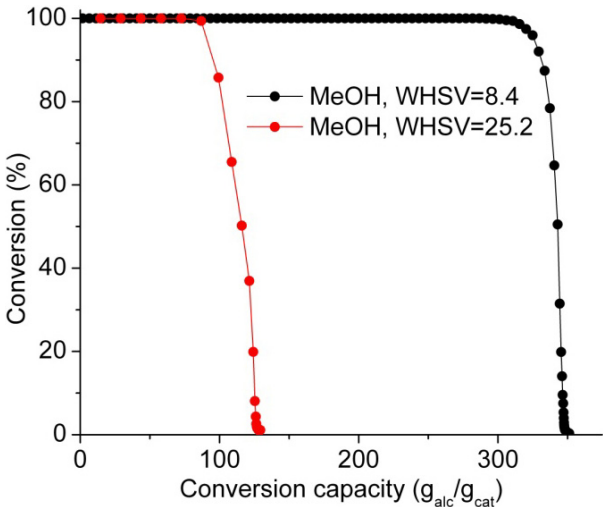

Figure 41: Conversion capacity of the catalyst (H-ZSM-5) for conversion of methanol at WHSV = 8.4 and 25.2, respectively (T = 400 °C, P = 1 bar)

As mentioned, the catalyst lifetime is much shorter when methanol is converted at high WHSV, but in order to truly compare the experiments, the conversion capacity has been calculated, and is plotted against the conversion in Figure 41. The conversion capacity is a measure of how much reactant the catalyst is able to convert before it is completely deactivated. As could be depicted from the very short lifetime at high feed rate, the catalyst is not able to convert nearly as much under these conditions. In fact, the conversion capacity is around three times higher at WHSV = 8.4, i.e. the catalyst deactivates disproportionately fast at high feed rates of methanol.

4.2.2.2 Conversion of ethanol over H-ZSM-5

The conversion of ethanol over H-ZSM-5 has been tested under similar conditions as the conversion of methanol (400 °C, 1 bar). The employed WHSV (12.1 h^{-1}) corresponds to the same molar feed rate of alcohol as 8.4 h^{-1} for methanol, meaning that when ethanol is converted under these conditions, the catalyst is actually subjected to twice as much carbon/h, compared to the conversion of methanol.

The conversion and production of aromatics and aliphatics are shown in Figure 42. The conversion graph is fundamentally different than for methanol conversion, since ethanol shows a much more gradual decline in conversion over time, indicating that ethanol is not converted through a “cigar-burn” type mechanism. As soon as active sites are lost due to deactivation, the conversion drops, indicating that ethene is converted throughout the entire bed. The dehydration of ethanol to ethene is assumed to happen almost instantly when ethanol reaches the catalyst bed, and ethanol or diethylether is not detected in the product stream, not even when the catalyst is deactivated.

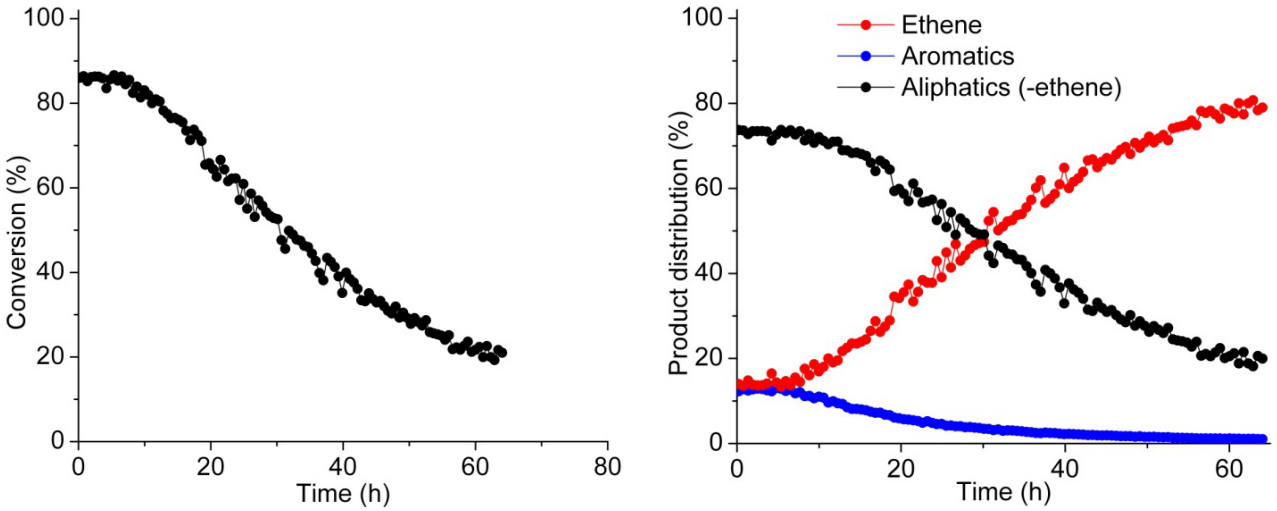

Figure 42: Conversion vs. time on stream for the reaction of ethanol over H-ZSM-5 (left) and the concentrations of ethene, aromatics, and aliphatics (apart from ethene) in the product stream vs. time on stream (right) (T = 400 °C, P = 1 bar, WHSV = 12.1 h^{-1})

When ethanol is converted, ethene is considered a reactant, but it is also a part of the normal products produced from conversion of oxygenates over H-ZSM-5. This means that even though the catalyst might be very active, full initial conversion is not observed since ethene leaves the reactor as a product, but is considered a reactant in the calculations.

The initial production of aromatics is somewhat lower than for methanol, and it declines with time on stream, and after around 40-50 h on stream very small amounts of aromatics are produced, while the catalyst is still somewhat active in the production of aliphatics.

Like methanol, ethanol produces large amounts of propene, C_4 and C_{5+} compounds, while propane quite rapidly declines along with the production of aromatics, as seen in Figure 43. No methane is produced from conversion of ethanol, supporting the hypothesis that methane is most likely produced directly from methanol independently of the working hydrocarbon pool. Ethane is produced in very small amounts, declining throughout the experiment from an initial value of 0.1 %. The selectivities within the aromatic compounds resemble what was observed for methanol, underlining the complexity of the reaction and the large extend of secondary reactions. Traces of ethylmethylbenzenes are observed, but in general very small amounts of ethylated species are observed in the outlet. The ethylmethylbenzenes are included in the triMBs in Figure 43.

As discussed earlier, ethene is not very reactive towards oligomerization under normal MTH conditions. This implies that ethene is not able to convert on its own, and is most likely converted through a hydrocarbon pool type mechanism where ethylated and methylated benzenes are likely to take part in the reaction as discussed in a publication from our group [100].

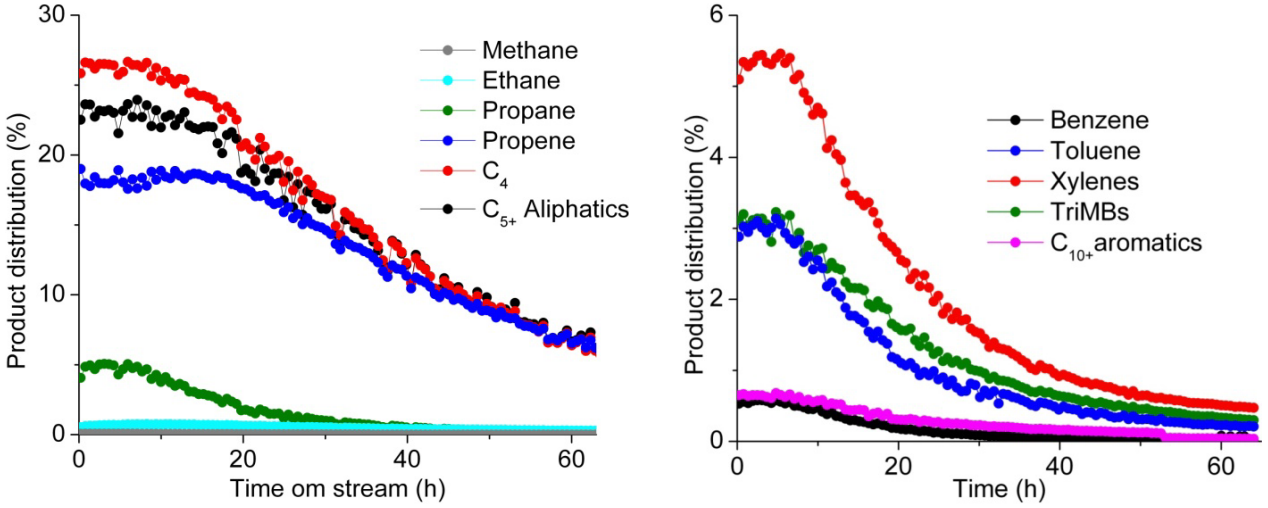

Figure 43: Detailed composition of the aliphatic (left) and aromatic (right) products for ethanol conversion over H-ZSM-5 (T = 400 °C, P = 1 bar, WHSV = 12.1 h^{-1})

Ethanol conversion has been performed at different feed rates and the graphs for conversions and conversion capacities are shown in Figure 44. Naturally, when the feed rate is increased, the catalyst lifetime is shorter, but interestingly the conversion capacity of the catalyst seems to be independent of the WHSV of ethanol, since the three curves for conversion capacity (right in Figure 44) can be extrapolated to approximately the same point on the X-axis. This behavior is contradictory to what was observed for methanol, where the conversion capacity is much lower at high WHSV.

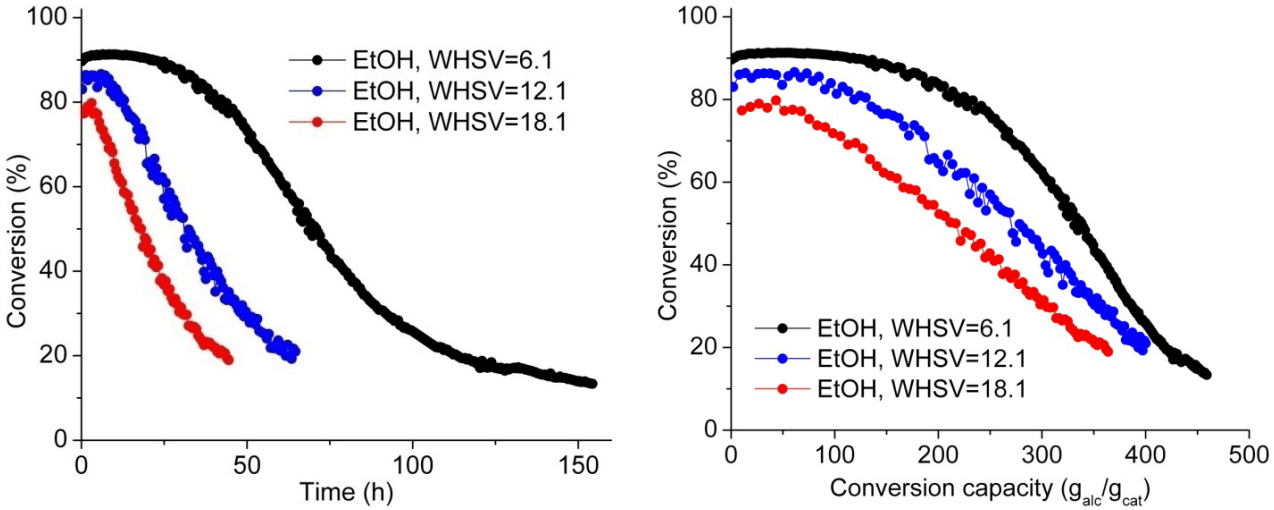

Figure 44: Conversion vs. time on stream and conversion capacity for the reaction of ethanol over H-ZSM-5 at different WHSV (T = 400 °C, P = 1 bar)

4.2.2.3 Conversion of 2-propanol over H-ZSM-5

The conversion of 2-propanol has been tested under similar conditions as the lower alcohols (400 °C, 1 bar), but in order to compare the different alcohols as reactants suitable values for the WHSV have to be employed. Table 4 shows values for WHSV and the molar feed rates on basis of the alcohol and carbon atoms, respectively. Naturally, when the molar feed rate of the alcohols is the same for conversion of methanol and 2-propanol, the catalyst is subjected to three times the amount of carbon/h when 2-

propanol is converted. By choosing the right values of WHSV, it is possible to obtain a series of experiments where methanol, ethanol and 2-propanol are converted at the same molar feed rate of the alcohol (0.26 mol_{alc}/g_{cat}*h) or carbon atoms in the feed (0.26 mol_C/g_{cat}*h).

	WHSV (h^{-1})	Feed rate alc. (mol_{alc}/g_{cat}*h)	Feed rate carbon (mol_C/g_{cat}*h)
Methanol	8.4	0.26	0.26
Methanol	25.2	0.79	0.79
Ethanol	6.1	0.13	0.26
Ethanol	12.1	0.26	0.53
Ethanol	18.1	0.39	0.79
2-Propanol	5.3	0.088	0.26
2-Propanol	15.8	0.26	0.79

Table 4: Values for WHSV for methanol, ethanol and 2-propanol, and corresponding values of molar feed rates of alcohol and carbon

When conversion data and conversion capacity of methanol, ethanol and 2-propanol at the same molar feed rate of carbon are plotted (see Figure 45) a dramatic difference in catalyst lifetime is observed. Within the timescale studied, the conversion of 2-propanol/propene only decreases slightly, and the experiment is discontinued after 3 weeks on stream, since it seems too time-consuming to wait for deactivation of the catalyst at this feed rate in order to find the catalyst lifetime and conversion capacity.

As soon as 2-propanol reaches the catalyst bed it is assumed to dehydrate to propene, which reacts further to form products, but since propene is also a product normally formed from catalytic conversion over H-ZSM-5, full conversion is not observed in the beginning of the experiment. This does not mean that the catalyst is not sufficiently active; propene leaving the reactor is simply considered a reactant in the calculations. As mentioned, this is also the case for conversion of ethanol.

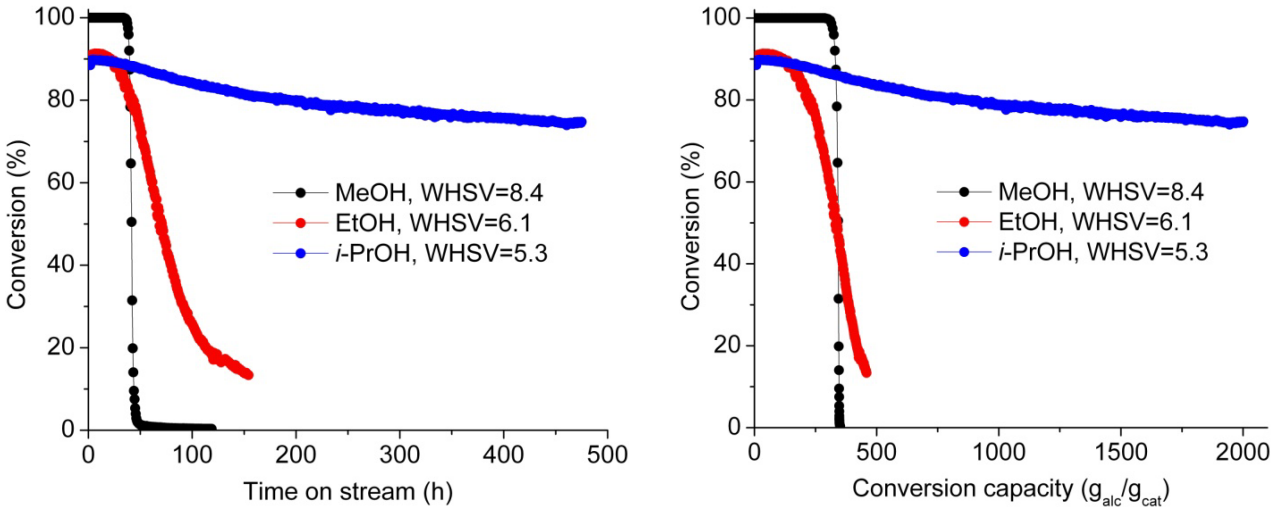

Figure 45: Conversion vs. time on stream (left) and conversion capacity (right) for conversion of methanol, ethanol and 2-propanol over H-ZSM-5. The molar feed rate of carbon atoms in the reactants is kept constant (0.26 mol_c/g_{cat}*h), resulting in the displayed values of WHSV (T = 400 °C, P = 1 bar)

Conversion data and conversion capacities for conversion of methanol, ethanol, and 2-propanol at the same molar feed rate of the alcohol are shown in Figure 46. At this feed rate the catalyst still has an extremely long lifetime for 2-propanol conversion, but it does deactivate within a reasonable timescale, and the experiment is discontinued after 6 weeks on stream. The missing data around 200 h on stream is due to a problem with the online GC, but the experiment itself was not affected by this.

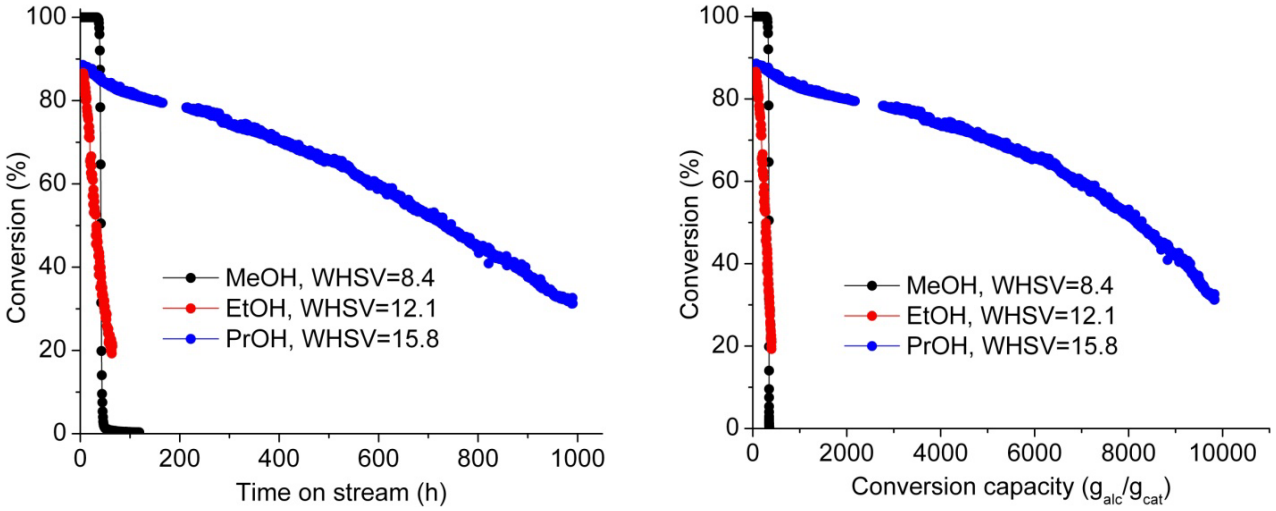

Figure 46: Conversion vs. time on stream (left) and conversion capacity (right) for conversion of methanol, ethanol and 2-propanol over H-ZSM-5. The molar feed rate of the reactants is kept constant, resulting in the displayed values of WHSV (T = 400 °C, P = 1 bar)

From extrapolation of the curves (Figure 46, right) it is possible to calculate the total conversion capacities of the catalyst in the different experiments and these are shown in Table 5. The catalyst is able to convert more than 30 times as much 2-propanol as methanol when calculated on mass basis, and 50 times as much on a molar basis of carbon atoms in the feed. As mentioned earlier, the conversion capacity for ethanol seems to be independent of the WHSV. This might also be the case for 2-propanol, but the experiment with the low WHSV of 2-propanol was discontinued prior to deactivation. If it was to reach the same conversion capacity as the other experiment it should have been on line for 4-5 months.

	WHSV (h^{-1})	Feed rate alc. (mol_{alc}/g_{cat}*h)	Conv. Cap. mol_C/g_{cat}	Conv. Cap. g_{alc}/g_{cat}
Methanol	8.4	0.26	11	350
Methanol	25.2	0.79	4	128
Ethanol	6.1	0.13	~22	~500
Ethanol	12.1	0.26	~22	~500
Ethanol	18.1	0.39	~22	~500
2-Propanol	5.3	0.088	>>100	>>2000
2-Propanol	15.8	0.26	~565	~11300

Table 5: Conversion capacities for conversion of methanol, ethanol and 2-propanol over H-ZSM-5 at different values of WHSV (T = 400 °C, P = 1 bar)

Apart from the extremely high conversion capacity, conversion of 2-propanol also shows interesting behavior concerning the product selectivity. The production of aliphatics and aromatics is shown in

Figure 47 alongside the product distribution within the aromatic compounds. As for the other reactants, the production of aromatics decline with time on stream, but in this case no aromatics are produced after around a third of the catalyst lifetime. This means that after approximately 300 h no aromatics are observed and the catalyst is still highly active delivering a product mixture exclusively consisting of aliphatic compounds.

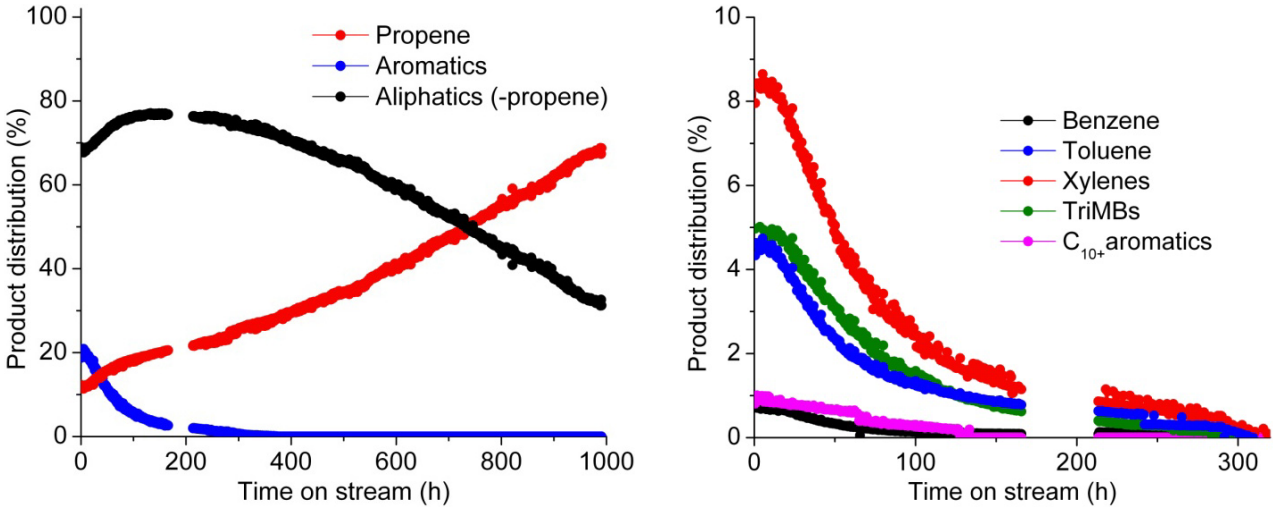

Figure 47: Production of aliphatics and aromatics vs. time on stream (left) and product distribution within the aromatic compounds (right) for conversion of 2-propanol over H-ZSM-5 (T = 400 °C, P = 1 bar)

The initial selectivity towards aromatics resembles what is observed for methanol, indicating that in both cases the fresh catalyst is able equilibrate the products. In other words, if there is enough fresh catalyst present, the product distribution is determined by the nature of the catalyst and the reaction conditions, meaning that the choice of reactant will not be decisive concerning the product selectivity (unless a reactant with a different H/C atomic ratio is employed).

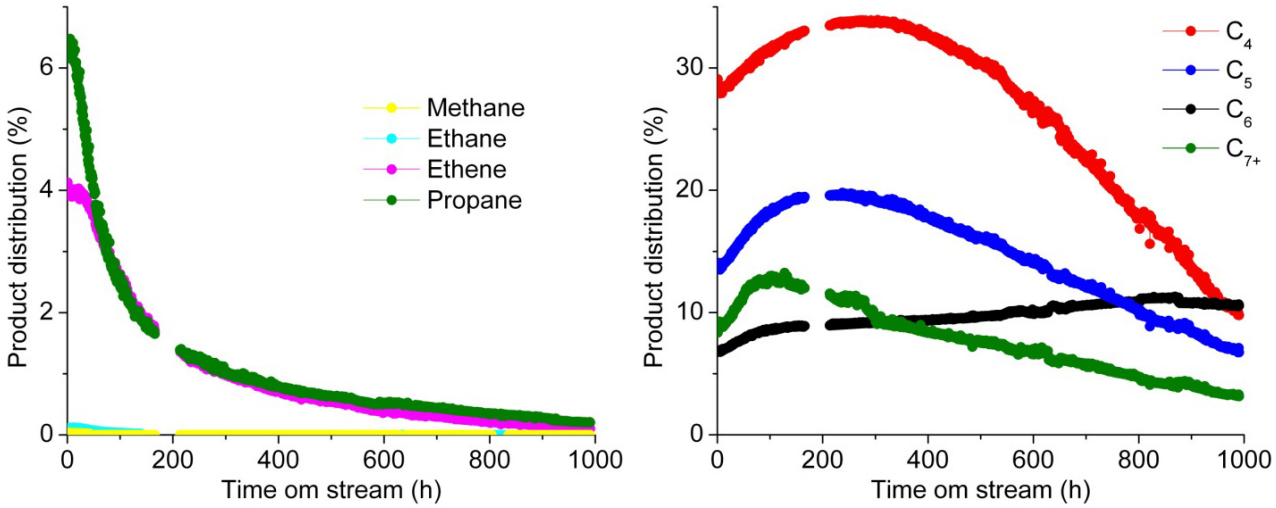

Figure 48: Distribution of aliphatic compounds vs. time on stream for conversion of 2-propanol over H-ZSM-5. Left: C_1-C_3, right: C_{4+} (T = 400 °C, P = 1 bar)

The product distribution of aliphatic compounds is shown in Figure 48. The selectivity towards propane decreases with time on stream, which is in good correspondence with the decrease in aromatics. The

production of ethene also decreases, reflecting that ethene is mainly produced from aromatics. Even though the catalyst is still active in the last part of the experiment almost no ethene is produced, while higher aliphatics (mainly alkenes) are produced in large amounts, illustrating that ethene is not produced from cracking of alkenes (or only to a minor extend).

The higher aliphatics (Figure 48 (right)) all show similar behavior, except the group of C_6 compounds, which does not decline when the catalyst approaches deactivation. This is simply due to the direct dimerization of propene which becomes more dominating in the last part of the run.

4.2.2.4 C_4 hydrogen transfer index

The selectivity towards aromatics is of interest since a product with low aromatic content is desired [32, 66]. Since aromatics are produced via hydrogen transfer reactions in the catalyst, a simple and indirect way of monitoring the selectivity towards aromatics is by observing the ability of the catalyst to perform hydrogen transfer. Since alkanes are always produced simultaneously with aromatics, a way to do this is to calculate the C_4 hydrogen transfer index (C_4-HTI), defined as the ratio between the sum of butanes and total C_4 compounds [106]:

$$C_4\text{-HTI} = \frac{\sum \text{butanes}}{\sum \text{butenes+butanes}}$$

The C_4-HTI gives a good indication of the activity of the catalyst [107] and the extent of secondary reactions happening downstream from the alcohol conversion zone.

Figure 49 shows the distribution of C_4 alkanes and alkenes for conversion of methanol (left) and 2-propanol (right). As expected, in both cases the amount of alkanes decline with time on stream, but in the case of methanol, the catalyst produces alkanes until full deactivation, while for 2-propanol a high C_4 alkene selectivity is observed, even when no alkanes are produced.

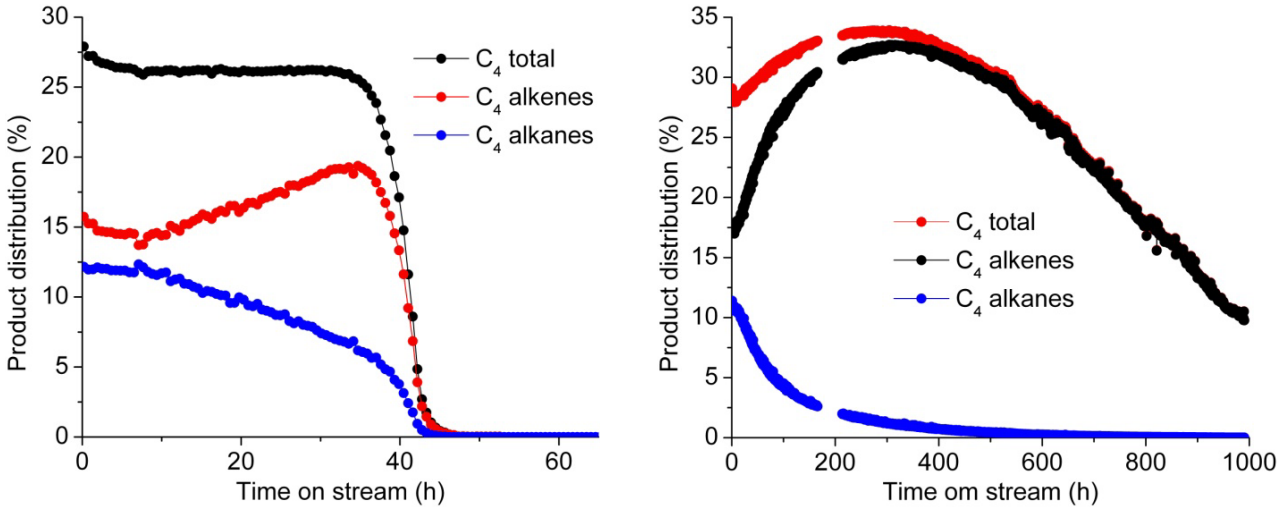

Figure 49: C_4 alkenes and alkanes from conversion of methanol (left) and 2-propanol (right) over H-ZSM-5 (T = 400 °C, P = 1 bar, WHSV = 8.4 h^{-1} for methanol and 15.8 h^{-1} for 2-propanol)

As described above, it is possible to calculate the C_4-HTI from the shown C_4 yields. The calculated C_4-HTI for methanol at different WHSV plotted against the conversion is shown in Figure 50. The C_4-HTI

gradually declines at full conversion until the catalyst is deactivated and the conversion drops when the C_4-HTI has a value around 0.2. When plotted against the conversion, the C_4-HTI seems rather independent of the space velocity.

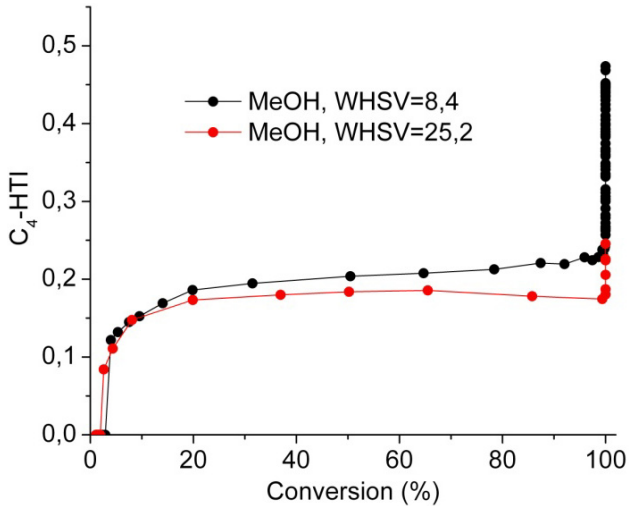

Figure 50: C_4-HTI for conversion of methanol at different values of WHSV (T = 400 °C, P = 1 bar)

Figure 51 shows the C_4-HTI for conversion of ethanol and 2-propanol. For ethanol the curve is less steep than for methanol due to the more gradual decline in conversion and the C_4-HTI reaches 0.1 while the catalyst is still somewhat active. In the case of 2-propanol, the decline in C_4-HTI is much more pronounced and it almost reaches zero at around 60 % conversion, meaning that while the catalyst is still highly active in oligomerization, cracking, and isomerization reactions, the ability to perform hydrogen transfer reactions is lost or at least suppressed significantly. At this point, the product mixture consists almost exclusively of alkenes. For both ethanol and 2-propanol the C_4-HTI seems rather independent of the WHSV, when plotted against the conversion.

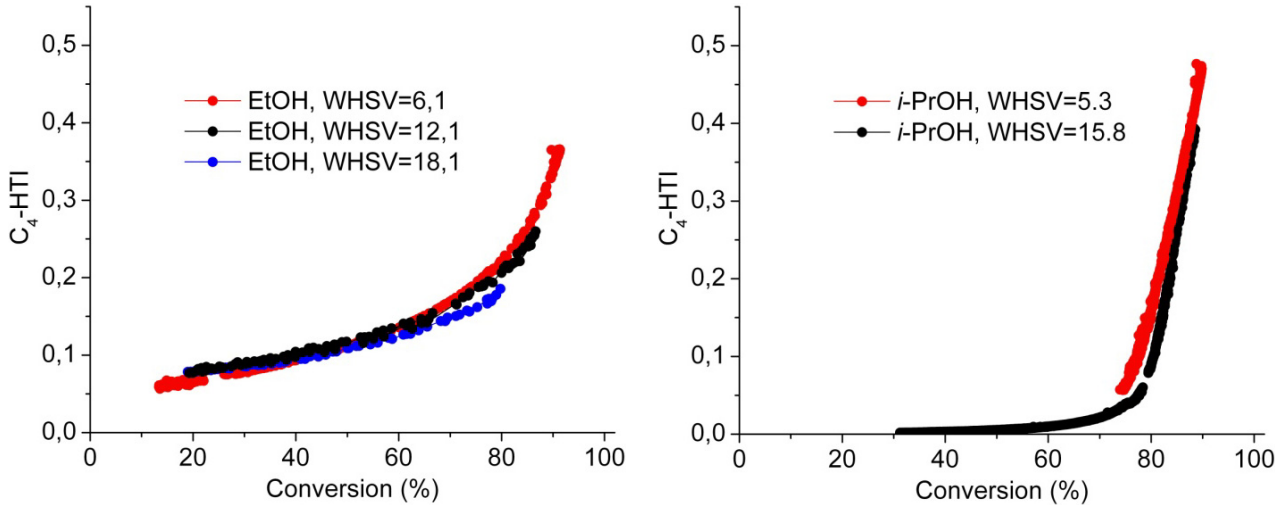

Figure 51: C_4-HTI for conversion of ethanol and 2-propanol at different values of WHSV (T = 400 °C, P = 1 bar)

4.2.3 Conversion of C_1-C_3 alcohols at elevated pressures

Conversion of methanol, ethanol and 2-propanol has been investigated under elevated pressures (up to 20 bars) in a dedicated pressure setup. The alcohols are converted at conditions similar to the non-pressurized experiments, and the molar feed rate of the alcohol is kept constant, see Table 6.

	WHSV (h^{-1})	Feed rate alc. (mol_{alc}/g_{cat}*h)	Feed rate carbon (mol_c/g_{cat}*h)
Methanol	8.4	0.26	0.26
Ethanol	12.1	0.26	0.53
***2*-Propanol**	15.8	0.26	0.79

Table 6: Employed feed rates for alcohol conversion at high pressure

The formation of liquid products from conversion of methanol and ethanol over H-ZSM-5 at 20 bar is illustrated in Figure 52. The data simply arise from the volume of liquid organics produced divided by the corresponding reaction time to give the rate of liquid formation. The amount of aromatics is calculated from the off-line GC analyses and displayed in the graphs as the red areas while the green areas represent aliphatics.

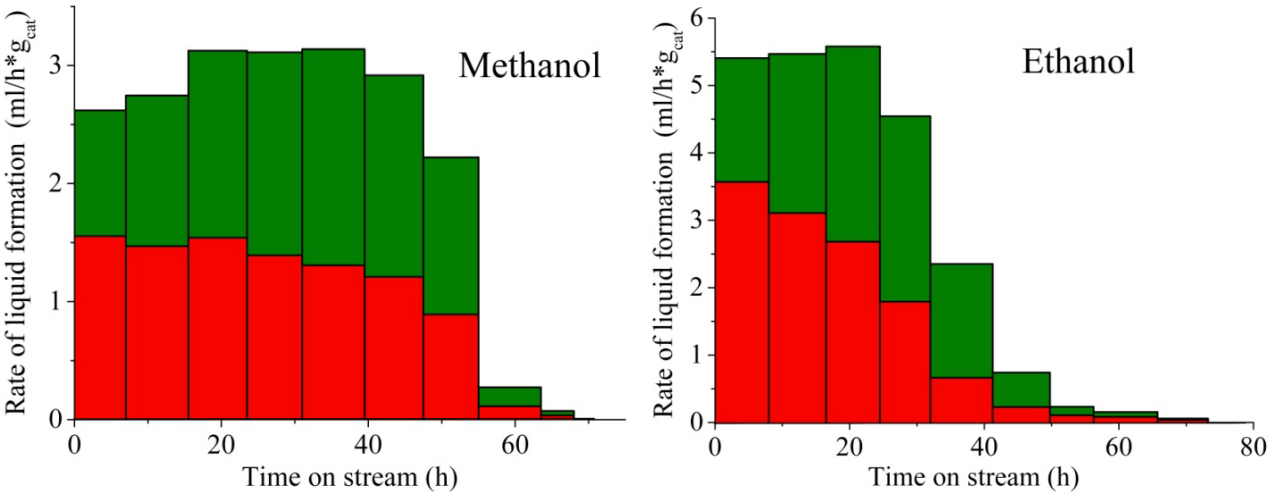

Figure 52: Rate of liquid product formation vs. time on stream for conversion of methanol (left) and ethanol (right) over H-ZSM-5 (400 °C, 20 bar). The red coloring represents aromatics and the green represents aliphatics

The liquid production from methanol is quite constant over time and declines rapidly when the catalyst is deactivated, which is in good correspondence with the conversion data from the non-pressurized experiments. The aromatic fraction declines with time on stream, from the initial value above 50 %, which at first glance seems quite high, but one should bear in mind that it is on the basis of liquid products only.

The formation of liquid products from ethanol is quite similar to methanol, but it declines more gradually. The higher initial rate of liquid formation for ethanol is simply due to the fact that the catalyst is subjected to twice the amount of carbon when ethanol is fed compared to methanol.

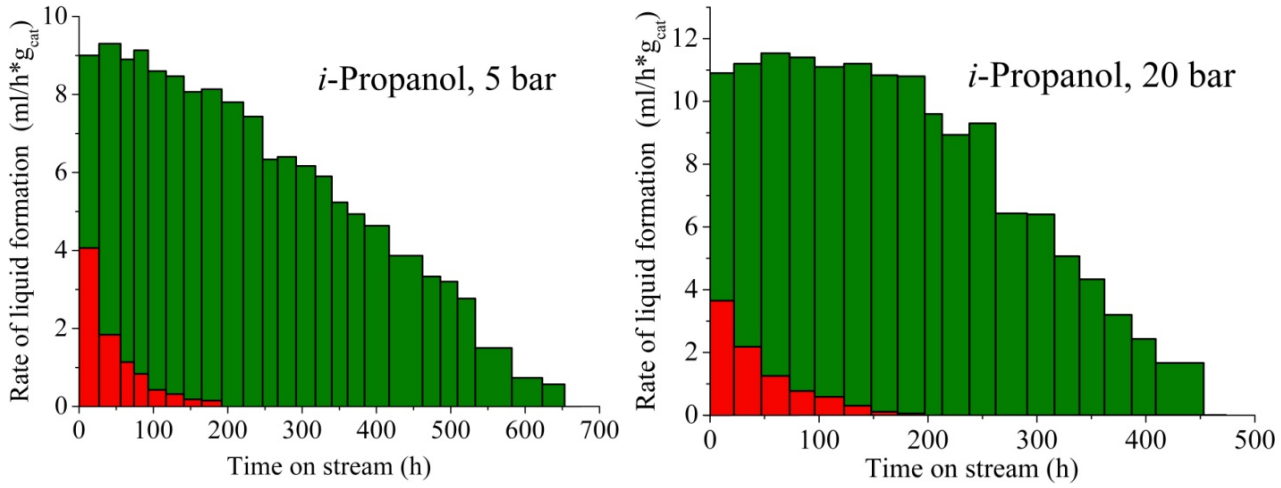

Figure 53: Rate of liquid product formation vs. time on stream for conversion of 2-propanol over H-ZSM-5 at 5 and 20 bar (400 °C). The red coloring represents aromatics and the green represents aliphatics

2-Propanol has been converted at 5 and 20 bar, see Figure 53. In both cases, the production of aromatics declines with time on stream, and after around 200 h, insignificant amounts of aromatics are present in the product mixture while aliphatic compounds (alkenes) are still produced in large amounts. As in the non-pressurized experiment, a gradual decrease in product formation is observed. The catalyst lifetime seems to be lower at elevated pressure; in the non-pressurized experiment (see Figure 46, page 52) the catalyst is still somewhat active after 1000 h on stream while liquid product formation seizes after 650 h and 450 h at 5 and 20 bar, respectively.

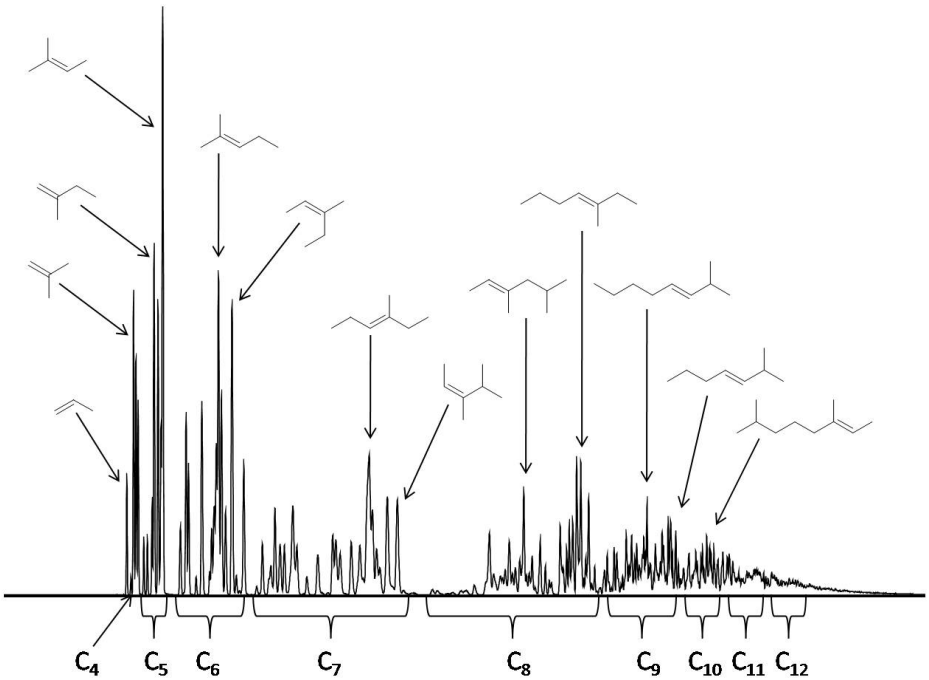

Figure 54: GC-MS chromatogram of the liquid product mixture after 250 h on stream from conversion of 2-propanol at 20 bar (400 °C). Major compounds are labeled for illustrative reasons

A GC-MS chromatogram of the liquid product mixture from conversion of 2-propanol at 20 bar is shown in Figure 54. The sample is withdrawn after 250 h on stream, which is when the production of aromatics

has just seized and the product mixture consists almost exclusively of C_3-C_{12+} alkenes as illustrated on the figure. Only traces of alkanes and aromatics are still present, confirming that the catalyst has lost its ability to perform hydrogen transfer reactions. For the smaller alkenes (up to C_6), it is possible to distinguish a number of peaks in the chromatogram corresponding to every possible structural alkene isomer (13 C_6 isomers, 5 C_5 isomers etc.), though it is not possible to identify the different peaks with 100 % certainty since many of the mass spectra are very similar. For the larger compounds, there is a clear tendency that only linear or methylated alkenes are produced due to the shape selective properties of the zeolite, i.e. the rate of diffusion of compounds with bulkier substituents is very low.

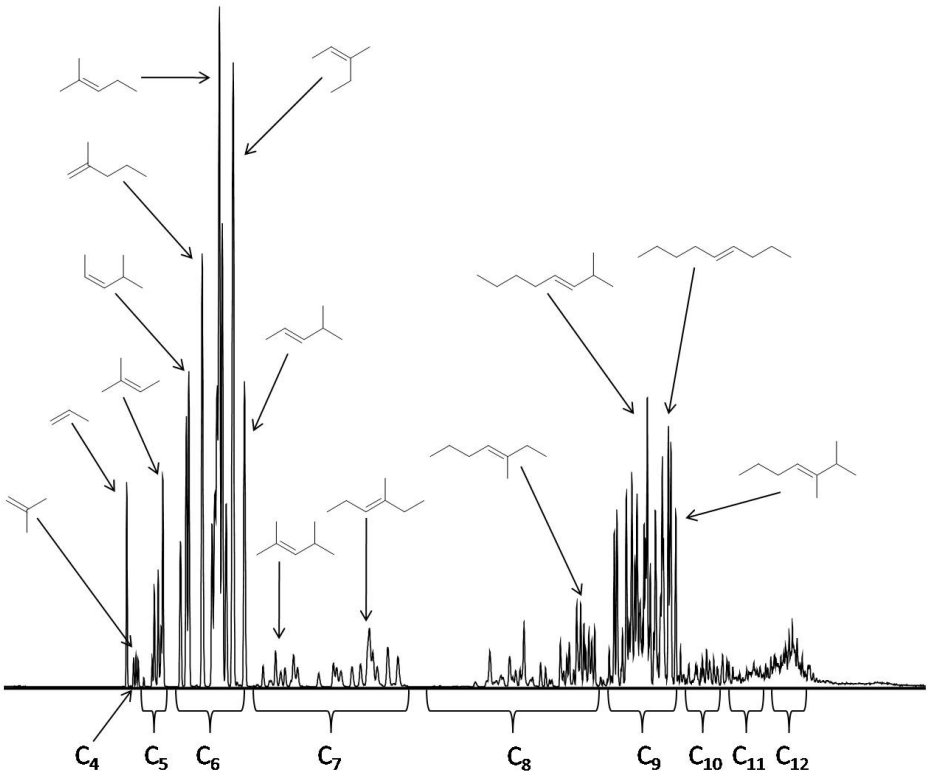

Figure 55: GC-MS chromatogram of the liquid product mixture after 425 h on stream from conversion of 2-propanol at 20 bar (400 °C). Major compounds are labeled for illustrative reasons

Figure 55 shows the composition of the very last liquid sample from the conversion of 2-propanol at 20 bar. There is a clear enrichment of the C_6, C_9 and even C_{12} compounds illustrating that the activity of cracking reactions is diminishing and the direct oligomerization products of propene become dominating.

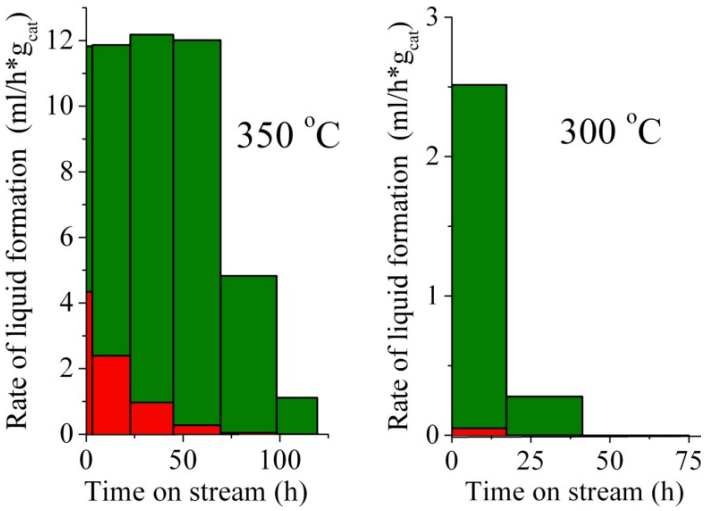

Figure 56: Rate of liquid product formation vs. time on stream for conversion of 2-propanol over H-ZSM-5 at 300 and 350 °C (P = 20 bar). The red coloring represents aromatics and the green represents aliphatics

In an attempt to push the selectivity towards larger compounds, the reaction was performed at lower temperature. This should decrease the relative rate of cracking reactions compared to oligomerization leading to production of larger molecules [104]. The rate of liquid production for conversion of 2-propanol at 350 and 300 °C is shown in Figure 56. At 350 °C, the production of aromatics declines quickly, but the aliphatics also decline shortly thereafter and at 300 °C only very small amounts of liquid is produced containing almost no aromatics. It seems like the catalyst is simply not active enough to perform the reaction at these temperatures. A plausible explanation for this behavior is the low activity towards cracking at low temperature, which leads to accumulation of large hydrocarbon compounds inside the zeolite. If these species are not cracked down at sufficient rate, they block the access to the zeolite and it has thus lost its activity. This is supported by the fact that the catalyst activity is normal as soon as the reaction temperature is raised upon deactivation at low temperature, increasing the cracking activity of the catalyst.

	Pressure (bar)	Temperature (°C)	Total organic liquid (mL)	Aromatics (%)
Methanol	20	400	160	47
Ethanol	20	400	200	50
2-Propanol	20	400	3550	6,1
2-Propanol	5	400	3556	6,3
2-Propanol	20	350	997	9,0
2-Propanol	20	300	50	1,7

Table 7: Total organic liquid produced before catalyst deactivation and total fraction of aromatics in the product from conversion of methanol, ethanol and 2-propanol at various pressures and temperatures over H-ZSM-5

Table 7 summarizes the total amount of organic liquid produced before catalyst deactivation and the summarized aromatic content in the liquid product from conversion of methanol, ethanol and 2-propanol under various conditions in the pressurized reaction setup. It is quite clear that conversion of 2-propanol produces a large amount of product with low aromatic contents compared to ethanol and methanol. Lowering the reaction temperature decreases the amount of product produced from 2-

propanol significantly. The slightly higher content of aromatics at 350 °C is simply due to shorter lifetime of the catalyst, leading to a lower production of olefinic compounds in the last part of the experiment.

4.2.4 Temperature programmed oxidation (TPO) of spent catalysts

In order to investigate the deposition of coke during the alcohol conversion, temperature programmed oxidation (TPO) has been performed on the spent zeolites in a dedicated experimental setup. From the raw data illustrated in Figure 57, the total content of carbon deposited on a spent catalyst is calculated through integration of the peaks for CO and CO_2 concentration.

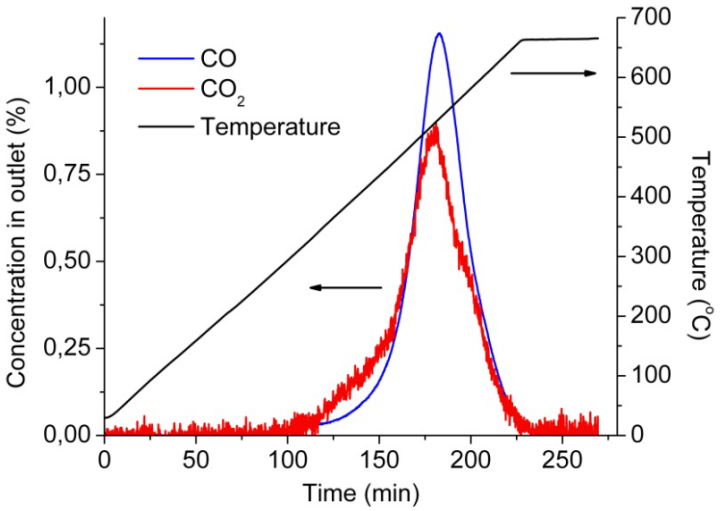

Figure 57: Example of raw data from a TPO experiment

Figure 58 shows the amount of carbon deposited on H-ZSM-5 upon deactivation after conversion of methanol, ethanol or 2-propanol at various reaction pressures. Conversion of methanol induces massive formation of coke (around 18 wt%) on the catalyst independently of the pressure. For ethanol and 2-propanol the amount of coke on the spent catalysts is lower, although it increases at elevated pressures. The fact that much more coke is produced from methanol conversion does not necessarily mean that the catalyst deactivates faster than for ethanol, in fact the lifetimes are quite similar. Methanol is simply more reactive than ethanol and the catalyst is not able to activate ethene when it is partially coked. The higher coke contents at elevated pressures for ethanol and 2-propanol might be an indication of better catalyst utilization under these conditions.

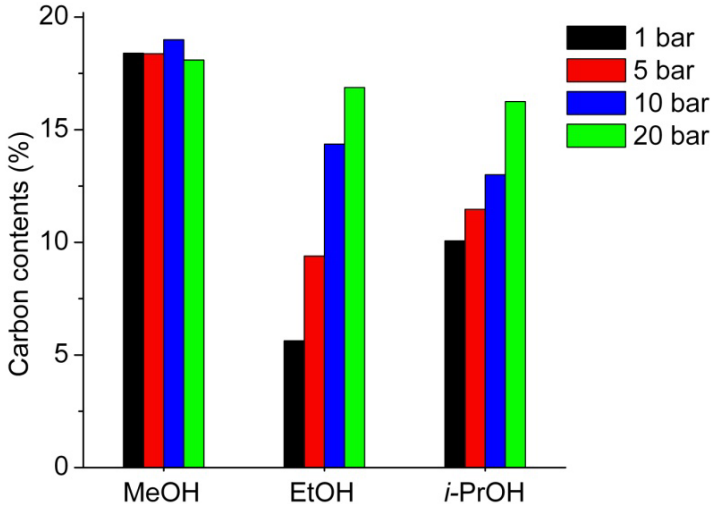

Figure 58: Carbon contents on spent H-ZSM-5 zeolite upon conversion of methanol, ethanol and 2-propanol at various reaction pressures (T = 400 °C)

Since the lifetime of the catalyst is very different for conversion of the various alcohols, the coke found on the spent catalysts has been deposited at very different rates. This is illustrated in Figure 59, where the molar ratios (mol/mol) between the amount of carbon converted and the amount of carbon deposited on the catalyst as coke during the entire lifetime of the catalyst are shown. For methanol, around 1 carbon atom in every 600 carbon atoms converted are deposited as coke. This is in stark contrast to conversion of 2-propanol, where the catalyst is able to convert as much as 53,500 carbon atoms pr. deposited carbon atom. For ethanol, around 1 in every 4,400 converted carbon atoms ends up as deposited coke.

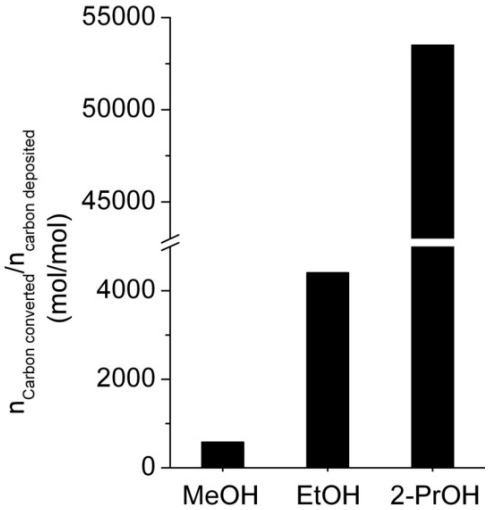

Figure 59: The molar (mol/mol) ratios between the amount of carbon converted and the amount of carbon deposited as coke on the catalyst during the entire lifetime of the catalyst for conversion of methanol, ethanol and 2-propanol over H-ZSM-5 at 400 °C and 1 bar

Figure 60 shows the amount of carbon deposited on H-ZSM-5 upon conversion of 2-propanol at different reaction temperatures and a clear trend is observed that higher reaction temperature leads to formation of more coke on the catalyst. This does not mean that the catalyst deactivates faster at 400 °C, on the contrary, when the temperature is 300 or 350 °C the catalyst lifetime is markedly lower than

at 400 °C. At lower temperatures, partial coking of the catalyst is apparently enough to suppress the reaction. An explanation for this could be that the activity towards cracking is low at lower temperatures, meaning that long aliphatic compounds might be retained inside the zeolite pores and the zeolite is deactivated without formation of large amounts of heavy aromatic coke on the exterior of the crystals.

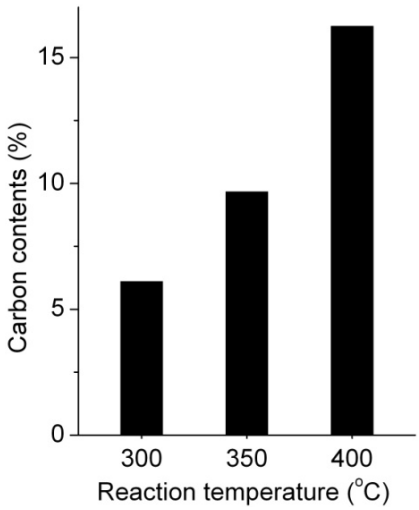

Figure 60: Carbon contents in H-ZSM-5 upon conversion of 2-propanol at 20 bar and at various reaction temperatures

In order to investigate the coke deposition as a function of reaction time, conversion of 2-propanol at 20 bar and 400 °C has been carried out for different reaction times; the reaction was simply stopped before full deactivation of the catalyst in order to analyze the amount of deposited carbon. Figure 61 (left) shows the carbon contents in the catalyst after different reaction times. From the carbon contents it is possible to calculate the average rate of carbon deposition in the period between the single data points as illustrated in Figure 61 (right). It is clear that the deposition of carbon is most pronounced in the very beginning of the reaction while the catalyst is most active and there is a high production of aromatics.

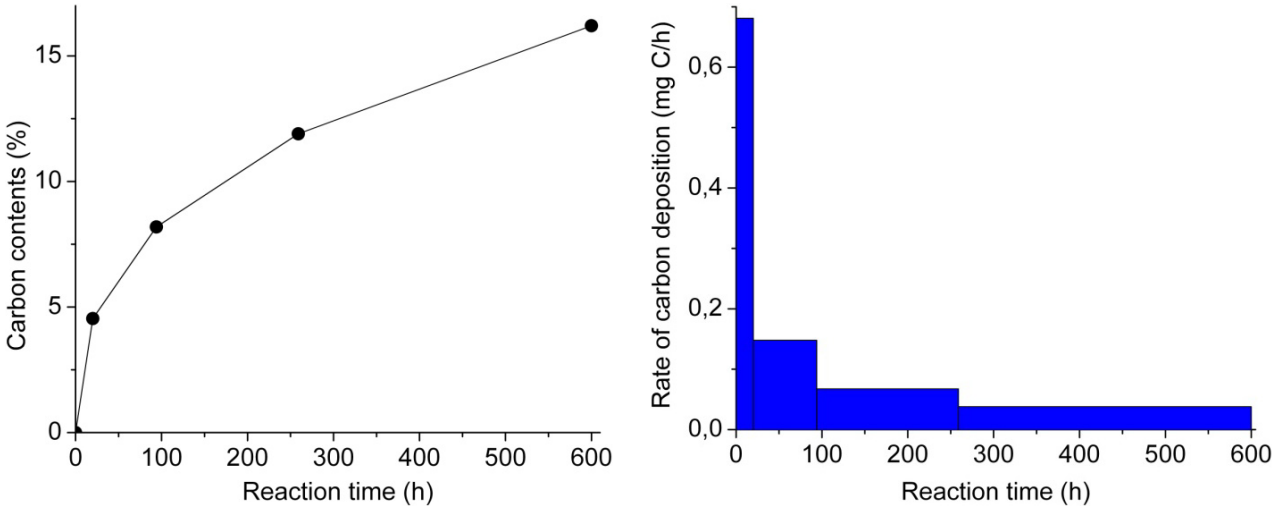

Figure 61: Carbon contents in H-ZSM-5 upon conversion of 2-propanol (P = 20 bar, T = 400 °C) as a function of the time of reaction (left) and calculated rate of carbon deposition (right)

After 200 h on stream the reaction produces no aromatic compounds (see Figure 53, page 57). One might think that when no aromatics are observed in the reactor outlet, the production of coke would also be negligible since coke mainly consists of aromatic structures, but this is not the case. Nevertheless, the rate of coke formation is much lower than in the beginning of the experiment.

4.3 Conversion of C_1-C_4 alcohols over H-ZSM-5 and H-Beta

In order to investigate the influence of the type of zeolite framework, methanol, ethanol, 2-propanol, and 1-butanol were converted over H-ZSM-5 and H-Beta zeolites.

4.3.1 Experimental

The employed catalysts were an H-ZSM-5 (Si/Al = 40) and an H-Beta (Si/Al = 19) supplied by Zeolyst International in their ammonia form. Prior to use they were calcined at 550 °C for 4 h to obtain the proton form.

The catalytic reactions were performed in a fixed bed reactor typically charged with 300 mg catalyst, which was pretreated in helium at the reaction temperature for 30 min. prior to the reaction. The reactant liquid was pumped with an HPLC pump and evaporated before reaching the reactor. The reaction temperature was 370 °C (measured inside the reactor, just below the catalyst bed). Helium was used as a carrier gas, with a flow of 40 mL/min, and the products from the reaction were analyzed by an on-line GC (HP 6890) equipped with an FID.

The TPO analyses were typically performed with 100 mg of spent catalyst which was heated in a flow of 5 % O_2 in helium (20 mL/min) with a heating ramp of 2.75 °C/min to an oven temperature of 700 °C. The final temperature was maintained for 2 h to ensure complete combustion of the carbonaceous species. The concentrations of CO and CO_2 in the outlet were monitored continuously by a BINOS detector.

4.3.2 Results and discussion

The employed flow rates for conversion over H-ZSM-5 are shown in Table 8. For practical reasons, the flow rates of the higher alcohols are quite high in order for the catalyst to deactivate within a reasonable timeframe.

	WHSV (h^{-1})	Feed rate alc. (mol_{alc}/g_{cat}*h)	Feed rate carbon (mol_c/g_{cat}*h)
Methanol	7.9	0.25	0.25
Ethanol	7.9	0.17	0.34
2-Propanol	33.0	0.55	1.65
1-Butanol	32.3	0.44	1.74

Table 8: Employed flow rates for the different alcohols converted over H-ZSM-5 (Si/Al = 40) at 370 °C

Conversion and conversion capacities are shown in Figure 62. Not surprisingly, the C_1-C_3 alcohols behave in a similar manner under these conditions as under the slightly different conditions employed earlier (see Figure 46, page 52). Furthermore, 1-butanol has a lifetime and conversion capacity similar to that of 2-propanol, indicating that it is a general trend that C_{3+} alcohols induce very slow deactivation to the catalyst. It should be mentioned that when the conversion is calculated for 1-butanol, all butenes are considered reactants. One could also have considered 1-butene as the only reactant, but low

temperature experiments have shown that alkene isomerization is observed as soon as 1-butanol dehydrates, making it more fair to consider all C_4 alkenes reactants.

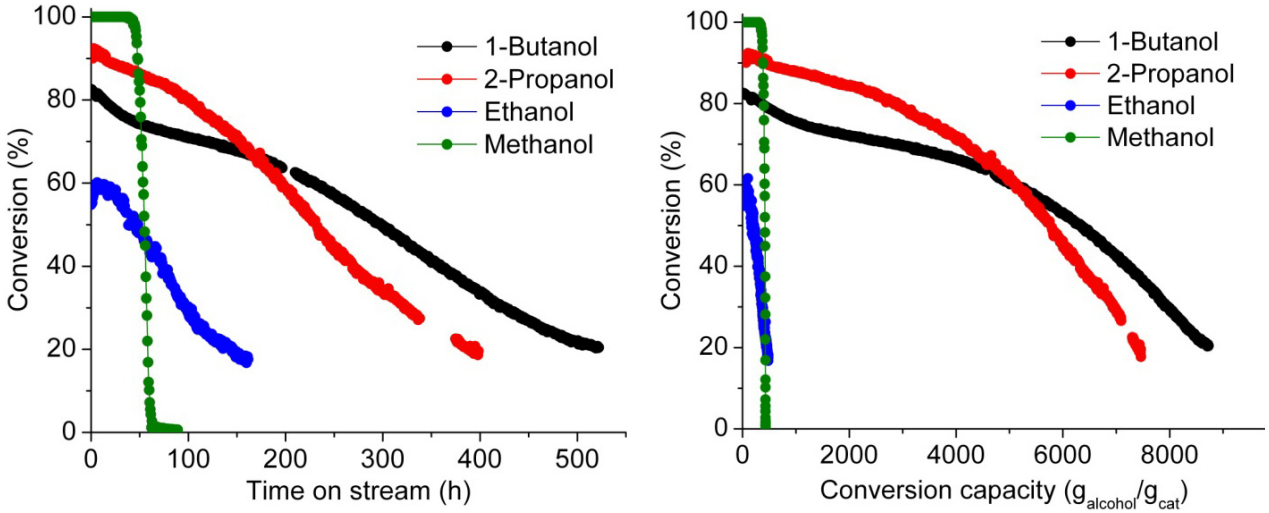

Figure 62: Conversion vs. time on stream (left) and conversion capacity (right) for conversion of C_1-C_4 alcohols over H-ZSM-5 at 370 °C and 1 bar

Due to higher space velocity, the lifetime for conversion of 2-propanol is shorter, than in the experiment shown in Figure 46, but the conversion capacity is also somewhat lower. This might reflect that a larger portion of the catalyst bed is required for dehydration of the alcohol at the high feed rate, leaving less catalyst available for the actual hydrocarbon conversion. The reaction temperature is also slightly lower (370 vs. 400 °C) which might also play a role in this context.

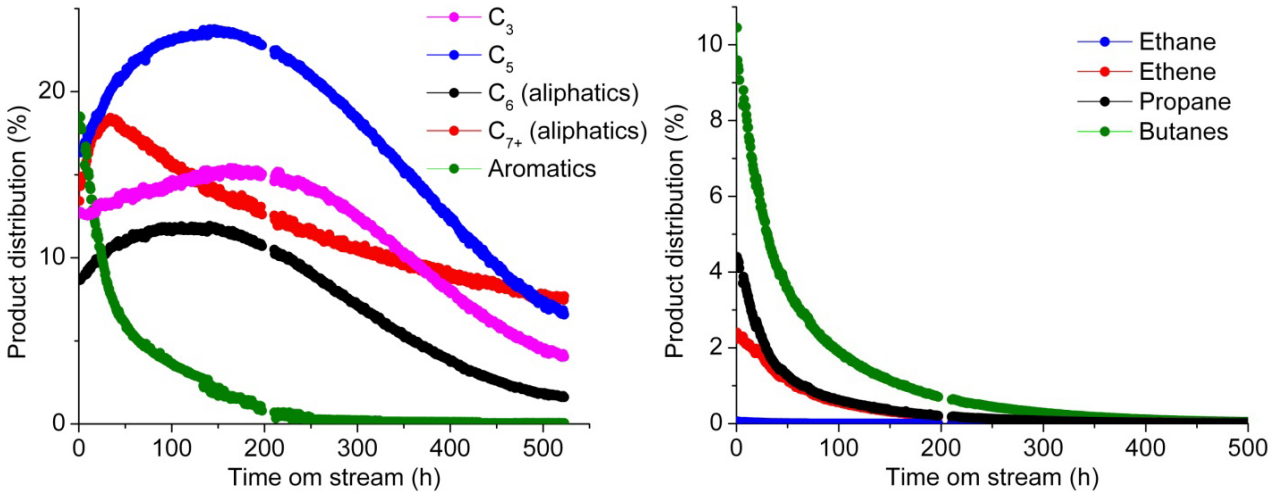

Figure 63: Product distribution from conversion of 1-butanol over H-ZSM-5 (T = 370 °C, P = 1 bar)

The product distributions from conversion of methanol, ethanol and 2-propanol are very similar to those shown earlier and they are therefore not shown here. The product distribution for conversion of 1-butanol is shown in Figure 63. As for 2-propanol, the amount of aromatics declines quickly over time, while large amounts of aliphatics are produced throughout the entire experiment. The concentration of alkanes declines along with the aromatics, and the concentration of ethene also declines since it is produced from decomposition of aromatic and not from alkene cracking. These observations are in good

accordance with the observations from conversion of 2-propanol. The amount of C_{7+} aliphatics declines slower than the other aliphatics, which reflects that the direct dimerization of butenes to produce C_8 alkenes becomes more dominating as the catalyst deactivates.

In order to investigate if the very long conversion capacities observed for conversion of higher alcohols is a general trend for different zeolite catalysts, H-Beta was employed in the conversion of the different alcohols. The main differences between H-Beta and H-ZSM-5 are that H-Beta has larger pores (12 T atoms, compared to 10 T atoms for H-ZSM-5) and a lower acid strength [108]. The specific sample of H-Beta employed in these experiments has an acid density twice as high as the employed H-ZSM-5 catalyst (Si/Al = 19 vs. Si/Al = 40).

	WHSV (h^{-1})	Feed rate alc. (mol_{alc}/g_{cat}*h)	Feed rate carbon (mol_c/g_{cat}*h)
Methanol	7.9	0.25	0.25
Ethanol	7.9	0.17	0.34
2-Propanol	6.5	0.10	0.31
1-Butanol	6.3	0.087	0.35

Table 9: Employed flow rates for the different alcohols converted over H-Beta (Si/Al = 19) at 370 °C

The employed flow rates of the different alcohols converted over H-Beta are shown in Table 9. Note that the feed rates of 2-propanol and 1-butanol are much lower than in the experiments with H-ZSM-5. The conversions and conversion capacities are shown in Figure 64. Clearly, deactivation of the catalyst is much more rapid for H-Beta than for H-ZSM-5. For all the alcohols, the catalyst is deactivated within a few hours on stream and the conversion drops to below 10 %. Another very interesting observation is that the catalyst actually has the highest lifetime and conversion capacity for conversion of methanol, which is in stark contrast to H-ZSM-5. This could be a consequence of alkylation of aromatics with propene or butene inside the zeolite to form aromatics with relatively long side chains, and due to the larger pores of zeolite H-beta these species are allowed to condense to large aromatics inside the pores leading to the formation of coke.

The initial conversion of ethanol is very low, when reacted over H-Beta at these conditions. Ethene is harder to activate than the larger alkenes which is also observed over H-ZSM-5. The lower acid strength of H-Beta is most likely responsible for the very low initial conversion observed.

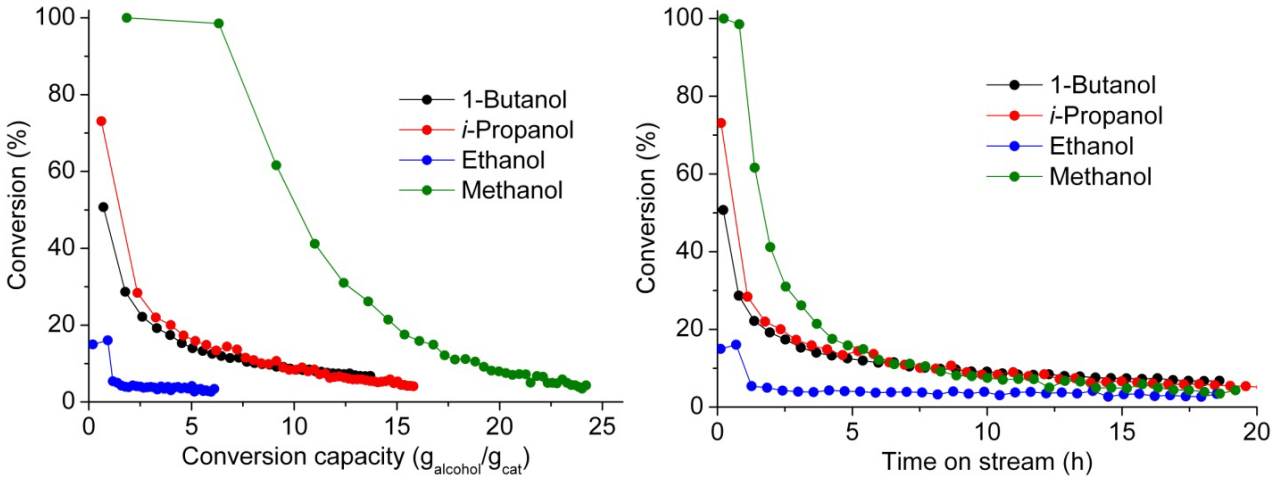

Figure 64: Conversion vs. time on stream (left) and conversion capacity (right) for conversion of C_1-C_4 alcohols over H-Beta at 370 °C and 1 bar

The initial selectivities towards aromatics and the initial values of C_4-HTI for conversion of the different alcohols over H-ZSM-5 and H-Beta are shown in Figure 65. For H-ZSM-5, the initial amount of aromatics produced and the C_4-HTI are rather independent of the reactant, except in the case of ethanol, where both values are markedly lower. Naturally, aromatics are produced through hydrogen transfer reactions and therefore the amount of aromatics is linked to the value of C_4-HTI. The situation is quite different for H-Beta where the amount of aromatics and the C_4-HTI seem highly dependent on the reactant, declining with the length of the carbon chain in the alcohol. Again ethanol is the exception producing very low amounts of aromatics while still retaining a very high value for C_4-HTI. This is most likely due to the fact that the initial conversion is quite low leading to a low yield of aromatics while the C_4-HTI is independent of the conversion.

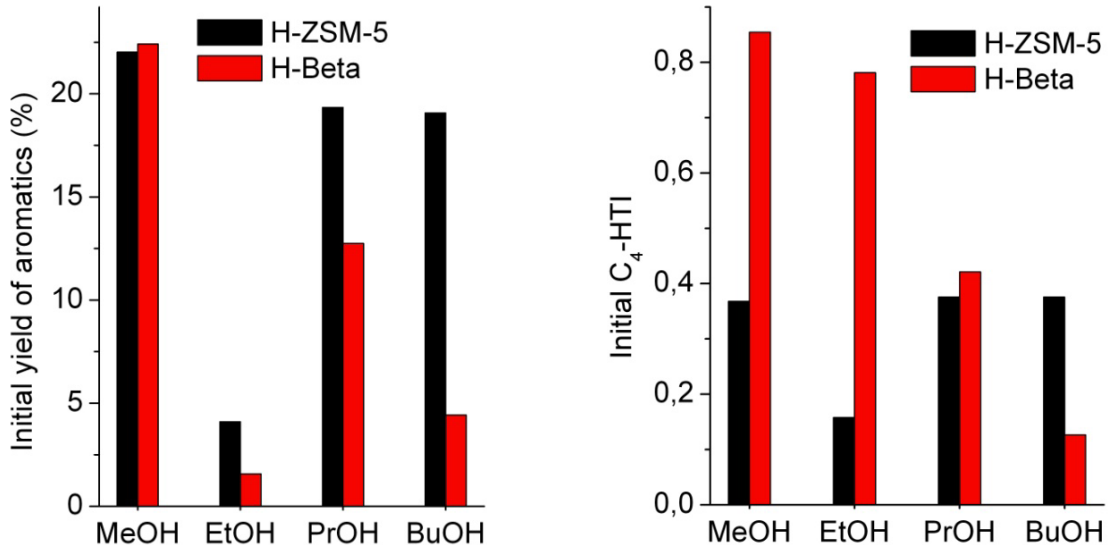

Figure 65: Initial yield of aromatics (left) and initial value of C_4-HTI (right) for conversion of methanol, ethanol, 2-propanol, and 1-butanol over H-ZSM-5 (Si/Al = 40) and H-Beta (Si/Al = 19) (T = 370 °C, P = 1 bar)

When a high value of C_4-HTI is observed and it is not accompanied by large amounts of aromatics in the product stream (at reasonable conversion) there is an excess of hydrogen in the products meaning that

some carbon seems to be missing. This carbon is either deposited on the catalyst as coke, or incorporated into very large aromatic compounds which do not reach the GC and are not accounted for in the product distribution. For all the reactants, H-Beta has a larger C_4-HTI to aromatics ratio than H-ZSM-5, indicating that some carbon is not accounted for.

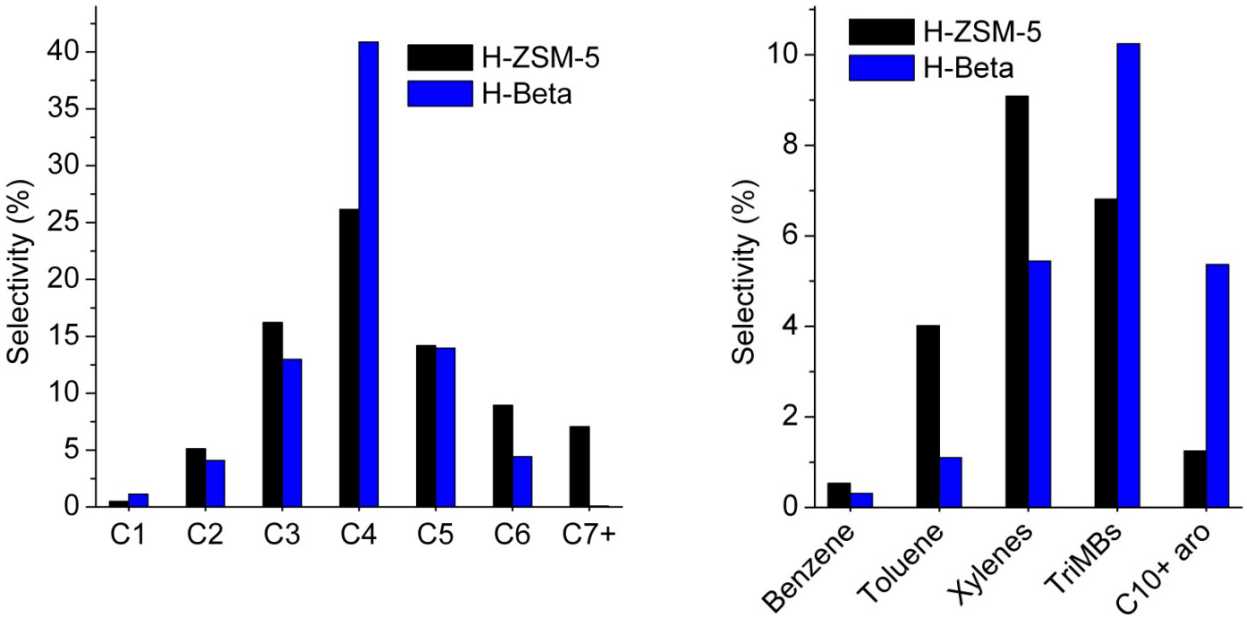

Figure 66: Initial product selectivities (left: Aliphatics, right: Aromatics) for conversion of methanol over H-ZSM-5 (Si/Al = 40) and H-Beta (Si/Al = 19) (T = 370 °C, P = 1 bar)

Initial selectivities for conversion of methanol over H-ZSM-5 and H-Beta are shown in Figure 66. For the aliphatic compounds the product distributions for both catalysts are centered around the C_4 group, but the distribution is more narrow for H-Beta than for H-ZSM-5. No aliphatics larger than C_6 are observed over H-Beta, indicating that these compounds react further as soon as they are formed, either by cracking to smaller aliphatics or by cyclization and hydrogen transfer to produce aromatics. This might be a consequence of the higher acid density of the specific H-Beta catalyst employed. The selectivity within the group of aromatic compounds is clearly shifted towards larger compounds for H-Beta, illustrating the effect of the larger pores of the zeolite structure. The large aromatic compounds include polymethyl benzenes and naphthalenic species.

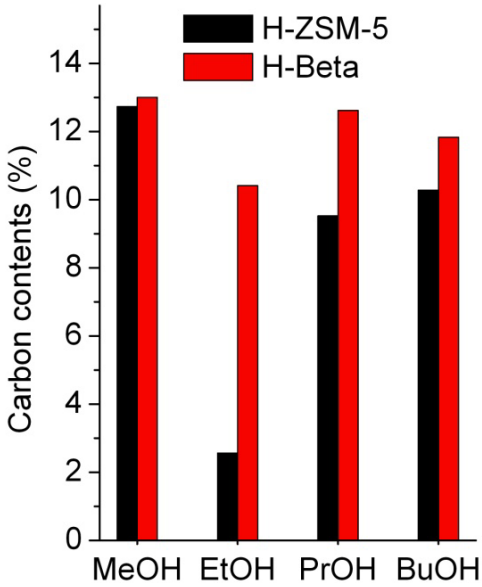

Figure 67: Carbon contents of the spent catalysts upon deactivation during conversion of methanol, ethanol, 2-propanol and 1-butanol over H-ZSM-5 (Si/Al = 40) and H-Beta (Si/Al = 19) (T = 370 °C, P = 1 bar)

The amount of carbon deposited on the spent catalysts is shown in Figure 67. Except for ethanol, there is not a large difference in the amount of coke on the two different zeolites upon deactivation, but due to the huge difference in catalyst lifetime, the rate of carbon deposition is much higher for H-Beta.

The low amount of deposited coke for conversion of ethanol over H-ZSM-5 is a consequence of the low conversion; the catalyst is simply not very effective for conversion of ethanol under these conditions. In experiments performed at slightly higher temperature (400 °C vs. 370 °C) and lower flow of carrier gas (20 mL/min vs. 40 mL/min) more coke is formed from the conversion of ethanol, and the formation of coke increases with the reaction pressure as shown in Figure 58 (page 61).

4.4 Mechanistic considerations

In the following, proposed mechanisms for conversion of C_1-C_4 alcohols are presented. Many aspects of the mechanisms for conversion of the different alcohols are similar, but there are also distinct differences which will be highlighted.

4.4.1 Conversion of methanol over H-ZSM-5

As discussed in Chapter 2, the mechanism for conversion of methanol to hydrocarbons has been debated extensively in literature, and a general acceptance of a hydrocarbon pool type mechanism has been achieved. The more specific “dual cycle” model (see Figure 17, page 20) is also well supported by experiments, but as discussed in Chapter 2 some details are not included in the mechanism. Figure 68 shows the dual cycle mechanism where a few more details have been incorporated.

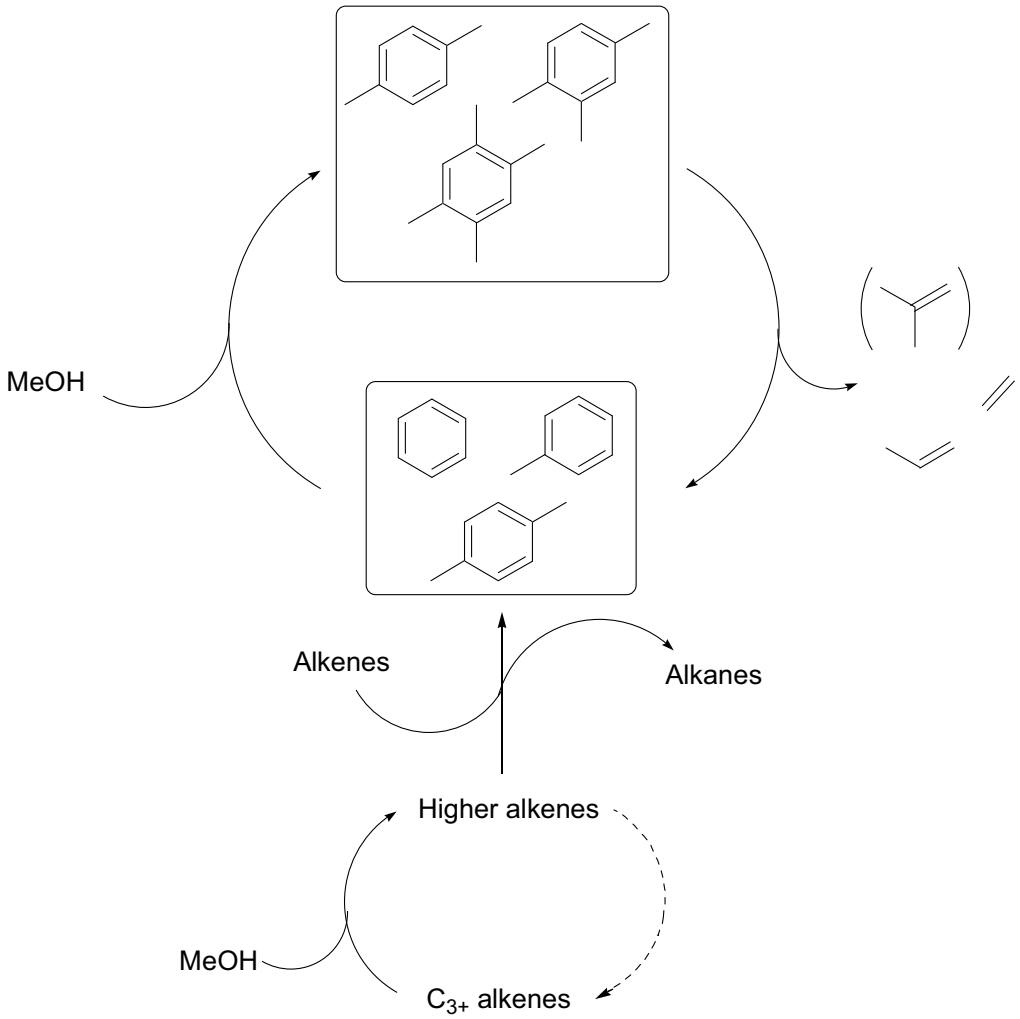

Figure 68: Proposed mechanism for conversion of methanol over H-ZSM-5

Methanol is able to be incorporated in either a C_{3+} alkene or an aromatic compound. The produced alkenes are able to undergo cyclization and hydrogen transfer reactions to form aromatics and alkanes. In the dual cycle mechanism the methylated aromatics are only able to split off ethene, but as discussed on page 20, it is possible to form ethene, propene, and small amounts of *i*-butene from the aromatic compounds. The other variation of the dual cycle mechanism is that cracking of the higher alkenes is suppressed (illustrated by the dashed arrow) when methanol is present in the catalyst bed [46], i.e. inside the methanol conversion zone. Naturally, outside the methanol conversion zone, where methanol is not present, the cycle of alkene oligomerization/cracking is active, but this is not directly connected to the conversion of methanol and is thus a part of the secondary reactions which are discussed below. These small adjustments of the dual cycle mechanism do not change the basic concept of the established mechanism, which is well supported by data.

Even though the proposed mechanism has incorporated a few more details than the dual cycle mechanism, some aspects of the reaction mechanism are not included. For instance methane is produced in fair amounts (above 1 %) from conversion of methanol. The mechanism for formation of methane is not well established in literature, but one could imagine that it is produced directly from

methanol (or surface methoxy groups) in a hydrogen transfer reaction (similar to production of ethane from ethene). Methane is not detected from conversion of ethanol or higher alcohols and therefore it must be produced directly from methanol, or at least it is not produced from aromatics, alkenes or alkanes.

Cycloalkanes and cycloalkenes are also present in the product mixture, but are only detected in very small amounts. These are most likely intermediates in the formation of aromatic compounds from alkenes and might play a role in the mechanism, but this is only speculations and they are not included in the proposed mechanism. The fact that the cyclic aliphatics are only detected in trace amounts in the product mixture indicates that they are dehydrogenated to aromatics very quickly.

4.4.2 Conversion of ethanol over H-ZSM-5

Several reaction pathways could be envisaged for the conversion of ethanol. Unlike methanol, ethanol already contains carbon-carbon bonds, and simple oligomerization of ethene could be envisaged, but this reaction would go via a primary carbocation and the intermediate would have to pass a high energy barrier. When the catalyst deactivates during conversion of propanol or butanol a distinct increase in the selectivity towards the direct dimerization products is observed, but this is not observed for ethanol. Also, for conversion of propanol and butanol, the alkene oligomerization/cracking cycle retains its activity after the production of aromatics has seized, but this is not the case for ethanol either. On the contrary the conversion of ethene declines with the production of aromatics, indicating that the activity of alkene oligomerization is minor and ethene needs the aromatic compounds to convert. These observations indicate that direct ethene oligomerization is most likely not the dominant route for conversion of ethanol, but it might play a minor role.

Many research groups have worked on the zeolite catalyzed conversion of ethanol to hydrocarbons [109, 110] and the direct coupling of ethene entities has been proposed as the main source of larger hydrocarbons [99, 111, 112, 113], but no solid evidence has been given. At higher temperatures this reaction is probably important, but in the temperature range of 350 – 400 °C it is not likely to be dominating, at least when H-ZSM-5 is employed as the catalyst, cf. the discussion above. The fact that oligomerization of ethene is slow compared to oligomerization of propene or butene is supported by quantum chemical modeling [114].

This means that ethanol (or ethene) is most likely converted via a hydrocarbon pool type mechanism as shown in Figure 69, where molecules of ethene are added to aromatic species which in turn split off ethene, propene and small amounts of *i*-butene similar to the conversion of methanol. Propene and butene produced from the hydrocarbon pool are able to oligomerize to higher alkenes, which subsequently can be converted to aromatics.

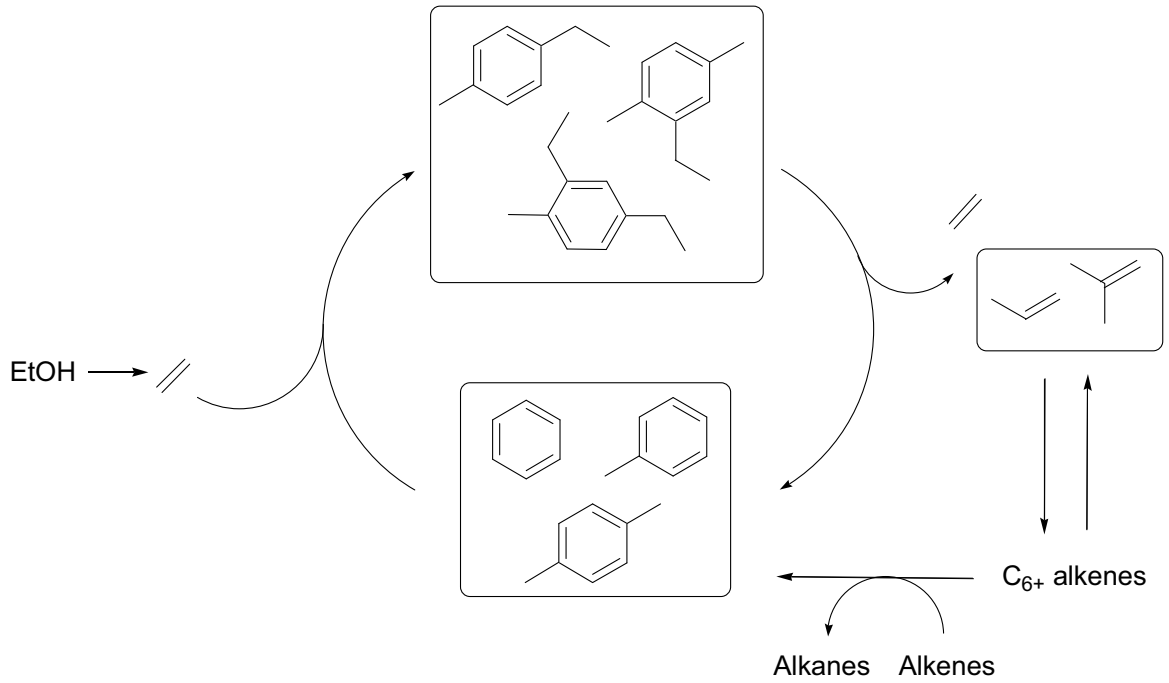

Figure 69: Proposed mechanism for conversion of ethanol over H-ZSM-5

The exact nature of the hydrocarbon pool in the conversion of ethanol is not known, but in a publication from our research group [100] it is shown that ethylated (and methylated) aromatic species are formed inside the zeolite during conversion of ethanol. The catalytic activity of these species is however not addressed, but it is fair to assume that these species split off small alkenes as for conversion of methanol. Due to the larger side chains it might even be possible to produce larger alkenes directly from the hydrocarbon pool. In the outlet of the reactor only minute traces of ethylbenzene are detected, indicating that it rapidly reacts further, if formed. Only small amounts of benzene are available for alkylation with ethene leading to a low formation rate of ethylbenzene. Due to the higher concentration of toluene in the catalyst bed, ethylmethylbenzenes are formed more readily and are detected in larger amounts in the product mixture than ethylbenzene, but still in minor quantities.

4.4.3 Conversion of C_{3+} alcohols over H-ZSM-5

When propanol or butanol is converted over H-ZSM-5, the alcohols dehydrate rapidly to the corresponding alkenes. In contrast to ethene, the larger alkenes (C_{3+}) are able to oligomerize readily under the employed conditions to a mixture of longer chained alkenes (C_{6+}). As for conversion of the smaller alcohols, the long alkenes are able to undergo hydrogen transfer and cyclization to form aromatics and alkanes, and the aromatics are able to split off small alkenes; see Figure 70.

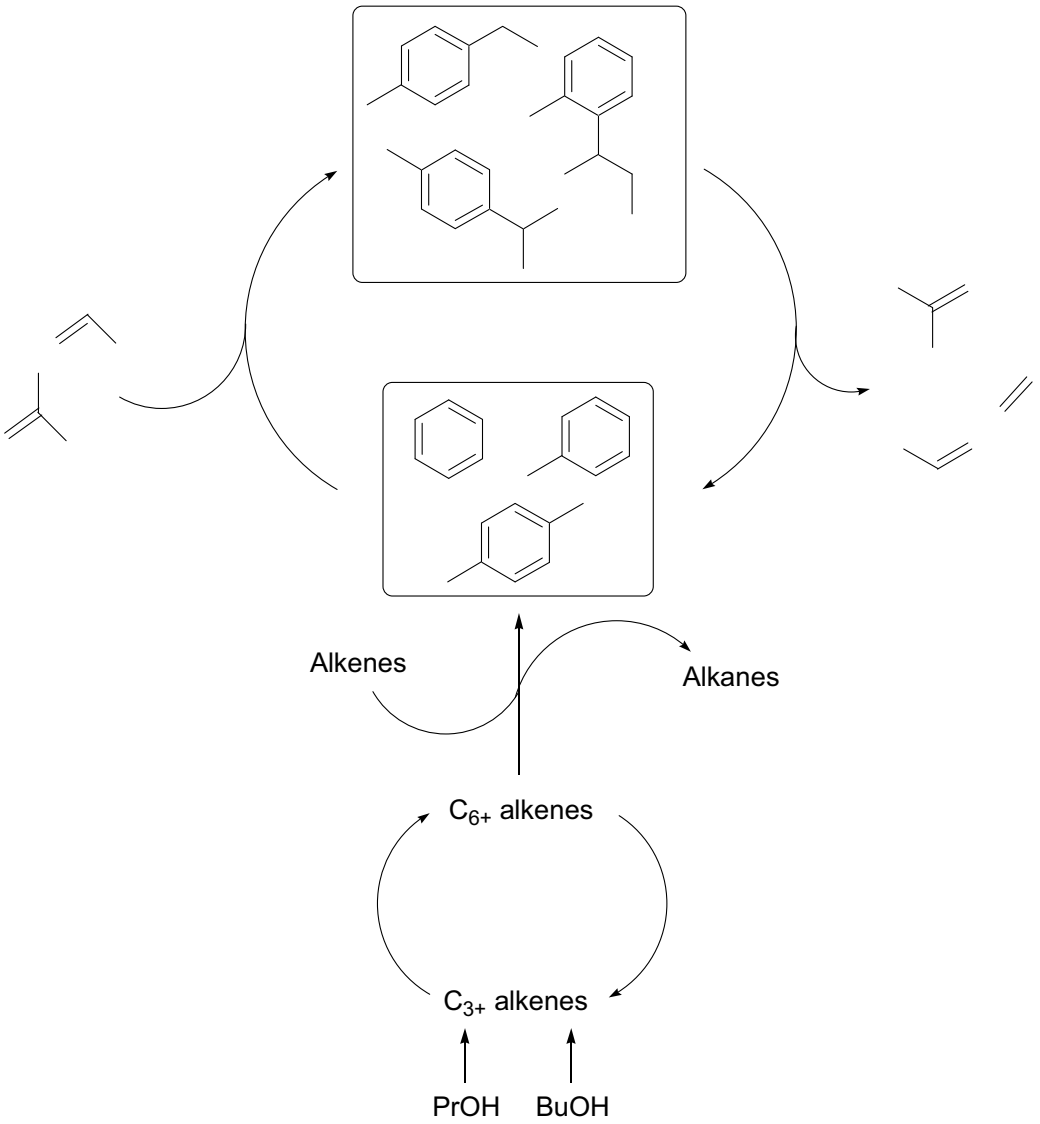

Figure 70: Proposed mechanism for conversion of C_{3+} alcohols over H-ZSM-5

Even though the alkene oligomerization/cracking cycle is very active, one could also imagine that propene or butene could be converted via a hydrocarbon pool type mechanism by addition to aromatic intermediates inside the zeolite as illustrated in Figure 70. This reaction is naturally more sterically hindered than for methanol and ethanol, but it is not implausible since alkylation of aromatics with propene and butene has been reported earlier [115, 116]. Nevertheless, no propylated species were found among the aromatic products during conversion of propanol, indicating that propylation reactions are probably not very active. To confirm this, a co-conversion experiment was performed with 10 wt% toluene in 2-propanol, and interestingly traces of propylated toluene were indeed found in the outlet. Even when the catalyst was almost completely deactivated and no other aromatic compounds were formed, propylated toluene was still observed. This shows that propylation of aromatics is actually taking place. Also, the produced propylated species seem to decompose quite rapidly when the catalyst is active, and it is actually plausible to assume that some propene (and butene) is converted via alkylation of aromatics.

Ethene is not produced from cracking of the higher alkenes. Conversion of 1-butanol over H-ZSM-5 at high temperature showed that even at 500 °C no ethene is produced from the alkene cracking/oligomerization cycle, it simply declines with the aromatics.

A very interesting feature of this mechanism is the fact that the alkene oligomerization/cracking cycle is still active when the cyclization and hydrogen transfer reactions have seized. This indicates that the cyclization and hydrogen transfer reactions take place on specific sites in the zeolite which are deactivated over time, but the oligomerization and cracking reactions of alkenes must take place on other catalytic sites which are deactivated much slower. Another explanation could be simple competition for the catalytic sites, if alkene interconversion reactions and cyclization/hydrogen transfer is occurring over the same sites in the zeolite. If such competition was responsible for the decline in selectivity towards aromatics and alkanes one would still expect to observe small amounts of aromatics when the catalyst is still highly active in alkene interconversion reactions, but this is not the case. Thus, partial deactivation of the catalyst leads to loss of the ability to perform cyclization/hydrogen transfer, while alkene interconversion reactions are still active.

4.4.4 Secondary reactions during conversion of methanol over H-ZSM-5

When zeolite catalyzed methanol conversion is performed, there is a large extend of secondary reactions occurring in the zeolite. Some of these have been summarized in Figure 71. Since ethene and higher alkenes are part of the normal products from methanol conversion, the mechanism for secondary reactions is basically a hybrid of the mechanisms for conversion of ethanol (ethene) and higher alcohols (C_{3+} alkenes). Small alkenes are converted via alkylation of aromatics and the alkene oligomerization/cracking cycle is active. Naturally, hydrogen transfer and cyclization reactions are also taking place.

A very important aspect is if the secondary reactions deactivate the catalyst. The catalyst in the lower part of the bed has performed secondary reactions for quite some time before the methanol front arrives, and coke formation from the secondary reactions might influence the performance of the catalyst in the methanol conversion. If we consider the normal product mixture it consists of alkanes, alkenes and aromatics. Alkanes are quite inert under the employed reaction conditions, and are not likely to form coke. Even though coke mainly consist of condensed aromatic compounds, free aromatic compound such as toluene do not tend to form coke directly, since they are not able to condense to larger compounds without addition of carbon atoms to the ring, which would allow for the aromatic compounds to grow and eventually form coke. Nevertheless, co-existence of small alkenes and aromatics might lead to formation of coke through alkylation and subsequent formation of larger aromatic species.

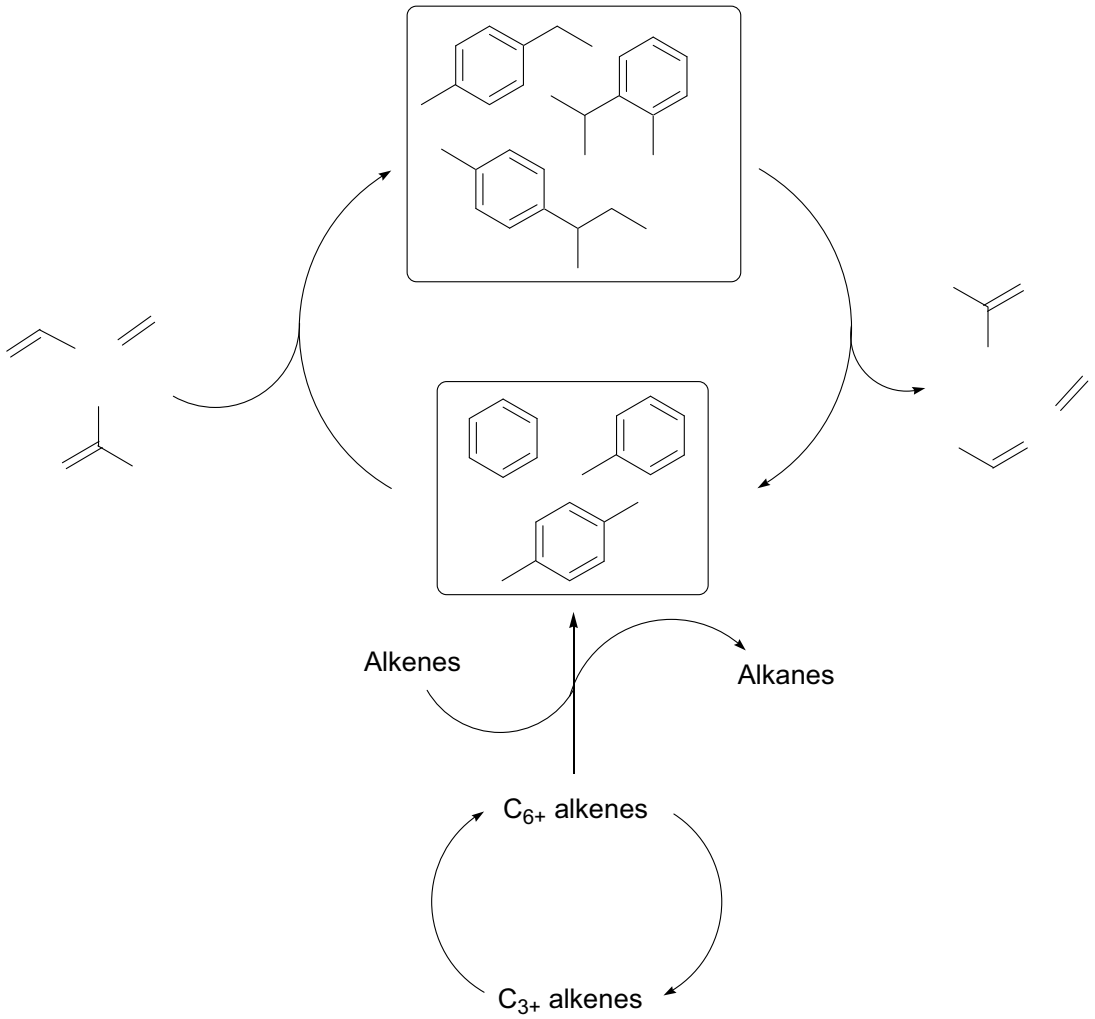

Figure 71: Proposed mechanism for secondary reactions during methanol conversion over H-ZSM-5

The fact that small alkenes are alkylating the aromatics, which in turn split off very similar small alkenes, might seem insignificant and a bit peculiar, but this reaction (among others) is responsible for obtaining the observed selectivity within aromatics and small alkenes. The rate of alkylation is dependent on the concentration of the alkylating agent (alkene) in the catalyst bed. If there is a large excess of a specific alkene, this will be consumed in the reaction, and the intrinsic reactivity of the specific aromatic species formed is responsible for which alkene is split off as a product. Also transalkylation [117] between different aromatic species could play an important role in obtaining the selectivity observed in the outlet.

4.5 Conversion of methanol and 2-propanol over conventional and mesoporous H-ZSM-5 and H-Ga-MFI

In this section a series of experiments concerning conversion of methanol and 2-propanol over conventional and mesoporous H-ZSM-5 and H-Ga-MFI is described.

The H-Ga-MFI zeolite is analogous to H-ZSM-5, but it has gallium atoms incorporated in the zeolite framework instead of aluminum. This decreases the intrinsic acidity of the individual active sites in the zeolite [118] without compromising the zeolite structure significantly, though minor distortion of the framework might take place due to the larger size of a gallium atom [119]. Several reports exists on conversion of methanol to hydrocarbons over H-Ga-MFI type zeolites [120, 121, 122, 123], and typically a higher selectivity towards small alkenes is observed compared to H-ZSM-5 due to the lower acid strength of the Brønsted sites leading to less secondary reactions converting the alkenes to aromatics [123]. Nevertheless, in some cases (especially at high gallium loadings), higher selectivity towards aromatics than for H-ZSM-5 is observed, which is ascribed to the presence of extra framework gallium species [122]. Conversion of higher alcohols such as 2-propanol to hydrocarbons over H-Ga-MFI type zeolites has not been reported, but conversion of propene results in a similar product mixture as for methanol [122]. During methanol conversion, the rate of formation of coke is reported to be somewhat slower for H-Ga-MFI than for H-ZSM-5, most likely as a consequence of the lower acidity of the Brønsted sites [118].

A mesoporous zeolite crystal contains pores in the range of 2-50 nm. This means that reactants gain much easier access to the micropores in the interior of the zeolite crystal improving the effectiveness of the catalyst by diminishing the transport limitations imposed by the micropores [124]. Mesoporosity can be introduced to the zeolite in a range of different ways, e.g. growing the zeolite crystals around carbon nanoparticles and subsequently burn off the carbon to leave mesopores (known as carbon templating [125]) or post synthesis base treatment of the zeolite to create mesopores by removal of silicon atoms from the zeolite framework (known as desilication [126]). Mesoporous H-ZSM-5 has been used to catalyze the MTH reaction in work from several research groups, and the main attribute of the mesoporous zeolites is a prolongation of the catalyst lifetime compared to their conventional counterparts [106, 127, 128].

The introduction of mesopores in a zeolite crystal will unavoidable lead to other changes in the material as well. In the case of desilication, removal of silicon from the framework causes the Si/Al ratio to rise and might also lead to deposition of extra framework aluminum species in the zeolite pores which affects the catalytic properties of the zeolite. For carbon templating, one could imagine that the zeolite contains isolated holes in the zeolite rather than truly interconnected mesopores. Furthermore, the carbon particles might affect the tendency towards formation of defect sites where the zeolite crystal is in contact with the carbon particles which will also affect the catalytic properties of the material.

Even though many catalytic studies on mesoporous zeolites have been performed, only methanol and ethanol [106] have been tested in alcohol conversion to hydrocarbons. Prompted by the interesting behavior of 2-propanol in conversion over H-ZSM-5 described earlier in this thesis, we decided to employ two different mesoporous catalysts in the conversion of 2-propanol to hydrocarbons. The

gallium-containing zeolites were chosen due to their lower acid strength, which should lead to higher selectivity towards alkenes as described above.

4.5.1 Experimental

The conventional H-ZSM-5 (Si/Al = 40) was supplied by Zeolyst International. Conventional H-Ga-MFI and mesoporous H-ZSM-5 and H-Ga-MFI were synthesized by Ph.D. student Karen Thrane Leth according to procedures described elsewhere [89, 129]. The mesoporosity was introduced to the zeolites by carbon templating.

The catalytic reactions were performed in a fixed bed reactor charged with 300 mg catalyst, which was pretreated in a flow of helium at the reaction temperature for 30 min. prior to the reaction. The reaction was performed at 370 °C and 1 bar, and the reactant liquid was pumped with an HPLC pump and evaporated before reaching the reactor. Helium was used as a carrier gas, with a flow of 40 mL/min, and the products from the reaction were analyzed by on-line GC equipped with an FID. The employed feed rates of methanol and 2-propanol are shown in Table 10.

	WHSV (h^{-1})	Feed rate alc. (mol_{alc}/g_{cat}*h)	Feed rate carbon (mol_c/g_{cat}*h)
Methanol	7.9	0.25	0.25
2-Propanol	33.0	0.55	1.65

Table 10: Feed rates for methanol and 2-propanol employed in conversion over H-ZSM-5, H-ZSM-5 meso, H-Ga-MFI, and H-Ga-MFI meso

The TPO analyses were typically performed with 100 mg of spent catalyst which was heated in a flow of 5 % O_2 in helium (20 mL/min) with a heating ramp of 2.75 °C/min to an oven temperature of 700 °C. The final temperature was maintained for 2 h to ensure complete combustion of the carbonaceous species. The concentrations of CO and CO_2 in the outlet were monitored continuously by a BINOS detector.

4.5.2 Catalyst characterization

X-ray diffraction (performed at Haldor Topsøe A/S) shows that all four catalysts are crystalline and posses the MFI structure, no traces of amorphous material is present. Surface areas and micro- and mesopore volumes are shown in Table 11 alongside the elemental compositions obtained from ICP-OES analyses. The gallium based zeolites have a somewhat lower acid density than their H-ZSM-5 based counterparts.

	BET surface area (m^2/g)	V_{micro} (cm^3/g)	V_{meso} (cm^3/g)	Elemental comp. (Si/Al or Si/Ga)
H-ZSM-5	398	0.11	-	37
H-ZSM-5 meso	462	0.11	0.55	40
H-Ga-MFI	296	0.10	-	66
H-Ga-MFI meso	375	0.13	0.48	62

Table 11: BET surface areas and micro- and mesopores volumes obtain from physisorption of nitrogen performed on a Micromeritics ASAP 2020 and elemental composition (Si/Al or Si/Ga ratios) obtained by dissolution of the zeolite in HF followed by ICP-OES analysis performed at Haldor Topsøe A/S

Ammonia TPD of the different catalysts is shown in Figure 72. As expected [118], the Brønsted peak for the gallium containing zeolites is shifted to lower temperature, due to the lower acidity of the active sites. The low temperature peak is usually ascribed to adsorption of multiple ammonia molecules on an acidic site [96], and the stronger acidity of the sites in H-ZSM-5 seems to lead to binding of larger amounts of ammonia pr. site than for the gallium based zeolites. Another explanation for the small low temperature peak for the gallium based zeolites could be that some of the peak is not observed because the sample is flushed with helium at 100 °C prior to the TPD measurement which might lead to desorption of some of the weakly bound ammonia.

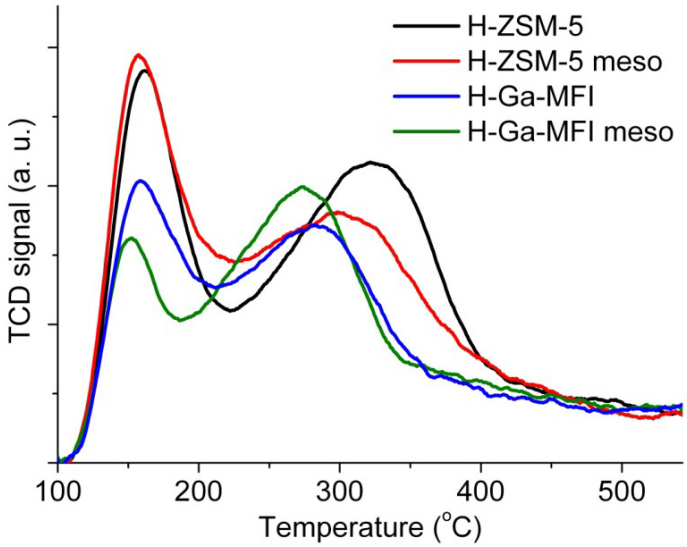

Figure 72: Temperature programmed desorption (TPD) of ammonia for H-ZSM-5, H-ZSM-5 meso, H-Ga-MFI, and H-Ga-MFI meso (Recorded on a Micromeritics Autochem 2920, heating ramp: 15 °C/min)

According to Parrillo *et al.* [130], H-Ga-MFI is indeed a weaker acid than H-ZSM-5, but it is not possible to observe this difference by NH_3-TPD, since the specific experimental conditions (flow rate, type/shape of sample bed, temperature ramp) seem to have a large influence on the results. The amount of sample employed and the acid density of the sample are also able to shift the maximum temperature. Nevertheless, we observe a distinct shift to lower temperatures for both gallium containing catalysts, when the NH_3-TPD is performed at the same conditions.

4.5.3 Results and discussion

4.5.3.1 Conversion of methanol

Conversions and conversion capacities for conversion of methanol over the four different zeolites are shown in Figure 73. The gallium containing zeolites exhibit shorter lifetime than H-ZSM-5, especially conventional H-Ga-MFI deactivates very fast. The mesoporous H-Ga-MFI deactivates much slower than the conventional, and has a lifetime which is almost comparable to H-ZSM-5. For the mesoporous H-ZSM-5, the breakthrough of methanol is observed a bit earlier than for conventional H-ZSM-5, but the decline in conversion is slower resulting in a somewhat higher conversion capacity. This less steep drop in conversion is also observed for mesoporous H-Ga-MFI.

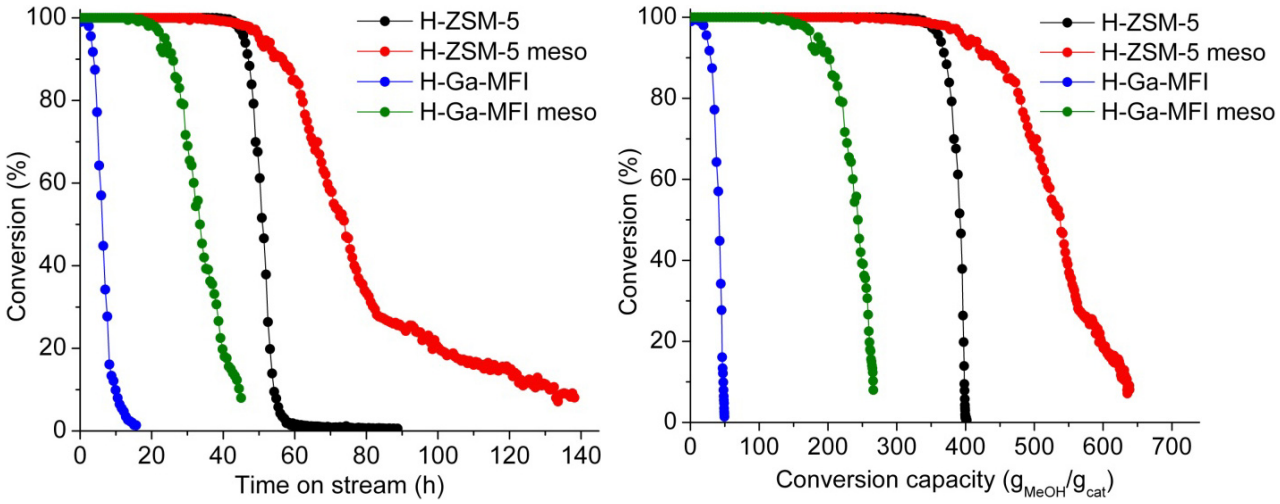

Figure 73: Conversion vs. time on stream and conversion capacities for conversion of methanol over H-ZSM-5, H-ZSM-5 meso, H-Ga-MFI, and H-Ga-MFI meso (T = 370 °C, P = 1 bar)

Figure 74 shows the yield of aromatics vs. time on stream and the C_4-HTI. It is clear that the gallium based zeolites has a distinct lower selectivity towards aromatics than H-ZSM-5, which is also reflected in a lower hydrogen transfer activity of the catalysts. For all the catalysts, the production of aromatics decline with time on stream due to loss of active catalyst.

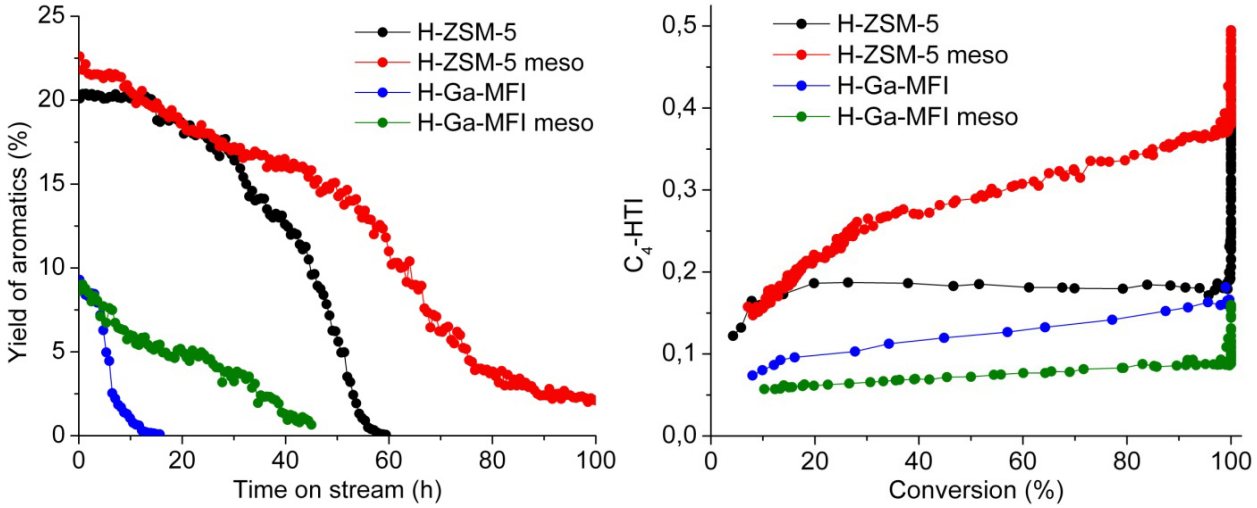

Figure 74: Yield of aromatics vs. time on stream (left) and C_4-HTI vs. conversion (right) for conversion of methanol over H-ZSM-5, H-ZSM-5 meso, H-Ga-MFI, and H-Ga-MFI meso (T = 370 °C, P = 1 bar)

Although the gallium based zeolites have a somewhat lower acid density than the H-ZSM-5 zeolites, the lower selectivity towards aromatics for the gallium containing zeolites most likely is a consequence of the intrinsic lower acidity of the individual active sites.

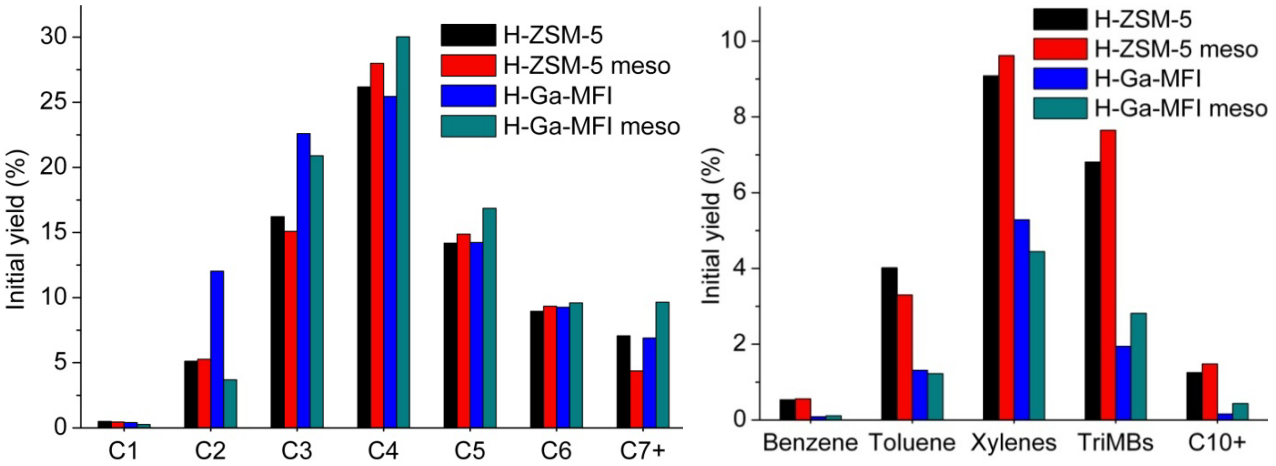

Figure 75: Initial product yields of aliphatics (left) and aromatics (right) for conversion of methanol over H-ZSM-5, H-ZSM-5 meso, H-Ga-MFI, and H-Ga-MFI meso (T = 370 °C, P = 1 bar)

Detailed initial product yields of aliphatics and aromatics for conversion of methanol are shown in Figure 75. Apart from the higher amount of aromatics produced from the two H-ZSM-5 based zeolites, the selectivities for the different catalysts are quite similar, which is reasonable since they all have the MFI structure. Nevertheless, H-Ga-MFI produces large amounts of propene and especially ethene, while the mesoporous H-Ga-MFI produce larger amounts of long chain aliphatics, indicating a lower cracking activity of this catalyst. Since ethene is produced from the aromatic compounds, one could expect the amount of aromatics to be significantly higher for H-Ga-MFI, but that is not the case. An explanation could be that the catalyst is simply not as active in conversion of ethene leading to a higher concentration in the outlet.

Another interesting observation is that the gallium containing zeolites produce only very small amounts of benzene. This might be a consequence of methanol being available for methylation reactions in a larger part of the catalyst bed, but it could also arise from the fact that benzene is simply produced in lower amounts due to the lower hydrogen transfer activity of the catalysts.

The mesoporous zeolites produce slightly larger amounts of large aromatic compounds than their conventional counterparts, which might be a direct effect of the mesoporosity leading to a shorter diffusion path for the larger compounds.

4.5.3.2 Conversion of 2-propanol

Figure 76 shows conversions and conversion capacities for conversion of 2-propanol over the four different zeolites. As for conversion of methanol, H-Ga-MFI shows a very short lifetime, and the conversion curve has a completely different shape than for the other catalysts; the conversion drops very rapidly in the beginning of the experiment. Interestingly mesoporous H-Ga-MFI has an exceptionally long lifetime. It clearly outperforms the conventional H-ZSM-5, and also the mesoporous H-ZSM-5 seems to deactivate faster than its gallium based counterpart. The catalyst is still highly active when the experiment is discontinued after almost 700 h on stream. This behavior is in stark contrast to the methanol conversion experiments, where the mesoporous H-Ga-MFI lost its activity faster than the conventional H-ZSM-5. For mesoporous H-ZSM-5, extrapolation of the curve gives a conversion capacity around 18,000 g/g, which is more than twice that of the conventional H-ZSM-5. For the mesoporous H-

Ga-MFI, this extrapolation is simply not possible, since the curve is too flat due to very slow deactivation of the catalyst.

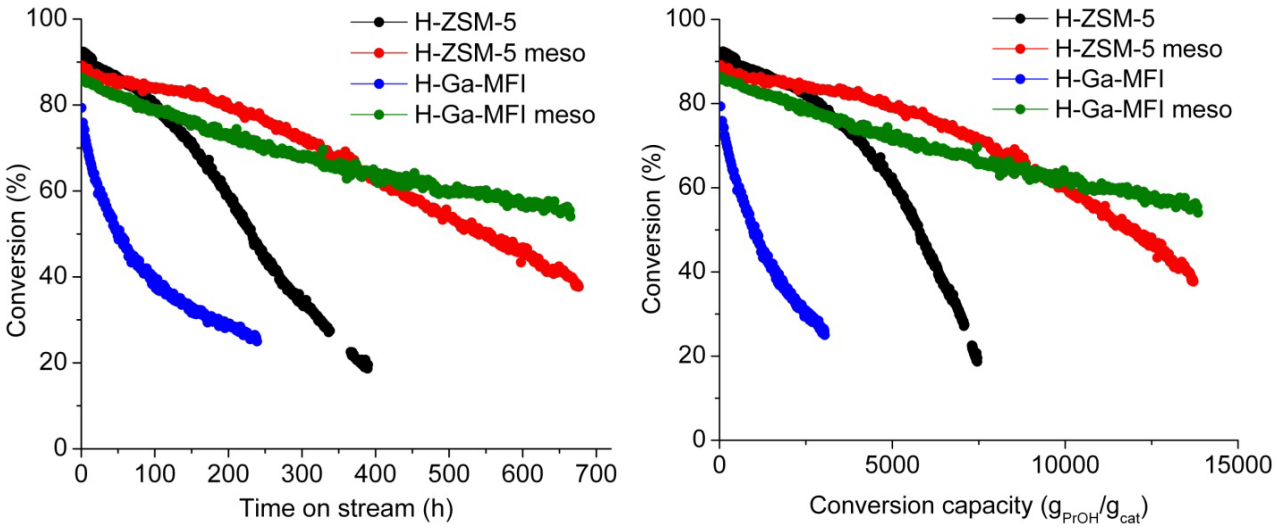

Figure 76: Conversion vs. time on stream (left) and conversion capacities (right) for conversion of 2-propanol over H-ZSM-5, H-ZSM-5 meso, H-Ga-MFI, and H-Ga-MFI meso (T = 370 °C, P = 1 bar)

The yield of aromatics as a function of time on stream for conversion of 2-propanol over the four different zeolites is shown in Figure 77 (left). As expected, the production of aromatics declines rapidly with time on stream for all the catalysts. Only H-ZSM-5 has an initial yield of aromatics comparable to what is observed for methanol conversion, while the other catalysts only produce small amounts of aromatics. Especially the gallium containing catalysts show a very low selectivity towards aromatics, which is accounted to the lower intrinsic acid strength of the active sites in the zeolite compared to H-ZSM-5. In the case of mesoporous H-Ga-MFI, this means that even though the catalyst is highly active in conversion of 2-propanol (propene), almost no aromatics are observed. The catalyst is simply able to perform reactions such as oligomerization, cracking and isomerization while the hydrogen transfer activity is diminished. The conventional H-Ga-MFI catalyst shows an even lower yield of aromatics, but as mentioned the catalyst deactivates quite rapidly. The reason for the very quick deactivation is not known, but one might think that something could be wrong with the specific zeolite sample employed in the experiments. Therefore, another sample (from another synthesis batch) was employed in the reaction and very similar results were obtained.

The mesoporous H-ZSM-5 and the two gallium containing zeolites have a lower initial selectivity towards aromatics for conversion of 2-propanol compared to methanol. When comparing these values, one should keep in mind that due to differences in the feed rate of the two reactants, the catalysts converts more than six times the amount of carbon when 2-propanol is converted (see Table 10). This means that the lower production of aromatics from 2-propanol might be due to occupancy of the catalytic sites for dehydration and oligomerization/cracking leaving less catalyst available for hydrogen transfer and cyclization.

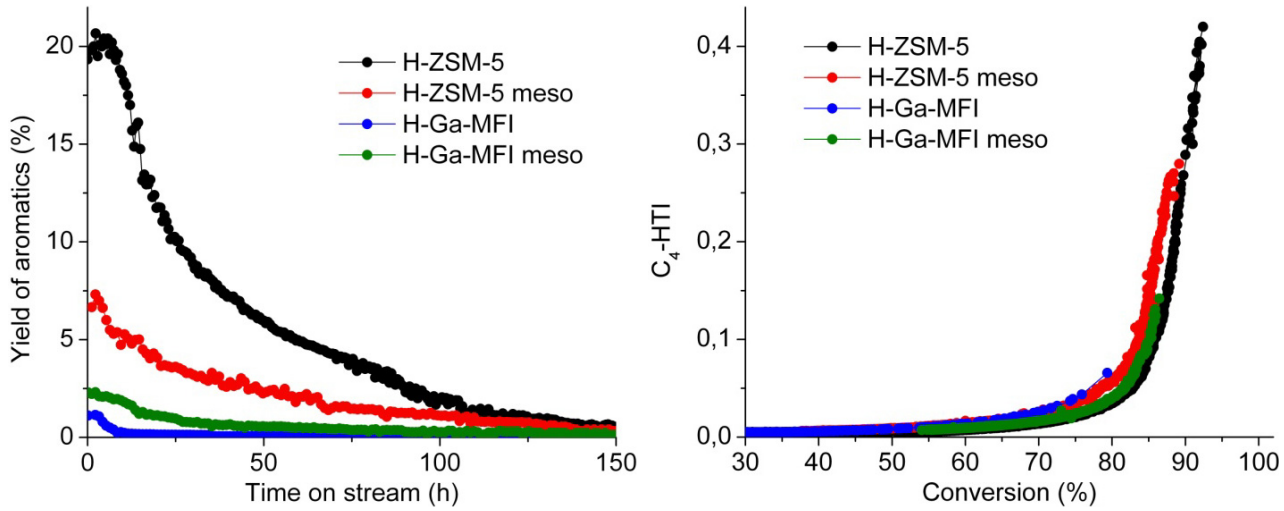

Figure 77: Yield of aromatics vs. time on stream (left) and C_4-HTI vs. conversion (right) for conversion of 2-propanol over H-ZSM-5, H-ZSM-5 meso, H-Ga-MFI, and H-Ga-MFI meso (T = 370 °C, P = 1 bar)

Figure 77 (right) shows the C_4-HTI plotted against the conversion. Interestingly, all the catalysts seem to follow the same trend as the catalyst deactivates, but the initial value of C_4-HTI is quite different for the four catalysts, which is expected when considering the difference in the production of aromatics. When considering the hydrogen transfer ability of the catalysts, one could argue that the gallium zeolites act as H-ZSM-5 which has been slightly deactivated.

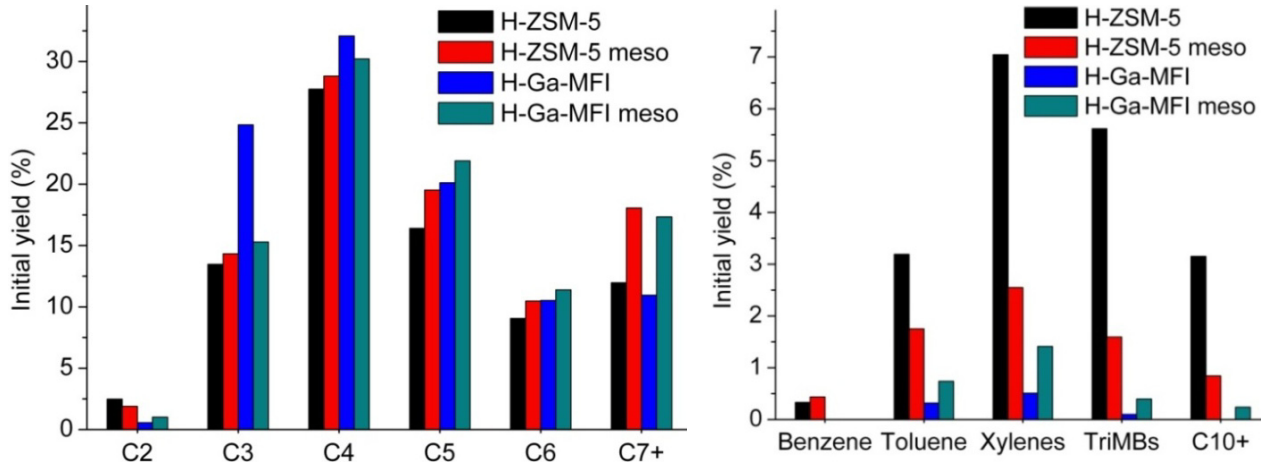

Figure 78: Initial product yields of aliphatics (left) and aromatics (right) for conversion of 2-propanol over H-ZSM-5, H-ZSM-5 meso, H-Ga-MFI, and H-Ga-MFI meso (T = 370 °C, P = 1 bar)

The detailed initial yields within aliphatics and aromatics for conversion of 2-propanol are shown in Figure 78. The high yield of propene for H-Ga-MFI is simply due to low conversion of propene. None of the catalysts produce any methane which is why it is not included in the graph. The gallium containing zeolites produce less ethene than the H-ZSM-5 zeolites since the production of ethene is linked to the concentration of aromatics. In general, the two mesoporous zeolites show higher selectivity towards larger aliphatic compounds; especially the group of C_{7+} compounds is enriched.

A low amount of benzene was observed for conversion of methanol over the two gallium containing zeolites, but in the case of 2-propanol benzene is not observed in measurable amounts. It is quite

peculiar that even though toluene and xylenes are formed in reasonable amounts, no benzene is detected at all. Benzene can be formed from C_6 alkenes through cyclizations and hydrogen transfer reactions, or it can be formed from decomposition of xylene or higher aromatics. Apparently these routes are not active for conversion of 2-propanol over the gallium based zeolites.

4.5.3.3 Coke deposition

The coke deposition on the various zeolites has been investigated through TPO analyses of the spent catalysts and the resulting carbon contents in the various zeolites upon conversion of methanol and 2-propanol are shown in Figure 79. Generally, the H-ZSM-5 based zeolites contain much more coke than the gallium based. In the case of conversion of methanol, H-Ga-MFI contains only 1 % carbon, while mesoporous H-Ga-MFI contains as little as 0.2 % carbon even though the catalysts are fully deactivated. This extremely low coke content is immediately apparent from visual inspection since the deactivated mesoporous H-Ga-MFI is light grey, while the H-ZSM-5 based catalysts are black (see Figure 80). Unfortunately, deactivated H-Ga-MFI is not included in the picture, but this was also light grey. Methanol does not seem to form significant amounts of coke when converted over the gallium based catalysts which is quite remarkable.

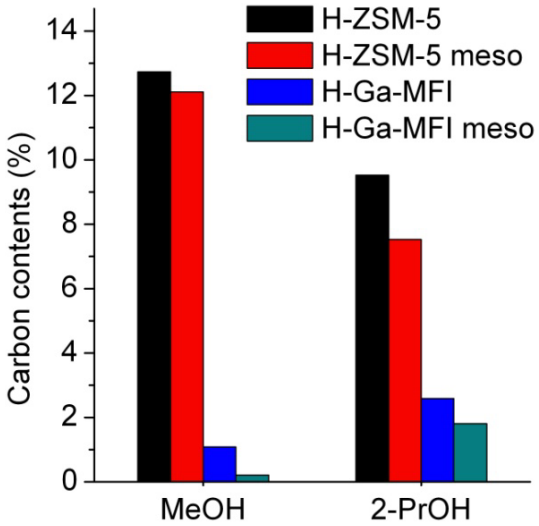

Figure 79: Carbon contents in spent catalysts upon conversion of methanol or 2-propanol over H-ZSM-5, H-ZSM-5 meso, H-Ga-MFI, and H-Ga-MFI meso (T = 370 °C and P = 1 bar)

For conversion of 2-propanol the H-ZSM-5 based catalysts contain less coke, while the gallium based zeolites contains more coke compared to the conversion of methanol. In the case of 2-propanol, the catalysts have not been fully deactivated; especially the mesoporous catalysts were still highly active when the experiments were discontinued. At full deactivation, the catalysts would contain somewhat larger amounts of coke.

Another interesting detail in the picture of deactivated catalysts in Figure 80 is the fact that the quartz wool holding the catalyst in place in dark grey at the end of the catalyst bed for the mesoporous catalysts. This indicates that large hydrocarbon compounds (most likely heavy aromatics) are able to leave the catalyst instead of forming coke, which might be part of the explanation of their superior lifetime.

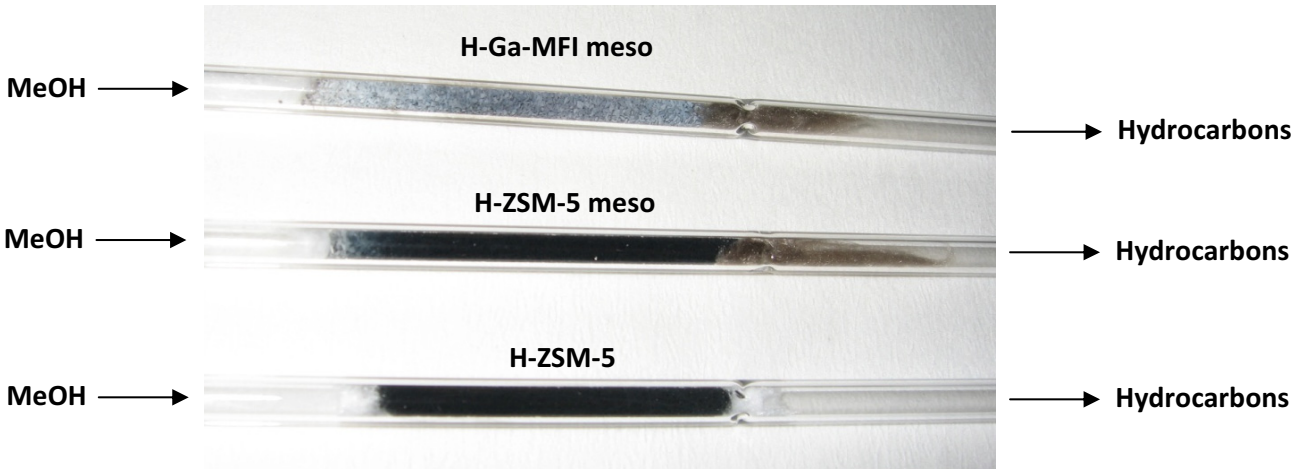

Figure 80: Picture of deactivated catalysts (mesoporous H-Ga-MFI, mesoporous H-ZSM-5, and conventional H-ZSM-5) upon conversion of methanol at 370 °C

For better comparison of the rate of coke formation, the ratios between the amount of carbon atoms converted and the amount of carbon atoms deposited on the catalyst during the entire catalyst lifetime are shown in Figure 81. For conversion of methanol, a combination of reasonable conversion capacity and a very small amount of deposited coke, leads to a remarkably high value for the mesoporous H-Ga-MFI. This catalyst is able to convert over 20 times as much carbon (in the form of methanol) pr. carbon atom deposited than any of the other catalysts even though it had a shorter lifetime than H-ZSM-5, which indicates that it deactivates through a different route. As mentioned in the introduction, H-Ga-MFI is reported to form coke at a slower rate than H-ZSM-5 during methanol conversion, but carbon contents above 10 % are measured at deactivation [118]. This is in stark contrast to what is observed for the gallium containing samples presented here.

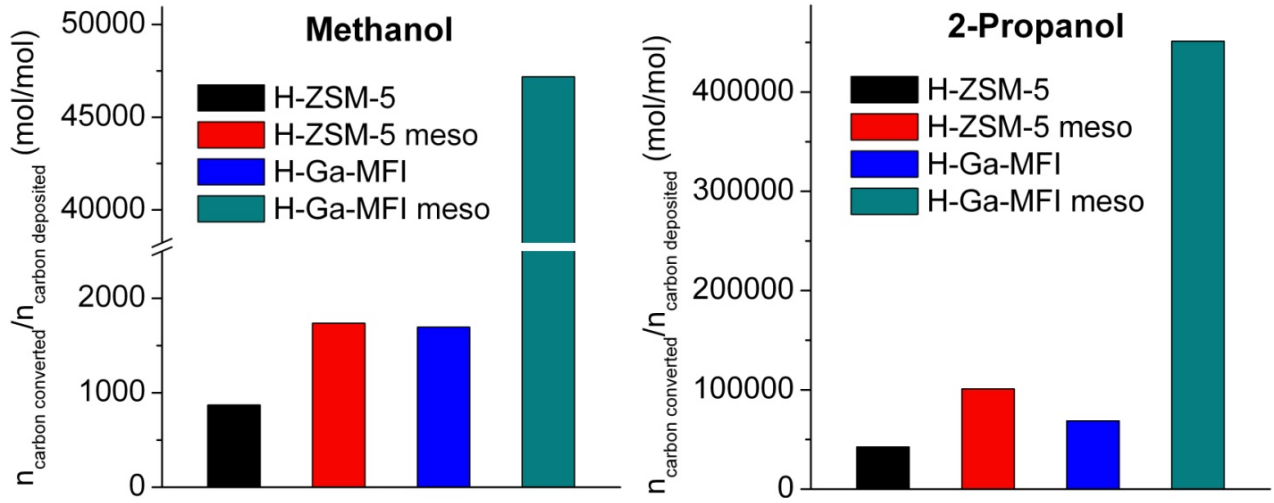

Figure 81: The molar ratios between the amount of carbon converted and the amount of carbon deposited as coke on the catalyst during the entire lifetime of the catalyst for conversion of methanol (left) or 2-propanol (right) over H-ZSM-5, H-ZSM-5 meso, H-Ga-MFI, and H-Ga-MFI meso (T = 370 °C, P = 1 bar)

Also for conversion of 2-propanol, mesoporous H-Ga-MFI is subjected to much less carbon deposition than the other catalysts. It is able to convert almost half a million carbon atoms pr. carbon atom

deposited as coke, which is over 4 times more than any of the other catalysts. The two mesoporous zeolites are not fully deactivated when the experiments were discontinued, and according to Figure 61 (page 62) the rate of coke formation during conversion of 2-propanol is very low in the last part of the experiment, meaning that the total amount of carbon converted pr. carbon deposited would probably be higher if the reaction was allowed to continue to deactivation.

Despite the fact that the spent mesoporous H-Ga-MFI only contains a very small amount of coke, it is still completely deactivated. This means, that the catalyst is either very sensitive towards the presence of coke, i.e. a very small amount of coke is enough to deactivate it, or it is deactivated in another way than coke deposition. The most obvious explanation would be steaming of the zeolite meaning that a combination of water presence and relatively high temperature causes the gallium-oxygen bonds in the zeolite to hydrolyze leading to loss of gallium from the framework and thereby loss of catalytic activity. For H-ZSM-5 this process requires higher temperatures to occur [131], but gallium might be more vulnerable than aluminum in this context. On the other hand, steaming of Ga-MFI is reported to occur under "mild" conditions at 550 °C in a stream of air saturated with water [132], which is much more severe conditions than in the methanol conversion experiment presented here. Also, if steaming was the cause of the deactivation it should also be observed during the conversion of 2-propanol where water is also formed. Naturally, 2-propanol does not lead to the formation of as much water pr. carbon atom as methanol, but the feed rate of 2-propanol is much higher and more water is actually present during conversion of 2-propanol compared to conversion of methanol in the shown experiments. If steaming takes place during conversion of 2-propanol it is either happening at an extremely slow rate since the catalyst only deactivates very slowly, or if the gallium atoms are in fact dislodged from the framework the generated extra framework gallium species might be active in propene oligomerization.

In order to investigate if the mesoporous H-Ga-MFI has lost its activity due to steaming, NH_3-TPD is performed on the fresh and regenerated (by combustion of coke, upon conversion of methanol) catalyst to investigate if acidity is lost, see Figure 82. Some acidic sites are lost, but a large part of the Brønsted peak is still present, indicating that some steaming might have taken place, but acidic sites are still present. The shift in temperature of the peak maximum is most likely a consequence of the lower number of acidic sites.

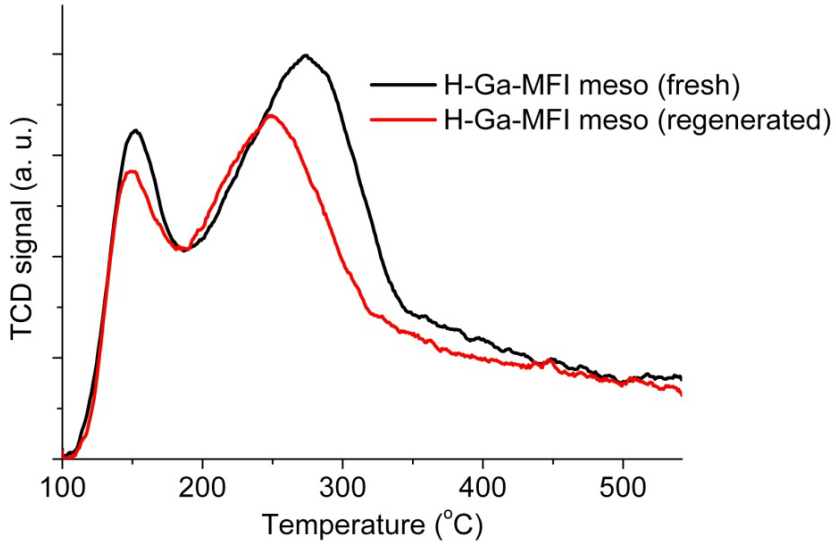

Figure 82: NH_3-TPD of mesoporous H-Ga-MFI, fresh and regenerated by combustion of coke in a flow of 5 % O_2 in helium at 550 °C (upon deactivation during conversion of methanol)

The presence of mesopores might make the zeolite structure more vulnerable, so in order to investigate if the zeolite structure was damaged/collapsed during the deactivation and regeneration, X-ray diffraction was performed on the fresh and regenerated mesoporous H-Ga-MFI resulting in the diffractograms shown in Figure 83. There are no observable differences between the two diffractograms, indicating that the zeolite structure is retained after regeneration.

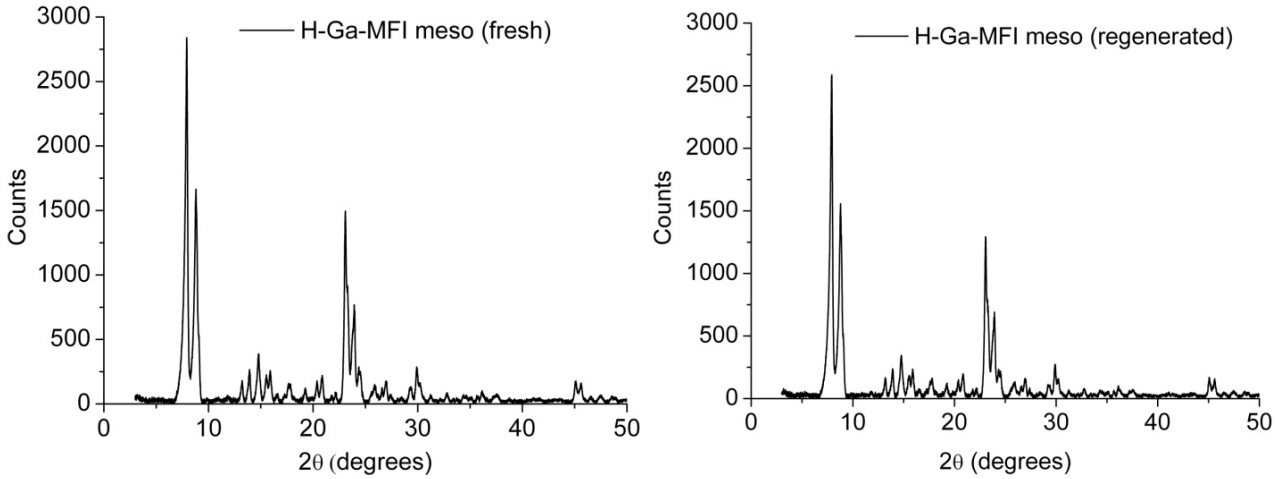

Figure 83: X-ray diffractograms of mesoporous H-Ga-MFI, fresh (left) and regenerated (right) by combustion of coke in a flow of 5 % O_2 in helium at 550 °C (upon deactivation during conversion of methanol)

The rather inconclusive results from NH_3-TPD led us to investigate the activity of the regenerated catalyst in a more direct manner. Upon deactivation during conversion of methanol, the catalyst was regenerated by combustion of the deposited coke, and subjected to methanol again in order to investigate the catalytic activity. This revealed that the catalyst is not active at all in the conversion of methanol upon combustion of coke which is not very surprising due to the very small amount of coke deposited. But as shown in Figure 84 when the feed is changed from methanol to 2-propanol over the same regenerated catalyst, high conversion of 2-propanol is observed for more than 70 h, until the feed

is stopped. In order to investigate if the catalyst is active in alkene methylation reactions, the feed is changed to a mixture of methanol (25 %) and 2-propanol (75 %). This results in high conversion of methanol while the conversion of 2-propanol (propene) is somewhat lower. This means that the regenerated catalyst which is completely inactive in the conversion of methanol by itself is able to convert 2-propanol readily, and furthermore it is also able to convert methanol when 2-propanol (propene) is present in large amounts in the catalyst bed, meaning that the catalyst is able to perform alkene methylation with methanol. Due to a high value of WHSV for the experiments concerning conversion of 2-propanol, the WHSV of methanol is the same in the methanol/2-propanol mixture as when methanol is converted on its own.

It should be mentioned, that when 2-propanol is fed to a deactivated H-ZSM-5 upon conversion of methanol, only minor conversion is observed. The catalyst is simply deactivated by formation of massive amounts of coke in contrast to the mesoporous H-Ga-MFI.

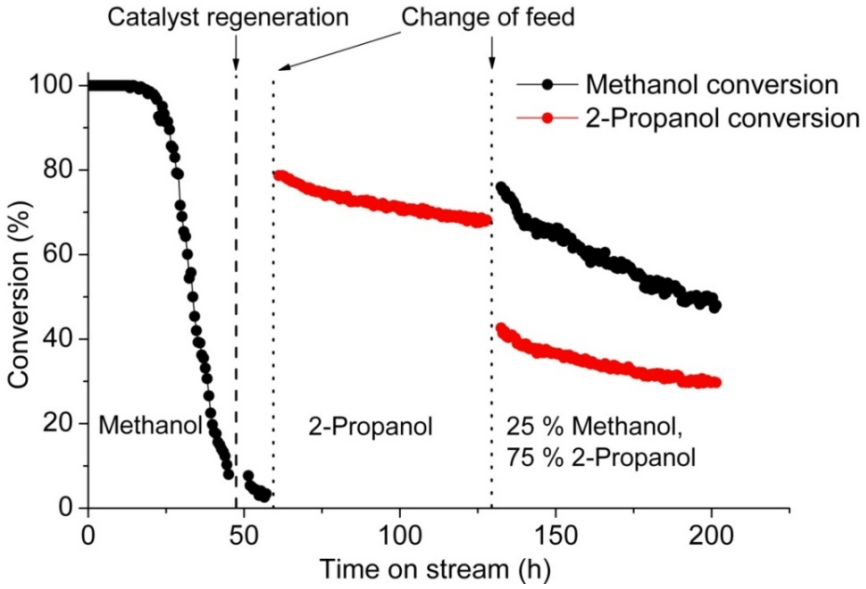

Figure 84: Conversion of methanol and 2-propanol over regenerated H-Ga-MFI meso. The catalyst is deactivated in methanol, regenerated by combustion of coke, and subjected to methanol (WHSV = 7.9 h^{-1}), followed by 2-propanol (WHSV = 32.0 h^{-1}) and 25 % methanol in 2-propanol (WHSV = 32.0 h^{-1}, corresponding to 8.0 h^{-1} for methanol)

The product distributions from the experiment concerning conversion of methanol and 2-propanol over regenerated mesoporous H-Ga-MFI are shown in Figure 85. When 2-propanol is led to the catalyst after deactivation in methanol almost no aromatics are formed. The product distribution is very similar to what is observed for conversion of 2-propanol, when the catalyst is partially deactivated and has lost its ability to perform hydrogen transfer reactions. This indicates that the ability to perform hydrogen transfer is not lost due to formation of coke (in the case of mesoporous H-Ga-MFI), since the coke has just been removed from the catalyst, meaning that the zeolite itself or at least the nature of the active sites must have been subjected to changes. If this is caused by partial steaming or by some other effect is not known. Due to the very small amount of deposited coke, the regeneration of the catalyst has most likely no major effect and the same reactivity of 2-propanol would be observed without preceding regeneration.

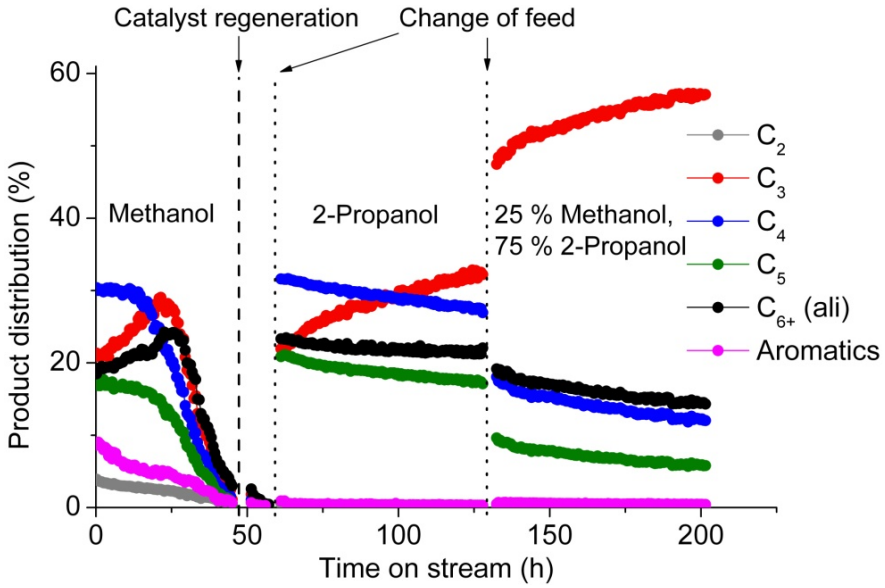

Figure 85: Product distributions for conversion of methanol and 2-propanol over regenerated H-Ga-MFI meso. The catalyst is deactivated in methanol, regenerated by combustion of coke, and subjected to methanol (WHSV = 7.9 h^{-1}), followed by 2-propanol (WHSV = 32.0 h^{-1}) and 25 % methanol in 2-propanol (WHSV = 32.0 h^{-1}, corresponding to 8.0 h^{-1} for methanol)

When the feed is changed from 2-propanol to 25 % methanol in 2-propanol, the production of aromatics is still negligible, and the product mixture consists almost exclusively of C_{3+} alkenes. This is a very interesting result, since methanol is actually converted to hydrocarbons without production of aromatics. In other words, if we consider the dual cycle mechanism for methanol conversion (Figure 17, page 20), cycle II is running independently of cycle I under these conditions, which is a highly desired goal for methanol conversion [28]. Of course, 2-propanol is needed in order for methanol to convert, but smaller amounts that 75 % might be enough, this has not been tested. Furthermore, instead of co-feeding 2-propanol, a part of the product mixture could easily be recycled which would most likely have the same effect, and the overall process would be conversion of methanol to C_{3+} alkenes.

The fact that mesoporous H-Ga-MFI is able to perform alkene methylation and interconversion reactions, without any significant hydrogen transfer activity of the catalyst makes one wonder what is actually the active catalytic sites for these reactions. The fact that no hydrogen transfer takes place indicates that no strong Brønsted acidic sites are present in the zeolite. But if the Brøndsted sites are altered somehow to weak acid sites, or if extra framework gallium species are responsible for the alkene methylation and interconversion is not known. Naturally, it would be very interesting to explore why the catalyst acts this way. An interesting experiment could be to address the possible activity of extra framework gallium species by employing an MFI silicalite impregnated with gallium species in the reaction. As discussed in Chapter 3, extra framework gallium species are active in dehydrogenation reactions and silicalite impregnated with extra framework Ga_2O_3 has been employed in dehydrogenation of propane at 600 °C [132]. Low conversion is observed and no aromatics are produced. Unfortunately, the authors do not reveal the detailed product composition, meaning that we do not know if oligomerization of propene formed in the reaction takes place.

If extra framework gallium species were present in the experiment, one could expect to observe dehydrogenated products, but this is not the case perhaps due to the relatively low temperature.

4.6 Conclusions

When methanol, ethanol, 2-propanol, and 1-butanol are converted to hydrocarbons over zeolite H-ZSM-5 the initial product distributions are quite similar, but the lifetime of the catalyst is markedly higher for conversion of the C_{3+} alcohols compared to methanol and ethanol. In fact the conversion capacity of the catalyst is more than 20 times higher for the C_{3+} alcohols than for methanol and ethanol. Furthermore, for conversion of C_{3+} alcohols the selectivity towards aromatics decline during the experiments and after ca. a third of the entire run-time the catalyst produces no aromatics and the product mixture consists almost exclusively of olefinic compounds in the range of C_3-C_{12}. When the reaction is performed at elevated pressure (up to 20 bar), the same tendencies concerning catalyst lifetime and shift in selectivity are observed.

TPO of the spent catalysts revealed that conversion of methanol leads to the formation of more coke on the catalyst than the other alcohols. Furthermore, the amount of deposited coke is independent of the reaction pressure for conversion of methanol, while elevated reaction pressures leads to higher amounts of coke on the deactivated catalyst for conversion of ethanol and 2-propanol. This indicates that for ethanol and 2-propanol the elevated pressure induces a more effective use of the catalyst.

For conversion of methanol, coke is deposited on the catalyst at a constant rate throughout the entire experiments, until the catalyst is completely deactivated and the methanol front reaches the end of the catalyst bed. This picture is very different for conversion of 2-propanol, where the rate of coke formation is high in the beginning of the experiment when the catalyst is highly active and the product mixture is rich in aromatics. In the last part of the experiment, when the selectivity has shifted towards the formation of alkenes, the rate of coke formation is much lower. Not surprisingly, there seems to be a link between the formation of coke on the catalyst and the activity of hydrogen transfer reactions of the catalyst reflected in the production of aromatics and alkanes.

When zeolite H-Beta is employed in the conversion of C_1-C_4 alcohols the catalyst lifetime and conversion capacity is very low compared to H-ZSM-5, and H-Beta shows very high initial hydrogen transfer ability, which declines with the length of the carbon chain of the alcohol. Furthermore, conversion of methanol leads to higher conversion capacity than the other catalysts, which is in stark contrast to H-ZSM-5. No experimental attempts were made to rationalize the very short lifetime for conversion of higher alcohols over H-Beta compared to H-ZSM-5, but a plausible explanation could be that the large pores of H-Beta allows this reaction to occur readily, leading to the formation of coke inside the zeolite pores.

For conversion of methanol over H-Ga-MFI a higher selectivity towards small alkenes is observed due to the lower acidity of the individual active sites compared to H-ZSM-5 leading to lower activity of hydrogen transfer reactions. Unfortunately, the lifetime of the specific H-Ga-MFI sample is very short. If a mesoporous H-Ga-MFI is employed in methanol conversion, the production of aromatics is still lower than for H-ZSM-5, and the lifetime of the catalyst is almost comparable to that of H-ZSM-5. As expected, mesoporous H-ZSM-5 has a slightly longer lifetime than the conventional H-ZSM-5, and the product

distributions are quite similar, although the mesoporous zeolites tend to produce slightly larger compounds than their conventional counterparts. Interestingly, when 2-propanol is employed as reactant over mesoporous H-Ga-MFI, the lifetime is much longer than for H-ZSM-5, which is in contrast to what was observed for conversion of methanol. Mesoporous H-ZSM-5 also shows significantly longer lifetime than its conventional counterpart, but not as long as the mesoporous H-Ga-MFI.

The gallium based zeolites contains only very small amounts of coke upon deactivation. In fact, for conversion of methanol, mesoporous H-Ga-MFI is able to convert more than 20 times the amount of carbon pr. carbon atom deposited as coke than H-ZSM-5. This is quite remarkable, but despite the very low content of coke the catalyst is still completely deactivated and has a shorter lifetime than H-ZSM-5. In an attempt to regenerate the catalyst the coke was removed by combustion, but subsequently the catalyst did not show any activity for methanol conversion, i.e. the formation of coke is not responsible for the loss of activity during methanol conversion. Interestingly, when the feed is changed to 2-propanol or a mixture of methanol and 2-propanol over the same deactivated catalyst high conversion is observed. This shows that the active sites for conversion of methanol are indeed different from the sites responsible for conversion of 2-propanol (propene), and furthermore it is possible to convert methanol over a presumably deactivated catalyst in the presence of 2-propanol via methylation of alkenes. The selectivity towards aromatics is negligible in this reaction, meaning that this process converts methanol to C_{3+} alkenes without production of aromatics. If the 2-propanol in the feed is replaced by mixed alkenes from recirculation of the products, it would be possible to convert methanol directly to C_{3+} alkenes without formation of aromatics.

5 Production of hydrocarbons from other oxygenates

Increasing crude oil prices and environmental concerns has prompted researchers worldwide to develop alternatives to the fossil energy sources. Hydrogen can be produced from alternative sources, and is a possible candidate for the energy carrier of the future, but as emphasized in Chapter 1 methanol might be a better choice. Concerning transportation fuels, liquid hydrocarbons are much more convenient than hydrogen since the use of hydrogen requires massive investments in infrastructure and new breakthroughs in storage/release systems. Besides direct utilization of CO_2 from the atmosphere, the only renewable source of carbon is biomass [133, 134] and the production of hydrocarbon fuels from biomass is of immense importance. Ethanol production from sugars through fermentation is the dominating commercial use of biomass for fuel production today [135]. But ethanol has a low energy density compared to gasoline and due to its high cost of production from cellulose it is not necessarily the best choice [136] and various processes for conversion of biomass to hydrocarbons are under development [135].

Biomass can readily be converted to hydrocarbon fuels with known technology through gasification followed by fuel synthesis (e.g. Fischer-Tropsch or methanol synthesis followed by MTH), but especially gasification is a very energy intensive process, and it must be performed in large scale in order to be economically viable [137]. It is therefore very attractive to develop processes for conversion of biomass to liquid fuels where gasification is circumvented.

As early as 1979 researchers from Mobil employed H-ZSM-5 in the direct conversion of various substances available from biomass including different types of oils and rubber latex to produce liquid hydrocarbon fuel, mainly consisting of aromatics [138]. Later, H-ZSM-5 was employed in the conversion of solutions of sugars either in water or methanol into aromatics [139, 140]. These processes result in very rapid deactivation of the catalyst due to coke deposition.

Pyrolysis oils obtained from thermal treatment of biomass has been widely investigated in zeolite catalyzed upgrading to hydrocarbons [141, 142, 143, 144]. The pyrolysis oils consists of compounds such as small carboxylic acids, aldehydes, ketones, esters, alcohols, phenols, and more functionalized compounds such as furfurals, and the composition of the pyrolysis oils differs greatly [142]. Nevertheless, H-ZSM-5 seems to be omnivorous, and it is possible to obtain a hydrocarbon fraction, mainly consisting of aromatics from these quite harsh reactant mixtures. Unfortunately, the catalyst still suffers from rapid deactivation due to coking [145].

Recently, Huber *et al.* has done a substantial amount of work on a process known as catalytic fast pyrolysis, where raw biomass (wood or sugars) is physically mixed with catalyst (H-ZSM-5) and heated rapidly (1000 °C/s) to 400 – 600 °C [146, 147, 148]. This can be considered as formation of pyrolysis oil and catalytic upgrading in one step and it results in the production of aromatics, CO, CO_2, and coke. Not surprisingly, the catalyst suffers from extremely fast deactivation due to coke deposition; in general the selectivity towards coke is in the same range as the selectivity towards aromatic products. Due to this massive coke formation it is necessary to employ large amount of catalyst (i.e. catalyst to feed ratio of

19 [146]), in order to obtain a decent product yield. Furthermore, the main product of the catalytic fast pyrolysis is actually naphthalene [147].

A completely different strategy for production of liquid fuels from biomass is pursued by the group of Dumesic. They have developed procedures where sugars are converted through a range of catalytic reactions including decarbonylation, decarboxylation and hydrogenation over platinum and rhenium containing catalysts [149]. This yields a mixture of partly defunctionalized intermediates (acids, alcohols, ketones, heterocycles), which are further upgraded to fuels, either through hydrogenation or conversion over H-ZSM-5. In a recent publication from their group, γ-valerolactone, which is obtainable from biomass [150, 151], is converted to liquid fuels through a series of catalytic reactions including ring opening and decarboxylation to form butene followed by oligomerization and hydrogenation [152]. The products in these reactions are obtained in high yields and are very suitable for implementation as liquid fuels, but the process consists of multiple steps employing different catalysts containing various rare (and expensive) metals.

Naturally, it would be very attractive to develop a cheap and simple process for conversion of biomass to fuels without compromising the quality and yield of the product or the process costs significantly. Many different approaches could be employed to pursue this goal including zeolite catalyzed conversion of substances available from biomass to hydrocarbon fuels. Various reactants have been tested in the reaction by many different research groups, including alcohols, phenols, acids, aldehydes, ketones, ethers, and esters [101, 153, 154, 155, 156]. Even scrap tires has been employed as reactant (via pyrolysis) [157]. H-ZSM-5 seems to be the catalyst of choice in these reactions due to its significant resistance towards coking compared to other zeolites.

Despite many publications within the area, there does not seem to be a consensus on which bioavailable compounds are sensible to employ in the reaction. The atomic ratio of H/C in the dehydrated reactant is important in terms of product selectivity and coke formation, which is mentioned in several papers [140, 155], but the more exact influence of the H/C ratio and the specific functional groups in the reactant needs to be further investigated. This prompted us to test a range of different oxygen containing compounds which are more or less directly available from biomass in the conversion to hydrocarbons over H-ZSM-5.

5.1 Experimental

The employed catalyst is the same H-ZSM-5 (Si/Al = 40) sample supplied by Zeolyst International as described and characterized in Chapter 4. In each experiment, the reactor was charged with 300 mg catalyst, which was heated to the reaction temperature in a flow of helium prior to the reaction. The reactant liquid was pumped by an HPLC pump at a flow of 0.05 mL/min and evaporated before reaching the catalyst bed. Helium was employed as the carrier gas with a flow of 40 mL/min. The reaction temperature was 370 °C (measured inside the reactor, just below the catalyst bed), and the reaction pressure was 1 bar. The organic products where analyzed by an online GC equipped with an FID followed by a BINOS detector, which continuously monitored concentration of CO and CO_2.

The experiments employing isotopically labeled reactants were performed with 2-3 g of reactant mixture, corresponding to around an hour of reaction time. Prior to the introduction of the reactant mixture, the tubing in the feeding system was filled with water. After introduction of the reactant mixture into the tubing, the feed was changed to water again. In this way a plug of isotopically labeled reactant mixture was fed to the catalyst without wasting large amounts of the labeled compounds.

The TPO analyses were typically performed with 100 mg of spent catalyst, which was heated in a flow of 5 % O_2 in helium (20 mL/min) with a heating ramp of 2.75 °C/min to an oven temperature of 700 °C. The final temperature was maintained for 2 h to ensure complete combustion of the carbonaceous species. The concentrations of CO and CO_2 in the outlet were monitored continuously by a BINOS detector.

5.2 Results and discussion

When oxygenates are converted to hydrocarbons over H-ZSM-5, the content of oxygen in the reactant has a large influence on the process. In most cases oxygen is released as water, leading to a depletion of hydrogen in the obtained hydrocarbon product mixture. This has given rise to the effective hydrogen to carbon ratio (H/C_{eff}) shown below [140, 146], where H, C, and O are the number of the different atoms in the specific molecules.

$$H/C_{eff} = \frac{H - 2O}{C}$$

This means that a high content of oxygen in the reactant leads to a low H/C_{eff} ratio, massive coke formation, and a product mixture which is rich in aromatics [140]. The H/C_{eff} ratios of a few selected compounds are shown in Table 12.

	H/C_{eff}
Methanol	2
Ethanol	2
Acetone	1.33
Glycerol	0.67
Acetic acid	0
Glucose	0
Cellulose	0

Table 12: H/C_{eff} ratios of selected compounds

The value of H/C_{eff} is 2 for the mono-alcohols, corresponding to an alkene. For glucose and cellulose the H/C_{eff} is zero, which is not surprising since dehydration of a carbohydrate results in nothing but water and carbon. This means that in order for these compounds to produce hydrocarbons, some of the oxygen in the reactant has to be expelled as CO or CO_2 instead of water which leads to an enrichment of hydrogen in the products. If the same variety of hydrocarbon products is formed from conversion of various oxygenates as for methanol conversion (alkenes (H/C = 2), alkanes (H/C > 2) and aromatics (H/C = ~0.8 – 1.4), the selectivity is bound to shift towards aromatics if reactants with low H/C_{eff} are employed, unless large amounts of CO or CO_2 are released.

Initial experiments performed on conversion of compounds such as glycerol, propanediols, ethylene glycol, etc. over H-ZSM-5 showed that the catalyst deactivated extremely fast (within 2 – 15 min.). Due to this very fast deactivation it was not convenient to measure a reliable catalyst lifetime, unless obscene amounts of catalyst were used in each catalytic test. In all experiments the reactant liquid was pump to the reactor at a rate of 0.05 mL/min, and when employing 300 mg of catalyst, this gives a WHSV around 7-10 h^{-1} depending on the density of the reactant and this space velocity is simply too high to obtain reliable data before deactivation.

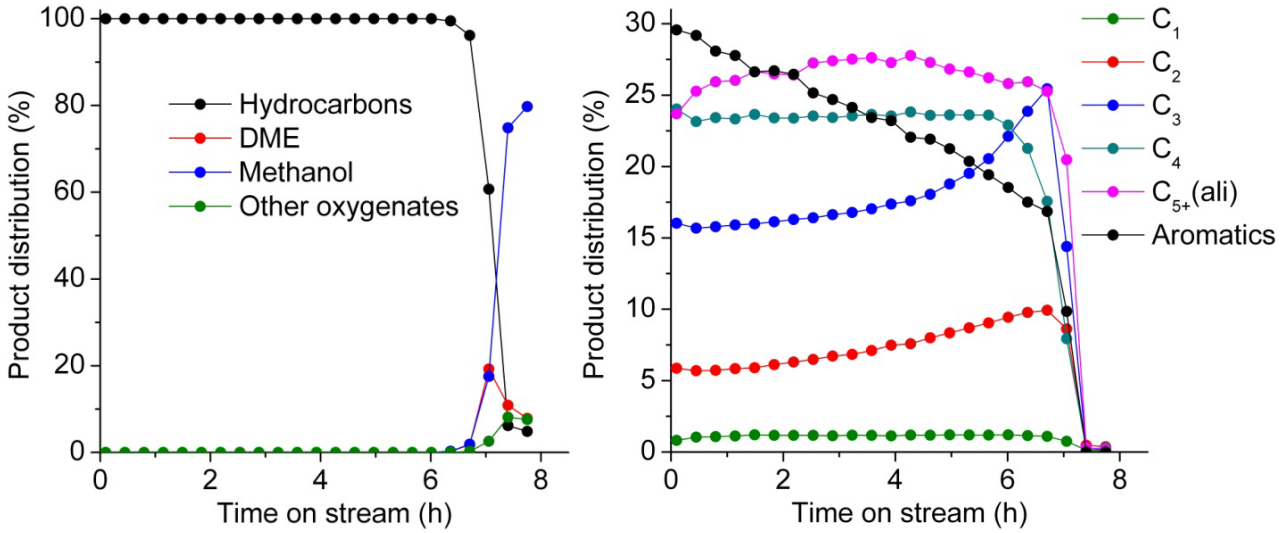

Figure 86: Yield of hydrocarbons and oxygenates (left) and hydrocarbon product distribution (right) vs. time on stream for conversion of 10 % glycerol in methanol over H-ZSM-5 at 370 °C (WHSV = 8.3 h^{-1})

In order to obtain measurable catalyst lifetimes, glycerol was diluted in different concentrations in methanol and the respective mixtures were converted over H-ZSM-5. Product distribution for conversion of 10 % glycerol in methanol is shown as an example in Figure 86. Clearly, the catalyst lifetime is much shorter than for conversion of methanol and the same types of products are formed (see Figure 37 and Figure 38, page 45), though the selectivity to aromatics is somewhat higher, which is not surprising when a co-reactant with a low H/C_{eff} ratio is employed.

When the catalyst deactivates, methanol, DME, and various oxygenates from dehydration of glycerol (mainly acrolein) are observed in the outlet. The fact that these oxygenates are observed simultaneously in the outlet (i.e. no acrolein is observed before breakthrough of methanol) indicates that methanol and glycerol are converted in the same band of active catalyst moving downstream in the bed. Another interesting observation is that DME is only observed in small amounts at deactivation. For conversion of methanol, DME and methanol are observed in equilibrium at deactivation, but apparently the presence of glycerol induces heavy deactivation leading to loss of the ability to dehydrate methanol to DME.

A range of solutions of glycerol in methanol in different concentrations have been converted over H-ZSM-5. Due to differences in the density of the different mixtures, the WHSV varies slightly, but in all cases the reactant was led to the bed at a liquid flow of ~0.05 mL/min. The catalyst lifetime is very short at high concentrations of glycerol and not surprisingly dilution in methanol leads to longer lifetimes. But the lifetime does not simply scale linearly according to the concentration of glycerol in the feed, for

instance the catalyst lifetime is around 5 times longer for 10 % glycerol than for 25 % glycerol. This is illustrated in Figure 87 (left) were the conversion capacities for glycerol and methanol are plotted for conversion of different solutions of glycerol in methanol. Methanol dilution has a clear positive effect on the amount of glycerol converted. Nevertheless, the catalyst lifetime is shorter when glycerol is present in the feed, leading to declining conversion capacity of methanol as a function of glycerol concentration. At low glycerol concentration, the positive effect of dilution is eclipsed by deactivation induced by methanol. This means that an optimum for glycerol conversion capacity is observed around a concentration of 5 %.

One could imagine that the increase in glycerol conversion capacity upon dilution in methanol is a consequence of lower space velocity of glycerol at low concentrations. In order to investigate this, 5 % glycerol in water was converted over H-ZSM-5 to obtain a low space velocity of glycerol. This experiment resulted in a conversion capacity of 0.6 g_{gly}/g_{cat}. Due to practical limitations, it has not been possible to perform conversion of 100 % glycerol, but the value of 0.6 g_{gly}/g_{cat} for conversion of the 5 % aqueous solution actually fits quite nicely with the data in Figure 87 (left), indicating that the lower space velocity of glycerol at low concentrations is not responsible for the higher conversion capacity, i.e. a clear synergistic effect is observed for co-reacting glycerol with methanol. Synergistic effects from dilution of the oxygenate reactant in methanol have been reported earlier for furfural [138] and sugars [140].

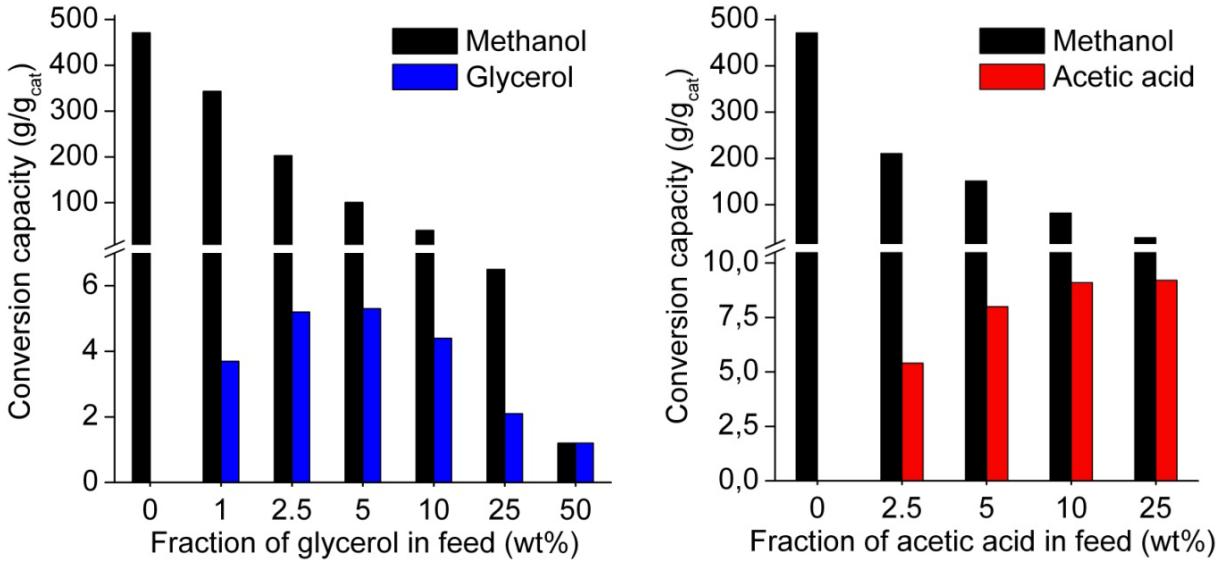

Figure 87: Total conversion capacities (g/g_{cat}) before full deactivation of the catalyst for conversion of mixtures with different concentrations of glycerol in methanol (left) and acetic acid in methanol (right) over H-ZSM-5 at 370 °C

Figure 87 (right) shows the conversion capacities obtained in a similar series of experiments performed with different concentrations of acetic acid in methanol. The conversion capacity for acetic acid is highest for the most concentrated solutions in methanol (10 and 25 %). Unfortunately, no data is available for higher concentrations of acetic acid, but one could imagine that it follows the same tendency as glycerol in the sense that a maximum conversion capacity for acetic acid is observed at a certain concentration.

When acetic acid is converted over H-ZSM-5 many different reactions take place. For instance ketonization of acetic acid to form acetone, CO_2, and water is observed which was already reported by Chang *et al.* in 1977 [13] and later by Hutchings *et al.* during conversion over H-Beta [154]. Acetone is able to react further to form *i*-butene in high selectivity over H-ZSM-5 [153] and H-Beta [154]. At high concentrations of acetic acid, unreacted acetic acid, methyl acetate, and acetone are observed in the outlet before breakthrough of methanol/DME, indicating that acetic acid and its derivatives needs a larger part of the catalyst bed to convert to hydrocarbons than methanol. At a concentration of 25 %, acetic acid, methyl acetate and acetone are observed already in the first product sample (after around 5-10 min. on stream) and the conversion gradually decreases. Furthermore, for conversion of acetone, *i*-butene is produced in fair amounts when the production of all other hydrocarbons has seized (not even isomerization of *i*-butene to other C_4 alkenes is observed), indicating that the reaction might be of thermal origin rather than catalytic, which makes it challenging to calculate a reliable conversion capacity for conversion of high concentrations of acetic acid in methanol.

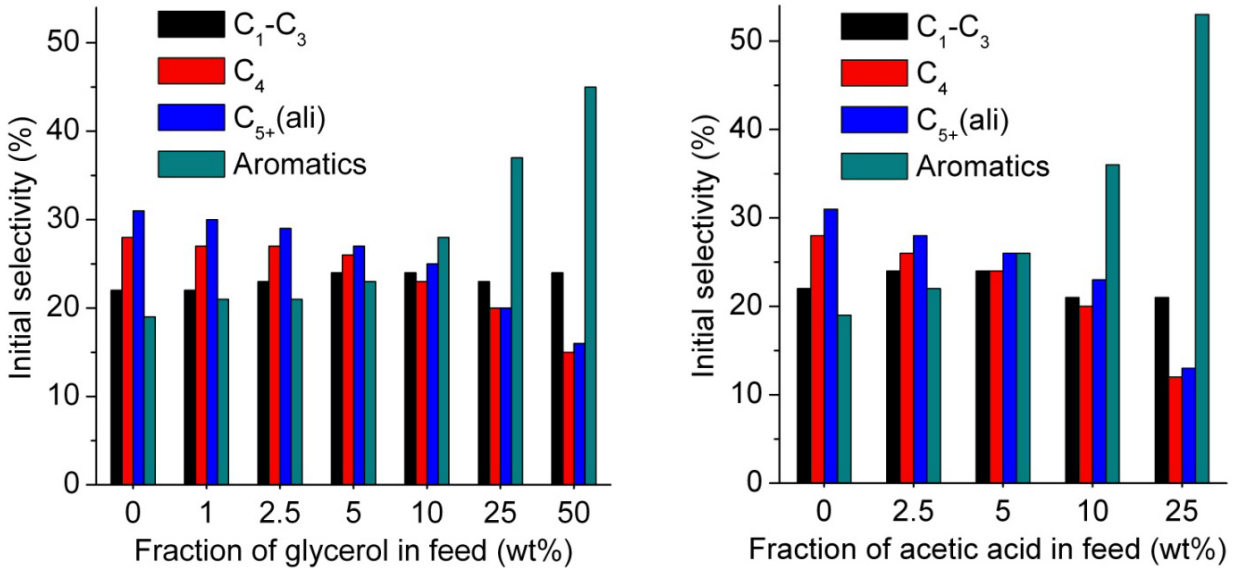

Figure 88: Initial product selectivities for conversion of mixtures with different concentrations of glycerol in methanol (left) and acetic acid in methanol (right) over H-ZSM-5 at 370 °C

Initial product selectivities for conversion of glycerol and acetic acid diluted in different concentrations in methanol are shown in Figure 88. At high concentrations of the additive (glycerol or acetic acid), the selectivity shifts towards production of aromatics. This is not surprising, since a lower H/C_{eff} of the reactant mixture must lead to higher selectivity towards aromatics (unless large amounts of CO or CO_2 are released). The selectivity towards small aliphatics (C_1-C_3), seems rather independent of the concentration of the additive while the increase of aromatics at high concentrations of additive seems to be at the expense of higher aliphatics (C_{4+}).

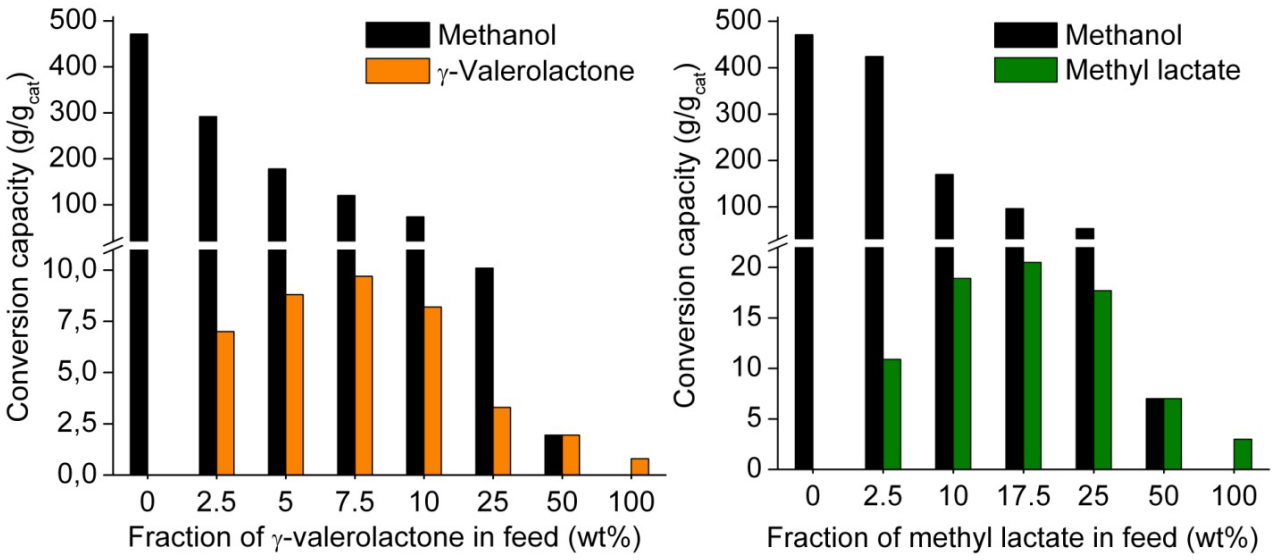

Figure 89: Total conversion capacities (g/g$_{cat}$) before full deactivation of the catalyst for conversion of mixtures with different concentrations of γ-valerolactone in methanol (left) and methyl lactate in methanol (right) over H-ZSM-5 at 370 °C

γ-Valerolactone has been acknowledged as a possible renewable platform molecule due to its availability from biomass [150, 151]. Also methyl lactate is available from biomass [158] and therefore the production of hydrocarbon fuels and chemicals from these two compounds is of great interest [159], especially if their production from biomass is industrialized.

Figure 89 shows conversion capacities for conversion of different concentrations of γ-valerolactone (left) and methyl lactate (right) in methanol over H-ZSM-5. As for glycerol, a beneficial effect of methanol dilution is observed and a maximum in conversion capacity for the additive is observed at a certain concentration. For γ-valerolactone, the conversion capacity is more than 10-fold higher when diluted to 7.5 % in methanol compared to conversion of 100 % γ-valerolactone. For methyl lactate, the increase in conversion capacity is slightly less than 10-fold.

Upon catalyst deactivation, gas samples were withdrawn and analyzed by GC-MS revealing the presence of 1,3-butadiene and CO from conversion of γ-valerolactone, and DME, acetaldehyde, and CO from conversion of methyl lactate, indicating that these compounds are produced initially by decomposition when the reactants reach the catalyst bed. As for conversion of glycerol/methanol mixtures, these direct decomposition products are not observed in the outlet until the catalyst is deactivated and breakthrough of methanol is also observed (except CO, which is not entering the hydrocarbon products).

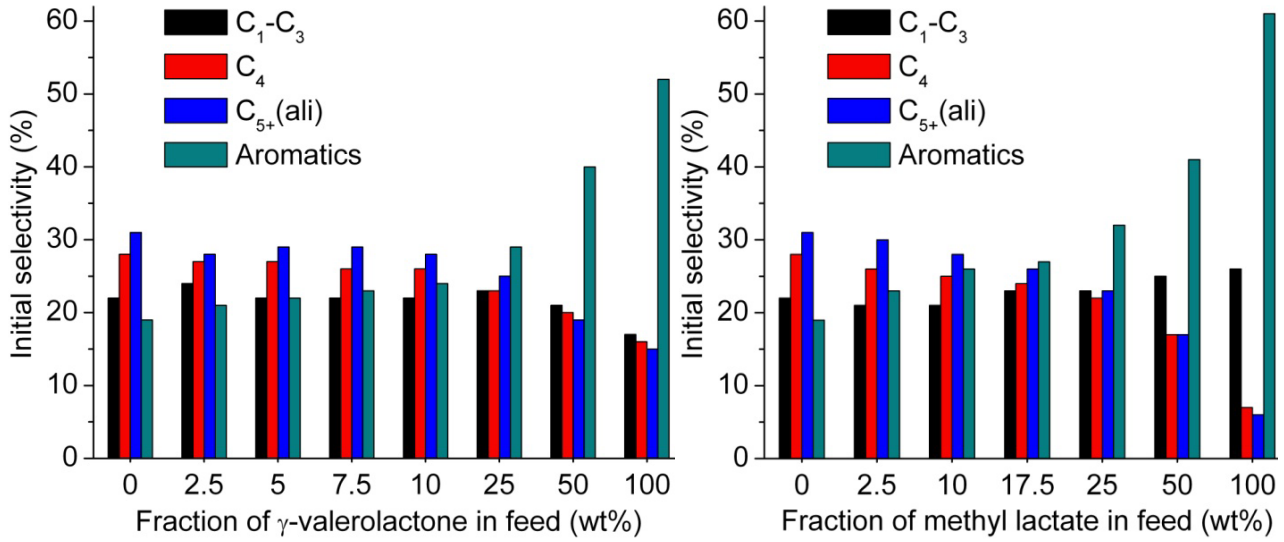

Figure 90: Initial product selectivities for conversion of mixtures with different concentrations of γ-valerolactone in methanol (left) and methyl lactate in methanol (right) over H-ZSM-5 at 370 °C

Figure 90 shows the product selectivities for conversion of different concentrations of γ-valerolactone and methyl lactate in methanol over H-ZSM-5. For methyl lactate, the same tendency as for glycerol and acetic acid is observed; at high concentrations of additive, the selectivity towards aromatics is high at the expense of C_{4+} aliphatics. For γ-valerolactone, also the selectivity towards C_1-C_3 compounds drops at high concentrations.

Table 13 shows the amount of CO and CO_2 produced from conversion of the various solutions of acetic acid, glycerol, methyl lactate, and γ-valerolactone as well as the H/C_{eff} of the reactant mixture and the initial C_4-HTI. CO and CO_2 are displayed as molar percentages of the amount of additive in the feed (for instance 100 % corresponds to 1 mole of CO pr. mole of methyl lactate in the feed). At high concentrations of additive, the amount of CO/CO_2 produced is in some cases very high meaning that the BINOS detector is outside its calibrated interval and reliable data is not obtained leading to the indication n/a in Table 13. Furthermore, the catalyst lifetime is very short also making the retrieval of reliable data challenging.

In general acetic acid and glycerol does not produce large amounts of CO or CO_2, though at higher concentrations glycerol produce fair amounts of CO, but almost no CO_2. Acetic acid has a higher selectivity towards CO_2 (9 % at a concentration of 25 %) which most likely is a consequence of the ketonization reaction mentioned above.

	Additive (wt%)	H/C_{eff} mixture	C_4-HTI	CO (mol/mol_{ad})	CO_2 (mol/mol_{ad})
Methanol	-	2	0.38	0 %	0 %
Acetic acid	2.5 %	1.95	0.34	0 %	0 %
Acetic acid	5 %	1.89	0.31	4 %	4 %
Acetic acid	10 %	1.79	0.27	5 %	3 %
Acetic acid	25 %	1.48	0.19	6 %	9 %
Glycerol	1 %	1.99	0.38	0 %	0 %
Glycerol	2.5 %	1.97	0.36	0 %	0 %
Glycerol	5 %	1.93	0.34	10 %	0 %
Glycerol	10 %	1.86	0.30	11 %	0 %
Glycerol	25 %	1.66	0.23	16 %	2 %
Glycerol	50 %	1.32	n/a	21 %	3 %
Methyl lactate	2.5 %	1.95	0.39	70 %	0 %
Methyl lactate	10 %	1.82	0.33	93 %	0 %
Methyl lactate	17.5 %	1.69	0.31	>95 %	1 %
Methyl lactate	25 %	1.56	0.27	>95 %	1 %
Methyl lactate	50 %	1.17	0.20	>95 %	1 %
Methyl lactate	100 %	0.50	n/a	n/a	2 %
γ-Valerolactone	2.5 %	1.95	0.39	76 %	2 %
γ-Valerolactone	5 %	1.91	0.38	78 %	6 %
γ-Valerolactone	7.5 %	1.86	0.35	77 %	7 %
γ-Valerolactone	10 %	1.82	0.32	78 %	7 %
γ-Valerolactone	25 %	1.58	0.27	73 %	9 %
γ-Valerolactone	50 %	1.26	0.24	72 %	11 %
γ-Valerolactone	100 %	0.8	n/a	n/a	n/a

Table 13: H/C_{eff}, initial C_4-HTI, and the initial selectivity towards CO and CO_2 (calculated as molar percentages of the additive (acetic acid, glycerol etc.)) for conversion of different mixtures of methanol and glycerol, acetic acid, methyl lactate, or γ-valerolactone over H-ZSM-5 at 370 °C

The results show that 1 mole of CO is released pr. mole of methyl lactate while only traces of CO_2 are produced. As mentioned above, GC-MS analyses have revealed that methyl lactate decompose to CO, acetaldehyde, and methanol (see Figure 91) and this reaction seems to be rather independent of the concentration of methyl lactate in the feed since the selectivity towards CO is quite constant at different concentrations. At low concentrations it is somewhat lower, indicating that large amounts of methanol in the feed suppress the initial decomposition of methyl lactate.

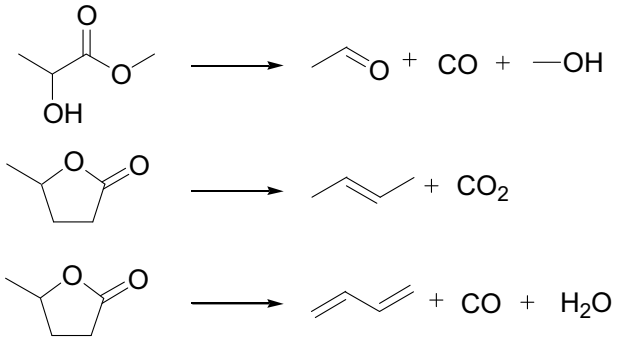

Figure 91: Proposed decomposition pathways for conversion of methyl lactate and γ-valerolactone over H-ZSM-5

γ-Valerolactone also produce large amounts of CO (from decomposition to CO, 1,3-butadiene, and water), but some CO_2 is also produced most likely from ring opening followed by decarboxylation to give CO_2 and butene in a reaction similar to the decarboxylation over SiO_2/Al_2O_3 reported by Dumesic *et al.* [152]. This decarboxylation seems to be more pronounced at high concentrations of γ-valerolactone. The two different proposed decomposition pathways for γ-valerolactone are shown in Figure 91.

The initial C_4-HTI (see Table 13) is low at high concentrations of the additive in the feed. Even though large amounts of aromatics are produced through hydrogen transfer reactions, this is not necessarily accompanied by production of alkanes since the reaction mixture is not a pool of alkenes, but a mixture less rich in hydrogen. Thus, even though the selectivity towards aromatics is high at low H/C_{eff} this does not induce high selectivity towards alkanes as observed for conversion of methanol.

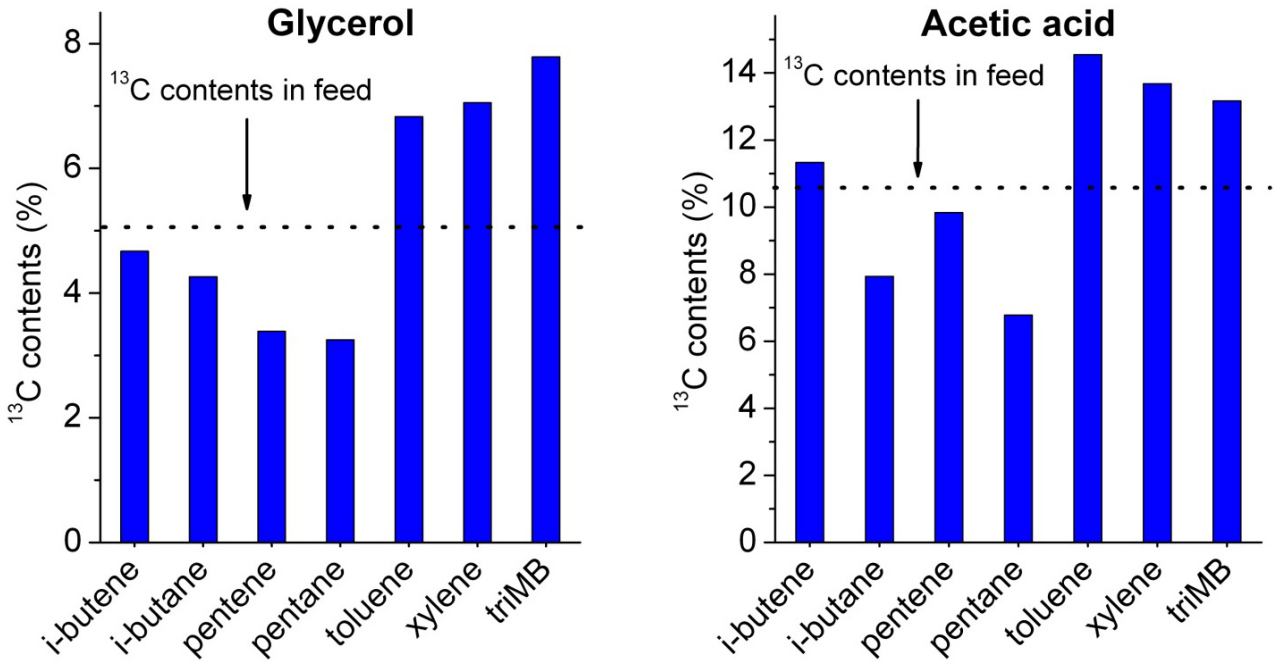

Figure 92: ^{13}C contents in various products formed from conversion of 5 % ^{13}C labeled glycerol in methanol (left) and 10 % ^{13}C labeled acetic acid (right). The dotted lines illustrate calculated values of ^{13}C contents in the reactant mixtures

In order to investigate if the carbon atoms from the various additives are actually incorporated into the hydrocarbon products, isotopic labeling studies have been performed. When performing these reactions, the reactant was led to the catalyst for around 1 h, meaning that the obtained data represents the initial product formation. During the experiments no changes in ^{13}C incorporation were observed.

Figure 92 illustrates the ^{13}C contents of selected products obtained from conversion of 5 % ^{13}C labeled glycerol in unlabeled methanol (left) and 10 % ^{13}C labeled acetic acid in unlabeled methanol (right). The ^{13}C contents of the reactant mixtures are illustrated on the graphs and the contents of ^{13}C in the products are in good correspondence with this value, indicating that the carbon atoms from the additives are incorporated into the hydrocarbon products. Unfortunately, the GC-MS is not able to separate smaller gasses than the C_4 fraction, making it impossible to obtain reliable isotopic data for propene and ethene (or CO/CO_2), so we have focused on the larger products.

In both reactant systems, there is a clear enrichment of ^{13}C in the aromatic products indicating that the carbon atoms from the additives are preferable incorporated into aromatic compounds. When glycerol or acetic acid is converted over H-ZSM-5 they will most likely dehydrate to unsaturated intermediates which are easily converted to aromatics, explaining the high degree of ^{13}C incorporation in the aromatic compounds. Another interesting observation is that *i*-butene contains more ^{13}C than the other aliphatics in the case of acetic acid. This can be explained by the ketonization of acetic acid to produce acetone which reacts further to *i*-butene as described above.

Even though some CO and CO_2 (5 % and 3 %) are produced, the isotopic data illustrate that both carbon atoms from acetic acid are predominantly inserted into the hydrocarbon products. This is quite remarkable since the carbon atom in the acid functionality has to go through a massive series of dehydration and reduction reactions (through hydrogen transfer) in order to avoid the formation of CO or CO_2. This must also involve methylation of reaction intermediates by methanol; otherwise acetic acid would simply dehydrate to carbon if CO or CO_2 is not expelled, since H/C_{eff} for acetic acid is 0.

Methyl lactate and γ-valerolactone are not commercially available as ^{13}C compounds, or at least extremely costly. Therefore, the incorporation of carbon atoms into the hydrocarbon products from these compounds was investigated by conversion of 10 % unlabeled γ-valerolactone and 25 % unlabeled methyl lactate in ^{13}C labeled methanol. Figure 93 shows the ^{12}C contents in selected products from these two experiments (left: γ-valerolactone, right: Methyl lactate). The ^{12}C contents in the reactant mixtures as well as the theoretical value for loss of 1 carbon atom as CO or CO_2 are shown as the dotted lines in the graphs.

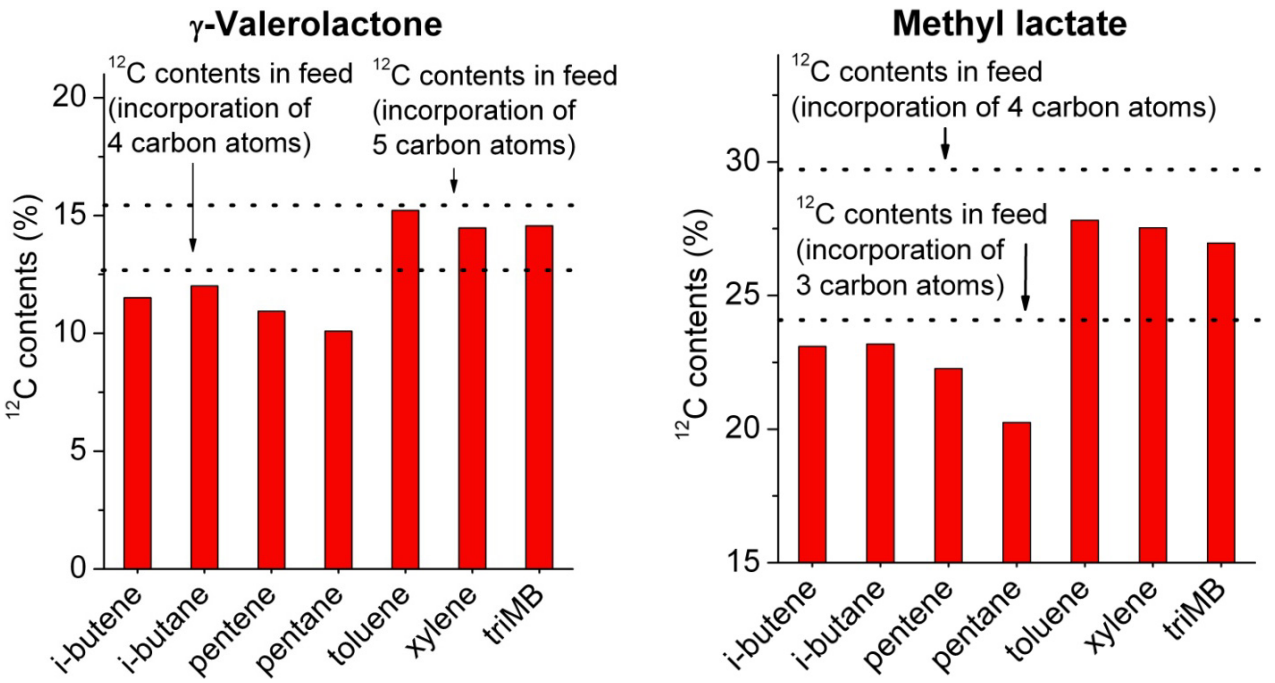

Figure 93: ^{12}C contents in various products formed from conversion of 10 % unlabeled γ-valerolactone in ^{13}C labeled methanol (left) and 25 % unlabeled methyl lactate in ^{13}C labeled methanol (right). The dotted lines illustrate calculated values of ^{12}C contents in the reactant mixtures, including the theoretical value for percentage of ^{12}C if 1 carbon atom is rejected as CO or CO_2 and thus not incorporated in the hydrocarbon products

The experiments confirm that the carbon atoms from the methyl lactate and γ-valerolactone are indeed incorporated into the hydrocarbon products and as for glycerol and acetic acid, the carbon atoms from the additive are preferably incorporated into the aromatic compounds. Furthermore, the isotopic data confirm the loss of close to 1 mole of CO from both reactant molecules since the ^{12}C contents in the products are in good correspondence with the calculated ^{12}C contents for loss of 1 carbon as CO or CO_2.

It is not possible to calculate the total summarized ^{13}C contents in the hydrocarbon products in these experiments, since the product mixture consist of a vast number of different products and detailed selectivity and isotopic distribution for each single compound is not obtainable. But from the CO and CO_2 data combined with the isotopic data, it is fair to state that the majority of the carbon atoms end up in the hydrocarbon products. Presumably, every reactant has its own reaction pathway, but since the performed experiments on isotopic labeling are performed over a fresh catalyst bed, secondary reactions have equilibrated the isotopic distribution within the hydrocarbon products to some extent before the product sample for the analysis is withdrawn.

The aliphatic compounds contain less carbon atoms from the additives than the aromatics. There is also a general trend that the C_5 aliphatics contain somewhat less carbon from the additives than the C_4 compounds, which might be ascribed to methylation of the C_4 compounds with methanol to form C_5 compounds. In general, alkene methylation by methanol followed by cracking to smaller alkenes might be responsible for incorporation of more carbon atoms from methanol in the aliphatic compounds.

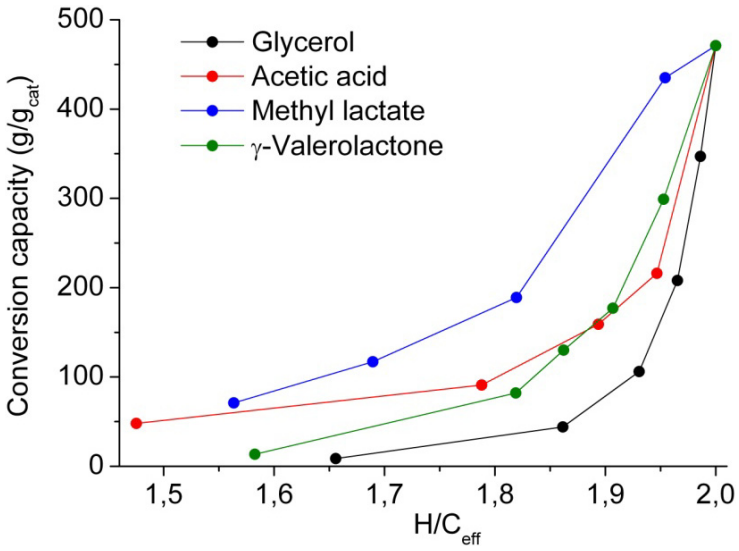

Figure 94: Total conversion capacities (i.e. the sum of the conversion capacities for methanol and additive) for conversion of glycerol, acetic acid, methyl lactate, and γ-valerolactone diluted in methanol at different concentrations (0 to 25 %) over H-ZSM-5 at 370 °C plotted as a function of H/C$_{eff}$ of the reactant mixture

As mentioned above, the value of H/C$_{eff}$ of the reactant mixture has a large effect on the total conversion capacity of the catalyst. This is illustrated in Figure 94, where the combined conversion capacities of methanol and additive for conversion of various solutions of glycerol, acetic acid, methyl lactate, and γ-valerolactone in methanol are plotted against H/C$_{eff}$ of the mixture. As expected, low conversion capacity is observed at low H/C$_{eff}$, but the nature of the reactant also seems to have a large effect. Thus, methyl lactate exhibits much higher conversion capacity than the other reactants at similar values of H/C$_{eff}$. Naturally, loss of CO from methyl lactate makes the reactant mixture richer in hydrogen, but even though γ-valerolactone also loses CO, it shows a significantly lower conversion capacity than methyl lactate at similar H/C$_{eff}$. Acetic acid and glycerol do not lose significant amounts of CO or CO_2, and a huge difference in conversion capacity for these two compounds is observed at similar H/C$_{eff}$ as well. This illustrates that, besides the H/C$_{eff}$ ratio, the functional groups present in the reactant mixture have a large effect on the conversion capacity of the catalyst.

In order to investigate this more thoroughly, a range of different oxygenates have been converted over H-ZSM-5 as 10 % solutions in methanol. Table 14 shows the H/C$_{eff}$ of the additive and reactant mixture as well as the conversion capacity and production of CO and CO_2 for conversion of C_2-C_4 diols, aldehydes, and ketones. These compounds are similar in the way that their H/C$_{eff}$ ratio is the same for compounds with the same number of carbon atoms, meaning that any major differences in their performance as reactants must arise from the specific functional groups. Initial hydrocarbon product selectivities and C_4-HTI for conversion of these 10 % solutions in methanol are shown in Table 15.

As seen from Table 14, major differences in conversion capacity are indeed observed for compounds with the same H/C$_{eff}$ ratio. For instance, within the group of C_4 compounds, the conversion capacity for 10 % butanone is more than twice that of 10 % butanal. Furthermore, 2,3-butanediol shows a conversion capacity similar to butanone, while the other butanediols are in the range of butanal. This observation is in good accordance with the fact that butanone is observed as the direct dehydration

product from 2,3-butanediol, while the other butanediols produce mixtures of butadiene, tetrahydrofuran (only from 1,4-butanediol), and butanal (not from 1,4-butanediol). A similar tendency is observed for the C_3 compounds, where acetone exhibits higher conversion capacity than propanal, and 1,2-propanediol outperforms 1,3-propanediol.

	H/C_{eff} (additive)	H/C_{eff} (mixture)	Conv. cap. (g_{feed}/g_{cat})	CO (mol/mol_{ad})	CO_2 (mol/mol_{ad})
Methanol	2	2	471	0 %	0 %
Ethyleneglycol	1	1.90	131	4 %	0 %
Acetaldehyde	1	1.86	72	7 %	0 %
1,2-Propanediol	1.33	1.92	190	1 %	0 %
1,3-Propanediol	1.33	1.92	96	1 %	0 %
Acetone	1.33	1.90	271	0 %	1 %
Propanal	1.33	1.90	138	3 %	0 %
1,4-Butanediol	1.5	1.93	139	0 %	0 %
1,3-Butanediol	1.5	1.93	120	0 %	0 %
1,2-Butanediol	1.5	1.93	166	n/a	n/a
2,3-Butanediol	1.5	1.93	320	0 %	0 %
Butanal	1.5	1.92	146	5 %	0 %
Butanone	1.5	1.92	327	0 %	0 %

Table 14: H/C_{eff} for the additive and reactant mixture, conversion capacity, and molar percent of CO and CO_2 (on the basis of the additive) in the products for conversion of 10 % solutions of C_2-C_4 diols, aldehydes and ketones in methanol over H-ZSM-5 at 370 °C

	C_1-C_3	C_4	C_{5+} (ali)	Aromatics	C_4-HTI
Methanol	22 %	28 %	31 %	19 %	0.38
Ethyleneglycol	23 %	24 %	25 %	28 %	0.31
Acetaldehyde	26 %	23 %	22 %	29 %	0.29
1,2-Propanediol	21 %	25 %	29 %	25 %	0.32
1,3-Propanediol	22 %	25 %	28 %	25 %	0.33
Acetone	22 %	24 %	26 %	27 %	0.29
Propanal	22 %	24 %	26 %	28 %	0.31
1,4-Butanediol	22 %	25 %	27 %	26 %	0.33
1,3-Butanediol	23 %	26 %	27 %	24 %	0.33
1,2-Butanediol	22 %	26 %	28 %	24 %	0.33
2,3-Butanediol	22 %	25 %	29 %	24 %	0.31
Butanal	22 %	25 %	27 %	26 %	0.34
Butanone	23 %	25 %	26 %	25 %	0.27

Table 15: Initial product selectivities and C_4-HTI for conversion of 10 % solutions of C_2-C_4 diols, aldehydes and ketones in methanol over H-ZSM-5 at 370 °C

In general, low amounts of CO and CO_2 are produced. The aldehydes seem to produce some CO, while acetone is the only compound producing any CO_2 (1 %). The production of CO and CO_2 is most likely suppressed by the large amount of methanol in the feed which is in accordance with data reported earlier [144].

The product selectivity (Table 15) seems to be quite independent of the functional groups in the additive. When comparing ethylene glycol, propanediol, and butanediol the smaller compounds have lower H/C_{eff}, leading to larger amounts of aromatics, but within for instance the C_4 compounds, no major variations are observed. Nevertheless, the aldehydes and ketones seem to produce slightly more aromatics than the diols which could be explained by the direct production of aromatics via aldol condensation followed by cyclization and dehydration to form aromatics as proposed by Deane *et al.* [160], but this effect might be significantly suppressed by the large amount of methanol in the feed. Another explanation could simply be that due to lower molecular weight of the aldehydes and ketones compared to the corresponding diols, the molar concentration of the reactant mixture is actually slightly higher which also leads to higher selectivity towards aromatics.

When acetic acid is converted over H-ZSM-5, early breakthrough of acetic acid, methyl acetate, and acetone is observed. This tendency is also observed for acetone and butanone, which are also present in the outlet before complete deactivation and breakthrough of methanol. There might be a connection between this behavior and the high conversion capacity observed for these compounds. Ketones seem to be harder to convert than other types of compounds and are most likely present in a larger part of the catalyst bed. This is supported by the fact that the initial C_4-HTI is lower for conversion of ketones than for aldehydes, indicating that less active catalyst is available for secondary reaction when ketones are present, most likely due to interaction of the ketone functionality with the active catalytic sites downstream from the methanol conversion zone.

Besides aldehydes, ketones, and diols, a range of other oxygenates including carboxylic acids and different compounds which are obtainable from biomass or present in significant amounts in pyrolysis oil have been converted over H-ZSM-5 as 10 % solutions in methanol. H/C_{eff} of the additives and the reactant mixtures, conversion capacities, and the amounts of CO and CO_2 are shown in Table 16, while the initial hydrocarbon product selectivities and C_4-HTI are shown in Table 17. Many of the reactants lose significant amounts of CO, while CO_2 is only produced in small amounts. Even for the carboxylic acids, where one could expect the formation of CO_2 from ketonization, mostly CO is produced, especially for butanoic acid and formic acid. This decarbonylation of carboxylic acids leads to the formation of alkenes (and water), except in the case of formic acid which is simply decomposed to CO and water, and high conversion capacity is observed, but most of the carbon from formic acid is lost as CO. This is supported by the fact that the hydrocarbon product selectivities are virtually the same for conversion of pure methanol and 10 % formic acid in methanol (see Table 17).

In general, low H/C_{eff} of the reactant mixture leads to a low conversion capacity, but there are many other effects than this. Especially anisol and dimethoxybenzene induce extremely rapid deactivation to the catalyst. Since phenolic compounds are major constituents of pyrolysis oil obtained from lignin, their conversion to more useful products has been investigated earlier, for instance over H-ZSM-5 [161], but generally very rapid coke formation [162] and low yield of hydrocarbons [163] are observed.

If we consider levulinic acid, γ-valerolactone, and 2-methyl-tetrahydrofuran, they are all based on the same carbon backbone but show very different H/C_{eff} ratios due to different degrees of oxidation. Levulinic acid can be hydrogenated into γ-valerolactone, which exhibits much higher conversion

capacity, or further hydrogenated into 2-methyl-tetrahydrofuran [151], and even higher conversion capacities are obtainable. Introduction of a hydrogenation step prior to conversion over H-ZSM-5 will make the overall process more complex and costly, but depending on the increase in conversion capacity it might be favorable.

	H/C_{eff} (additive)	H/C_{eff} (mixture)	Conv. cap. (g_{feed}/g_{cat})	CO (mol/mol_{ad})	CO_2 (mol/mol_{ad})
Methanol	2	2	471	0 %	0 %
Formic acid	-2	1.71	496	85 %	2 %
Acetic acid	0	1.79	91	5 %	3 %
Propanoic acid	0.67	1.83	109	26 %	4 %
Butanoic acid	1	1.86	219	62 %	0 %
Formaldehyde dimethylacetal	1.33	1.92	62	0 %	0 %
Glycolaldehyde dimethylacetal	1	1.88	40	43 %	3 %
Methyl glycolate	0	1.79	86	91 %	0 %
Glycerol	0.67	1.86	44	11 %	0 %
Methyl lactate	0.5	1.82	189	93 %	0 %
Methyl acrylate	0.5	1.79	27	26 %	10 %
Levulinic acid	0.4	1.79	37	90 %	0 %
γ-Valerolactone	0.8	1.82	82	78 %	7 %
2-Methyl tetrahydrofuran	1.6	1.93	255	0 %	0 %
Anisole	0.86	1.79	10	0 %	0 %
1,2-Dimethoxy benzene	0.75	1.79	9	0 %	0 %

Table 16: H/C_{eff} for the additive and reactant mixture, conversion capacity, and molar percent of CO and CO_2 (on the basis of the additive) in the products for conversion of 10 % solutions of various oxygenates in methanol over H-ZSM-5 at 370 °C

	C_1-C_3	C_4	C_{5+} (ali)	Aromatics	C_4-HTI
Methanol	22 %	28 %	31 %	19 %	0.38
Formic acid	22 %	28 %	32 %	18 %	0.38
Acetic acid	21 %	20 %	23 %	36 %	0.26
Propanoic acid	22 %	24 %	25 %	29 %	0.30
Butanoic acid	21 %	25 %	30 %	24 %	0.35
Formaldehyde dimethylacetal	22 %	25 %	28 %	25 %	0.34
Glycolaldehyde dimethylacetal	23 %	26 %	28 %	23 %	0.31
Methyl glycolate	23 %	25 %	26 %	26 %	0.34
Glycerol	24 %	23 %	25 %	28 %	0.33
Methyl lactate	21 %	25 %	28 %	26 %	0.33
Methyl acrylate	24 %	22 %	25 %	29 %	0.27
Levulinic acid	24 %	25 %	25 %	26 %	0.29
γ-Valerolactone	22 %	26 %	28 %	24 %	0.33
2-Methyl tetrahydrofuran	20 %	25 %	29 %	26 %	0.36
Anisole	26 %	21 %	21 %	32 %	0.23
1,2-Dimethoxy benzene	28 %	20 %	26 %	26 %	0.22

Table 17: Initial product selectivities and C_4-HTI for conversion of 10 % solutions of various oxygenates in methanol over H-ZSM-5 at 370 °C

Another interesting comparison can be drawn between methyl lactate and methyl acrylate. These compounds are very similar, methyl acrylate is simply the dehydration product of methyl lactate, and consequently they also have the same H/C_{eff} ratio. Nevertheless, the conversion capacities for the two 10 % solutions in methanol are very different; 189 g/g_{cat} for methyl lactate and 27 g/g_{cat} for methyl acrylate. This clearly shows that the functionalities in the reactants and the decomposition pathways are essential to the rate of deactivation. As mentioned methyl lactate decomposes (almost quantitatively) to CO, acetaldehyde and methanol, while methyl acrylate only produces 26 % CO and 10 % CO_2. The compound is simply not able to decompose in the same manner as methyl lactate due to the fact that it contains a carbon-carbon double bond instead of the alcohol group present in methyl lactate. If methyl acrylate was to decompose in a similar way as methyl lactate it would result in the formation of acetylene, which seems very unlikely.Since the concentration of the additive in methanol is only 10 %, the initial hydrocarbon product selectivities (Table 17) do not vary much, though there is a general trend that reactant mixtures with low H/C_{eff} produce larger amounts of aromatics. This is illustrated in Figure 95, where the initial yield of aromatics for the various compounds in Table 15 and Table 17 is plotted against H/C_{eff} of the reactant solution. Compounds which split off significant amounts of CO are marked with red dots while the rest are blue. Besides the trend that low H/C_{eff} of the reactant mixture gives high initial yield of aromatics, it is also clear that loss of CO leads to lower yield of aromatics, simply due to the fact that more hydrogen is retained in the hydrocarbon products when oxygen is removed as CO instead of water.

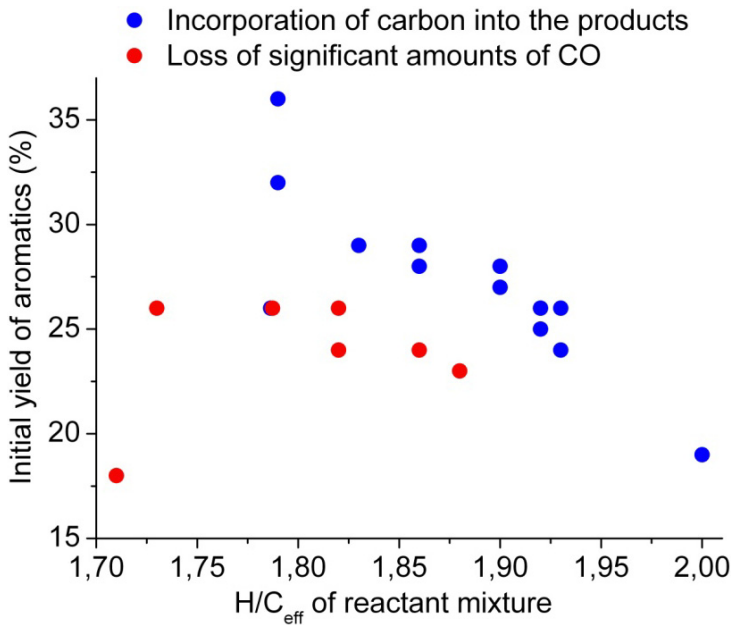

Figure 95: Initial yield of aromatics for conversion of various oxygenates as 10 % solutions in methanol (data from Table 15 and Table 17) as a function of H/C_{eff} of the reactant mixture. Compounds which lose significant amounts of CO are marked with red while the rest are blue

Figure 96 shows the conversion capacity data for the 10 % solutions of different oxygenates listed in Table 14 and Table 16 plotted against the H/C_{eff} of the reactant mixture. The type of functional group in the reactant is indicated on the graph and reactants which lose significant amounts of CO are marked

with a circle. Generally, low H/C_{eff} of the reactant mixture leads to low conversion capacity, but as mentioned large differences in conversion capacity are observed for compounds with similar H/C_{eff}.

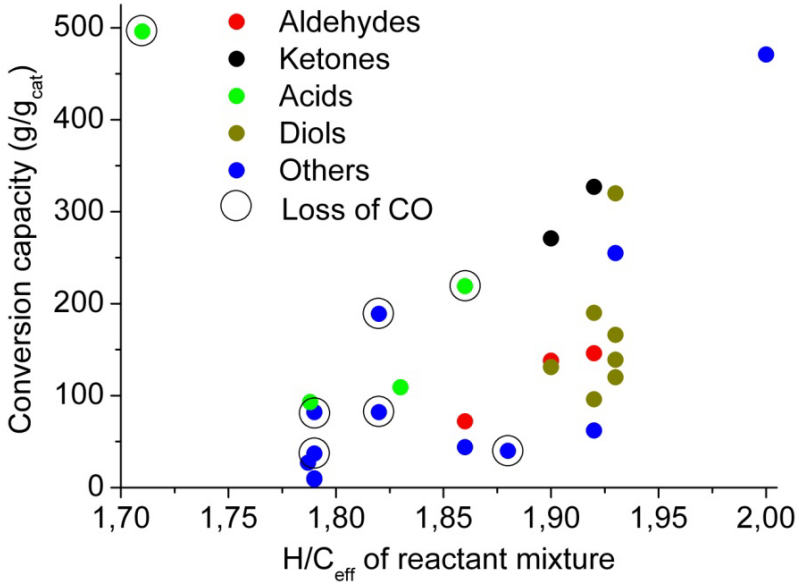

Figure 96: Conversion capacity for conversion of 10 % solutions of various oxygenates in methanol over H-ZSM-5 at 370 °C (data from Table 14 and Table 16) plotted against H/C_{eff} of the reactant mixture. Compounds which lose significant amounts of CO are marked with a circle

Loss of oxygen from the reactants as CO instead of water leads to a reaction mixture which is richer in hydrogen and one could imagine that this would result in slower coke deposition and thereby higher conversion capacity, but this is not a clear trend, since some molecules lose CO and still deactivate the catalyst rapidly.

When an oxygenate mixture is converted over H-ZSM-5, the resulting hydrocarbon mixture is subjected to secondary reactions downstream from the oxygenate conversion zone which might result in formation of coke. Large differences in conversion capacity are observed for compounds with similar H/C_{eff} indicating that coke on the catalyst is predominantly formed in the oxygenate conversion zone, and that each type of compound/functional group has an intrinsic ability towards formation of coke leading to the large differences in conversion capacities observed for reactant mixtures with similar H/C_{eff} ratio.

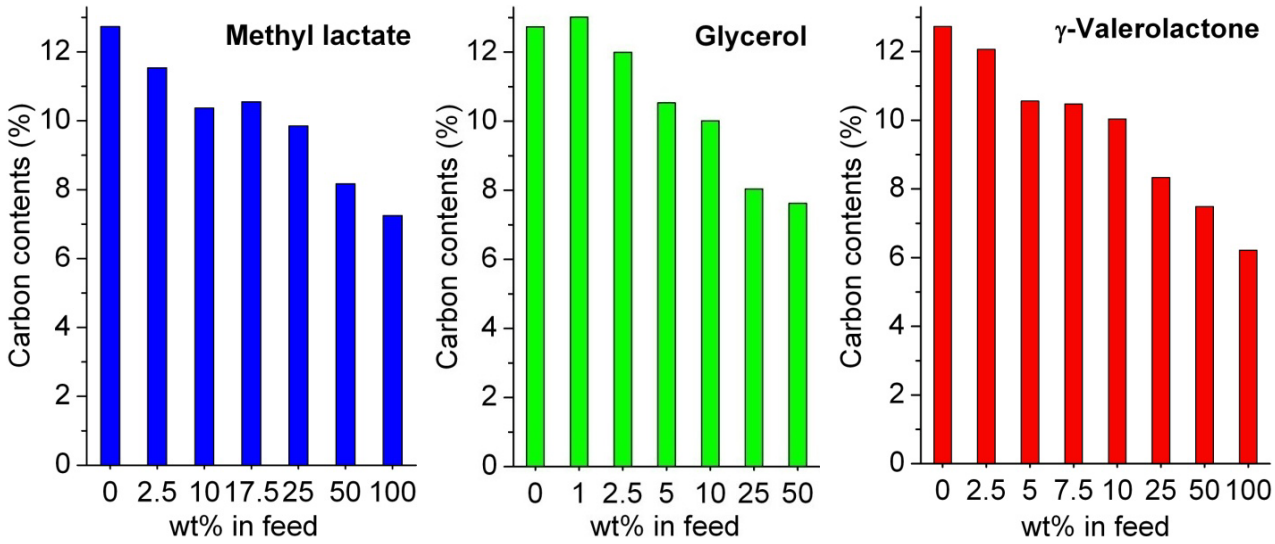

Figure 97: Carbon contents in deactivated H-ZSM-5 upon conversion of solutions of methyl lactate (left), glycerol (middle), and γ-valerolactone (right) in different concentrations in methanol

In order to determine the amount of coke formed on the catalyst during conversion of solutions of the different oxygenates in methanol, TPO analyses have been performed. The resulting carbon contents in the deactivated catalyst samples from conversion of solutions of methyl lactate, glycerol, γ-valerolactone are shown in Figure 97. For all three additives there is a clear tendency that high concentration of the additive leads to lower carbon content on the deactivated zeolite. Due to shorter catalyst lifetimes, the coke is deposited at much higher rate for reactant mixtures containing large amounts of additive, but the catalyst simply seems to deactivate at a lower final content of coke. This effect is most likely a consequence of the high reactivity of methanol, meaning that when methanol is present in large amounts in the feed it is able to convert to hydrocarbons (and form coke) even though the catalyst is partially deactivated. Another effect could be that at longer catalyst lifetimes (low additive concentrations) methanol is allowed to add to the coke species already formed in the deactivated part of the catalyst bed for longer times to build larger carbonaceous species.

Figure 98 shows the carbon contents in deactivated H-ZSM-5 upon conversion of various oxygenates as 10 % solutions in methanol. In most cases the catalyst contains around 10 % carbon, but for the phenolic compounds the carbon content is somewhat lower. This might seem counterintuitive at first glance since the phenolic compounds induce the fastest deactivation of all compounds tested, but as a consequence of the very short lifetime, the catalyst is only subjected to small amounts of methanol and the coke is not allowed to grow.

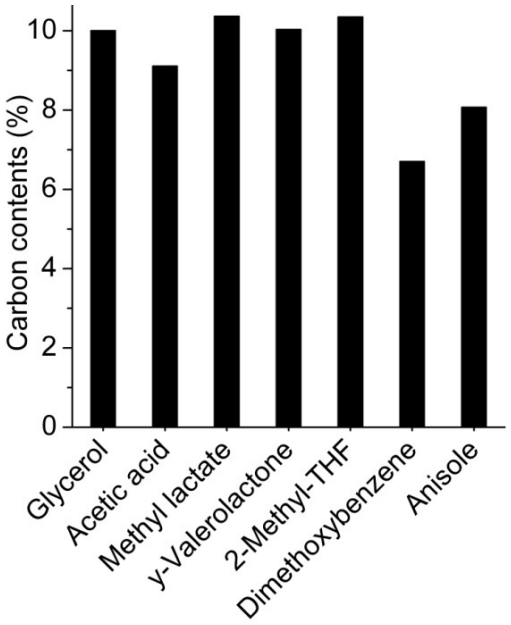

Figure 98: Carbon contents of deactivated H-ZSM-5 upon conversion of various oxygenates as 10 % solutions in methanol

When 10 % glycerol in methanol is converted over H-ZSM-5, the catalyst loses its ability to dehydrate methanol to DME when it deactivates, see Figure 86 (page 93). This is also observed for most of the other oxygenate additives (e.g. methyl lactate and γ-valerolactone), but not for the phenolic species, indicating that the catalyst is not subjected to as massive external coking leading to complete blockage of the zeolite crystals.

The fact that some compounds (ketones, carboxylic acids, etc.) show higher conversion capacity than other compounds with similar H/C_{eff} means that isomerization of intermediates obtained from biomass to compounds which are suitable for conversion over H-ZSM-5 might be a plausible pathway for conversion of biomass to hydrocarbon fuels. For instance methyl lactate shows a quite good conversion capacity, and results from our research group demonstrate that it is available through isomerization of triose sugars [164] or through reverse aldol condensation of hexose sugars followed by isomerization [158] by employing a Sn-Beta zeolite developed by Corma *et al.* [165, 166]. In this way, sugars, which themselves lead to extremely fast deactivation if converted to hydrocarbons over H-ZSM-5 are transformed to an intermediate (methyl lactate), which shows a much more reasonable catalyst conversion capacity in the production of hydrocarbons over H-ZSM-5. Furthermore, when methyl lactate is converted over H-ZSM-5, the CO formed in the reaction could be subjected to water gas shift, leading to the formation of hydrogen which could be used to hydrogenate the reactant mixture leading to longer catalyst lifetimes.

Zeolite upgrading of pyrolysis oils obtained from lignocellulosic biomass has been widely investigated, and massive deactivation of the catalyst is observed. Controlled isomerization of bio-oil prior to zeolite upgrading does not seem viable due to the very complex composition of bio-oil. Furthermore, the presence of phenolic species originating from lignin induces massive deactivation and has to be

removed from the reactant mixture if reasonable catalyst lifetimes are desired, or alternatively lignin could be removed from the biomass prior to the pyrolysis.

5.3 Conclusions

When oxygenates such as diols, aldehydes, ketones, carboxylic acids, and others are converted to hydrocarbons over H-ZSM-5 extremely rapid catalyst deactivation by coking is observed. Co-feeding of methanol has a distinct positive effect on this and not only the catalyst lifetime but also the total conversion capacity of the oxygenate is increased significantly. For instance, the amount of γ-valerolactone converted before catalyst deactivation is more than 10-fold higher for conversion of a 7.5 % solution in methanol than for pure γ-valerolactone. Glycerol and methyl lactate show similar behavior. When oxygenates with low H/C_{eff} ratios are converted to hydrocarbons, the product mixture is very rich in aromatics (>50 %), and co-feeding with methanol leads to higher selectivity towards aliphatics, especially C_{4+} alkenes.

The incorporation of the carbon atoms from glycerol, acetic acid, methyl lactate, and γ-valerolactone into the hydrocarbon products during co-feeding with methanol is confirmed by ^{13}C labeling experiments. Methyl lactate and γ-valerolactone lose close to 1 mole of carbon as CO during conversion over H-ZSM-5, which is confirmed by the isotopic data. For glycerol the vast majority of the carbon atoms are incorporated into the products, and interestingly for conversion of acetic acid only minor amounts of CO and CO_2 are produced, while most of the carbon atoms are incorporated into the hydrocarbon products (at least at a concentration of 10 % in methanol). This means that the majority of the oxygen atoms in the acid functionality are actually removed as water and the carbon atoms are incorporated to the products.

A range of different oxygenates including diols, ketones, aldehydes, acids and various more functionalized compounds obtainable from biomass have been converted to hydrocarbons over H-ZSM-5 as 10 % solutions in methanol. In general a low H/C_{eff} ratio of the reactant solutions leads to low conversion capacity, but there is also a distinct difference in the conversion capacity for different compounds displaying similar H/C_{eff}. For instance ketones display much higher conversion capacity than aldehydes, and diols display major differences in conversion capacity depending on the position of the alcohol groups on the carbon chain. Furthermore, carboxylic acids seem to induce much slower deactivation to the catalyst than other compounds with similar low H/C_{eff} ratios.

Many of the employed reactants lose some of the oxygen in the structure as CO, while almost no CO_2 is produced. This loss of oxygen as CO instead of water leads to an enrichment of the hydrogen contents in the product mixture and the yield of aromatics is decreased.

To avoid heavy deactivation of the catalyst when converting highly functionalized compounds to hydrocarbons over H-ZSM-5, the experiments described here show that isomerization of the reactants to ketones, acids, esters, or other suitable compounds might be a good strategy. Combined with co-feeding of methanol, reasonable catalyst conversion capacities are obtainable.

6 Concluding remarks

In this thesis, different catalytic transformations concerning production of hydrocarbon fuels from alternative sources have been investigated. The investigated processes have the potential of being a part of the future chemical industry based on methanol as carrier of energy and carbon. Whether this future scenario will emerge is not known, but one thing is certain: The fossil resources will not last forever, and massive changes and investments are necessary to adjust to new energy sources and chemical processes. Unless massive breakthroughs are done within a certain area, one type of technology will not be sufficient to replace the fossil resources and a combination of all relevant technologies is necessary.

Even though the fossil resources might last for relatively long time, we have the opportunity and obligation to pursue the development of other energy sources and processes for production of fuels and chemicals in due time. This is a necessity in order to maintain our wealth in the future and to ensure that enough resources are present to sustain the entire world population which will most likely continue to increase. Even though energy conservation is a natural part of making the future resources adequate, it is very hard to imagine a declining energy consumption pr. capita worldwide when considering the current development in countries like India and China.

Atmospheric CO_2 represents an inexhaustible carbon source and is equally available to everybody on earth as well as sustainable energy sources like the sun and the wind. Biomass is also available worldwide, but is more abundant in some regions. If sufficiently efficient processes for conversion of these different energy and carbon sources to fuels and chemicals are developed, the future depletion of fossil resources will not only lead to a change in the chemical industry, but a new worldwide situation will emerge where no countries own the major part of the world resources.

7 References

1. Marbán, G.; Valdés-Solís, T., *Int. J. Hydrogen Energy* **2007**, *32*, 1625
2. Muradov, N. Z.; Veziroglu, T. N., *Int. J. Hydrogen Energy* **2008**, *33*, 6804
3. Olah, G. A.; Goeppert, A.; Surya Prakash, G. K., *Towards a methanol economy*, Wiley, Los Angeles, CA, **2006**
4. Wiswall Jr., R. H.; Reilly, J. J.; Wallace, W. E., *Science* **1974**, *186*, 1158
5. Züttel, A., *Mater. Today* **2003**, *6*, 24
6. Christensen, C. H.; Sørensen, R. Z.; Johannessen, T.; Quaade, U. J.; Honkala, K.; Elmøe, T. D.; Køhler, R.; Nørskov, J. K., *J. Chem. Mater.* **2005**, *15*, 4106
7. Sørensen, R. Z.; Hummelshøj, J. S.; Klerke, A. K.; Reves, J. B.; Vegge, T.; Nørskov, J. K.; Christensen, C. H., *J. Am. Chem. Soc.* **2008**, *130*, 8660
8. Olah, G. A., *Angew. Chem. Int. Ed.* **2005**, *44*, 2636
9. Cole, E. B.; Lakkaraju, P. S.; Rampulla, D. M.; Morris, A. J.; Abelev, E.; Bocarsly, A. B., *J. Am. Chem. Soc.* **2010**, *132*, 11539
10. Liu, X.-M.; Lu, G. Q.; Yan, Z.-F.; Beltramini, J., *Ind. Eng. Chem. Res.* **2003**, *42*, 6518
11. Kamarudin, S. K.; Daud, W. R. W; Ho, S. L.; Hasran, U. A., *J. Power Sources* **2007**, *163*, 743
12. Meisel, S. L., *Chemtech* **1988**, *18*, 32
13. Chang, C. D.; Silvestri, A. J., *J. Catal.* **1977**, *47*, 249
14. Meisel S. L.; McCullough, J. P.; Lechthaler, C. H.; Weisz, P. B., *Chemtech* **1976**, *6*, 86
15. Chang, C. D.; Silvestri, A. J., *Chemtech* **1987**, *17*, 624
16. Stöcker M., *Microporous Mesoporous Mater.* **1999**, *29*, 3
17. 2008 Financial & Operating Review, ExxonMobil, www.exxonmobil.com
18. www.uop.com
19. Mokrani, T.; Scurrell, M., *Catal. Rev.* **2009**, *51*, 1
20. www.topsoe.com
21. Keil, F. J., *Microporous Mesoporous Mater.* **1999**, *29*, 49
22. Grosse, A. V.; Snyder, J. C., US Patent 2,492,984, **1950**
23. Adkins, H.; Perkins, P. D., *J. Phys. Chem.* **1928**, *32*, 221
24. Cullinane, N. M.; Chart, S. J.; Meatyard, R., *J. Soc. Chem. Ind.* **1948**, *67*, 142
25. www.iza-structure.org
26. Corma, A., *J. Catal.* **2003**, *216*, 298
27. Svelle, S.; Joensen, F.; Nerlov, J.; Olsbye, U.; Lillerud, K. P.; Kolboe, S.; Bjørgen, M., *J. Am. Chem. Soc.* **2006**, *128*, 14770
28. Bjørgen, M.; Svelle, S.; Joensen, F.; Nerlov, J.; Kolboe, S.; Bonino, F.; Palumbo, L.; Bordiga, S.; Olsbye, U., *J. Catal.* **2007**, *249*, 195
29. Kvisle, S.; Fuglerud, T.; Kolboe, S.; Olsbye, U.; Lillerud, K. P.; Vora, B. V., *Handbook of Heterogeneous Catalysis, Chapter 13.14*, Eds. Ertl, G.; Knözinger, H.; Schüth, F.; Vietkamp, J., Wiley, Los Angeles, CA, **2008**
30. Haw, J. F.; Song, W.; Marcus, D. M.; Nicholas, J. B., *Acc. Chem. Res.* **2003**, *36*, 317

31. Liu, Z.; Sun, C.; Wang, G.; Wang, Q.; Cai, G., *Fuel Proc. Tech.* **2000**, *62*, 161
32. Haw, J. F.; Marcus, D. M., *Nanotechnology in Catalysis, Chapter 13*, Eds. Zhou S.; Hermans, S.; Samorjai, G. A., Kluwer Academic/Plenum, NY, **2004**
33. Wilson, S. T., *Stud. Surf. Sci. Catal., Chapter 4.4.1* **2007**, *168*
34. Cormerias, F. X.; Perot, G.; Chevalier, F.; Guisnet, M., *J. Chem. Res. S.* **1980**, 362
35. Ono, Y.; Mori, T., *J. C. S. Faraday Trans. 1* **1981**, *77*, 2209
36. Olah, G.A.; Doggweiler, H.; Felberg, J. D.; Frohlich, S.; Grdina, M. J.; Karpeles, P.; Keumi, T.; Inaba, S.; Ip, W. M.; Lammertsma, K.; Salem, G.; Tabor, T. C., *J. Am. Chem. Soc.* **1984**, *106*, 2143
37. Olah, G.A.; Doggweiler, H.; Felberg, J. D., *J. Org. Chem.* **1984**, *49*, 2112
38. Olah, G.A.; Doggweiler, H.; Felberg, J. D., *J. Org. Chem.* **1984**, *49*, 2116
39. Zatorski, W.; Krzyzanowski, S., *Acta. Phys. Chem.* **1978**, *29*, 347
40. Dahl, I. M.; Kolboe, S., *Catal. Lett.* **1993**, *20*, 329
41. Dahl, I. M.; Kolboe, S., *J. Catal.* **1994**, *149*, 458
42. Langner, B. E., *Appl. Catal.* **1982**, *2*, 289
43. Dessau, R. M.; LaPierre, R. B., *J. Catal*. **1982**, *78*, 136
44. Dessau, R. M., *J. Catal.* **1986**, *99*, 111
45. Svelle, S.; Rønning, P. O.; Kolboe, S., *J. Catal.* **2004**, *224*, 115
46. Svelle, S.; Rønning, P. O.; Olsbye, U.; Kolboe, S., *J. Catal.* **2005**, *234*, 385
47. Mole, T.; Bett, G.; Seddon, D., *J. Catal.* **1983**, *84*, 435
48. Mikkelsen, Ø.; Rønning, P. O.; Kolboe, S., *Microporous Mesoporous Mater.* **2000**, *40*, 95
49. Olsbye, U.; Bjørgen, M.; Svelle, S.; Lillerud, K. P.; Kolboe, S., *Catal. Today* **2005**, *106*, 108
50. Song, W.; Nicholas, J. B.; Sassi, A.; Haw, J. F., *Catal. Lett.* **2002**, *81*, 49
51. Bjørgen, M.; Bonino, F.; Kolboe, S.; Lillerud, K. P.; Zecchina, A.; Bordiga, S., *J. Am. Chem. Soc.* **2003**, *125*, 15863
52. Bjørgen, M.; Olsbye, U.; Petersen, D.; Kolboe, S., *J. Catal.* **2004**, *221*, 1
53. Svelle, S.; Bjørgen, M.; Kolboe, S.; Kuck, D.; Letzel, M.; Olsbye, U.; Sekiguchi, O.; Uggerud, E., *Catal. Lett.* **2006**, *109*, 25
54. Sullivan, R. F.; Egan, C. J.; Langlois, G. E.; Sieg, R. P., *J. Am. Chem. Soc.* **1961**, *83*, 1156
55. Sassi, A.; Wildman, M. A.; Ahn, H. J.; Prasad, P.; Nicholas, J. B.; Haw, J. F., *J. Phys. Chem. B* **2002**, *106*, 2294
56. Xu, T.; Barich, D. H.; Goguen, P. W.; Song, W.; Wang, Z.; Nicholas, J. B.; Haw, J. F., *J. Am. Chem. Soc.* **1998**, *120*, 4025
57. Song, W.; Nicholas, J. B.; Sassi, A.; Haw, J. F., *Catal. Lett.* **2002**, *81*, 49
58. Song, W.; Nicholas, J. B.; Haw, J. F., *J. Phys. Chem.* **2001**, *105*, 4317
59. Arstad, B.; Kolboe, S., *J. Am. Chem. Soc.* **2001**, *123*, 8137
60. Svelle, S.; Kolboe, S. Swang, O.; Olsbye, U., *J. Chem. Phys.* **2005**, *109*, 12874
61. Bjørgen, M.; Joensen, F.; Lillerud, K. P.; Olsbye, U.; Svelle, S., *Catal. Today* **2009**, *142*, 90
62. McCann, D. M.; Lesthaeghe, D.; Kletnieks, P. W.; Guenther, D. R.; Hayman, M. J.; Van Speybroeck, V.; Waroquier, M.; Haw, J. F., *Angew. Chem. Int. Ed.* **2008**, *47*, 5179
63. Song, W.; Marcus, D. M.; Fu, H.; Ehresmann, J. O.; Haw, J. F., *J. Am. Chem. Soc.* **2002**, *124*, 3844
64. Lesthaeghe, D.; Van SpeyBroeck, V.; Marin, G. B.; Waroquir, M., *Angew. Chem. Int. Ed.* **2006**, *45*, 1714

65. Marcus, D. M.; McLachlan, K. A.; Wildman, M. A.; Ehresmann, J. O.; Kletnieks, P. W.; Haw, J. F., *Angew. Chem. Int. Ed.* **2006**, *45*, 3133
66. Haw, J.F.; Marcus, D. M., *Top. Catal.* **2005**, *34*, 41
67. Janssens, T. V. W., *J. Catal.* **2009**, *264*, 130
68. Chang, C. D.; Lang, W. H.; Smith, R. L., *J. Catal.* **1979**, *56*, 169
69. Voltz, S. E.; Wise, J. J., *Development Studies on Conversion of Methanol and Related Oxygenates to Gasoline* Final Report, US ERDA Contract No E(49-18)-1773 **1976**
70. Teketel, S.; Svelle, S.; Lillerud, K. P.; Olsbye, U., *ChemCatChem* **2009**, *1*, 78
71. Choudhary, T. V.; Aksoylu, V.; Goodman, D. W., *Catal. Rev.* **2003**, *45*, 151
72. Hagen, A.; Roesnner, F., *Catal. Rev.* **2000**, *42*, 403
73. Schulz, P.; Baerns, M., *Appl. Catal.* **1991**, *78*, 15
74. Chetina, O. V.; Vasina, T. V.; Lunin, V. V., *Appl. Catal.* **1995**, *131*, 7
75. Pidko, E. A.; Kazansky, V. B.; Hensen, E. J. M.; van Santen, R. A., *J. Catal.* **2006**, *240*, 73
76. Nishi, K.; Komai, S.; Inagi, K.; Satsuma, A.; Hattori, T., *Appl. Catal. A* **2002**, *223*, 187
77. Choudhary, T. V.; Kinage, A.; Banerjee, S.; Choudhary, V. R., *Catal. Commun.* **2006**, *7*, 166
78. Sun, C.; Yao, S.; Shen, W.; Lin, L., *Catal. Lett.* **2007**, *122*, 84
79. Tessonnier, J.-P.; Louis, B.; Rigolet, S.; Ledoux, M. J.; Pham-Huu, C., *Appl. Catal. A* **2008**, *336*, 79
80. Inazu, K.; Koyama, T.; Miyaji, A.; Baba, T. *J. Jpn. Petrol. Inst.* **2008**, *51*, 205
81. Kusmiyti; Amin, N. A. S., *Catal. Today.* **2005**, *106*, 271
82. Baba, T.; Abe, Y., *Appl. Catal. A* **2003**, *250*, 265
83. Choudhary, V. R.; Kinage, A. K.; Choudhary, T. V., *Science* **1997**, *275*, 1286
84. Anunziata, O. A.; Mercado, G. G., *Catal. Lett.* **2006**, *107*, 111
85. Anunziata, O. A.; Mercado, G. V. G.; Pierella, L. B., *Catal. Lett.* **2003**, *87*, 167
86. Pierella, L. B.; Wang, L. S.; Anunziata, O. A., *React. Kinet. Catal. Lett.* **1997**, *60*, 101
87. Choudhary, V. R.; Mondal, K. C.; Mulla, S. A. R., *Angew. Chem. Int. Ed.* **2005**, *44*, 4381
88. Rovik, A. K.; Hagen, A.; Schmidt, I.; Dahl, S.; Chorkendorff, I.; Christensen, C. H., *Catal. Lett.* **2006**, *109*, 153
89. Leth, K. T.; Rovik, A. K.; Holm, M. S.; Brorson, M.; Jakobsen, H. J.; Skibsted, J.; Christensen, C. H., *Appl. Catal. A* **2008**, *348*, 257
90. Lücke, B.; Martin, A.; Günschel, H.; Nowak, S., *Microporous Mesoporous Mater.* **1999**, 145
91. Safronova, S. S.; Koval, L. M.; Erofeev, V. I., *Theor. Found. Chem. Eng.* **2008**, *42*, 550
92. Mier, D.; Aguayo, A. T.; Atutxa, A.; Gayubo; A. G., Bilbao, J., *Int. J. Chem. React. Eng.* **2007**, *5*, A60
93. Bolotov, V. V.; Poddubnyi, V. V.; Koval, L. M., *Russ. J. Phys. Chem. A* **2007**, *81*, 1521
94. Safronova, S. S.; Koval, L. M.; Chernov, E. B.; Bolotov, V. V., *Russ. J. Phys. Chem. A* **2005**, *79*, 55
95. Magnoux, P.; Roger, P.; Canaff, C.; Fouche, V.; Gnep, N. S.; Guisnet, M., *Stud. Surf. Sci. Catal.* **1987**, *34*, 317
96. Lónyi, F.; Valyon, J., *Microporous Mesoporous Mater.* **2001**, *47*, 293
97. Costa, E.; Uguina, A.; Aguado, J.; Hernández, P. J., *Ind. Eng. Chem. Process Des. Dev.* **1985**, *24*, 239
98. Aguayo, A. T.; Gayubo, A. G.; Tarrío, A. M.; Atutxa, A.; Bilbao, J., *J. Chem. Technol. Biotechnol.* **2002**, *77*, 211

99. Derouane, E. G.; Nagy, J. B.; Dejaifve, P. van Hoff, J. H. C.; Spekman, B. P.; Védrine, J. C.; Naccache, C., *J. Catal.* **1978**, *53*, 40
100. Johanson, R.; Hruby, S. L.; Rass-Hansen, J.; Christensen, C. H., *Catal. Lett.* **2009**, *127*, 1
101. Gayubo, A. G.; Aguayo, A. T.; Atutxa, A.; Aguado, R.; Bilbao, J., *J. Ind. Eng. Chem. Res.* **2004**, *43*, 2610
102. Tau, L.-M.; Davis, B. H., *Fuel Processing Technol.* **1993**, *33*, 1
103. Tau, L.-M.; Fort, A. W.; Bao, S.; Davis, B. H., *Fuel Processing Technol.* **1990**, *26*, 209
104. Tabak, S. A.; Krambeck, F. J.; Garwood, W. E., *AIChE J.* **1986**, *64*, 72
105. Gujar, A. C.; Guda, V. K.; Nolan, M.; Yan, Q.; Toghiani, H.; White, M. G., *Appl. Catal. A* **2009**, *363*, 115
106. Bjørgen, M.; Joensen, F.; Holm, M. S.; Olsbye, U.; Lillerud, K. P.; Svelle, S., *Appl. Catal. A* **2008**, *345*, 43
107. Platon, A.; Thomson, W. J., *Catal lett.* **2005**, *101*, 15
108. Haw, J., *Phys. Chem. Chem. Phys.* **2002**, *4*, 5431
109. Gayubo, A. G.; Alonso, A.; Valle, B.; Aguayo, A. T.; Bilbao, J., *Appl. Catal. B* **2010**, *97*, 299
110. Inoue, K.; Inaba, M.; Takahara, I.; Murata, K., *Catal. Lett.* **2010**, *136*, 14
111. Inaba, M.; Murata, K.; Saito, M.; Takahara, I., *React. Kinet. Catal. Lett.* **2006**, *88*, 135
112. Oikawa, H.; Shibata, Y.; Inazu, K.; Iwase, Y.; Murai, K.; Hyodo, S.; Kobayashi, G.; Baba, T., *Appl. Catal. A* **2006**, *312*, 181
113. Ferreira Madiera, F.; Gnep, N. S.; Magnoux, P.; Maury, S.; Cadran, N, *Appl. Catal. A* **2009**, *367*, 39
114. Svelle, S.; Kolboe, S.; Swang, O., *J. Phys. Chem. B* **2004**, *108*, 2953
115. Wichterlová, B.; Čejka, J.; Žilková, N., *Microporous Mater.* **1996**, *6*, 405
116. Bejblová, M.; Žilková, N.; Čejka, J., *Res. Che. Intermed.* **2008**, *34*, 439
117. Aitani, A. M.; Ali, A. M.; Waziri, S. M.; Al-Khattaf, S., *Chem. Eng. Technol.* **2010**, *33*, 1193
118. Handreck, G. P.; Smith, T. D., *J. Catal.* **1990**, *123*, 513
119. Kosslick, H.; Tuan, V. A.; Parlitz, B.; Fricke, R.; Peuker, C.; Storek, W., *J. Chem. Soc. Faraday Trans.* **1993**, *89*, 1131
120. Fricke, R.; Kosslick, H.; Lischke, G.; Richter, M., *Chem. Rev.* **2000**, *100*, 2303
121. Lalik, E.; Liu, X.; Klinowski, J., *J. Phys. Chem.* **1992**, *96*, 805
122. Choudhary, V. R.; Kinage, A. K., *Zeolites* **1995**, *15*, 732
123. Romannikov, V. N.; Chumachenko, L. S.; Mastikhin, V. M.; Ione, K. G., *React. Kinet. Catal. Lett.* **1985**, *29*, 85
124. Pérez-Ramirez, J.; Christensen, C. H.; Egeblad, K.; Christensen, C. H.; Groen, J. C., *Chem. Soc. Rev.* **2008**, *37*, 2530
125. Jacobsen, C. J. H.; Madsen, C.; Janssens, T. V. W., Jakobsen, H. J.; Skibsted, J., *Microporous Mesoporous Mater.* **2000**, *39*, 393
126. Groen, J. C.; Jansen, J. C.; Moulijn, J. A.; Pérez-Ramirez, J., *J. Phys. Chem.* **2004**, *108*, 13062
127. Sun, C.; Du, J.; Liu, J.; Yang, Y.; Ren, N.; Shen, W.; Xu, Hualong, Tang, Y., *Chem. Commun.* **2010**, *46*, 2671
128. Kim, J.; Choi, M.; Ryoo, R., *J. Catal.* **2010**, *269*, 219
129. Jacobsen, C. H. J.; Madsen, C.; Houzvicka, J.; Schmidt, I.; Carlsson, A., *J. Am. Chem. Soc.* **2000**, *122*, 7116

130. Parillo, D. J.; Lee, C.; Gorte, R. J.; White, D.; Farneth, W. E., *J. Phys. Chem.* **1995**, *99*, 8745
131. Triantafillidis, C. A.; Vlessidis, A. G.; Nalbandian, L.; Evmiridis, N. P., *Micrporous Mesoporous Mater.* **2001**, *47*, 369
132. Bayense, C. R.; van der Pol, A. J. H. P.; van Hooff, J. H. C., *Appl. Catal.* **1991**, *72*, 81
133. Huber, G. W.; Iborra, S.; Corma, A., *Chem. Rev.* **2006**, *106*, 4044
134. Lin, Y.-C.; Huber, G. W., *Energy. Environ. Sci.* **2009**, *2*, 68
135. Regalbuto, J. R., *Science* **2009**, *325*, 822
136. Hasegawa, F.; Yokoyama, S.; Imou, K., *Biores. Technol.* **2010**, *101*, S109
137. Puig-Arnavat, M.; Bruno, J. C.; Coronas, A., *Renew. Sus. Energy Rev.* **2010**, *14*, 2841
138. Weisz, P. B.; Haag, W. O.; Rodewald, P. G., *Science* **1979**, *206*, 57
139. Haniff, M. I.; Dao, L. H., *Appl. Catal.* **1988**, *39*, 33
140. Chen, N. Y.; Degnan Jr., T. F.; Koenig, L. R., *Chemtech* **1986**, *16*, 506
141. Dao, L. H.; Haniff, M.; Houle, A.; Lamothe, D., *Prepr. Pap. - Am. Chem. Soc. Div. Fuel Chem.* **1987**, *32*, 308
142. Bridgwater, A. V.; Cottam, M.-L., *Energy & Fuels* **1992**, *6*, 113
143. Gayubo, A. G.; Valle, B.; Aguayo, A. T.; Olazar, M.; Bilbao, J., *Energy Fuels* **2009**, *23*, 4129
144. Gayubo, A. G.; Valle, B.; Aguayo, A. T.; Olazar, M.; Bilbao, J., *Ind. Eng. Chem. Res.* **2010**, *49*, 123
145. Sharma, R. K.; Bakhshi, N. N., *Biomass and Bioenergy* **1993**, *5*, 445
146. Carlson, T. R.; Vispute, T. P.; Huber, G. W., *ChemSusChem* **2008**, *1*, 397
147. Carlson, T. R.; Topsett, G. A.; Conner, W. C.; Huber, G. W., *Top. Catal.* **2009**, *52*, 241
148. Carlson, T. R.; Jae, J.; Huber, G. W., *ChemCatChem* **2009**, *1*, 107
149. Kunkes, E. L.; Simonetti, D. A.; West, R. M.; Serrano-Ruiz, J. C.; Gärtner, C. A.; Dumesic, J. A., *Science* **2008**, *322*, 417
150. Heeres, H.; Handana, R.; Chunai, D.; Rasrendra, C. B.; Girisuta, B.; Heeres, H.J., *Green Chem.* **2009**, *11*, 1247
151. Mehdi, H.; Fabos, V.; Tuba, R.; Bodor, A.; Mika, L. T.; Horvath, I. T., *Top. Catal.* **2008**, *48*, 49
152. Bond, J. Q.; Alonso, D. M.; Wang, D.; West, R. M.; Dumesic, J. A., *Science* **2010**, *327*, 1110
153. Gayubo, A. G.; Aguayo, A. T.; Atutxa, A.; Aguado, R.; Olazar, M.; Bilbao, J., *Ind. Eng. Chem. Res.* **2004**, *43*, 2619
154. Hutchings, G. J.; Johnston, P.; Lee, D. F.; Warwick, A.; Williams, C. D.; Wilkinson, M., *J. Catal.* **1994**, *147*, 177
155. Fuhse, J.; Bandermann, F., *Chem. Eng. Technol.* **1987**, *10*, 323
156. Danuthai, T.; Jongpatiwut, S.; Rirksomboon, T.; Osuwan, S.; Resasco, D. E., *Appl. Catal. A* **2009**, *361*, 99
157. Williams, P. T.; Brindle, A. J., *J. Anal. Appl. Pyrolysis* **2003**, *67*, 143
158. Holm, M. S.; Saravanamurugan, S.; Taarning, E., *Science* **2010**, *328*, 602
159. Serrano-Ruiz, J. C.; Dumesic, J. A., *Green Chem.* **2009**, *11*, 1101
160. Deane, S; Wilshier, K.; Western, R.; Mole, T.; Seddon, D., *J. Catal.* **1984**, *88*, 499
161. Chantal, P. D.; Kaliaguine, S.; Grandmaison, J. L., *Appl. Catal.* **1985**, *18*, 133
162. Horne, P. A.; Williams, P. T., *Renew. Energy* **1996**, *7*, 131
163. Zhu, X.; Mallinson, R. G.; Resasco, D. E., *Appl. Catal. A* **2010**, *379*, 172

164. Taarning, E.; Saravanamurugan, S.; Holm, M. S.; Xiong, J.; West, R. M.; Christensen, C. H., *ChemSusChem* **2009**, *2*, 625
165. Corma, A.; Nemeth, L. T.; Renz, M.; Valencia, S., *Nature* **2001**, *412*, 423
166. Renz, M.; Blasco, T.; Corma, A.; Fornés, V.; Jensen, R.; Nemeth, L., *Chem. Eur. J.* **2002**, *8*, 4708

8 Included publications

Catal Lett (2009) 127:44–48
DOI 10.1007/s10562-008-9726-8

Co-conversion of Ethane and Methanol into Higher Hydrocarbons over Ga/H-ZSM-5, Mo/H-ZSM-5 and Ga-Mo/H-ZSM-5

Uffe V. Mentzel · Anne K. Rovik · Claus Hviid Christensen

Received: 16 July 2008 / Accepted: 8 October 2008 / Published online: 11 November 2008

Abstract Ethane and methanol are converted simultaneously over Ga/H-ZSM-5, Mo/H-ZSM-5 and Ga-Mo/H-ZSM-5 to produce light olefins and aromatics. The presence of methanol in the reactant stream is intended to facilitate activation of ethane following literature reports on co-conversion of methane and methanol. However, the conversion of ethane actually decreases significantly when methanol is present. To gain insight into mechanistic details, ^{13}C-labeled methanol is co-converted with unlabeled ethane. These isotopic labeling studies show that carbon atoms from ethane and methanol are mixed in the products and in the carbonaceous compounds deposited on the catalysts. This indicates that both reactants take part in the formation of the hydrocarbon pool, which is the origin of all products.

Keywords Ethane conversion · MTH · Co-conversion · Mo/H-ZSM-5 · Ga/H-ZSM-5

U. V. Mentzel · A. K. Rovik · C. H. Christensen
Center for Sustainable and Green Chemistry, Department of Chemistry, Technical University of Denmark, 2800 Kgs. Lyngby, Denmark

A. K. Rovik
Department of Chemical Engineering, Technical University of Denmark, 2800 Kgs. Lyngby, Denmark

A. K. Rovik
Center for Individual Nanoparticle Functionality, Technical University of Denmark, 2800 Kgs. Lyngby, Denmark

C. H. Christensen (✉)
Haldor Topsøe A/S, Nymøllevej 55, 2800 Kgs. Lyngby, Denmark
e-mail: chc@topsoe.dk

1 Introduction

Natural gas is often produced at remote places and needs to be transported over large distances. This has proved to be a challenge. The gas can be transported in pipelines, which requires massive investments and maintenance, or alternatively it can be compressed or liquefied, but these processes consume a lot of energy. Therefore some of the produced natural gas is still being flared at the well site, whereby valuable products are lost and a considerable amount of CO_2 is emitted to the atmosphere. In the future, flaring of natural gas will most likely be banned or at least extremely costly, so it must be circumvented. As a consequence it could be very attractive to convert natural gas into valuable and easily transportable products at the well site.

One way of exploiting the low-molecular-weight hydrocarbons in the natural gas is by non-oxidative catalytic conversion into olefins or aromatics over metal-containing acidic zeolites [1, 2]. These reactions are endothermic and the thermodynamic equilibrium does not favor the desirable products unless the temperature is relatively high. When the reaction temperature is increased, the possibility of coking the catalyst is also increased, so an intermediate temperature is used, where the conversion is reasonably high while coking is suppressed. A possible way of circumventing these temperature restrictions is by activating the hydrocarbons by the addition of suitable compounds to the reactant stream. Several research groups have studied this approach, e.g., activation of methane by addition of various alkanes [3–6], alkenes [7–10], or light gasoline [11].

In another well-investigated reaction, hydrocarbons are produced by converting methanol into gasoline (MTG) or into olefins (MTO) over an acidic ZSM-5 zeolite catalyst [12–14]. This reaction is exothermic and is typically performed at 350–400 °C.

A combination of the non-oxidative dehydroaromatization of alkanes and the methanol conversion might prove useful, since the heat produced in the exothermic methanol conversion can be exploited in the endothermic hydrocarbon aromatization. In principle, a thermoneutral reaction can be obtained in this way. The working hypothesis is that the alkane is activated by a combination of the dehydrogenating metal sites and the methanol generated hydrocarbon species on the catalyst [15].

Several research groups attempted to use methanol to promote the conversion of alkanes over different zeolite catalysts in cracking as well as aromatization reactions. Nowak and co-workers [16, 17] studied the methanol activated cracking of hydrocarbons by co-converting methanol with hydrocarbons like *n*-decane, *n*-hexane, cyclohexane, naphta, *n*-butane, and C_4 olefins over different Fe-containing modified H-ZSM-5 catalysts. The main products in these reactions were olefins. In another series of studies, Safronova et al. [18–24] co-converted methanol with a mixture of propane and butane over H-ZSM-5, and also observed an increase in the production of olefins when methanol was present. Methanol was also used by Chang et al. [25, 26] to improve the catalytic cracking of *n*-hexane over an H-ZSM-5 zeolite.

In a different study, Choudhary et al. [15] investigated the co-conversion of methane and methanol over Ga-, Zn-, In-, and Mo-modified H-ZSM-5 zeolites in the production of olefins and aromatics. Choudhary et al. reported that the conversion of methane was highly promoted by the presence of methanol in the feed. At conditions where methane by itself was not converted at all, it converted readily with methanol present. In fact, methane and methanol were converted in equimolar amounts.

This work by Choudhary et al. prompted us to investigate the possible activation of ethane by co-conversion with methanol over metal-containing H-ZSM-5 catalysts.

2 Experimental

2.1 Catalyst Preparation

The NH_4-ZSM-5 zeolite obtained from Zeolyst (CBV3024E, Si/Al = 15) was calcined at 550 °C for 4 h to obtain the acidic form. The zeolite was subsequently impregnated by the incipient wetness technique using aqueous solutions of $Ga(NO_3)_3 \cdot xH_2O$ and/or $(NH_4)_6 Mo_7O_{24} \cdot 4H_2O$, dried overnight at 110 °C, and calcined at 550 °C for 4 h. The catalyst powder was pelleted, crushed, and sieved to obtain the desired particle size of 180–355 μm. The prepared catalysts contained 3 wt% Ga, 3 wt% Mo, and 2 wt% Ga + 2 wt% Mo, respectively.

2.2 Catalytic Tests

The catalytic tests were carried out with 500 mg of catalyst in a plug flow quartz reactor with an inner diameter of 3.7 mm. All the catalysts were pretreated at 550 °C prior to test. The Ga/H-ZSM-5 catalyst was pretreated in a flow of He for 2 h, while the molybdenum containing catalysts were pretreated in a H_2/CH_4 mixture (6% H_2) for 4 h to produce the catalytically active molybdenum carbide [15]. Tests were carried out at atmospheric pressure and at an oven temperature of 500 °C. The flow of ethane was 590 mL(SATP)/h. A uniform stream of methanol (WHSV = 0.16 gg^{-1} h^{-1}) was obtained by leading 550 mL(SATP)/h of He through a bubble flask containing methanol at room temperature followed by another flask kept at 16 °C. The product stream from the reaction was analyzed by an online HP6890A gas chromatograph equipped with a TCD and an FID connected in series. The conversion of ethane was calculated from the TCD using Ar as an internal standard and the conversion of methanol was 100% in all runs. When ^{13}C-labeled methanol was used, gas samples were taken out manually through a septum immediately after the oven using a gas syringe of 1 mL. These gas samples were analyzed by GC–MS (Agilent 5975 MSD/6850 GC) to identify the distribution of labeled and unlabeled carbon atoms in the products.

2.3 Dissolution of the Catalyst

In order to analyze the carbonaceous compounds deposited on the catalysts the zeolites were dissolved in hydrofluoric acid after the catalytic tests using a method introduced by Guisnet and co-workers [27]. About 100 mg of the spent catalyst was placed in a closed teflon vial, 2 mL of 20% HF was added, and the zeolite was left to dissolve for 30 min. The liberated carbonaceous deposits were extracted by adding 1 mL of CH_2Cl_2 and analyzed by GC–MS.

3 Results and Discussion

The catalytic experiments are designed to resemble the methane and methanol co-conversion experiments performed by Choudhary et al. [15].

The Ga/H-ZSM-5 catalyst shows an ethane conversion of around 4% under the chosen test conditions (Fig. 1) with no methanol present. When methanol is added to the feed, the conversion drops significantly to around 2%. Thus, the conversion of ethane is apparently not increased by the presence of methanol; in fact, the opposite seems to be the case. The same tendency is observed for the Mo/H-ZSM-5 and Ga-Mo/H-ZSM-5 catalysts; especially

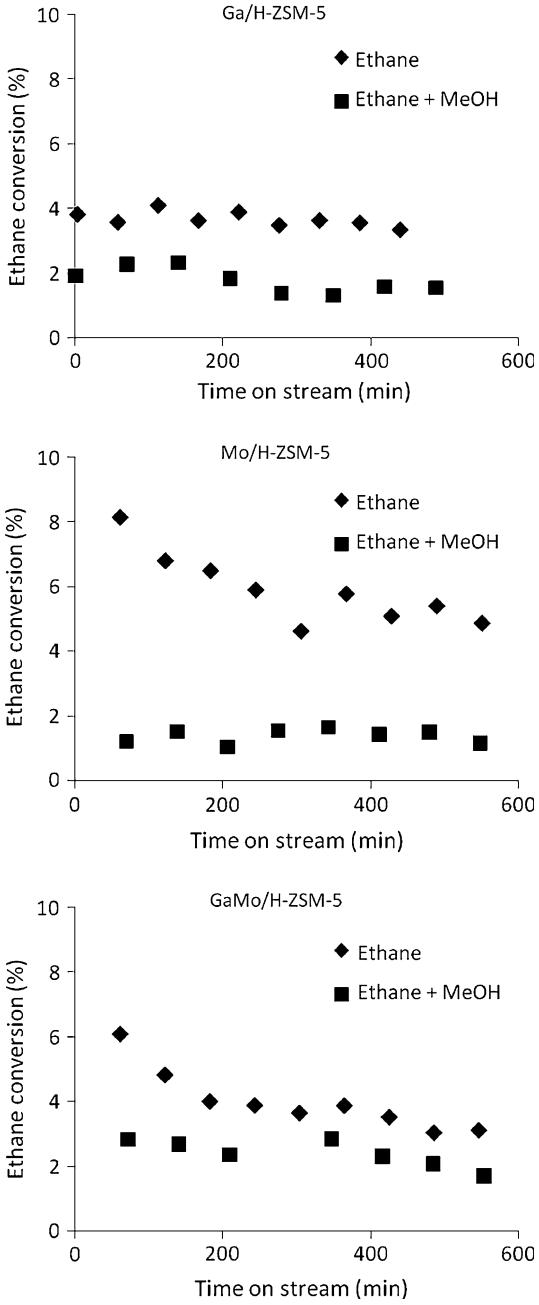

Fig. 1 Conversion of ethane, with and without methanol present ($T = 500$ °C, GHSV(ethane) = 1,180 $cm^3\ g^{-1}\ h^{-1}$, GHSV(He) = 1,100 $cm^3\ g^{-1}\ h^{-1}$, WHSV(MeOH) = 0.16 $gg^{-1}\ h^{-1}$)

in the case of Mo/H-ZSM-5, the presence of methanol suppresses the conversion of ethane significantly.

The product selectivities for the co-conversion of ethane and methanol and for the conversion of the two reactants alone over Ga/H-ZSM-5 are shown in Fig. 2. The selectivities are relatively constant throughout the entire test period. The main products in the reactions are aromatics and small olefins. The presence of methanol induces production of heavier aromatics and more methane compared

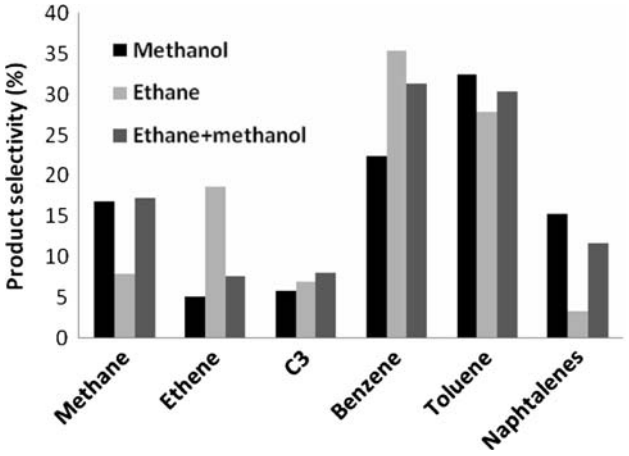

Fig. 2 Product selectivities in the conversion of methanol, ethane and ethane + methanol over Ga/H-ZSM-5 after at 500 °C, time on stream = 200 min

to when ethane is converted alone. It is interesting to note that the reaction does not produce aliphatics larger than C3 in detectable amounts. When methanol is converted alone, only insignificant amounts of ethane are produced. The decrease in the conversion of ethane is therefore not due to production of ethane from methanol.

There could be several possible reasons for the decrease in ethane conversion in the presence of methanol. We believe that the most plausible explanation is that methanol and ethane are competing for the same catalytic sites. Ethane needs a combination of a dehydrogenating metal site and an acidic site on the zeolite to convert into aromatics; however methanol and hydrocarbon species generated from methanol are also able to bind to the metal sites, leaving fewer sites to convert ethane. Methanol is much more reactive than ethane or ethene, and is therefore converted at the inlet of the reactor, whereas ethane is converted throughout the entire catalyst bed. Due to the relatively high reaction temperature (500 °C) methanol is converted immediately, and there will not be any methanol present in the lower part of the reactor. However, methanol is converted to a range of products (small olefins and aromatics) which might be able to promote the conversion of ethane [7]. Even though these species might activate ethane, it is apparently not enough to make up for all the active sites occupied by the conversion of methanol.

Another factor that might be responsible for the suppressed ethane conversion is that methanol induces heavy coking of the catalyst, mainly at the inlet. This will naturally deactivate the catalyst and could lead to a lower conversion. However, Fig. 1 shows that the catalyst does not deactivate faster when methanol is present, within the timescale studied. The fact that the initial conversion is much lower when methanol is present supports the

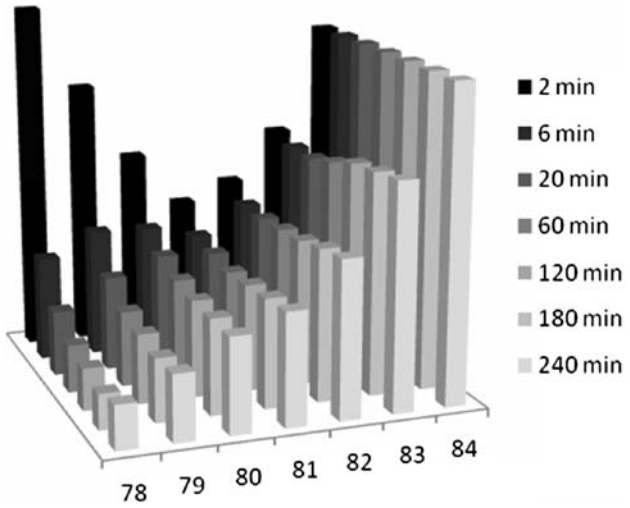

Fig. 3 Mass spectra of benzene, produced at different reaction times in a co-conversion experiment of unlabeled ethane and ^{13}C-labeled methanol over Ga/H-ZSM-5 at 500 °C. Normalized with respect to M = 84

hypothesis described above, that methanol and ethane simply compete for the same catalytic sites.

To trace if the carbon atoms in the products originate from ethane or methanol, co-conversion of unlabeled ethane and ^{13}C-labeled methanol was performed over Ga/H-ZSM-5. Gas samples were taken out from the product stream at different reaction times and analyzed by GC–MS. Figure 3 shows the mass spectra of benzene produced after different reaction times. There is a clear tendency, that in the first few minutes there is a high degree of ^{12}C incorporation (from ethane), which quite rapidly levels off, giving a smoother isotope distribution. All the aromatic products show this tendency.

We believe that this phenomenon is caused be a stoichiometric reaction between ethane and Ga_2O_3 on the catalyst, whereby ethane is oxidized and Ga_2O_3 is reduced to its catalytically active state. However, another possibility is that methanol is mainly used to generate a hydrocarbon pool in the catalyst during the first minutes, which would lead to an excess of ^{12}C from ethane in the products.

After the induction period, we see that carbon atoms from ethane and methanol are still mixed in the products. This clearly shows that we have a hydrocarbon pool mechanism, where both methanol and ethane are incorporated, leading to scrambling of isotopes in the products.

To extract information about the hydrocarbon pool in the catalysts, the zeolites are dissolved after the catalytic tests and the deposited carbon species are investigated by GC–MS. Figure 4 shows mass spectra of some hydrocarbon species generated in the catalyst in a co-conversion experiment of unlabeled ethane and ^{13}C-labeled methanol over Ga/H-ZSM-5. The fact that the isotopes are completely mixed confirms that a hydrocarbon pool, where both ethane and methanol are incorporated, is generated in the catalyst. But even though both reactants are involved in the mechanism, they may have completely different reaction pathways in the hydrocarbon pool. For instance, naphthalene has a much higher content of ^{12}C (from ethane) than both trimethylbenzene and tetramethylbenzene, indicating that they are produced via different reaction mechanisms. We have not looked further into the mechanistic details, since it is beyond the scope of this study.

4 Conclusions

The presence of methanol is not beneficial for the conversion of ethane in our experiments; the conversion of ethane actually drops when methanol is present. We believe this is due to competition for the active sites; methanol simply takes up the sites leaving ethane unreacted. The fact that the presence of methanol has a pronounced negative effect on the conversion of ethane is somewhat surprising since Choudhary et al. [15] reported a successful activation of methane in the presence of methanol using similar conditions and catalysts as in our study.

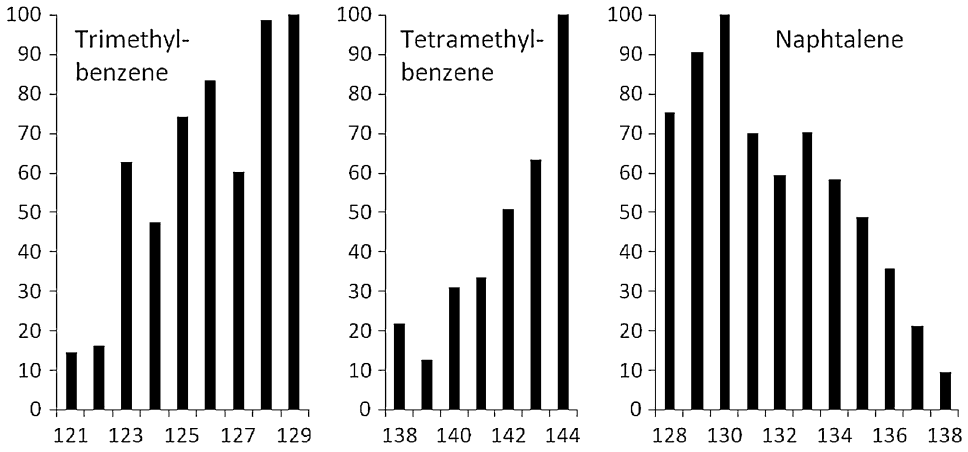

Fig. 4 Mass spectra of different carbonaceous compounds deposited on the catalyst after co-conversion of unlabeled ethane and ^{13}C-labeled methanol over Ga/H-ZSM-5 for 2 h

^{13}C-labeling studies indicate an initial activation of the catalyst where ethane reduces Ga_2O_3 to its catalytically active state. The labeling studies also clearly show that carbon atoms from ethane and methanol are mixed in the products and in the deposited carbonaceous material on the zeolite. This indicates that both ethane and methanol take part in the formation of a hydrocarbon pool in the catalyst, from where the products are formed, i.e., ethane and methanol are successfully co-converted in the sense that they are involved in the same overall reaction mechanism. However, the co-conversion does not promote the conversion of ethane.

Acknowledgments The Center for Sustainable and Green Chemistry is sponsored by the Danish National Research Foundation. Anne Krogh Rovik would like to thank Copenhagen Graduate School for Nanoscience and Nanotechnology (CONT) for funding. Haldor Topsøe A/S is acknowledged by Anne Krogh Rovik and Uffe Vie Mentzel for funding.

References

1. Hagen A, Roessner F (2000) Catal Rev 42:403
2. Choudhary TV, Aksoylu V, Goodman DW (2003) Catal Rev 45:151
3. Anunziata OA, Mercado GG, Pierella LB (2004) Catal Commun 5:401
4. Anunziata OA, Mercado GVG, Pierella LB (2003) Catal Lett 87:167
5. Liu JF, Liu Y, Peng LF (2008) J Mol Catal A: Chem 280:7
6. Anunziata OA, Eimer GA, Pierella LB (2000) Appl Catal A Gen 190:169
7. Choudhary VR, Kinage AK, Choudhary TV (1997) Science 275:1286
8. Baba T, Abe Y (2003) Appl Catal A Gen 250:265
9. Baba T, Sawada H (2002) Phys Chem Chem Phys 4:3919
10. Kusmiyati , Amin NAS (2005) Catal Today 106:271
11. Anunziata OA, Mercado GG (2006) Catal Lett 107:111
12. Stöcker M (1999) Microporous Mesoporous Mater 29:3
13. Olsbye U, Bjørgen M, Svelle S, Lillerud K-P, Kolboe S (2005) Catal Today 106:108
14. Bjørgen M, Svelle S, Joensen F, Nerlov J, Kolboe S, Bonino F, Palumbo L, Bordiga S, Olsbye U (2007) J Catal 249:195
15. Choudhary VR, Mondal KC, Mulla SAR (2005) Angew Chem Int Ed Engl 44:4381
16. Martin A, Nowak S, Lücke B, Günschel H (1989) Appl Catal 50:141
17. Lücke B, Martin A, Günschel H, Nowak S (1999) Microporous Mesoporous Mater 29:145
18. Safronova SS, Koval LM, Chernov EB, Bolotov VV (2005) Russ J Phys Chem 79:47
19. Erofeev VI, Shabalina LB, Koval LM, Minakova TS (2002) Russ J Appl Chem 75:752
20. Erofeev VI, Shabalina LB, Koval LM, Minakova TS (2002) Russ J Appl Chem 75:1646
21. Shabalina LB, Erofeev VI, Minakova TS, Koval LM (2002) Russ J Appl Chem 75:1979
22. Koval LM, Safronova SS, Chernov EB, Bolotov VV, Zhukova NV (2003) Russ J Appl Chem 76:1461
23. Koval LM, Bolotov VV, Zhukova NV, Safronova SS, Tregubkin RA (2005) Russ J Appl Chem 78:769
24. Bolotov VV, Poddubnyi VV, Koval LM (2007) Russ J Phys Chem A 81:1521
25. Chang F, Wei Y, Liu X, Zhang D, He Y, Liu Z (2006) Catal Lett 106:171
26. Chang F, Wei Y, Liu X, Zhao Y, Xu L, Sing Y, Zhang D, He Y, Liu Z (2007) Appl Catal A 328:163
27. Magnoux P, Roger P, Canaff C, Fouche V, Gnep NS, Guisnet M (1987) Stud Surf Sci Catal 34:317

J|A|C|S
ARTICLES

Published on Web 10/30/2009

High Yield of Liquid Range Olefins Obtained by Converting *i*-Propanol over Zeolite H-ZSM-5

Uffe V. Mentzel,*[,†,‡] Saravanamurugan Shunmugavel,[†] Sarah L. Hruby,[§] Claus H. Christensen,[‡] and Martin S. Holm*[,†,‡]

Department of Chemistry, Technical University of Denmark, DK-2800 Kgs. Lyngby, Haldor Topsøe A/S, 2800 Kgs. Lyngby, and Department of Chemical and Biological Engineering, Iowa State University, Ames, Iowa 50011

Received September 10, 2009; E-mail: uvm@kemi.dtu.dk; msh@kemi.dtu.dk

Abstract: Methanol, ethanol, and *i*-propanol were converted under methanol-to-gasoline (MTH)-like conditions (400 °C, 1−20 bar) over zeolite H-ZSM-5. For methanol and ethanol, the catalyst lifetimes and conversion capacities are comparable, but when *i*-propanol is used as the reactant, the catalyst lifetime is increased dramatically. In fact, the total conversion capacity (calculated as the total amount of alcohol converted before deactivation in $g_{alcohol}/g_{zeolite}$) is more than 25 times higher for *i*-propanol compared to the lower alcohols. Furthermore, when *i*-propanol is used as the reactant, the selectivity toward alkanes and aromatics declines rapidly over time on stream, and at 20 bar of pressure the liquid product mixture consists almost exclusively of C_4-C_{12} alkenes after approximately a third of the full reaction time. This discovery could open a new route to hydrocarbons via *i*-propanol from syn-gas or biobased feedstocks.

Introduction

The methanol-to-hydrocarbons (MTH) reaction was discovered and commercialized more than two decades ago. However, due to the situation on the global oil market, the gasoline synthesis was discontinued.[1,2] Currently, the MTH reaction is receiving renewed attention due to the focus on renewable fuel sources.[3] The level to which this reaction can contribute to a sustainable nonfossil-based energy sector naturally depends on the origin of the methanol.[4] Methanol is traditionally produced from coal or natural gas via syn-gas, but many interesting nonfossil routes for the production of methanol as well as higher alcohols are investigated today.[5] Methods for production of higher alcohols from syn-gas are also under development[6,7] as is the gasification of biomass to syn-gas.[8]

Since the MTH reaction was discovered in the early 1970s and published in 1977,[9] the reaction mechanism has been widely debated.[10] The "hydrocarbon pool mechanism" in which carbonaceous species in the zeolitic pores are part of the catalytic system has become generally accepted. This idea was originally suggested by Mole[11] and Langner,[12] and a decade later Kolboe et al.[13,14] introduced a more general mechanism. Through isotopic labeling experiments Bjørgen et al.[15] uncovered further mechanistic details about the hydrocarbon pool and suggested "the dual cycle mechanism". Recently, mechanistic modeling has also been used to gain insight into the mechanistic details.[16,17]

In the MTH reaction, the zeolite catalyst suffers from deactivation due to coking and frequent regeneration by combustion of the deposited coke is required. It is thus a key research area to improve the catalyst lifetime between regenerations. Another important objective is to suppress the formation of aromatic compounds and shift the selectivity toward the production of olefins (the MTO reaction).[18,19] Numerous approaches have been tried to obtain these goals, most of them dealing with optimization of the catalyst or modifying the reaction conditions.[20−24]

[†] Technical University of Denmark.
[‡] Haldor Topsøe A/S.
[§] Iowa State University.

(1) Stöcker, M. *Microporous Mesoporous Mater.* **1999**, *2*, 9–3.
(2) Topp-Jørgensen, J. *Stud. Surf. Sci. Catal.* **1998**, *36*, 293.
(3) Suntana, A. S.; Vogt, K. A.; Turnblom, E. C.; Upadhye, R. *Appl. Energy* **2009**, *86*, 215.
(4) Vogt, K. A.; Vogt, D. J.; Patel-Weynand, T.; Upadhye, R.; Edlund, D.; Edmonds, R. L.; Gordan, J. C.; Suntana, A. S.; Sigurdardottir, R.; Miller, M.; Roads, P. A.; Andreu, M. G. *Renew. Energ.* **2009**, *34*, 233.
(5) Atsumi, S.; Hanai, T.; Liao, J. C. *Nature.* **2008**, 451.
(6) Iranmahboob, J.; Hill, D. O.; Toghiani, H. *Appl. Catal., A* **2002**, *231*, 99.
(7) Spivey, J. J.; Egbebi, A. *Chem. Soc. Rev.* **2007**, *36*, 1514.
(8) Al Arni, S.; Bosio, B.; Arato, E. *Renew. Energ.* **2010**, *35*, 29.
(9) Chang, C. D.; Silvestri, A. J. *J. Catal.* **1977**, *47*, 249.
(10) Haw, J. F.; Song, W.; Marcus, D. M.; Nicholas, J. B. *Acc. Chem. Res.* **2003**, *36*, 317.
(11) Mole, T.; Whiteside, J. A.; Seddon, D. *J. Catal.* **1983**, *82*, 261.
(12) Langner, B. E. *Appl. Catal.* **1982**, *2*, 289.
(13) Dahl, I. M.; Kolboe, S. *Catal. Lett.* **1993**, *20*, 329.
(14) Dahl, I. M.; Kolboe, S. *J. Catal.* **1994**, *149*, 458.
(15) Bjørgen, M.; Svelle, S.; Joensen, F.; Nerlov, J.; Kolboe, S.; Bonino, F.; Bordiga, S.; Olsbye, U. *J. Catal.* **2007**, *249*, 195.
(16) McCann, D. M.; Lesthaeghe, D.; Kletnieks, P. W.; Guenther, D. R.; Hayman, M. J.; Speybroeck, V. V.; Waroquier, M.; Haw, J. F. *Angew. Chem., Int. Ed.* **2008**, *47*, 5179.
(17) Svelle, S.; Tuma, C.; Rozanska, X.; Kerber, T.; Sauer, J. *J. Am. Chem. Soc.* **2009**, *131*, 816.
(18) Haw, J. F.; Marcus, D. M. *Nanotechnology in Catalysis*; Plenum Publishers: New York, 2004; Vol. 1, Chapter 13.
(19) Bjørgen, M.; Joensen, F.; Lillerud, K.-P.; Olsbye, U.; Svelle, S. *Catal. Today* **2009**, *142*, 90.
(20) Chen, J. Q.; Bozzano, A.; Glover, B.; Fuglerud, T.; Kvisle, S. *Catal. Today* **2005**, *106*, 103.
(21) Mokrani, T.; Scurrell, M. *Catal. Rev.* **2009**, *51* (1), 145.

Table 1. Feed Rates and Observed Conversion Capacities

	P (atm)	WHSV (h^{-1})	feed rate $n_{alcohol}$ (mmol/g_{cat}*h)	feed rate n_{carbon} (mmol/g_{cat}*h)	conv. cap. $mol_{carbon}/g_{zeolite}$	conv. cap. $g_{alcohol}/g_{zeolite}$
methanol	1	8.4	263	263	11	350
ethanol	1	12.1	263	526	22	505
i-propanol	1	15.8	263	789	565	11300

In the literature, many different reactants have been tested under MTH-like reaction conditions. Already in the first article on MTH[9] a number of different oxygen containing reactants (higher alcohols, carbonyl compounds, acids, and esters) were screened in the reaction, all resulting in a mixture of hydrocarbon products. Recently, Gayubo et al.[25,26] did a thorough screening of reactants, including higher alcohols (propanol and butanol) phenols, aldehydes, ketones, and carboxylic acids. In all cases, a mixture of hydrocarbon products containing olefins, paraffins, and aromatics was produced, illustrating that H-ZSM-5 is virtually omnivorous. In an attempt to elucidate mechanistic information, mixtures of methanol and higher alcohols (ethanol, *i*-propanol, and 1-butanol), were reacted over H-ZSM-5 by Tau et al.[27] Through isotopic labeling experiments it was concluded that the carbon atoms from the different alcohols are scrambled and distributed randomly in the products. Lifetime and deactivation of the catalyst however was not addressed in these studies.

Tabak et al. have converted propene and butene to hydrocarbons over ZSM-5.[28] They show that the small alkenes oligomerize and by varying the reaction temperature and pressure they are able to change the reactivity of oligomerization versus cracking and thereby controlling the molecular weight of the products.

In an early study,[29] methanol and ethanol were compared as reactants over H-ZSM-5, and very similar product distributions were obtained. This was confirmed in a recent article from our research group, where the differences in the hydrocarbon pool were also discussed.[30]

Very recently, Gujar et al. studied the conversion of C_1-C_4 alcohols over H-ZSM-5 in a batch reactor. They concluded that the higher alcohols produce more organic liquid than methanol, when allowed to react for the fixed time in the reactor.[31]

Even though several different reactants and cofeeding experiments have been tested in the catalytic conversion over H-ZSM-5, almost no emphasis has been put on the dependence of the reactant on catalyst lifetime and deactivation when using other reactants than methanol or ethanol. In the present study, methanol, ethanol, and *i*-propanol are compared as reactants over H-ZSM-5 and the focus is placed on the beneficial effects observed on product selectivity as well as lifetime of the catalyst when feeding *i*-propanol.

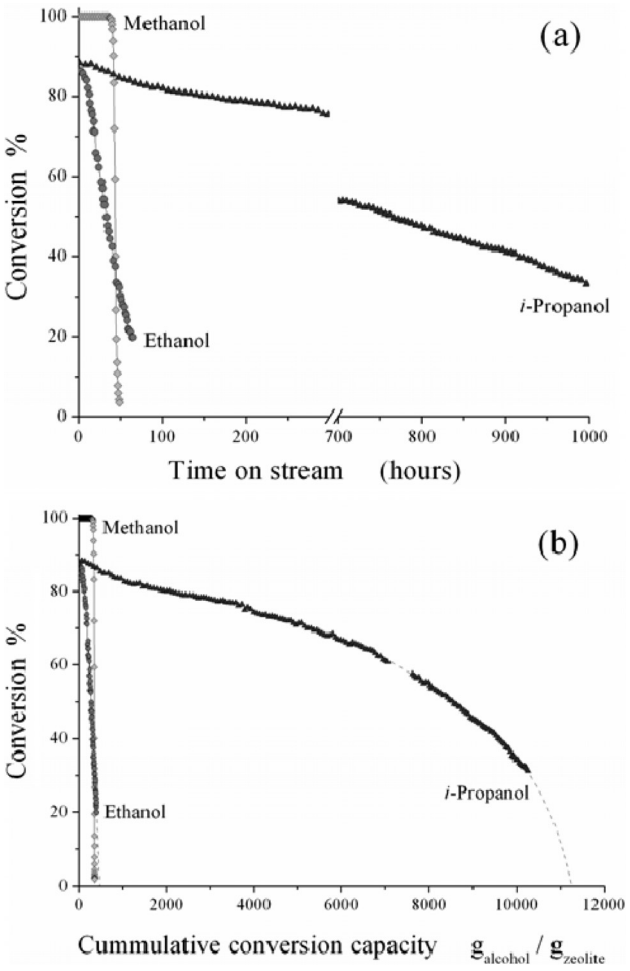

Figure 1. (a) Conversion profiles of methanol, ethanol, and *i*-propanol reacted over H-ZSM-5 at 400 °C. (b) Cumulative conversion capacities in $g_{alcohol}/g_{zeolite}$ given as a function of the alcohol conversion.

Experimental Section

The catalyst used was a commercially available zeolite ZSM-5 (Si/Al = 40) kindly provided by Zeolyst International. The catalytic reactions were performed in a fixed bed reactor at a reaction temperature of 400 °C and a pressure of 1 or 20 bar. In all runs, 300 mg of fractioned (350−500 μm) zeolite catalyst was used. The reactant liquid was introduced by a HPLC pump and evaporated before the catalyst bed. The feed rates of the various alcohols were normalized to introduce an equivalent molar amount of alcohol per unit of time. This resulted in a significantly larger WHSV for the higher alcohols compared to methanol. The feed rates for the different alcohols are listed in Table 1.

For reactions performed at 1 bar, the products were analyzed by an online GC equipped with a flame ionization detector. Helium was used as an inert carrier gas with a flow of 20 mL/min in all nonpressurerized experiments.

When performing the reaction at 20 bar of pressure, the products were condensed at room temperature while still pressurized. The

(22) Bjørgen, M.; Joensen, F.; Holm, M. S.; Olsbye, U.; Lillerud, K. P.; Svelle, S. *Appl. Catal., A* **2008**, *345*, 43.
(23) Christensen, C. H.; Johannsen, K.; Törnqvist, E.; Schmidt, I.; Topsoe, H.; Christensen, C. H. *Catal. Today* **2007**, *128*, 177.
(24) Teketel, S.; Svelle, S.; Lillerud, K. P.; Olsbye, U. *ChemCatChem* **2009**, *1*, 78.
(25) Gayubo, A. G.; Aguayo, A. T.; Atutxa, A.; Aguado, R.; Bilbao, J. *Ind. Eng. Chem. Res.* **2004**, *43*, 2610.
(26) Gayubo, A. G.; Aguayo, A. T.; Atutxa, A.; Aguado, R.; Olazar, M.; Bilbao, J. *Ind. Eng. Chem. Res.* **2004**, *43*, 2619.
(27) Tau, L. M.; Davis, B. H. *Fuel Process. Technol.* **1990**, *26*, 209.
(28) Tabak, S. A.; Krambeck, F. J.; Garwood, W. E. *AIChE J.* **1986**, *64*, 72.
(29) Derouane, E. G.; Nagy, J. B.; Dejaifve, P.; van Hoff, J. H. C.; Spekman, B. P.; Védrine, J. C.; Naccache, C. *J. Catal.* **1978**, *53*, 40.
(30) Johanson, R.; Hruby, S. L.; Rass-Hansen, J.; Christensen, C. H. *Catal. Lett.* **2009**, *127*, 1.
(31) Gujar, A. C.; Guda, V. K.; Nolan, M.; Yan, Q.; Toghiani, H.; White, M. G. *Appl. Catal., A* **2009**, *363*, 115.

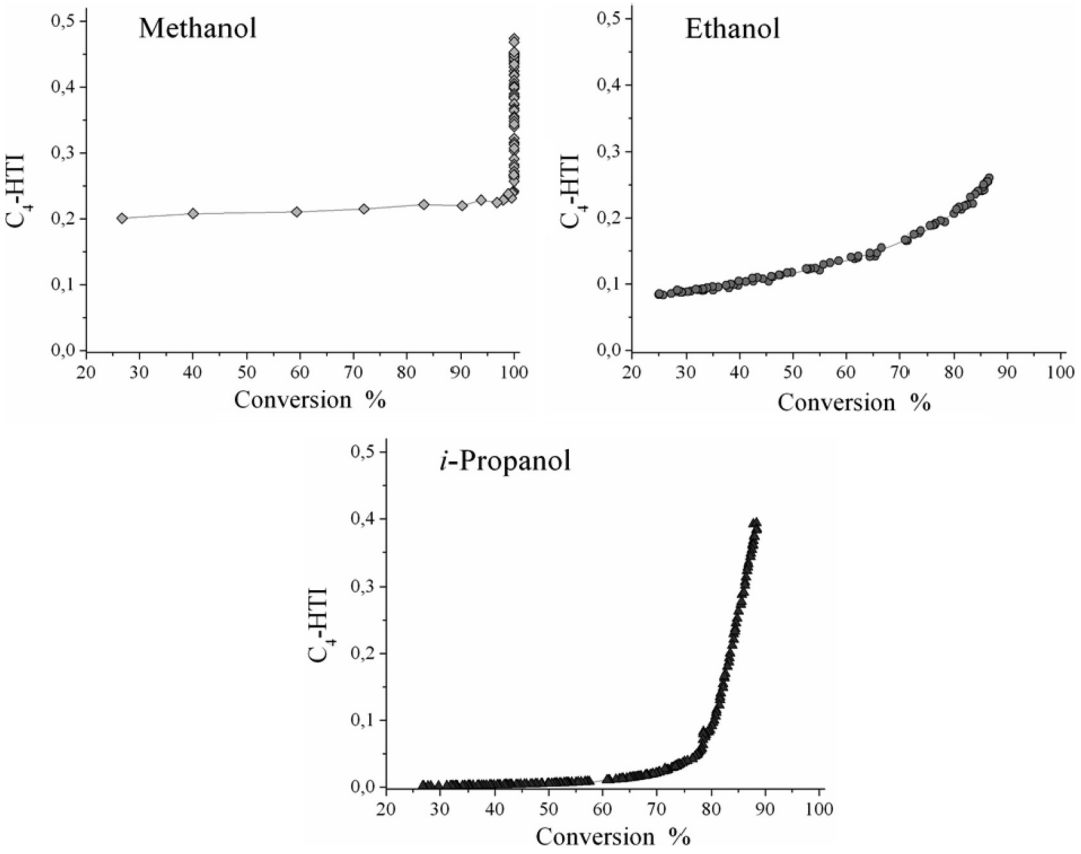

Figure 2. C_4−HTI plotted as a function of the conversion for the three alcohols tested.

gas phase was continuously monitored by an online GC whereas the liquid products were analyzed by offline GC after decompressing the liquid sample to ambient pressure. Helium was used as the carrier gas with a flow of 40 mL/min in all pressurized experiments.

Results and Discussion

The lifetime of the catalyst (conversion vs time on stream) for the different alcohol feeds is illustrated in Figure 1a. When the conversions of the different alcohols are calculated, the direct dehydration products (dimethyl ether, diethyl ether, ethene, dipropyl ether, and propene, respectively) are considered reactants. These dehydration products are still produced over the completely deactivated catalyst, although dipropyl ether was never formed in significant amounts. Initially, we do not observe full conversion in the cases of ethanol and *i*-propanol. This does not mean that the catalyst is not sufficiently active; the (dehydrated) reactants are simply part of the normal products formed during the reaction.

From Figure 1a it is seen that when methanol or ethanol is fed, the catalyst is deactivated within in a few days, but when *i*-propanol is used, the catalyst is still active (>30% conversion) after more than 1000 h on stream.

In addition, the *molar* feed rates are kept constant for the different alcohols, meaning that the catalyst converts three times the amount of carbon/h when *i*-propanol is fed compared to methanol, see Table 1. If *i*-propanol is fed with a WHSV of 8.4 as in the case of methanol, the deactivation of the catalyst scales accordingly, simply making the reaction times required to reach deactivation impractical.

For conversion of methanol, coke is deposited on the catalyst, and a deactivation zone moves through the catalyst bed, resulting in the sudden drop in conversion when the whole catalyst bed is deactivated. This sudden drop in conversion is not observed to the same degree for ethanol and especially not for *i*-propanol.

The cumulative conversion capacity is plotted in Figure 1b, and values showing the total amount (calculated on a weight basis) of alcohol converted over the entire lifetime of the catalyst are summarized in Table 1. When propanol is fed, the catalyst is able to convert more than 25 times the amount of alcohol before reaching complete deactivation, compared to the smaller alcohols.

When the catalytic activity in the MTH reaction is described, the "C_4 hydrogen transfer index" (C_4−HTI) is often used.[22] This is defined as the amount of butanes (iso-butane and *n*-butane) divided by the total amount of C_4-compounds and thus gives a good indication of the development of the hydrogen transfer ability of the working catalyst. When the C_4−HTI is high, the catalyst is able to convert alkenes to aromatics and alkanes. The C_4−HTI as a function of conversion for the three alcohols is presented in Figure 2. For methanol the C_4−HTI is quite high (ca. 0.47) in the beginning and drops steadily as the catalyst deactivates to around 0.22, at which point we observe breakthrough of methanol and the catalyst is completely deactivated. For ethanol and *i*-propanol, the initial values are around 0.26 and 0.38, respectively, and they decline with conversion. Interestingly, for *i*-propanol, the C_4−HTI approaches zero already when the conversion is around 60−70%. This means that the catalyst is no longer able to convert alkenes to aromatics and alkanes, and therefore the product mixture consists almost exclusively of alkenes. A decrease in the C_4−HTI is expected during deactivation due to a decrease in the effective acid site

Table 2. Product Selectivities for Conversion of the Three Alcohols Calculated as Carbon Percentages

	methane	ethane	ethene	propane	propene	C_4-butenes	C_4-butanes	C_{5+}(aliphatics)	aromatics
Methanol									
Initially	0.7	0.2	5.3	6.2	11.8	14.7	12.0	28.3	20.8
~80% conv.	2.4	0.1	8.6	1.1	25.4	14.6	4.0	33.5	10.1
~60% conv.	3.0	0.1	10.9	0.8	24.7	13.2	3.5	33.5	10.0
~40% conv.	4.0	0.1	13.8	0.7	24.2	11.8	3.0	31.1	11.0
Ethanol									
Initially	0.1	0.7	−	5.7	20.6	22.9	7.8	27.3	14.5
~80% conv.	0.1	0.9	−	3.9	23.8	25.2	6.1	27.7	12.4
~60% conv.	<0.1	1.0	−	2.2	27.0	27.8	4.3	29.9	7.8
~40% conv.	<0.1	1.1	−	1.3	29.5	28.5	3.0	30.2	6.5
i-Propanol									
Initially	<0.1	0.1	4.4	7.3	−	19.2	12.4	35.5	21.1
~80% conv.	<0.1	<0.1	2.4	2.2	−	37.1	3.7	50.2	4.4
~60% conv.	<0.1	<0.1	0.7	0.8	−	46.7	0.5	50.8	0.5
~40% conv.	<0.1	<0.1	0.4	0.5	−	38.2	0.1	60.8	<0.1

density present in the catalyst bed.[22,32,33] However, as is the case for the presented methanol experiment, the catalyst will normally be completely deactivated before the C_4−HTI approaches zero. In the case of *i*-propanol this is not true, since the catalyst is still able to perform oligemerization and cracking reactions forming a rich mixture of long branched alkenes when the C_4−HTI is approximately zero.

Product selectivities for the three tested alcohols as a function of the conversion are listed in Table 2. We note that the initial product selectivities are quite similar for all the alcohols, as they all produce a significant amount of aromatics. The selectivity toward aromatics compounds (mainly toluene, xylenes and trimethyl benzene isomers) however decreases significantly for *i*-propanol over time. This is naturally expected from the presented low C_4−HTI of the catalyst at intermediate conversions. Again this observation is in strong contrast to the methanol experiment where the catalyst produces aromatic compounds right up to the point of complete deactivation. Another interesting observation when using *i*-propanol as the reactant is, that the production of ethene also decreases over time. This is in good accordance with conclusions drawn by Svelle et al.,[34] suggesting that the production of ethene is mechanistically linked to the production of aromatics; thus, when a smaller amount of aromatics is produced, a smaller amount of ethene is produced. The fact that the concentration of ethene decreases so dramatically also indicates that only a minor fraction (if any) of the produced ethene is formed from cracking of larger alkenes, since the alkene oligemerization/cracking cycle is still very active at this point. This observation is very important since only small amounts of the lower value products methane, ethane, and ethene are produced.

To confirm the above findings under reaction conditions closer to the industrially used and to push the selectivity toward liquid products, similar experiments with methanol, ethanol and *i*-propanol were performed in a pressure setup operated at 20 bar. The condensed liquid products were periodically withdrawn to atmospheric pressure for GC analysis. The rates of formation of liquid products per gram of zeolite are illustrated in Figure 3 for the three alcohols. Again we observe that the lifetime of the catalyst when feeding *i*-propanol is far superior to the other alcohols. Naturally, the rate of liquid product formation is highly dependent on the WHSV, but in Table 3 the total yields of liquid products before reaching complete deactivation are summarized. Here we see that methanol produces around 160 $mL/g_{zeolite}$ whereas *i*-propanol yields as much as 3550 $mL/g_{zeolite}$.

The dark coloring of the columns in Figure 3(a−c) represents the carbon% present in aromatic compounds. In accordance with the nonpressure experiments *i*-propanol initially produce an aromatic rich liquid but for the latter ~2/3 of the experiment solely C_4−C_{12} alkenes are formed. In Table 3, the total averaged aromatic carbon% of the liquid products is given.

When the reaction is performed at 20 bar, the initial selectivity toward aromatics is higher than at 1 bar, and it declines more rapidly. Furthermore, the lifetime of the catalyst when converting *i*-propanol is around 50% shorter, than at 1 bar. This effect is not observed for methanol and ethanol, where the catalyst shows similar lifetimes at 1 and 20 bar.

Along with the much higher conversion capacity of *i*-propanol, the low aromatic carbon% illustrates the pronounced difference of using *i*-propanol compared to methanol or ethanol as the reactant. GC-MS analysis was used to identify the various compounds formed during the experiment. Figure 4 shows the product distribution in the organic liquid when using *i*-propanol. The sample presented in Figure 4a was obtained after approximately 250 h on stream representing a case from Figure 3c where insignificant amounts of aromatics are formed. Clearly we see that a huge range of different alkene isomers is produced from the reaction. There are no detectable aromatic compounds and only minute traces of alkanes present in the liquid at this point. Alkene contribution ranges from C_4 to C_{12} species. The shape selectivity of the zeolite is clearly affecting the larger products, no bulky products are able to escape the zeolite pores and mainly methylated long chains are present in the products. Interestingly, as the catalyst deactivates further from this point the product distribution changes systematically. In the last hours of operation we observe a pronounced enrichment in the C_6, C_9 and C_{12} alkenes indicating that cracking of the formed alkenes is diminished and we thus mainly observe the direct oligomerization products of propene, see Figure 4b.

Conclusions

It has been shown here that the lifetime and conversion capacity of the zeolite catalyst is increased dramatically when *i*-propanol is used as reactant instead of methanol or ethanol in the catalytic conversion over H-ZSM-5.

Furthermore, when reacting *i*-propanol the C_4−HTI approaches zero after approximately a third of the full experimental

(32) Janssens, T. V. W. *J. Catal.* **2009**, *264*, 130.
(33) Bjørgen, M.; Kolboe, S. *Appl. Catal., A* **2002**, *225*, 285.
(34) Svelle, S.; Joensen, F.; Nerlov, J.; Olsbye, U.; Lillerud, K. P.; Kolboe, S.; Bjørgen, M. *J. Am. Chem. Soc.* **2006**, *128*, 14770.

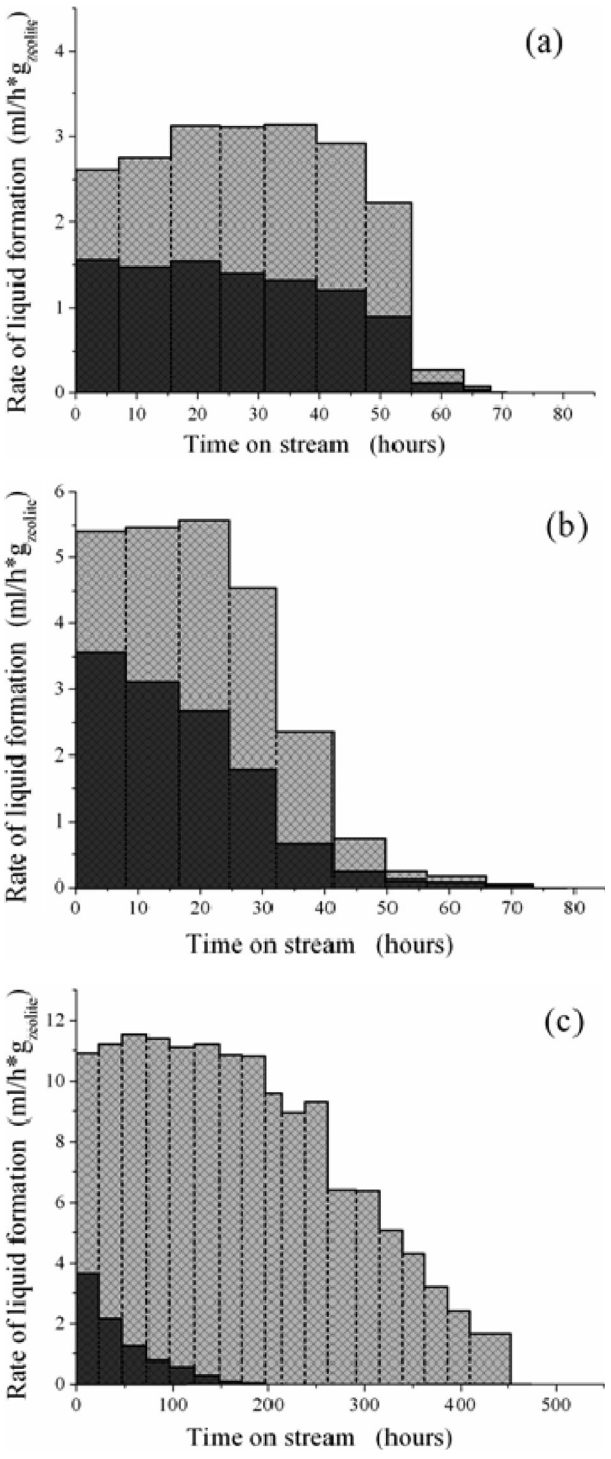

Figure 3. Rate of formation of the organic phase from reacting (a) methanol, (b) ethanol, and (c) *i*-propanol over H-ZSM-5 at 400 °C. The dark coloring represents the carbon% present in aromatics.

run time, meaning that the selectivity is almost exclusively shifted toward the production of alkenes, and only minute amounts of aromatics and alkanes are formed. The resulting alkene rich liquid product which is very low in aromatic content can serve as an attractive raw material for the chemical industry, or could easily be hydrogenated to produce high quality clean fuel. On the basis of the results presented here, an alternative route from syn-gas or biobased feedstocks to hydrocarbons going via *i*-propanol instead of methanol can be envisaged.

Table 3. Total Yield and Selectivities at 20 bar

	P bar	WHSV gg^{-1}h^{-1}	org. liq. mL/g$_{cat}$	total carbon in aromatics
Methanol	20	8.4	160	46.9%
Ethanol	20	12	200	49.9%
i-Propanol	20	16	3550	6.1%

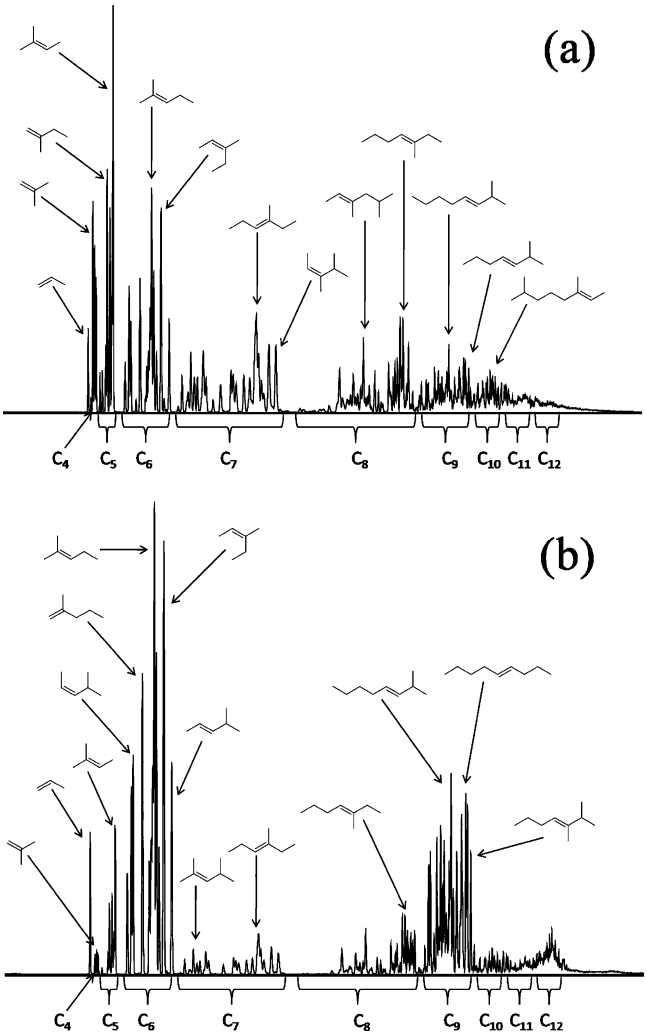

Figure 4. GC-MS analysis of the organic phase feeding *i*-propanol (a) after 250 h on stream and (b) after 425 h on stream. Major compounds are labeled for illustrative reasons.

Acknowledgment. The Centre for Catalysis and Sustainable Chemistry is sponsored by the Danish National Research Foundation. S.L.H. acknowledges the National Science Foundation's Partnership for International Research and Education (PIRE) (NSF grant OISE 0730277) for financial support.

JA907692T

DOI: 10.1002/cctc.200((will be filled in by the editorial staff))

Utilization of Biomass: Conversion of Model Compounds to Hydrocarbons over Zeolite H-ZSM-5

Uffe V. Mentzel,*[a] and Martin S. Holm*[a]

Zeolite catalyzed deoxygenation of small oxygenates present in bio-oil or selected as model compounds was performed under Methanol-to-Hydrocarbons (MTH) like reaction conditions using H-ZSM-5 as the catalyst. Co-feeding of the oxygenates typically decreased catalyst lifetime due to coking and resulted in higher selectivities towards aromatics as compared to pure methanol. The reaction pattern of the different oxygenates was seen not to simply follow the effective H/C ratio of the additives since structural isomers, having identical effective H/C ratios, showed significant differences concerning catalyst lifetimes and product selectivities. A distinct positive effect was observed for methanol dilution, and up to 10 times the amount of additive could be converted before catalyst deactivation if the additive was diluted in methanol as compared to reacted pure. We observe that in particular acid/ester functionalities favor oxygen removal through decarbonylation over dehydration which preserves hydrogen in the hydrocarbon product mixture. By employing ^{13}C labeled substrates we confirmed an efficient deoxygenation of the additives as well as a pronounced affinity of the additive carbon towards incorporation into the aromatic products.

Introduction

A strive towards a sustainable and more environmentally friendly production of chemicals and transportation fuels is pursued today.[1] The use of a biomass derived additive e.g. bio-ethanol or bio-diesel to conventional fuels represent examples of current strategies towards "greener" fuels. [2,3]

Bio-oil can be produced from numerous types of biomass e.g. straw through a rapid thermal treatment with no or only little oxygen present. Bio-oil represents an abundant and near CO_2 neutral resource which could find application if sufficiently robust upgrading strategies could be identified. Dependent on the starting material and the specific treatment conditions large compositional discrepancies are seen within bio-oils but in general it is a highly complex mixture of oxygenates produced by depolymerization and fragmentation of cellulose, hemi-cellulose and lignin.[4] Bio-oil is immiscible with hydrocarbons, contains large amounts of water and is relatively unstable, however the liquid has an advantage with respect to handling and transport over untreated biomass.[5,6] Homogenization of bio-oil into a mixture of hydrocarbons through zeolite catalyzed deoxygenation has been a long-time goal and could ensure compatibility with conventional gasoline.[7] In fact, researchers at Mobil already in the years following the discovery of the Methanol-to-gasoline (MTG) process [8] investigated this idea of converting biomass into hydrocarbons primarily over zeolite ZSM-5.[9,10] They introduced the effective H/C ratio of a substrate (see below), with H, O and C being the moles of hydrogen, oxygen and carbon present in the compound, as a convenient measure of the hydrogen content left in the products once oxygen was removed in the form of water.[11]

$$\frac{H}{C}effective = \frac{(H-2O)}{C}$$

Excessive deactivation of the catalyst by coking was discovered as a major problem when reacting compounds with an effective H/C ratio below 2. A carbohydrate with a molecular formula of $C_6H_{12}O_6$ has an effective H/C ratio of 0 and will thus be able to produce only carbon if fully dehydrated. However, if the reactants are deoxygenated by decarbonylation or decarboxylation (CO or CO_2 formation, respectively) hydrogen is retained in the hydrocarbon products. Consequently, if a gasoline product mixture with a

[a] *U. V. Mentzel and M. S. Holm*
Centre for Catalysis and Sustainable Chemistry
Department of Chemistry, Technical University of Denmark
Anker engelundsvej 1
2800 Kgs. Lyngby
Denmark, DK
e-mail: uvm@kemi.dtu.dk, msh@kemi.dtu.dk

similar H/C content as conventional MTG fuel is desired a hexose would need to dissociate 1/3 third the carbon as CO_2 which resemble what is done during fermentation when CO_2 and ethanol is formed.

Several authors have reported on zeolite catalyzed conversion of bio-oil/pyrolysis vapors [12,13,14,15,16,17] or selected model compounds present in bio-oil [18,19,20,21,22,23,24,25,26,27,28,29] over mainly zeolite ZSM-5 at MTG-like reaction conditions. Due to the very complex nature of bio-oil only limited information regarding the reactivity of the individual components is obtained when feeding the entire bio-oil mixture which merits the investigation of representative compounds. Very interestingly the reports show that hydrocarbons can indeed be produced from virtually any oxygenate but generally the catalyst suffers from extremely fast deactivation by coking. The addition of methanol, which has an effective H/C ratio of 2, will increase the combined H/C ratio of the feed and has been reported to have a positive effect e.g. on the conversion of furfural.[30,31,11] Also dilution of bio-oil with methanol has been reported [32] and recently Bilbao and co-workers showed that a major effect of methanol is attenuation of the condensation of pyrolytic lignin when the feed is heated prior to introduction to the reactor. Significant improvements were thus achieved in a two-step process where the bio-oil and methanol mixture was volatilized in a separate unit before the catalytic conversion.[33,34,35]
The use of zeolite catalysts for the conversion of biomass derived compounds in the high temperature range of FCC have also recently been reported.[36,37,38] In relation to this, Huber et al. used finely dispersed sugar physically blended with the catalyst while applying extremely rapid heating and were able to produce single- and poly-aromatics alongside CO_2 and water although also excessive coking of the catalyst occurs.[39,40,41]

Here we present a study investigating the reactivity of selected oxygenates when co-feed with methanol at MTG reaction conditions over zeolite H-ZSM-5. The additives were selected to cover a wide range of H/C ratios and contain different functionalities. We chose to co-react the oxygenates as 10 wt. % solutions to obtain lifetimes between one hour and 2 days which made a comparison of their compatibility with MTG possible. The simple effective H/C ratio does not take account for oxygen being present as different functionalities or as positional isomers and we find significant differences between compounds having similar effective H/C ratios. The most interesting compounds were further tested in a wt.% series intended to quantify the positive effect of methanol dilution with respect to conversion capacity of the additive before catalyst deactivation. A total conversion capacity of the additive as well as changes in the product selectivity were investigated and we could identify concentration optima where up to 10 times the amount of additive could be converted as compared to converting the additive without any methanol present. By using ^{13}C-labeled additives (or ^{13}C methanol) we were able to address whether the carbon atoms from the most oxidized and hydrogen deficient additives were in fact quantitatively and/or selectively incorporated into the hydrocarbon products.

Results and Discussion

Additive screening

An initial screening of pure compounds with relatively high effective H/C ratios (≤1,5) was done at MTG reaction conditions (370 °C) over H-ZSM-5. This resulted in catalyst lifetimes in the order of minutes which was in strong contrast to reacting methanol giving a catalyst lifetime of around 65 hours. Clearly, this illustrated that excessive coking of the zeolite catalyst occurred when non-mono alcohols were converted. In order to be able to examine all molecules under similar conditions we therefore chose to react the compounds diluted to 10 wt.% in methanol. This resulted in catalyst lifetimes spanning from as little as 2% to approximately equal that of pure methanol thus giving an idea of the "toxicity" of co-converting the individual molecules. Table 1 presents the additives chosen for co-feeding, the total conversion capacities in $g_{feed}/g_{zeolite}$ and the amount of CO and CO_2 formed (given as a percent relative to the molar amount of additive introduced). The initial product distribution is described by the C_4-HTI (hydrogen transfer index) being a descriptor of the hydrogen transfer activity of the catalyst in combination with grouped selectivities.[42] Both taken approximately 10% into the full experiment run time. As is the case in conventional MTG, the product selectivity in the co-feeding experiments shifted from high aromatic and paraffinic products towards olefins as the catalyst gradually deactivated.[43]

From the data in Table 1 we see that any additive leads to a lower conversion capacities as compared to pure methanol with the exception of water, formic acid and the higher alcohols. The later is in good correlation with results published elsewhere [44] while water and formic acid (formic acid dissociates into CO and water) leads to a lower WHSV of methanol with an increased water concentration which presumably suppresses coke formation.[27] Co-feeding a 10 wt.% solution of the phenolic species anisole or 1,2-dimethoxybenzene results in conversion capacities of only <10 $g_{feed}/g_{zeolite}$ compared to 471 $g_{feed}/g_{zeolite}$ for pure methanol. The huge difficulty in converting these species is in good agreement with previous reports.[18,19] Additional compounds which deactivated the catalyst strongly were levulinic acid, glycerol and formaldehyde dimethyl acetal. These compounds gave conversion capacities around 10% that of pure methanol and all represent highly hydrogen deficient molecules with critically low effective H/C ratios of 0.4, 0.6 and 1.33, respectively. As we would expect compounds which are more compatible are indeed candidates with higher effective H/C ratio such as 1,5-pentanediol. Generalizing the tendencies from Table 1 it can be seen that lower conversion capacities are obtained as a function of decreasing H/C ratio of the additives. Illustrative examples of this include hydroxy acetaldehyde (introduced as the dimethyl acetal) which deactivates the catalyst faster than acetaldehyde, glycerol is harder to convert than

Table 1. Conversion capacities, initial selectivities, C_4-HTI and CO/CO_2 production from the 10 wt.% series.

Additive	Eff. H/C (additive)	Conversion Capacity [a]	C_4-HTI [c]	CO [b]	CO_2 [b]	C_{1-3} [c]	C_4 [c]	C_{5+} [c] (aliphatic)	C_{6-10} [c] (aromatic)
H_2O	-	512	0,36	0%	0%	22%	28%	31%	19%
Methanol	2	471	0,38	0%	0%	22%	28%	31%	19%
Formaldehyde dimethyl acetal	1,33	62	0,34	0%	0%	22%	25%	28%	25%
Formic acid	-2	496	0,38	85%	2%	22%	28%	32%	18%
Ethanol	2	487	0,36	0%	0%	24%	27%	31%	18%
Ethyleneglycol	1	131	0,31	4%	0%	23%	24%	25%	28%
Acetaldehyde	1	72	0,29	7%	0%	26%	23%	22%	29%
Acetic acid	0	91	0,26	5%	3%	21%	20%	23%	36%
Glycolaldehyde dimethyl acetal	1	40	0,31	43%	3%	23%	26%	28%	23%
Methyl glycolate	0	86	0,34	91%	0%	23%	25%	26%	26%
2-Propanol	2	578	0,38	0%	0%	21%	28%	32%	19%
1,2-Propanediol	1,33	190	0,32	1%	0%	21%	25%	29%	25%
1,3-Propanediol	1,33	96	0,33	1%	0%	22%	25%	28%	25%
Glycerol	0,67	44	0,33	8%	0%	24%	23%	25%	28%
Acetone	1,33	271	0,29	0%	1%	22%	24%	26%	27%
Propionaldehyde	1,33	138	0,31	3%	0%	22%	24%	26%	28%
Propionic acid	0,67	109	0,30	26%	4%	22%	24%	25%	29%
Methyl lactate	0,5	189	0,33	93%	0%	21%	25%	28%	26%
Methyl acrylate	0,5	27	0,27	26%	10%	24%	22%	25%	29%
1-Butanol	2	679	0,39	0%	0%	20%	27%	32%	21%
1,4-Butanediol	1,5	139	0,33	0%	0%	22%	25%	27%	26%
1,3-Butanediol	1,5	120	0,33	0%	0%	23%	26%	27%	24%
1,2-Butanediol	1,5	166	0,33	n.a.	n.a.	22%	26%	28%	24%
2,3-Butanediol	1,5	320	0,31	0%	0%	22%	25%	29%	24%
Butyraldehyde	1,5	146	0,34	5%	0%	22%	25%	27%	26%
Butanone	1,5	327	0,27	0%	0%	23%	25%	26%	25%
Butyric acid	1	219	0,35	62%	0%	21%	25%	30%	24%
1,5-Pentanediol	1,6	299	0,34	0%	0%	22%	25%	28%	25%
Levulinic acid	0,4	37	0,29	90%	0%	24%	25%	25%	26%
γ-Valerolactone	0,8	82	0,33	78%	7%	22%	26%	28%	24%
2-methyl-tetrahydrofuran	1,6	255	0,36	0%	0%	20%	25%	29%	26%
Toluene	1,14	412	0,33	0%	0%	19%	20%	21%	40%
Anisole	0,86	10	Na.	0%	0%	26%	21%	21%	32%
1,2-dimethoxybenzene	0,75	9	Na.	0%	0%	28%	20%	26%	26%

[a] $g_{feed}/g_{zeolite}$, [b] $mol/mol_{additive}$, [c] initial

propanediol and butanoic acid performs better than the lower acids, however several additional features should be noted.

Figure 1 presents the conversion capacities from Table 1 plotted as a function of the effective H/C ratio of the pure additive. Here it can be seen that compounds which have the same effective H/C ratio do not give identical conversion capacities. This is true for molecules containing oxygen in different functionalities as well as for positional isomers. A pronounced differences in conversion capacity between 2,3-butanediol and the other three butanediols is seen disregarding that they all have an effective H/C ratio of 1.5 and contain the same functional groups. Interestingly butanone reacts similar to 2,3-butanediol whereas butanal groups along with the other diols which have one or two hydroxyl groups at a terminal carbon. The same tendency of higher conversion capacities of the ketone over the aldehyde is seen for the C_3-series when comparing acetone and propanal, where also 1,2-propanediol is significant better than the corresponding 1,3-propanediol.

Levulinic acid and γ-valerolactone can be derived from biomass [45, 46] and represent along with 2-methyl-tetrahydrofuran a series of molecules with an identical

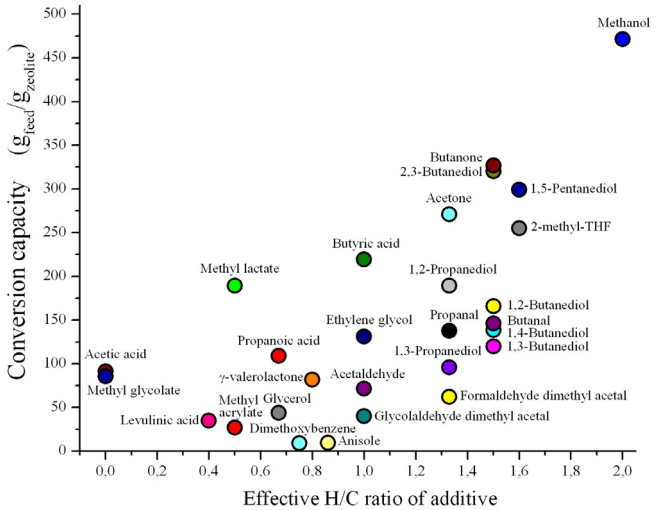

Figure 1. Conversion capacities from experiments having 10 wt.% of additive plotted as a function of the effective H/C ratio of the additive.

carbon backbone but increasingly hydrogenated. From Figure 1 (and Table 1) we see that this series does indeed group according to their oxidation state, with the most reduced compounds performing superior, giving conversion capacities of ~10%, ~20% and ~55% as compared to that of pure methanol, respectively. This observation can prove important since the use of 1 equivalent of H_2 when going from levulinic acid to γ-valerolactone actually doubles the conversion capacity thus showing that partial hydrogenation could be advantageous.

Further from Figure 1 it is apparent that the acids and in particular methyl lactate performs significantly better than could be expected from their low H/C ratios. In conventional MTG the alcohol oxygen is removed by dehydration, it would however be advantageous when reacting higher oxidized compounds to remove oxygen by decarboxylation or to a lesser extend decarbonylation in order to preserve hydrogen in the products through the sacrifice of one carbon atom. Analyzing the $C_{2\text{-}4}$ acids in Table 1 is an illustrative example. Acetic acid forms only minor amounts of CO and CO_2 (5%, 3%) while propanoic acid (26%, 4%) and butyric acid (62%, 0%) produces increasing amounts of CO. The high oxidation state of acetic acid in combination with a negligible tendency to dissociate CO and/or CO_2 (at this concentration) leads to a very high initial aromatic carbon percentage of 35% compared to 29% for propanoic acid, 24% for butanoic acid and only 19% for pure methanol.

Figure 2 shows the initial carbon % located in aromatic products plotted as a function of the effective H/C ratio in the combined feed (methanol+additive) for the compounds in Table 1. The coloring differentiates between molecules able to dissociate significant amounts of CO and/or CO_2 when converted (red) and those unable (blue). Clearly a trend exists that those compounds deoxygenating through dehydration (blue) experience a relatively high selectivity towards aromatics while the red (decarboxylation/decarbonylation) can have low effective H/C ratios without a corresponding large aromate selectivity. We interpret these results as to intrinsic selectivity of the MFI zeolite forces the product distribution within the gasoline range but preserving hydrogen in the products increases the selectivity towards aliphatic over the hydrogen deficient aromatic compounds.

Dissociation of CO is also relevant to explain the extraordinary good performance of methyl lactate. Initially we see more than 90% of the introduced methyl lactate dissociating CO which is in good agreement with recent results.[47] In fact after complete deactivation of the catalyst we observe a continued formation of mainly CO, acetaldehyde and DME (dimethyl ether) indicating that acetaldehyde with a higher effective H/C ratio of 1 as compared to methyl lactate with 0.5 is the “true” reactant.

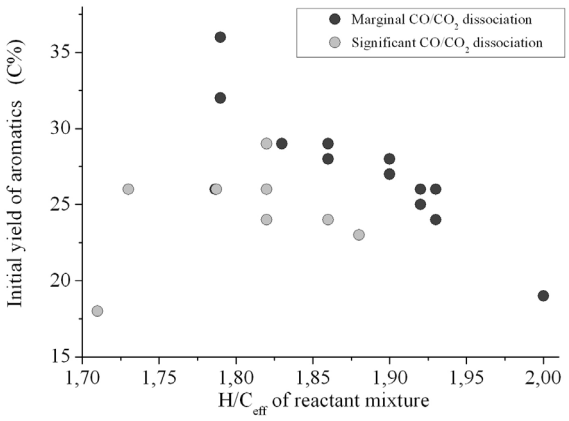

Figure 2. Initial aromatic carbon % plotted as a function of the effective H/C ratio of selected additives from Table 1.

Also levulinic acid and γ-valerolactone forms large amounts of CO and in the case of γ-valerolactone also small amounts of CO_2 are produced. γ-valerolactone has previously been reported to decompose into CO_2 and butene over a weak solid acid at a lower temperature.[48] In our case however, when CO is predominantly dissociated we observe butadiene as the main product appearing over a deactivated catalyst.

Based on the data from Table 1 in combination with knowledge of very short lifetimes when reacting the pure compounds we speculated whether the lifetime improvement from diluting in methanol correlated linearly with the wt.% or it was possible to convert more of the additive at suitable concentrations. To investigate this we chose the 4 most interesting compounds from Table 1 (methyl lactate, γ-valerolactone, glycerol, and acetic acid) and tested them in a concentration series. Figure 3 presents the conversion capacities of methanol as well as the additive obtained from experiments with different wt.% of additive. Figure 3 illustrates that reacting pure methyl lactate or pure γ-valerolactone results in very poor conversion capacities. However, looking at the lower levels of methyl lactate in the feed (Figure 3a) we clearly see that an optimum in the conversion capacity exists from approximately 10-25 wt.%. Conclusively, the dilution of methanol does not only increase the lifetime proportional to the dilution level but fine tuning the concentration leads to an increased total conversion capacity of methyl lactate before the catalyst is deactivated (see Table 2). The lower limit can be understood by considering that with only small amounts of methyl lactate added conventional deactivation from methanol conversion dominates and even if the catalyst had a similar lifetime as that of pure methanol a 2,5 wt.% solution of methyl lactate could not convert as much additive as a feed in the 10-25 wt.% range.

Table 2. Conversion capacities, initial selectivities, C_4-HTI and CO/CO_2 production from the wt.% series.									
Additive	**wt.%**	**Eff. H/C of feed [a]**	**C_4-HTI**	**CO [b]**	**CO_2 [b]**	**C_{1-3}**	**C_4**	**C_{5+} (aliphatic)**	**C_{6-10} (aromatic)**
Methanol	-	2	0.38	0%	0%	22%	28%	31%	19%
Acetic acid	2.5%	1.95	0.34	0%	0%	24%	26%	28%	22%
Acetic acid	5%	1.89	0.31	4%	4%	24%	24%	26%	26%
Acetic acid	10%	1.79	0.27	5%	3%	21%	20%	23%	36%
Acetic acid	25%	1.48	0.19	6%	9%	21%	12%	13%	53%
Glycerol	1%	1.99	0.38	0%	0%	22%	27%	30%	21%
Glycerol	2.5%	1.97	0.36	0%	0%	23%	27%	29%	21%
Glycerol	5%	1.93	0.34	10%	0%	24%	26%	27%	23%
Glycerol	10%	1.86	0.30	11%	0%	24%	23%	25%	28%
Glycerol	25%	1.66	0.23	16%	2%	23%	20%	20%	37%
Glycerol	50%	1.32	Na.[c]	21%	3%	24%	15%	16%	45%
Methyl lactate	2.5%	1.95	0.39	70%	0%	21%	26%	30%	23%
Methyl lactate	10%	1.82	0.33	93%	0%	21%	25%	28%	26%
Methyl lactate	17.5%	1.69	0.31	>95%	1%	23%	24%	26%	27%
Methyl lactate	25%	1.56	0.27	>95%	1%	23%	22%	23%	32%
Methyl lactate	50%	1.17	0.20	>95%	1%	25%	17%	17%	41%
Methyl lactate	100%	0.50	Na.[c]	Na.[c]	Na.[c]	26%	7%	6%	61%
γ-Valerolactone	2.5%	1.95	0.39	76%	<2%	24%	27%	28%	21%
γ-Valerolactone	5%	1.91	0.38	78%	6%	22%	27%	29%	22%
γ-Valerolactone	10%	1.82	0.32	78%	7%	22%	26%	28%	24%
γ-Valerolactone	25%	1.58	0.27	73%	9%	23%	23%	25%	29%
γ-Valerolactone	50%	1.26	0.24	72%	11%	21%	20%	19%	40%
γ-Valerolactone	100%	0.80	Na.[c]	Na.[c]	Na.[c]	17%	16%	15%	52%
[a] calculated from the dehydrated H/C ratios, [b] $mol/mol_{additive}$, [c] too rapid catalyst deactivation to obtain data									

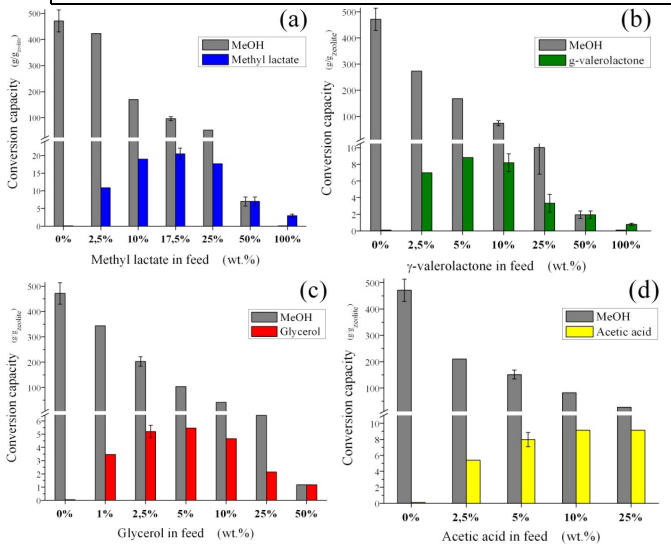

Figure 3. Conversion capacities plotted as a function of the wt.% of additive in the feed. (a) methyl lactate, (b) γ-valerolactone, (c) glycerol and (d) acetic acid. Error bars represent a 96% confidence interval. Note the different scales below the break.

Figure 3b shows a similar dilution behavior for converting γ-valerolactone as seen for methyl lactate. Also here we can identify an optimum in the conversion capacity, though it should be noted that the optimum is lower namely around 5-10 wt.%. In the case of glycerol the experiments revealed an optimum around 2,5-5 wt.% and high loadings above 50 wt.% deactivate the catalyst so rapidly that we chose not to react pure glycerol under these reaction conditions. Glycerol has a very low effective H/C ratio of 0.67 which correlate well with the low optimum limit of addition and the rapid deactivation seen in Table 1. Furthermore, glycerol reacts with only modest levels of CO and CO_2 formation which support the fact that it is one of the most unwanted molecules to co-convert with methanol from a catalyst lifetime perspective.

From analyzing the series of acetic acid experiments a somewhat different trend is revealed. Increasing amounts of acetic acid in the feed results in larger amounts of CO and CO_2 formation which can be explained by an increased tendency of the ketonization reaction forming acetone and CO_2.[26] The conversion capacity of acetic acid thus increases with the concentration correlating with the fact that acetone does not induce massive deactivation (see Table 1). However, very early breakthrough of methyl acetate in the 25 wt.% experiment complicates the quantitative interpretation and tentatively a higher temperature is required to reach a satisfactory conversion.

Product distributions

Clearly not only the conversion capacity but also a change in product selectivity is crucial when co-feeding various compounds. If the deoxygenation proceeds through dehydration reactions and not through decarboxylation and decarbonylation we inevitably will produce an overall more hydrogen deficient product mixture as compared to that of conventional MTG. This point is rather important since it has previously been argued that the high aromatic content in MTG derived gasoline prohibits its implementation.[49,50] Table 2 lists the initial product selectivities as a function of increasing oxygenate addition. We note that reacting small amounts of additive leads to very similar product

compositions as seen for pure methanol. However, as expected with increasing amounts of additive we observe a rise in the abundance of aromatics (mainly benzene, toluene, xylenes and tri-methylbenzenes) at the cost of the C_{4+} aliphatic products while no oxygenated aromatic products are seen. Further from Table 2 it is clear that the increasing aromatic carbon% comes alongside a decreasing hydrogen transfer activity within the aliphatic products, here illustrated by the C_4-HTI. We explain this low C_4-HTI by the possibility of arene production without necessity of co-production of alkanes.

It should be noted that in the high concentration experiments (with run times below one hour) the HTI-index decreases rapidly as deactivation is very pronounced.

With respect to the formation of CO and CO_2 it can be seen from the glycerol and acetic acid experiments in Table 2 that increasing the concentration favors the decarboxylation/decarbonylation route which is in good correlation with a previous report.[34] This can also be seen for very low concentration of methyl lactate and γ-valerolactone which indicate that this is a more general trend.

Isotopic labeling

Through decarbonylation and decarboxylations reactions carbon atoms are sacrificed and will not add to the gasoline product. In order to preserve hydrogen in the fuel we were screening for functionalities which favored this route. The surveillance of the product stream, with respect to CO and CO_2, gives us some indications of what is occurring but a concern was whether the carbon atoms present in the additive did indeed end up as conventional gasoline products. In order to investigate this issue in detail we chose to use ^{13}C labeled additives or ^{13}C labeled methanol and analyze the ^{13}C content in selected main products (butene, butane, pentane, pentene, toluene, xylene and trimethylbenzene). For labeling experiments we chose the additives investigated in Table 2 because these compounds could potentially be derived from biomass, some had the ability to dissociate CO/CO_2 and we could react them in a concentration close to the optimum. In the case of glycerol and acetic acid the additives were ^{13}C labeled whereas for methyl lactate and γ-valerolactone we used standard additives and ^{13}C labeled methanol. The experiments were conducted for <1 hour corresponding to less than 1/10 the total reaction time which makes the data representative to the initial product selectivities given in Table 1 and Table 2. During this time span no change in the pattern of ^{13}C incorporation was observed.

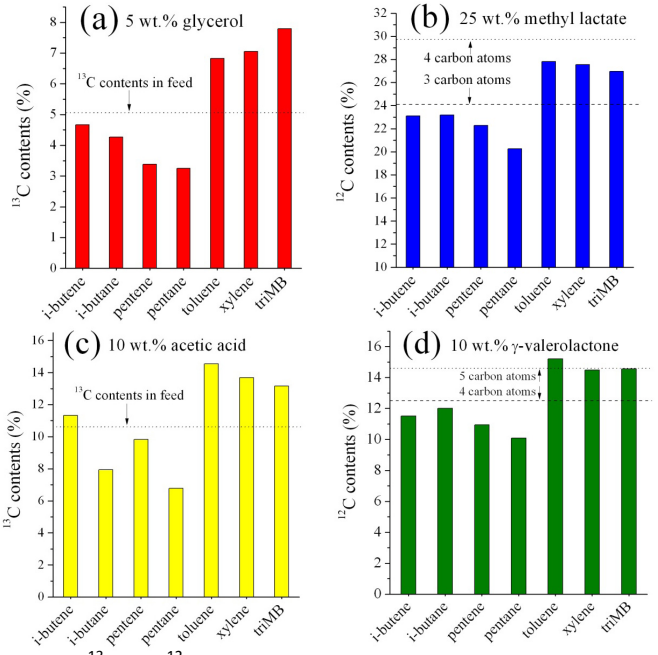

Figure 4. ^{13}C and ^{12}C content observed in typical main products for MTG. In the case of (a) 5 wt.% glycerol and (c) 10 wt.% acetic acid we used ^{13}C labeled additives in unlabeled methanol whereas ^{13}C methanol was used in (b) 25 wt.% methyl lactate and (d) 10 wt.% γ-valerolactone. The dotted lines correspond to the ^{13}C content in the feed and the dashed lines in (b) and (d) correspond to incorporation of all additive carbon after CO dissociation.

Figure 4 presents results from these labeling experiments using glycerol, methyl lactate, acetic acid and γ-valerolactone, respectively. From Figure 4a we see the ^{13}C carbon content when reacting 5 wt.% of ^{13}C labeled glycerol in methanol while the dotted line represents the ^{13}C content in the feed. If all additive carbons were incorporated and distributed evenly in the products 5.05% ^{13}C would be expected in all products. Interestingly, we see that the aromatic products (toluene, xylene and trimethylbenzene) actually contain significantly more ^{13}C than the average while the aliphatic products contain correspondingly less. It thus appears that the reaction path of glycerol favors the formation of aromatics which eventually through alkylation and alkene dissociation equilibrate into the remaining products as described in detail elsewhere.[51] This observation is in good agreement with a recent report by Mallinson and co-workers where they found an increased affinity for aromatization of propanal as compared to propanol when reacted over HZSM-5.[52] In the aliphatic compounds only a small difference exists between the incorporation into saturated and unsaturated compounds even though the longer pentane and pentene have a markedly lower content than their C_4 analogues.

Figure 4b presents the case of reacting 25 wt.% methyl lactate in ^{13}C labeled methanol. We know from Table 2 that >95% of CO is produced suggesting that we "lose" 1/4 of the carbons from methyl lactate. The dotted lines in Figure 4b represents the average ^{13}C content in the feed while the dashed line represent the ^{13}C content we would expect if only 3 of the carbon atoms in methyl lactate were incorporated into the products. Note that the Y-axis shows

the ^{12}C content since we are using ^{13}C labeled methanol instead of labeled additive in this experiment. As was the case for glycerol we clearly see that the aromatic products are a larger sink for additive carbon compared to the aliphatic products and again the longer pentane and pentene have less additive carbon compared to the C_4 compounds. Further, we see that the ^{12}C content of the individual products is located above and below the limit for 3 carbon atoms in correlation with the fact that one carbon atom from methyl lactate is removed by decarbonylation and the remaining 3 are incorporated into the products. At present we are unable to explain the diminished incorporation into pentane but we note that this trend is also present in the other experiments though to a lesser extend.

Figure 4c shows data from the experiment co-reacting 10 wt.% of ^{13}C labeled acetic acid in methanol. From Table 1 and Table 2 we know that at 10 wt.% of acetic acid small amounts of CO and CO_2 are formed (3% and 5%) along with a tremendous amount of aromatic carbon (35%) already in this modest concentration of acetic acid. We recognize the pattern of incorporation with high levels in the aromatic compounds and less in the aliphatic as described previously. The total incorporation distributes below and above the ^{13}C content of the feed which means that we are probably incorporating the vast majority of even the acid carbon from acetic acid into the traditional gasoline products. This is somewhat surprising since significant amounts of hydrogen is required transferred to acetic acid (H/C effective = 0) if it is to produce the even modest H/C ratio of 1,14 present in for example toluene. The aliphatic ^{13}C incorporation is somewhat inconsistent with the other experiments which can partly be explained by the reaction path of acetic acid described elsewhere.[9,26] Acetic acid can form acetone and further iso-butene in sequence. We do however only detect relatively low amounts of CO_2 which would be formed in the ketonization leading to acetone but it could be enough to enrich isobutene above the expected value. Finally in Figure 4d γ-valerolactone was co-reacted with ^{13}C methanol. The results are very similar to what we saw for methyl lactate. Around 4/5 of the carbon from the additive is incorporated into the products (predominantly into the aromatics) which corresponds well with the significant CO and CO_2 formation detected.

From this type of GC-MS analysis it would be impossible to analyze the content of all of the hundreds of products in order to calculate a true average ^{13}C content in the gasoline product. However, based on the detected levels of CO and CO_2 as well as the presented data using labeled substrates in Figure 4 it seems likely that the majority of the carbon present in the additive does indeed end up in the gasoline products. Presumably the different additives have individual reaction paths highly dependent on the specific concentration and we are only able to observe the composition after some equilibration (by cracking, isomerization, oligomerization etc.) over the full catalyst bed has occurred. To address the enrichment of additive carbon in the aromatic products we repeated the experiment with ^{13}C labeled acetic acid while loading decreasing amounts of catalyst in order to suppress secondary reactions. The results are given in Figure 5 and in all cases we have >99% conversion of methanol/DME and acetic acid.

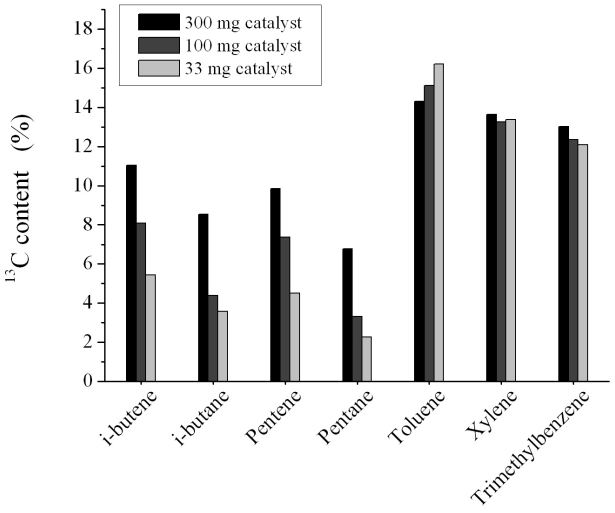

Figure 5. ^{13}C content in selected products when reacting ^{13}C labeled acetic acid in methanol over decreasing catalyst amounts.

Figure 5 reveals that as less catalyst is used we observe a pronounced decrease in the ^{13}C carbon % of the aliphatic while the content is relatively unchanged in the aromatics products. It is also clear that less additive carbon is present in the saturated aliphatics compared to the corresponding olefins. These result support a reaction path where the oxygenate initially forms aromatics. Over an active catalyst the aromatic products will subsequently split off alkenes which through hydrogen transfer reactions can produce alkanes effectively distributing the additive carbon into all products.

Temperature programmed oxidation (TPO)

A catalyst deactivated in methanol conversion is able to catalyze the methanol-DME equilibrium yielding predominantly DME for numerous hours after hydrocarbons are no longer formed in significant amounts. In the case of reacting 10 wt.% of γ-valerolactone, methyl lactate and glycerol in methanol the DME formation decreases rapidly after deactivation whereas DME is continually produced in the experiment with acetic acid added. Deactivating the catalyst with 10 wt.% of anisole which have the lowest conversion capacity of all the additives (see Table 1) does however not stop the production of DME. We performed TPO on the catalysts used in the concentration series presented in Table 2 as well as on selected catalysts from Table 1 to determine the amount of coke present once the catalysts where run to full deactivation.

Bilbao and co-workers have done thorough coke analysis when reacting bio-oil diluted in methanol over H-ZSM-5 and reported a distinction between thermal and catalytic coke. The thermal coke having a higher H/C ratio were attributed to bio-oil and could be combusted at a lower temperature as compared to coke from a conventional methanol experiment.[18,33]

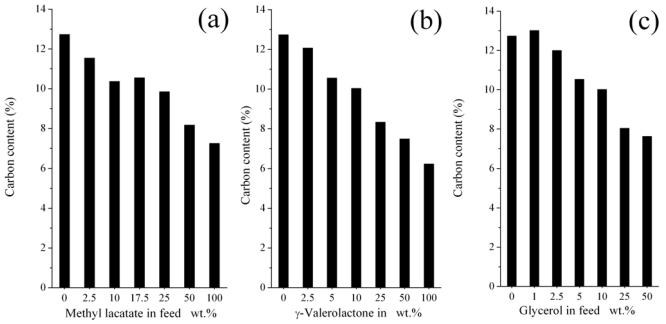

Figure 6. TPO experiments presenting the amount of coke deposited on the fully deactivated catalysts as a function of additive concentration. (a) methyl lactate, (b) γ-valerolactone and (c) glycerol

Figure 6 shows our results from TPO experiments of the concentration series from Table 2 and it is clear that the total amount of coke deposited before deactivation decreases as the wt.% of additive is increased. We were however unable to correlate the combustion temperature to specific fractions on the catalysts but merely note that a catalyst converting methanol for less than an hour (the lifetime of experiments having ≥50 wt.% of additive) contain negligible amounts of coke which underline that conversion of the hydrogen deficient additives from Table 1 results in excessive deactivation by coking. No clear trend in levels of coke deposition was observed from the catalysts in Table 1 where most catalysts contained approximately 10 wt.% coke although anisole and dimethoxybenzene had slightly less (~8 wt.%).

Conclusion

We have investigated the co-conversion of various model compounds in methanol under MTG reaction conditions which represents an alternative strategy to simply using "green" additives to conventional gasoline. The effective H/C ratio has previously been used as an indicator of whether an oxygenate would lead to rapid deactivation and we confirm the overall tendency. However, we present results that also show that structural isomers can indeed perform very differently with conversion capacities of approximately only half that of the other isomer. Molecules capable of dissociating CO_2 or CO generally experience higher conversion capacities highlighting that the specific functionalities in the additive are crucial in order to understand the specific reactivity. Converting the pure compounds leads to very short lifetimes of the zeolite catalyst and depending on the molecule we show how an optimal dilution in methanol can give up to 10 times higher conversion capacities of the additive before regeneration of the catalyst is required.

Experiments using ^{13}C labeling show that we are effectively able to remove the oxygen present in the additive (as water, CO or CO_2) independent of the type of functionality (triol, acid, lactone or alpha-hydroxyester) and overall oxidation state of the additive. The carbon in the additive is distributed into the hydrocarbon products with a favored affinity for the aromatics. And we can thus rule out that the additive carbon ends up in single "dead end" hydrocarbon or form new unconvertible oxygenates.

Experimental Section

The zeolite catalyst used in this study was a commercially available zeolite ZSM-5 with a Si/Al ratio of 40 kindly supplied by Zeolyst. The NH_4-ZSM-5 was transformed into proton form by calcination at 550 °C for 6 hours reached with a heating ramp of 2 °C/min. before use.

Catalytic experiments were performed employing 300 mg of pure zeolite crushed and sieved to obtain particle size of 350-500 µm and fixated by quartz wool in a quartz reactor having an internal diameter of 4 mm. Before reaction and during heating to 370 °C the catalyst was kept in a He flow of 40 ml/min. The reactants were introduced by an HPLC pump at a rate of 0.05 ml/min through a stainless steel tube (1/16 inch) heated to above the boiling point of the respective additives. The constant feed volume gave a typical WHSV of around 8 h^{-1} depending on the density of the specific feed composition. Conversion capacities reported in $g/g_{zeolite}$ for the individual experiments were calculated from the measured WHSV multiplied by the observed lifetime until only 50% conversion of methanol/DME.[43]

The reaction temperature was measured inside the reactor approximately 0.5 cm below the catalyst bed and was stabilized at 370 °C before the experiments. Steel piping (1/4 inch) heated to >200 °C directed the products to on-line GC equipped with a FID. Response factors of all hydrocarbons were assumed to be 1 while 0.63 and 0,81 was used for DME and methanol, respectively. Response factors for other oxygenates were estimated to be equal to that of DME. The concentrations of CO and CO_2 in the effluent were determined by a BINOS instrument placed after condensation in a cold-trap kept at 0 °C.

In the case of experiments converting ^{13}C enriched reactants; the same setup, scaling and reaction conditions were used. The conversion and product selectivities were monitored by on-line GC in order to verify similarity with conventional runs while additional product samples could continuously be withdrawn for GC-MS analysis. Calculating the ^{13}C content in the products was done based on a reference containing 99% ^{13}C obtained from reacting pure ^{13}C labeled methanol. In a typical ^{13}C experiment enough substrate was used to continue operation for 1-2 hours. In all cases only minor deactivation occurs in this short time range thus giving us information on the fate of additive carbon incorporation over a "fresh" catalyst.

TPO (temperature programmed oxidation) of the deactivated catalysts was performed on 100 mg of sample. The coked catalyst was heated from RT to 670 °C at a rate of 2.7 °C/min in a flow of 20 ml/min of 5% O_2 in He. The formed CO and CO_2 were detected by a BINOS.

All chemicals were used as purchased without further purification. Methanol, ≥99.7%, Sigma-Aldrich; 2-propanol, , ≥99.8%, Sigma-Aldrich; Acetone, ≥99%, Sigma-Aldrich; Methyl glycolate, 98%, Aldrich; Glycolaldehyde

dimethylacetal, 98%, Alfa Aesar; 1,4-butanediol, ≥98%, Fluka; 1-butanol, ≥99,5%, Sigma-Aldrich; Butyraldehyde, ≥99,0%, ≤1% butyric acid, stabilized w. ~1% water and 0,1% 2,6-ditertbutyl-p-cresol, Fluka; Ethyleneglycol, ≥99%, spectrophometric grade, Sigma-Aldrich; γ-valerolactone, 99%, Aldrich; 2,3-butanediol, ≥98%, mixture of racemic and meso forms, Fluka; 1,3-propanediol, 99%, Aldrich; Propyleneglycol, ≥99,5%, Fluka; Methyl propionate, ≥99,0%, Fluka; Propionic acid, ≥99,5%, Sigma-Aldrich; Butyric acid, ≥99%, Aldrich; 1,2-dimethoxybenzene, 99%, Sigma-Aldrich; Methyl-(S)-(-)-lactate, 98%, Aldrich; Methyl-(L)-lactate, 98%, Aldrich; 1,2-butanediol, ≥98,0%, Fluka; 1,3-butanediol, ≥99,0%, Fluka; 1,5-pentanediol, ≥97%, Fluka; Acetic acid, 98-100%, Bie & Berntsen A/S; Ethanol, anhydrous, 99,9%, Kemetyl; Levulinic acid, 98%, Aldrich; Glycerol, ≥99%, Sigma-Aldrich; Formaldehyde dimethyl acetal, ≥99%, Fluka; Formic acid, 98%, Fluka; Acetaldehyde, ≥99%, Sigma-Aldrich; Methyl acetate, ≥99,5%, Fluka; Propionaldehyde, 97%, Sigma-Aldrich; Butanone, ≥99%, Sigma-Aldrich; 2-Methyltetrahydrofuran, ≥97%, Fluka; Toluene, 99,9%, Sigma-Aldrich; Anisole, 99%, Sigma-Aldrich; Glycerol $^{13}C_3$, 99 atom% ^{13}C, Isotec; Methanol ^{13}C, 99 atom% ^{13}C, Isotec; Acetic acid, $^{13}C_2$, 99 atom% ^{13}C, Isotec; demineralized water.

Acknowledgements

We thank the Danish National Research Foundation and Haldor Topsoe A/S for financial support.

Keywords: Zeolite • ZSM-5 • Methanol-to-Hydrocarbons • Bio-oil • Oxygenate • Biomass

Entry for the Table of Contents
Layout 1:

Co-conversion of oxygenates in the Methanol-to-Hydrocarbons (MTH) reaction has been investigated. The positive effect of methanol dilution on conversion capacities of the additives was quantified and the use of ^{13}C labeled substrates reveals additional information of the fate of oxygenate carbon.

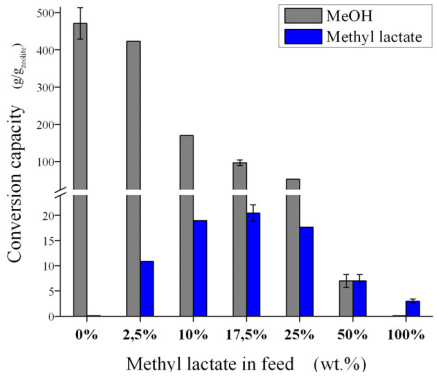

Uffe V. Mentzel* & Martin S. Holm*

Page No. – Page No.

Utilization of Biomass: Conversion of Model Compounds to Hydrocarbons over Zeolite H-ZSM-5

[1] G. W. Huber, S. Iborra, A. Corma, *Chem. Rev.* **2006**, 106, 4044-4098.

[2] J. R. Regalbuto, *Science* (**2009**), 325, 822-824.

[3] A. Demirbas, *Energy Convers. Manage*. **2009**, 50, 2239-2249.

[4] A. V. Bridgewater, M. L. Cottam, *Energy Fuels* **1992**, 6, 113-120.

[5] S. Czernik, A. V. Bridgwater, *Energy Fuels* **2004**, 18, 590-598.

[6] D. Mohan, C. U. Pittman, P. H. Steele, *Energy fuels* **2006**, 20, 848-889.

[7] R. French, S. Czernik, *Fuel Process. Technol.* **2010**, 91, 25-32.

[8] M. Stöcker, *Microporous Mesoporous Mater.* **1999**, 29, 3-48.

[9] C. D. Chang, A. J. Silvestri, *J. Catal.* **1977,** 47, 249-259.

[10] P. B. Weisz, W. O. Haag, P. G. Rodewald, *Science*, **1979,** 206, 57-58.

[11] N. Y. Chen, T. F. Degan, Jr., L. R. Koenig, *Chemtech* **1986, A**ugust, 506-511.

[12] P. D. Chantal, S. Kaliaguine, J. L. Grandmaison, A. Mahay, *Appl. Catal.* **1984**, 10, 317-332.

[13] P. A. Horne, P. T. Williams, *J. Anal. Appl. Pyrolysis* **1995**, 34, 65-85.

[14] J. D. Adjaye, N. N. Bakhshi, *Fuel Process. Technol.* **1995**, 45, 185-202.

[15] R. French, S. Czernik, *Fuel Process. Technol.* **2010**, 91, 25-32.

[16] R. K. Sharma, N. N. Bakhshi, *Fuel Process. Technol.* **1993**, 35, 201-218.

[17] P. T. Williams, A. J. Brindle, *J. Anal. Appl. Pyrolysis* **2003**, 67, 143-164.

[18] A. G. Gayubo, A. T. Aguayo, A. Atutxa, B. Valle, J. Bilbao, *J. Chem. Technol. Biotechnol.* **2005**, 80, 1244-1251.

[19] P. A. Horne, P. T. Williams, *Renewable Energy* **1996**, 7, 2, 131-144.

[20] X. Zhu, R. G. Mallinson, D. E. Resasco, *Appl. Catal., A* **2010**, 379, 172-181.

[21] M. C. Samolada, A. Papafotica, I. Vasalos, *Energy Fuels* **2000**, 14, 1161-1167.

[22] P. D. Chantal, S. Kaliaguine, J. L. Grandmaison, *Appl. Catal.* **1985**, 18, 133-145.

[23] J-L. Grandmaison, P. D. Chantal, S. C. Kaliaguine, *Fuel* **1990**, 69, 1058-1061.

[24] R. J. Evans, T. Milne, *ACS Symposium Series*, Pyrolysis oils from Biomass, **1988**, 376, 27, 311-327.

[25] T. Q. Hoang, X. Zhu, L. L. Lobban, D. E. Resasco, R. G. Mallinson, *Catal. Commun.* **2010**, 11, 977-981.

[26] G. J. Hutchings, P. Johnston, D. F. Lee, A. Warwick, C. D. Williams, M. Wilkinson, *J. Catal.* **1994,** 147, 177-185.

[27] A. G. Gayubo, A. T. Aguayo, A. Atutxa, R. Aguado, J. Bilbao, *Ind. Eng. Chem. Res*. **2004,** 43, 2610-2618.

[28].A. G. Gayubo, A. T. Aguayo, A. Atutxa, R. Aguado, M. Olazar, J. Bilbao, *Ind. Eng. Chem. Res*. 2004, 43, 2619-2626.

[29] J. D. Adjaye, N. N. Bakhshi, *Biomass Bioenergy* **1995**, 8, 131-149.

[30] L. H. Dao, M. Haniff, A. Houle, D. Lamothe, *ACS Symposium Series*, Pyrolysis oils from Biomass **1988**, 376, 27, 328-341.

[31] L. H. Dao, M. Haniff, A. Houle, D. Lamothe, *193. National meeting of the American Chemical Society*, **1987**, 32:2, 308-316.

[32] R. K. Sharma, N. N. Bakhshi, *Bioresour. Technol.* **1991**, 35, 57-66.

[33] A. G. Gayubo, B. Valle, A. T. Aguayo, M. Olazar, J. Bilbao, *Energy Fuels* **2009,** 23, 4129-4136.

[34]. A. G. Gayubo, B. Valle, A. T. Aguayo, M. Olazar, J. Bilbao, *Ind. Eng. Chem. Res*. **2010**, 49, 123-131.

[35] B. Valle, A. G. Gayubo, A. Alonso, A. T. Aguayo, J. Bilbao, *Appl. Catal., B* **2010**, 100, 318-327.

[36] A. Corma, G. W. Huber, L. Sauvanaud, P. O'Connor, *J. Catal.* **2007**, 247, 307-327.

[37] A. Corma, G. W. Huber, L. Sauvanaud, P. O'Connor, *J. Catal.* **2008**, 257, 163-171.

[38] I. Graca, F. R. Ribeiro, H. S. Cerqueira, Y. L. Lam, M. B. B. de Almeida, *Appl. Catal., B* **2009**, 90, 556-563.

[39] T. R. Carlson, T. P. Vispute, G. W. Huber, *ChemSusChem* **2008,** 1, 397-400.

[40] T. R. Carlson, G. A. Tompsett, W. C. Conner, G. W. Huber, *Top. Catal.* **2009**, 52, 241-252.

[41] T. R. Carlson, J. Jae, Y-C. Lin, G. A. Tompsett, G. W. Huber, *J. Catal.* **2010**, 270, 110-124.

[42] M. Bjørgen, F. Joensen, M. S. Holm, U. Olsbye, K.-P. Lillerud, S. Svelle, *Appl. Catal., A* **2008**, 345, 43-50.

[43] T. V. W. Janssens, *J. Catal.* **2009**, 264, 130-137.

[44] U. V. Mentzel, S. Shunmugavel, S. L. Hruby, C. H. Christensen, M. S. Holm, *J. Am. Chem. Soc.* **2009**, 131, 17009-17013.

[45] H. Heeres, R. Handana, D. Chunai, C. B. Rasrendra, B. Girisuta, H. J. Heeres, *Green Chem*. **2009**, 11, 1247-1255.

[46] H. Mehdi, V. Fabos, R. Tuba, A. Bodor, L. T. Mika, I. T. Horvath, *Top. Catal.* **2008**, 48, 49-54.

[47] B. Kartryniok, S. Paul, F. Dumeignil, *Green Chem.* **2010**, 12, 1910-1913.

[48] J. Q. Bond, D. M. Alonso, D. Wang, R. M. West, J. A. Dumesic, *Science* **2010**, 327, 1110-1114.

[49] J. F. Haw, D. M. Marcus, *Top. Catal.* **2005,** 34, 41-48.

[50] J. F. Haw and D. M. Marcus, *Nanotechnology in Catalysis*, Eds. B. Zhou, S. Hermans, and G.A. Somorjai, **2004,** ch. 13, Kluwer Academic/Plenum, NY.

[51] M. Bjørgen, S. Svelle, F. Joensen, J. Nerlov, S. Kolboe, F. Binino, L. Palumbo, S. Bordiga, U. Olsbye, *J. Catal.* **2007**, 249, 195-207.

[52] T. Q. Hoang, X. Zhu, T. Sooknoi, D. E. Resasco, R. G. Mallinson, *J. Catal.* **2010**, 271, 201-208.